TRACING MULTIPLE AQUATIC ECOSYSTEM STRESSORS ACROSS A LAND-USE INTENSIFICATION GRADIENT: A MULTI-TOOLED ENVIRONMENTAL FORENSIC APPROACH

A thesis submitted to the Faculty of Science in the fulfillment of the requirements for the degree of

Doctor of Philosophy in Ecohydrology

In the School of Animal, Plant and Environmental Sciences,

University of the Witwatersrand

by

Jonathan Chaim Levin

May 2024

UNIVERSITY OF THE WITWATERSRAND, JOHANNESBURG

Supervisor: Prof. D.J. Woodford (University of the Witwatersrand)

Co-supervisor: Prof. C.J. Curtis (University of Johannesburg)

DECLARATION

I, Jonathan Chaim Levin, submit this thesis to the Faculty of Science for the Degree of Doctor of Philosophy at the University of the Witwatersrand, Johannesburg. I declare this thesis to be of my own, unaided work, that has not been submitted for any other degree or examination at any other university.

____

Signed on 20th day of May 2024 at the University of the Witwatersrand, Braamfontein, Johannesburg, South Africa.

ABSTRACT

South Africa requires advanced freshwater management approaches to address complex catchment stressors acting on aquatic ecosystems. An environmental forensics toolbox could help disentangle pollution sources, informing stressor-focused adaptive management. Existing national, spatial resource strategies that define aquatic resource objectives, overlook modelling different aquatic stressor-linked components across spatio-temporal scales to disentangle individual stressor effects along land-use intensification gradients. This thesis investigated how spatio-temporal, physico-chemical water quality parameters, dissolved and sediment-bound trace metals as well as fish tissue $\delta^{34}S$ all collected from 15 river sites in the tributaries of the Gwathle River Catchment, positioned in the Platinum Belt of South Africa across a land-use intensification gradient, can be used to disentangle aquatic stressors. Through using a spatio-temporal generalised linear mixed effects model (GLMM) approach, the importance of employing a multi-hydrological-spatial (sub-basin, cumulative basin and riparian buffer) scale approach to link stressors (drivers) to changes in key catchment water quality parameters as opposed to a single scale approach was identified. At the sub-basin scale, ammonium concentrations were best explained by urban stress through wastewater effluent, Cu increased with mining via leaching from pollution control dams and mineral discharges, while turbidity increased with higher agricultural coverage, following greater tillage practices and irrigation. River pH was positively predicted for by slope heterogeneity at the cumulative-basin scale, while sulfate increased with mining at the cumulative 100 m riparian buffer, from leaching and discharges. Dissolved inorganics, including trace metals, are routinely assessed in national aquatic resource assessments, yet metals in sediments demonstrating legacy effects, are yet to be integrated. Using geo-spatial models across seasons, dissolved and sediment Cr concentrations were found to be driven primarily by mining both at the sub-basin scale, while dissolved Zn concentrations reflected sub-basin lithology and sediment-bound Zn reflected cumulative basin scale urban stress and lithology. Concordance correlation indicated that the Cr had a substantial positive stress-tracking agreement between the two media, with both tracking Cr land-use intensification gradient inputs while Zn displayed negligible concordance. While fish tissue $\delta^{15}N$ has been used to trace nutrient pollution, no local or international research has assessed time-integrated fish tissue $\delta^{34}S$ as a sulfur stress-tracer from interacting urban, agricultural and mining stressors. Using a spatio-temporal GLMM modelling approach, it was found to be possible to distinguish key agricultural and mining stressors on aquatic ecosystems, with $\delta^{34}S$ being relatively enriched following sub-basin scale agriculture and relatively depleted following cumulative basin scale mining activities. The outcomes of this research expands our knowledge base on using aquatic physico-chemical parameters, inorganic media indicators, and biotic tracers, towards the development of a potential environmental forensic toolbox to elucidate complex pollution sources and pathways for enhanced catchment management and freshwater governance in South Africa.

ACKNOWLEDGEMENTS

Throughout this Ph.D. journey, I have been fortunate enough to be surrounded by incredible support that played fundamental roles in allowing for the completion of this research. Firstly, I would like to express my deepest gratitude to my primary scientific advisory committee, including Darragh Woodford, my late supervisor Robert (Bob) Scholes and Chris Curtis for their scholarly inputs during this journey.

Darragh, I sincerely appreciate the support you provided within the Aquatic Laboratory that enabled me to conduct my Ph.D. research. Your willingness to listen open-mindedly as I worked through ideas was invaluable. I was fortunate enough to be mentored by Bob as a supervisor during the foundational phase of my Ph.D. Throughout my undergraduate degree and into my doctorate, he challenged me to become a ‘big picture’ scientist. I value all the inspiration and knowledge during consultations, over dinners, during citizen science excursions to KwaZulu-Natal and on hiking trips in the Magaliesberg Mountains. The systems thinking inspiration he imparted will remain with me forever, and I will carry it throughout the rest of my career. For this lifelong impact, I am incredibly grateful. To Chris, who readily and selflessly stepped up to fill the supervisory void, I sincerely appreciate your kindness and support in taking on this role when needed. Your willingness to give your time and guidance so generously is greatly appreciated.

Myself, Darragh, Bob and Stephan Woodborne (iThemba Laboratories and University of Pretoria) conceptualised and submitted a successful Water Research Commission (WRC) proposal (Project No. 3079/1/23), published by Levin et al. (2023) that in its entirety funded the collection of all the data presented in this thesis. With that, I would like to express my sincere gratitude to the WRC, who without my Ph.D. research in the field of Ecohydrology, would not have been possible. I want to thank Yazeed van Wyk at the WRC, for being a kind and supportive Research Manager, overseeing to completion the WRC report and providing key insight into the availability of stable isotope processing facilities in South Africa. To the National Research Foundation (NRF), thank you for providing partial bursary funding.

I would also like to thank Stephan Woodborne, Marc Humphries (University of the Witwatersrand) and Jaclyn Hill (Maurice Lamontagne Institute, Canada) for their guidance on field data collection, as well as for providing revisions on specific data chapters, ensuring coherence of critical ideas. Stephan and Jaclyn also played integral roles in supporting the correct execution of the protocols used in the collection of stable isotope samples. Marc provided amicable training of all necessary equipment in the Environmental Geochemistry laboratory at the University of the Witwatersrand to process and analyse water as well as sediment trace metals. To my peers, Mandlenkosi Nkala, Nompendulo Khoza and Lethabo Sebothoma, who assisted me in the laboratories to ensure the samples were prepared on schedule, I thank you. I thank Chris Yarnes and James Farlin at the University of California, Davis Stable Isotope Facility for processing the isotope samples for this thesis.

My Ph.D. research took me to sections of the magnificent Magaliesberg Mountain range. I want to thank Gert Easters of Cherry Ridge (Pty), Mark Ashfield at the Maretlwane Wilderness School and staff at the Utopia Nature Resort for access to river sites for the purpose of data collection. A big thank you to Rene Shields at Milorho Lodge for providing accommodation with the necessary back-up energy solutions to securely store collected samples. I wish to extend my deep appreciation to Patrick Lacey, who offered invaluable field assistance for the data presented in this thesis.

To my friends and fellow peers during my registration, Gina Walsh, Catiuscia Pino, Blair Cowie, Alekzandra Szewczuk, I am extremely grateful for all your support and laughs that have made this journey so memorable. My friend Joshua Polakow, who often reminded me that it was important to take a break during this academic journey, I am extremely grateful for the sincere friendship.

Lastly, to those who are the most instrumental in ensuring the completion of this research, my family. To my mom, you have provided me with the utmost compassion and patience during this journey. Thank you for always believing in me and my potential. Even when my ideas or ambitions seemed unbelievable, your unwavering support of my abilities has pushed me to become the who I am today. To my brother Doron, the best field assistant, equipment troubleshooter and moral support buddy, I am incredibly thankful for all your help. To my aunt Janine, you have always been my greatest cheerleader. I thank you for always ensuring I am in the best mood possible throughout my Ph.D.

Publication preparation

The **Chapter 2** from this thesis has been publication in a peer-reviewed journal, Science of the Total Environment:

Levin, J.C., Curtis, C.J. and Woodford, D.J., 2024. A multi-spatial scale assessment of land-use stress on water quality in headwater streams in the Platinum Belt, South Africa. *Science of the Total Environment*, *927*, 1 – 14. https://doi.org/10.1016/j.scitotenv.2024.172180

Grey literature publication

The **following chapters** have written work with the literature content and/or data included from my previous research submitted as grey literature as a requirement of the WRC Project No. 3079/1/23, cited as:

Levin, J.C., Woodford, D.J., Woodborne, S. and Curtis, C., 2023. Assessing water user impacts on eco-hydrology using stable isotopes, Water Research Commission, Report number: 3079/1/23, Pretoria, ISBN 978-0-6392-0440-6.

Chapter 1 – Written literature review

Chapter 2 – River water quality data

Chapter 3 – Dissolved trace metal data

Chapter 4 – Water quality data and fish tissue $\delta^{34}S$ values

TABLE OF CONTENTS

LIST OF FIGURES

LIST OF TABLES

ACRONYMS

AICc – Akaike's Information Criterion with small-sample correction

BIC – Bushveld Igneous Complex

CCC – Concordance correlation analysis

CMA – Catchment Management Agencies

COHESION – connectedness to patches with the same landcover class

DWS – Department of Water and Sanitation

EDXRF – Energy Dispersive X-Ray Fluorescence

EF – enrichment factor

FEPA – Freshwater Ecosystem Priority Area

GLMM – Generalised linear mixed effects model

GWT – Gwathle River

ICP-MS – inductively coupled plasma mass spectrometry

ICP-OES – inductively coupled plasma optical emission spectrometry

MRT – Maretlwane River

NFEPA – National Freshwater Ecosystem Priority Areas

NWA – National Water Act (Act No. 36 of 1996)

PCA – Principal Component Analysis

PCD – pollution control dam

PES – Present Ecological Status

PGE – platinum group elements

PLAND – percentage cover of each land cover class

RDM – Resource Directed Measures

REMP – River Eco-Status Monitoring Programme

RQO – Resource Quality Objectives

RWQOs – Receiving water quality objectives

SDC – Source Directed Controls

STK – Sterkstroom River

TDS – total dissolved solids

TPC – Thresholds of potential concern

Chapter 1 – General introduction

1.1. Concern for global freshwater resources

There is a mounting global freshwater resource crisis driven by population growth, escalating socio-economic resource demands and intensifying catchment land-use pressures from expanding urban, agricultural and industrial activities (stressors) (du Plessis, 2023). By 2030, global freshwater demand is expected to exceed supply by 40%, with water security defined as one of the greatest threats to global prosperity (Caretta et al., 2022; Day and Davies, 2023). This deficit, coupled with the mismanagement and contamination of water resources to support socio-economic growth, leads to substantial degradation of aquatic ecosystems. River pollution alone is estimated to be responsible for 30% of global aquatic biodiversity losses (Vörösmarty et al., 2010). Characteristic of the Anthropocene era, human activities are the primary drivers of global aquatic system modification, with climate pressures placing further stress on freshwater resources (Crutzen and Stoermer, 2021).

Since 1990, substantial research has brought attention to the alarming exponential decline in the suitability of global freshwater for human use, already a scarce resource constituting only 3% of the world's total water (du Plessis, 2023). Countries experiencing threats to their freshwater resources and aquatic life consistently suffer from the combined impacts of extensive water extraction and pervasive pollution. These interconnected activities amplify the pressures on already strained and depleted freshwater ecosystems. One central obstacle for sustainable and fair management of water resources is the complex interplay of multiple stressors acting upon aquatic ecosystems that reduce their capacity to continuously provide crucial ecosystem services (Jackson et al., 2016; Birk, 2019). This complex interaction poses major challenges for straightforward management interventions that aim to alleviate such stress.

Agricultural and domestic activities are key socio-economic stressors that routinely co-occur in river catchments and strongly correlate with water pollution. As pollution of freshwater resources increases in tandem with population growth, it critically drives escalating water scarcity by restricting suitability across various usage needs (Vörösmarty et al., 2010). This is with the suitability and sustainability of these resources being expected to worsen, while demand is anticipated to increase between 20% to 30% by 2050 to align with global population growth, with Africa anticipated to experience the greatest population growth (du Plessis, 2023). Already 27% of the global population resides in water-scarce countries, and projections estimate this figure to rise between 42% and 95% by 2050 (du Plessis, 2023). Of concern are the increasing numbers and concentrations of legacy and in particular emerging contaminants in global and local freshwater systems, such as pharmaceuticals (e.g., Ritonavir) and industrial ingredients (e.g., Triclosan) (Selwe et al., 2022).

Approximately 2.5 billion people globally do not have adequate access to sanitation services, resulting in uncontained raw sewage entering nearby surface waters. In addition, the poor maintenance of sewerage infrastructure has led to the discharge of raw and partially treated sewage into river systems (Gqomfa et al., 2022; du Plessis, 2023). Domestic sewage is a major driver of poor river water quality in developing countries, where the high cost of treatment and the necessary infrastructure often prevent discharge standards from being met (du Plessis, 2023). To support the rising demand for food production, given rapid human population growth, chemical fertilizers and pesticides have been used unsustainably, along with the ineffective storage of animal waste products (Carey et al., 2013; Xu et al., 2022). These pose immense threats to river health through the discharge and runoff of excess chemicals and nutrients, contributing to water contamination, eutrophication, and biodiversity loss.

Already, certain fertilizer-linked nutrients, such as phosphorus, have exceeded planetary boundaries (Li et al., 2019), with further increases in certain nutrients predicted (Richardson et al., 2023). While agriculture remains the largest freshwater resource user, it is anticipated that global domestic and industrial water requirements will grow at a faster rate (du Plessis, 2023). Industrial activities ranging from manufacturing to mining can generate and lead to the improper storage and/or disposal of effluent containing hazardous pollutants that can enter aquatic ecosystems, compromising water quality and aquatic life (Ouma et al., 2022). Urban expansion and the proliferation of impervious surfaces can also facilitate the rapid transport of leaked sewage, nutrient-rich domestic detergents, and other pollutants into stormwater drains before being discharged into river systems (Paul and Meyer, 2001).

1.2. State of South Africa's surface water resources

South Africa is among the 30th driest countries in the world, receiving ~465 mm of unequally distributed rainfall, well below the global annual average rainfall of 860 mm (Day and Davies, 2023; Daniell and van Tonder, 2023). With 21% of the country's landmass receiving less than 200 mm annually (Colvin and Muruven, 2017), its' surface water resources, and in particular headwater streams, are considered highly variable, with only ~8.6% of the rainfall becoming runoff; being among the lowest globally (Nkosi et al., 2021; Day and Davies, 2023). A large driver of such is the high average surface temperatures (17°C), which leads to three times more water lost through evaporation than rainfall can replenish in some regions (King and Pienaar, 2011; Colvin and Muruven, 2017). Ultimately, geographical and climatic factors result in the available surface water resources being temporally and spatially variable, threatening consistent freshwater access across the country (King and Pienaar, 2011).

With 77% of the country's water supply supported by fragile surface water resources, like headwater streams and main-stem rivers, careful management is crucial (Colvin et al., 2019; du Plessis, 2023). Most of the nation's river basins and water management areas, after water allocation for environmental flows (to support aquatic ecosystem integrity), are already considered to be in a water deficit (van Wyk et al., 2007; du Plessis, 2023). As a result, major inter-basin transfer schemes, such as the complex Lesotho Highlands Water Project, are required to transport significant volumes of freshwater to support socio-economic well-being (Matumba, 2019). Approximately 60% of South Africa's rivers are considered to be overexploited, with only one-third of the main-stem rivers said to be in good condition (Donnenfeld et al., 2018). Although the country's dams store ~65% of all runoff, 35% of those dams are already considered impaired by eutrophication (Frost and Sullivan, 2010).

With South African society reliant upon abundant, high-quality freshwater resources, it is also the major source of its degradation. Over-exploitation (e.g. extraction) of freshwater resources threatens aquatic ecosystem integrity and the sustainable provision of ecosystem services (Grizzetti et al., 2016). Such exploitation is driven by the rising demand for water, particularly among agricultural, municipal and industrial sectors, accounting for the highest water demands respectively (Matumba, 2019). As the demand for water rises by 1% per annum, it is anticipated that there will be a 17%

deficit in South Africa’s water supply by 2030 (Colvin and Muruven, 2017), with other research suggesting that demand already exceeded supply in 2017 (Matumba, 2019). In addition, not all the surface water resources are available for extraction, as some of the surface water needs to be retained to support downstream ecosystem requirements (i.e. environmental flows), as per the Ecological Reserve outlined in the National Water Act (NWA; No. 36 of 1998) (du Plessis, 2023).

Performing key ecosystem services, such as nutrient cycling, rivers also collect and transport organic matter, sediments and additional constituents obtained from the surrounding catchment area. Nutrient loading occurs in headwater and large order streams, due to agricultural (fertilizers) and domestic (detergents and sewage) activities. In addition, the introduction of trace metals, chemical waste and additional constituents associated with industry (from mining etc.) can disturb the physico-chemical and biological condition of the ecosystem (Erasmus et al., 2020). Poor land management and waste practices can lead to aquatic pollution that causes certain water quality parameters to exceed acceptable limits or Thresholds of Potential Concern (TPC). These thresholds are outlined in the South African Water Quality Guidelines Volumes 1–7 (DWAF, 1997) for protecting specific water users including aquatic ecosystems. Exceeding these thresholds can disadvantage downstream users by rendering the resource unusable as well as harm the environment.

There has been a significant deterioration in the country’s surface water resources in the last ~20 years with rising and concerning levels of contaminants (Day and Davies, 2023; du Plessis, 2023). The rate and extent of pollution places an incredible financial burden on local water treatment entities to deliver high-quality drinking water to an increasing population. It is predicted that additional and often advanced methods of treatment are going to be required to deal with the increasing extent of new and persistent pollutants entering aquatic ecosystems into the foreseeable future (du Plessis, 2023).

1.3. South African National Water Act and resource management structures

Within the NWA, the ‘Reserve’, specific to each freshwater resource, consists of two major interdependent components. These include the “Basic Human Needs Reserve” and “Ecological Reserve”, both outlining the adequate water quality and quantity required for basic human needs and to sustain the ecological integrity of the ecosystem, respectively (King and Pienaar, 2011; du Plessis, 2023). Two key mechanisms used in executing the Ecological Reserve, outlined in Chapter 3 of the NWA, are Resource Directed Measures (RDMs) and Source Directed Controls (SDCs). The RDM is directly concerned with the state (i.e. condition) of the resource and is key in setting resource-specific objectives, while the SDCs are used in limiting aquatic ecosystem impacts i.e. identifying the stressors at the source to mitigate downstream effects (Von der Meden et al., 2005; DWAF, 2008)

The RDMs measures provide the protocol used to protect the country's water resources, ensuring the resource's current condition meets the Reserve's requirements and preventing resource over-exploitation (Wepener et al., 2015). Resource Directed Measures are implemented by Catchment Management Agencies (CMAs) through the use of Catchment Management Strategies and thus, form part of the legislated protection of South Africa's water resources (Wepener et al., 2015). The RDMs consist of the Reserve determination, establishing Resource Quality Objectives (RQO) and the classification of the water resource. To determine the desirable condition at which a water resource must be upheld, it is important to define the Reserve of the resource in question (King and Pienaar, 2011). To uphold the Reserves' quantity and quality requirements, RQOs are implemented.

Such RQOs provide the quantitative and/or descriptive conditions of the water resources quality, quantity, habitat and biota, thus providing for the Reserves requirements (desirable conditions) (King and Pienaar, 2011). Clear and measurable goals pertaining to the resource are established within each RQO. Through these goals, the RQOs aim to achieve a sustainable balance between societal water use and the protection of the water resource (King and Pienaar, 2011; du Plessis, 2023). Associated with each RQO is a TPC, which represents the range at which the conditions of the water resource become undesirable. If conditions do breach the TPC, additional research is conducted to determine the breach and implement the corrective measures (i.e. through SDCs), however, the RQOs can also be revisited and improved if deemed to have been too stringent in representing the typical conditions. However, to determine whether the requirements of the Reserve are compromised, baseline monitoring is first required to define the resource's current condition (Kleynhans et al., 2007).

To assess the condition of the resource and whether the Reserve's requirements have been breached, it is important to determine the Present Ecological Status (PES). Within the national River Eco-Status Monitoring Programme (REMP), aquatic ecosystems consist of two main components, each assessed by different monitoring types (techniques) (Kleynhans et al., 2007). The first component being physical drivers are monitored using abiotic techniques, while the second includes a suite of rapid biomonitoring indices (e.g. South African Scoring System Version 5 (SASS5); Dickens and Graham, 2002).

Each assessment provides the current condition of the ecosystem in the form of a Present Ecological Status (PES), which forms part of the Eco-Classification process (Kleynhans et al., 2007). While the rapid biotic indices effectively track spatio-temporal integrated changes in river health, some have been shown to be sensitive to hydrodynamic variations, like floods, that temporarily affect community structure and reflect such, rather than true long-term changes in river water quality (Foord and Fouché, 2015). In addition, they are limited in their forensic ability to identify specific sources of river impact in multi-user catchments where stressors coexist.

The SDCs are measures used to protect the water resources by preventing potentially harmful effects, through identifying pollution activities at the source and then implementing corrective action (DWAF, 2008; DWS, 2023). In doing so, the SDCs are used to ensure the aquatic ecosystem conditions remains within an acceptable range outlined by the resources RQOs within the RDMs. There are a range of SDCs activities, which include the development of guidelines and suitable protocols aimed at limiting harm to aquatic ecosystems, as well as the activities of compliance and enforcement, such as water use licensing.

1.4. Controlling effluent discharge: Water use licenses

The Department of Water and Sanitation (DWS), the custodian of South Africa's freshwater resources, can set river-specific 'receiving water quality objectives' (RWQO), to ensure the effluent entering aquatic systems does not impede upon the rivers social and environment suitability (Day and Davies, 2023). Each user that discharges effluent into the river is required by law to apply and hold a water use license. This license instructs the user as to the volume and quality of effluent that is to be discharged into the aquatic system, thereby upholding the RWQOs and ensuring downstream suitability. The RWQOs are river and stressor dependent, based on the variables of potential concern that enter the river from the activity. The South African Water Quality Guidelines Volumes 1–7 (DWAF, 1997) are specific to different uses of the river, and result in separate river RWQOs needing to be upheld (Day and Davies, 2023).

River water quality monitoring is (in theory) routinely performed, and the specifics of which are outlined in the user's allocated water use license to ensure compliance. The water quality tests are benchmarked against the 'water quality standards' and 'effluent standards' to ensure the effluent disposed of does not exceed certain TPCs (Day and Davies, 2023). In determining whether a user would be allocated a water use license by the issuer to discharge effluent, two key principles are considered, being the 'precautionary' and 'polluter pays' principles. The 'precautionary principle' indicates that if the proposed discharged effluent is likely to cause harm on the receiving aquatic system, it ought not to be discharged. The second, 'polluter pays principle' mentions that the polluting activity must fund the clean-up or pay a waste-discharge fee, which is to be facilitated by CMAs (Day and Davies, 2023). Such charges, however, are yet to be implemented and are held back by institutional challenges surrounding the establishment of most CMAs around the country.

1.5. Recognition and shortcomings of the National Water Act

The National Water Act (No. 36 of 1998), is recognised globally as one of the most advanced pieces of water legislation in translating integrated water resources management concepts into national law (Schreiner, 2013). The implementation of the Act, however, has been considered only partially successful, as essential components have not been acted upon nor enforced, constrained by technological deficiencies and skilled personnel (Schreiner, 2013). Examples of inadequate implementation include the low number of CMAs to support RDMs and enforce key functions such as the 'polluter pays principle' (Day and Davies, 2023). Additional concerns include the delayed equitable reallocation of water resources to previously disadvantaged farmers (Schreiner, 2013).

Outlined by the allocated water use license, key and routine aquatic health biomonitoring and/or river water quality monitoring using key parameters should be conducted in-field by professionally registered scientist(s) and/or using accredited water quality laboratories. These are used to identify potential transgressing activities that are in breach of the outlined water use license condition(s) (Day and Davies, 2023). Monitoring reports are then submitted to the license issuer, the DWS or Department of Mineral Resources, for review and consideration before further enforcement action is taken by the necessary authorities. Cases of infringement and thereafter, inadequate enforcement, have been identified with water use license-holding entities country-wide (Pollard and du Toit, 2011).

Instances of systemic pollution from major license-holding, non-compliant polluters have included industrial companies, mining corporations and municipalities failing to ensure compliance of discharged wastewater treatment work-related effluent (Gqomfa et al., 2022). The current national aquatic management systems do not offer the environmental forensic techniques or tools (i.e. no recommendations) to assess the relationship between specific or multiple water quality stressors that may operate in antagonistic, additive or even synergistic ways on the receiving aquatic ecosystem. Additional research and management guidelines are thus needed to bridge the knowledge gap regarding human-water stressors. Supplemental tools analysing spatio-temporal water quality variation, deployed at appropriate spatial scales, could disentangle stressors in mixed-use catchments where sources closely co-exist. This could enable the identification of key polluters in these catchments.

1.6. Spatial considerations for local surface water quality monitoring

In South Africa, river water quality monitoring is often conducted through private water-use license compliance, baseline and follow-up environmental impact assessment monitoring, as well as less frequent large-scale government catchment health assessments. These ecosystem-supporting assessments, however, often use variable sampling locations without considering spatial scale effects (Day and Davies, 2023). This makes it challenging to unravel the impact of interacting water quality stressors from key land-use activities in complex multi-user catchments, where stressors rarely exert influence in isolation. Effective monitoring and spatial-assessment techniques are needed to disentangle and pinpoint pollution sources to provide stressor-focused information for adaptive catchment management and/or enforcement actions.

No widely adopted national sampling protocols adequately address the significance of accounting for different hydrological spatial scales when collecting and analyzing *in-situ* river water quality data. Only the National Freshwater Ecosystem Priority Areas (NFEPA) project, which is a freshwater resource strategy, mentions fine-scaled sample node placement, defined by spatially-aligned FEPAs (Freshwater Ecosystem Priority Areas), but without the geo-spatial analysis (Driver et al., 2011). Incorporating spatial considerations is critical for accurately attributing contamination sources and elucidating how ecohydrological processes transform and/or transport pollutants between interconnected land-water systems. Such an approach enables the precise disentangling of multiple catchment stressors (Day and Davies, 2023). International research has demonstrated the importance of considering spatial-scale(s) in catchment assessments (for each independent study area) to best detect key sources of modified water quality constituents. In some regions, research studies have found nutrient loading (and retention) to be best predicted for by stressors at the catchment (cumulative or nested) basin scale (King et al., 2005; Ding et al., 2016), while other research has shown that riparian buffers and local sub-basin scales are more ideal, owing to the natural filtering ability of rivers along the continuum (Shen et al., 2015; Zhang et al., 2019).

Few studies in the developing world have investigated suitable spatial scales to disentangle stressor effects on river water quality across land-use intensification gradients (Mello et al., 2018). There is an especially notable lack of research on this topic in mineral-rich countries like South Africa, where catchments experience substantial mining pollution but also agricultural and domestic threats (Namugize et al., 2018). For example, South Africa's Bushveld Igneous Complex contains significant global deposits of Platinum Group Elements, yet this mining region is juxtaposed within catchments and is also facing the latter water quality stressors. Despite multiple pressures, the disentangling of such impacts on water quality using spatial scale assessments in the Bushveld Complex remains understudied. Techniques to assess stressors linked to legacy metal contaminants would also provide an integrated perspective on key exposures faced by headwater streams draining industrialised catchments.

1.7. Transient and legacy metals in current water resource management

Recent investigations have reported a concerning rise in aquatic metal pollution globally and in South Africa (Dalu et al., 2017; Erasmus et al., 2020; Kodikara et al., 2022). This has led to inorganic pollution posing a major threat to aquatic biota (Gurrieri, 1985; Amundsen et al., 1997) and escalating challenges for freshwater resource management, governance and policy (Balaram et al., 2023). Currently, metal pollution is widely assessed for water use license compliance monitoring and river health assessments. The fingerprinting of such sources of stress (primarily for academic research) in local aquatic ecosystems is mainly achieved through collected water samples analysed via inductively coupled plasma mass spectrometry (ICP-MS) and inductively coupled plasma optical emission spectrometry (ICP-OES) (Chetty et al., 2021; Madikizela et al., 2023). Unlike biomonitoring techniques in the REMP that provide relatively long-term river water quality indications over organism lifespans, *in-situ* collected water quality data is often highly variable (transient) (Beck et al., 1991). In particular, *in-situ* sample collection for the analysis of metals and other inorganics often lacks enough long-term consistency (demonstrating short-term variability across space and time) to reflect legacy contamination effects prior to recent monitoring efforts, making it challenging to identify the source of previous aquatic pollution (Förstner, 1979).

Applying an approach that can capture legacy metal pollution effects and be integrated into routine South African river health monitoring could enable resource managers to pinpoint specific contaminant sources and pathways. This would allow highly targeted mitigation efforts guided by elucidating the particular origins of pollution entering headwater streams (Albuquerque et al., 2021; Laha et al., 2022; Balaram et al., 2023). For example, the non-degradable nature and deposition of metals in sediment, would allow water resource managers to assess legacy effects of inorganic pollution in such media instead of only considering transient water samples. Analytical techniques, such as ICP-MS, can be used to assess inorganics in water as well as sediment, however, such analyses in accredited laboratories can be costly in South Africa, particularly when applied to both forms of media.

Energy Dispersive X-Ray Fluorescence (EDXRF) presents a relatively rapid, highly cost-effective yet largely unapplied alternative (compared to international systems) for assessing and tracing sources of legacy metal pollution in South African river sediments (Albuquerque et al., 2021). Comparing sediment EDXRF results to commonly used but transient water quality data, measured by ICP-MS analysis, can provide insights into the spatial detection capabilities of these complementary methods for tracking metal pollutants within mixed land-use South African river systems. As different ecohydrological processes can influence contaminant fate across hydrological scales and media, understanding where the techniques provide similar versus divergent catchment information on metals represents a key knowledge gap.

Determining if sediment EDXRF analysis can identify legacy polluters also fills an important local water management need. This is because such an approach can also be incorporated into broader river health assessments, with the intention of pinpointing current and legacy pervasive metal polluters, contributing to adaptive water resource management. Filling these gaps and clarifying the complementarity of techniques can strengthen long-term monitoring, help prioritize remediation of concerning legacy sites, and bolster the safeguarding of aquatic ecosystem health.

1.8. The use of the stable sulfur isotopes in South Africa's freshwater management

Over the past 20 years, global research has rarely used aquatic consumer tissue stable isotopes of sulfur ($\delta^{34}S$) to distinguish aquatic pollutants, even though such provide time-integrated $\delta^{34}S$ signals (Hesslein et al., 1991; Levin et al., 2023) that can effectively monitor and trace long-term pollution (Wayland and Hobson, 2001). Instead, it has been widely applied in tracking and identifying food resources in aquatic food web assessments (Hesslein et al., 1991; Croisterière et al., 2009). While some studies globally have assessed aquatic tissue $\delta^{34}S$, none attempted to use it to disentangle more than two distinct stresses along one river (Wayland and Hobson, 2001). Given this, there is substantial innovative potential in applying aquatic consumer tissue $\delta^{34}S$ globally to discriminate leading freshwater ecosystem stressors (e.g. agriculture, urban and mining) within mixed land-use catchments for improved water resource management. Conversely, tissue $\delta^{13}C$ and $\delta^{15}N$ have received more global and local attention in aquatic ecosystem assessments when compared to $\delta^{34}S$ (see Levin et al., 2023).

In South Africa (and globally), tissue $\delta^{13}C$ and $\delta^{15}N$ are two key stable isotopes that have been commonly used in aquatic ecosystem assessments. In peer-reviewed literature, both $\delta^{13}C$ and $\delta^{15}N$ have been used to monitor aquatic ecosystem recovery following the removal of alien invasive aquatic plant species, as well as ecological functionality of aquatic food webs, in dietary assessments as well as tracing and mapping sewage and agricultural pollution in river systems (Jackson et al., 2020; Motitsoe et al., 2020; de Necker et al., 2020; Motitsoe et al., 2022). Government-related reports have used $\delta^{15}N$ in aquatic assessments as an early warning system for eutrophication (Hill et al., 2011). From the available literature, which is discussed in further length in Levin et al. (2023), the current academic and grey South African literature on stable isotope stressors has demonstrated effectiveness with regards to tracing nitrogen pollution, with no indication of aquatic tissue $\delta^{34}S$ applied to trace sulfur-based pollution.

Although international aquatic-tissue $\delta^{34}S$ assessments have made an effort to trace and sewage and industrial sources, none have attempted to distinguish the impacts of multiple coexisting stressors along land-use intensification gradients, especially involving extensive mining activities. While $\delta^{34}S$ derived from aquatic animal tissues (invertebrates) has shown potential to identify sulfur-polluting mining stressors in aquatic ecosystems (see Corson, 2017), it has not yet been used to trace sulfur pollution inputs from concurrent multiple stressors (i.e. agriculture and urbanisation) across a watershed, locally or internationally in higher trophic levels. Using aquatic tissue $\delta^{34}S$ signatures as complementary tracers alongside other tools for disentangling the impacts of activities, like mining, could make a valuable contribution to the local stable isotope toolbox and ultimately support improved water governance strategies. However, the potential of fish tissue $\delta^{34}S$ for distinguishing the intricate blend of agricultural, urban, and industrial mining pressures in heavily impacted catchments currently represents a local and international knowledge gap.

1.9. Advancing South Africa's freshwater management through Environmental Forensics

Environmental Forensics is a growing international field involving scientific techniques linked to the surrounding environment. Its purpose is to investigate key contamination events in ecosystems in a manner that can identify their sources, potential historical release date, fate and pathways based on available evidence (Mudge, 2008; ed.

Petrisor, 2014). It is often considered the key 'link' between environmental and forensic sciences, integrating knowledge from fields such as chemistry, geology and biology; it considers processes and the timing of how certain evidence was received in a location (ed. Petrisor, 2014). It is particularly important in river systems, which may experience chronic pollution episodes – low exposure over a long time period leading to long-term detrimental ecological and social effects (ed. Petrisor, 2014).

Environmental forensics is important in systems that already experience a degree of natural background inputs (e.g. via weathering), coupled with stressor-derived pollution (Almécija et al., 2017). For example, river systems can experience natural stressors that are essential for their structure and functionality (Birk, 2019), but also receive confounding harmful interacting anthropogenic stressors, that can often be considered difficult to tease apart owing to causing similar effects (Feld et al., 2016). For instance, the polluting nutrient phosphorus enters ecosystems naturally as well as artificially, and is a key constituent in aquatic eutrophication, which has significant social and ecological implications (Griffin, 2017).

This makes tracing anthropogenic stressors (chronic/acute and perpetual/sporadic) especially important in multi-user contexts, where stressors can act in isolation or interact in unexpected ways. In aquatic ecosystems, complex biological and ecological interactions that are not yet fully understood can challenge and limit the effectiveness of conventional, straightforward management interventions. Rather scientists who apply environmental forensics can disentangle aquatic stressor-sourced effects and understand spatial scale-dependent ecohydrological processes interacting with such inputs, which is necessary to adequately inform adaptive management strategies.

Literature searches revealed no mentions of 'Environmental Forensics' being applied to prosecutions or directly informing freshwater management strategies in South Africa. While separate academic studies have used various statistical and environmental analysis techniques to fingerprint contamination sources and pathways, an opportunity exists to develop a tailored environmental forensic toolbox for targeted deployment to improve national catchment and transboundary water stewardship. General water parameters like metals (Gqomfa et al., 2022) and landscape-pollutant examinations (Namugize et al., 2018), alongside stable isotopes (Motitsoe et al., 2020), have determined some catchment stressors locally, though spatial considerations were limited. Few have traced legacy metal contaminants using rapid analytical methods, and stable isotope sulfur remains unapplied as a complementary tracer for discriminating watershed pollution sources. Developing such a fit-for-purpose toolbox combining emerging forensic methods with spatially explicit persistent pollutant fingerprinting could strengthen evidentiary bases to prosecute local offenders and better safeguard aquatic health through directed protections when paired with current REMP biotic and abiotic monitoring techniques.

1.10. Study area description

This investigation was conducted within the Gwathle River Catchment (Quaternary catchment A21K), in the North West Province of South Africa. Spanning approximately 160 km^2 with elevations from 986 m to 1843 m, the semi-arid watershed sees mean yearly precipitation of 629 mm. It has a rainy period from November to March with a peak in January, and a dry spell from April to October (Funk et al., 2015). Average monthly temperatures vary from 4.94 – 31.76°C, with June and February being the coldest and hottest months, respectively (SAWS, 2023).

The headwaters originate on the northern slopes of the Magaliesberg mountain range and flow between the towns of Rustenburg and Mooinooi. The rivers within form a confluence with the Crocodile (West) River at Roodekoppies Dam. The catchment headwaters are partially enclosed within the Magaliesberg Protected Environment, a provincial protected area containing several private nature reserves which is encapsulated within the Magaliesberg Biosphere Reserve, a region designated for ecotourism and sustainable development under the UNESCO Man and Biosphere program (Pool-Stanvliet, 2013). The Magaliesberg Biosphere was established in 2015 and is governed by a board of local landowners and stakeholders to promote conservation and prevent ecologically damaging economic growth in this mountainous area.

The headwaters of the Gwathle consist of several small mountain tributaries that converge into two rivers, the Sterkstroom and the Maretlwane (**Figure 1-1**). These flow north through agricultural, urban, and highly developed mining areas before merging into the Gwathle River. Both rivers originate in sandstone mountain watersheds, characterised by naturally low conductivity and pH. They then enter the bushveld basin, where dolomitic bedrock produces more alkaline groundwater with higher natural conductivity (Sappa et al., 2013). The geology of the catchments lowlands is characterised by the Western Lobe of the platinum group metal-containing Bushveld Igneous Complex, a narrow geological formation along the northern edge of the Magaliesberg (Magalhães et al., 2018) that supports several chrome and platinum mines, with supporting smelting activities. While the upper Sterkstroom lies within the Western Bankenveld aquatic ecoregion (Level 1 ecoregion 7), its lower reaches, the whole Maretlwane and the Gwathle fall within the Bushveld Basin aquatic ecoregion (Level 1 Ecoregion 8; Kleynhans et al., 2005).

The Sterkstroom's upper tributaries pass through lightly farmed land before entering the Buffelspoort Dam reservoir, a water source for agriculture and nearby settlements. Downstream of the dam, the river flows through a commercial platinum mine, then drains the large peri-urban area of Marikana. Several other platinum mines with large waste structures (mine dumps, pollution control dams) also drain into the Sterkstroom before it enters the Gwathle River. The Maretlwane's upper catchment drains near-pristine mountain bushveld, then flows past the town of Mooinooi, receiving agricultural and urban (treated wastewater) inputs. Further downstream, it passes an active commercial chrome mine and several legacy platinum mine waste storage facilities, collecting runoff from each until flowing through the peri-urban settlement of Wonderkop where it receives more urban wastewater and runoff. The Gwathle River flows mostly through rural landscapes with little adjacent urban or mining activity (**Figure 1-1**).

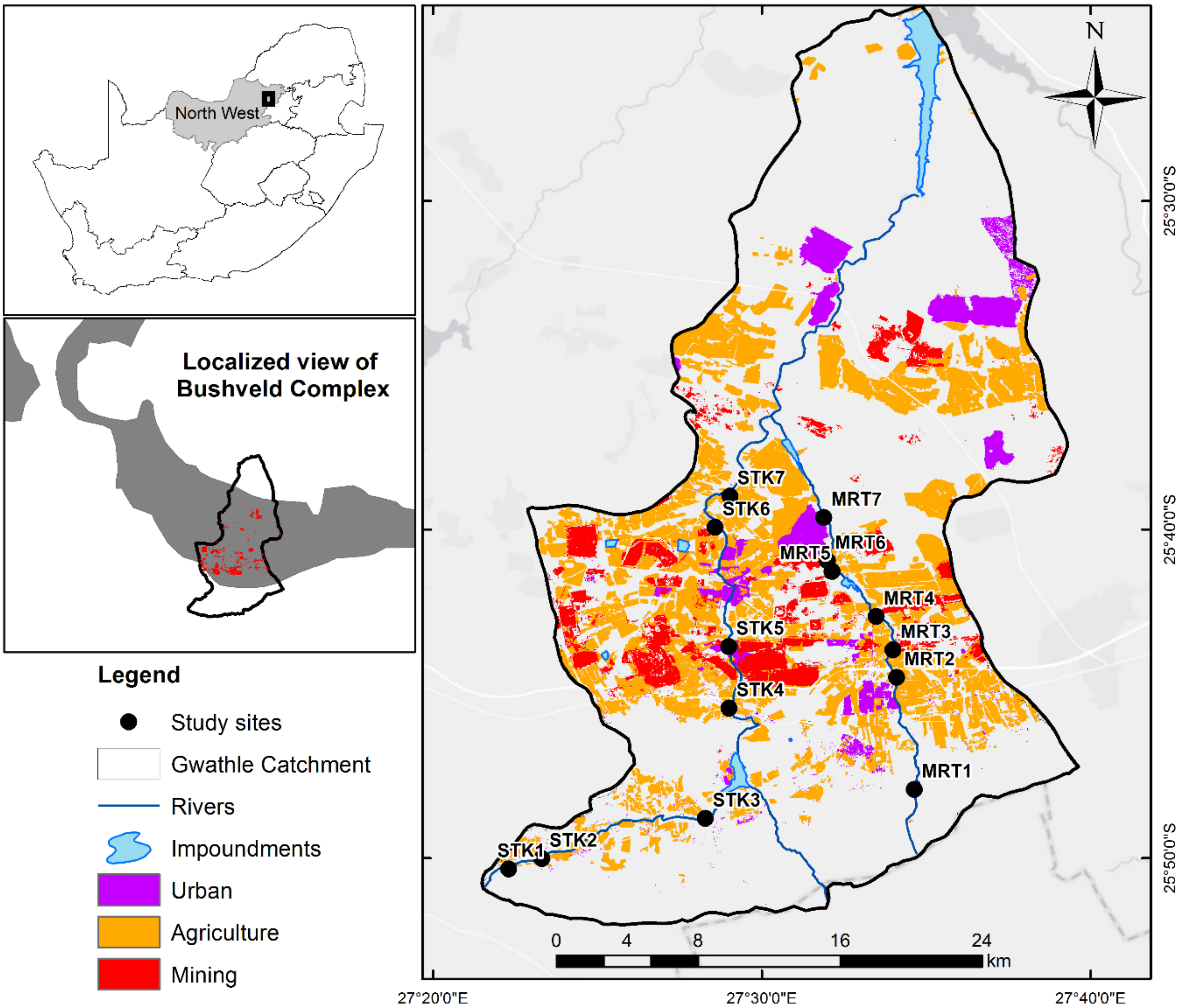

Figure 1-1: Map of the Gwathle study catchment within the Bushveld Complex (the mafic-ultramafic layered intrusion which hosts platinum group element deposits) as well as the sampling sites across the Sterkstroom (STK) and Maretlwane (MRT) rivers, draining an intensification gradient including natural (greyed area within), urban, agriculture and mining stressor activities.

1.11. Thesis Organisation

This thesis has been written as three stand-alone data chapters formatted as scientific papers intended for publication, bookended by an introduction and a concluding synthesis chapter of the key findings. Some repetition can be found in each of the three data chapters, including their introductions and method site description sections. At the end of each chapter is its respective reference list and supplementary material. Although the chapters have received input from co-authors, whose contributions are listed in the individual data chapter acknowledgements, the statistical analysis, data presentation and writing are primarily my own. **Chapter two** has been submitted to and published in the journal *Science of the Total Environment*.

Chapter two describes a multi-hydrological spatial scale assessment to disentangle the distinct spatial signatures and mechanistic effects of specific land-use stressors (urban, fallow-land, agriculture, impoundments and mining) as well as topographic drivers on individual water quality parameters in tributaries of the Gwathle River Catchment. Using class-level 1) composition and 2) connectedness metrics together with topographic data, models were developed at multiple spatial scales (sub-basin, cumulative catchment or nested, and 100 m riparian buffers at each of the latter two respective scales) to identify the dominant land-use stressor and/or topographic driver of each water quality parameter.

In **Chapter three** I perform a comparative geospatial assessment of dissolved and sediment-bound trace metals, analysed using separate analytical techniques, being ICP-MS (high analysis expense) and EDXRF (cost-effective, but only suitable for sediments), respectively. This is to determine the effectiveness and complementarity in tracking metal pollution from surrounding catchment stressors using the two media types. Wet and dry seasonal variation in in-stream metals between the two media were analysed. I determine at which spatial scale, either the sub-basin or the cumulative basin scale (demonstrating nesting), enabled the most robust prediction of trace metals (from each sample type) based on catchment stressors (pinpointing the source), while controlling for the confounding effects of catchment geology. Finally, I assess the agreement and, thus, consistency of the dissolved and sediment trace metal spatial detection patterns across the intensification gradient.

In **Chapter four** I examine fish tissue $\delta^{34}S$ as an ecotoxicological tracer along a land-use intensification river gradient to disentangle the effects of key aquatic stressors in the mixed-use Gwathle Catchment. The key water quality conditions at the time of tissue sampling were characterised and the stressor's proportionate coverage was assessed for each river's respective watershed. The dual ability of *in-situ* determined total dissolved solids as well as fish-tissue $\delta^{34}S$ as an approach to visually disentangle key stressors was assessed. Longitudinal trends in tissue $\delta^{34}S$ as well as the key catchment stressors were assessed at sub-basin and cumulative basin scales to elucidate primary land-use drivers of fish tissue $\delta^{34}S$ variation, while accounting for confounding atmospheric $SO_{2(g)}$ effects on tissue $\delta^{34}S$ from catchment mining and smelting activities.

Finally, in **Chapter five**, I provide the thesis's key findings and the potential of developing a tailored environmental forensic toolbox for pinpointing the polluter with the intention of improving catchment water stewardship across the country. I also highlight the research's limitations and the additional knowledge gaps identified that are suitable for future research

1.12. References

Albuquerque, P.T., Fredou, T., Barcellos, R.L., Melo, J.T., Arruda, G.N. and De França, E.J., 2022. Anthropogenic influences on sedimentary geochemistry of Itapessoca Estuarine Complex, Pernambuco, Brazil, *Environmental monitoring and assessment*, *194*(43), 1-18.

Almécija, C., Cobelo-García, A., Wepener, V. and Prego, R., 2017. Platinum group elements in stream sediments of mining zones: the Hex River (Bushveld Igneous Complex, South Africa), *Journal of African Earth Sciences*, *129*, 934-943.

Amundsen, P.A., Staldvik, F.J., Lukin, A.A., Kashulin, N.A., Popova, O.A. and Reshetnikov, Y.S., 1997. Heavy metal contamination in freshwater fish from the border region between Norway and Russia, *Science of the total environment*, *201*, 211-224.

Balaram, V., Copia, L., Kumar, U.S., Miller, J. and Chidambaram, S., 2023. Pollution of water resources and application of ICP-MS techniques for monitoring and management–A comprehensive review, *Geosystems and Geoenvironment*, 1-24.

Beck, M.B., Adeloye, A.J., Finney, B.A. and Lessard, P., 1991. Operational water quality management: transient events and seasonal variability, *Water Science and Technology*, *24*(6), 257-265.

Birk, S., 2019. 'Detecting and Quantifying the Impact of Multiple Stress on River Ecosystems' in S. Sabater., A. Elosegi., and R. Ludwig (eds.), *Multiple Stressors in River Ecosystems: Status, Impacts and Prospects for the Future*, pp. 235-253, Elsevier.

Caretta, M.A., A. Mukherji, M. Arfanuzzaman, R.A., Betts, A. Gelfan, Y., Hirabayashi, T.K. Lissner, J. Liu, E. Lopez Gunn, R. Morgan, S. Mwanga, and S. Supratid, 2022: 'Water' In (eds) Pörtner, H.O., Roberts, D.C., Tignor, M., Poloczanska, E.S., Mintenbeck, K., Alegría, A., Craig M., Langsdorf S., Löschke, S., Möller, V., Okem, A. and Rama, B, *Climate Change 2022: Impacts, Adaptation and Vulnerability. Contribution of Working Group II to the Sixth Assessment Report of the Intergovernmental Panel on Climate Change*, Cambridge University Press, Cambridge, UK and New York, NY, USA, 551–712.

Carey, R.O., Hochmuth, G.J., Martinez, C.J., Boyer, T.H., Dukes, M.D., Toor, G.S. and Cisar, J.L., 2013. Evaluating nutrient impacts in urban watersheds: Challenges and research opportunities. *Environmental Pollution*, *173*, 138-149.

Chetty, S., Pillay, L. and Humphries, M.S., 2021. Gold mining's toxic legacy: Pollutant transport and accumulation in the Klip River catchment, Johannesburg, *South African Journal of Science*, *117*(7/8), 1-11.

Colvin, C. and Muruven, D. 2017. *Scenarios for the Future of Water in South Africa*, World Wide Fund For Nature (WWF) and the Boston Consulting Group, viewed 23 July 2017, from http://www.wwf.org.za/what_we_do/marine2/?20461/Scenarios-for-the-future-of-water-in-South-Africa.

Corson, K.B. 2017. 'Coal ash derived sulfur and mercury in the Dan River invertebrate food web', Master of Science Thesis, Faculty of The Graduate School, University of North Carolina at Greensboro.

Croisetiere, L., Hare, L., Tessier, A. and Cabana, G., 2009. Sulphur stable isotopes can distinguish trophic dependence on sediments and plankton in boreal lakes, *Freshwater Biology*, *54*, 1006-1015.

Crutzen, P.J., Stoermer, E.F., 2021. The 'Anthropocene' (2000). In Benner, S., Lax, G., Crutzen, P.J., Pöschl, U., Lelieveld, J., Brauch, H.G. (eds.) Paul J. Crutzen and the *Anthropocene: A New Epoch in Earth's History.* The Anthropocene: Politik—Economics—Society—Science, vol 1, Springer, Germany.

Dalu, T., Wasserman, R.J., Tonkin, J.D., Mwedzi, T., Magoro, M.L. and Weyl, O.L., 2017. Water or sediment? Partitioning the role of water column and sediment chemistry as drivers of macroinvertebrate communities in an austral South African stream, *Science of the total environment*, *607*, 317-325.

Daniell, A. and van Tonder, D.M., 2023. Opportunity for increasing the soil quality of non-arable and depleted soils in South Africa: A review, *Journal of Soil Science and Plant Nutrition*, *23*, 2476-2487.

Day, J. and Davies, B., 2023. *Vanishing Waters – Third Revised Edition*, SP 160/23, Water Research Commission, Pretoria.

de Necker, L., Manfrin, A., Ikenaka, Y., Ishizuka, M., Brendonck, L., Van Vuren, J.H.J., Sures, B., Wepener, V. and Smit, N.J., 2020. Using stable δ13C and δ15N isotopes to assess foodweb structures in an African subtropical temporary pool, *African Zoology*, *55,* 79-92.

Dickens, C.W. and Graham, P.M., 2002. The South African Scoring System (SASS) version 5 rapid bioassessment method for rivers, *African Journal of Aquatic Science*, *27*, 1-10.

Ding, J., Jiang, Y., Liu, Q., Hou, Z., Liao, J., Fu, L. and Peng, Q., 2016. Influences of the land use pattern on water quality in low-order streams of the Dongjiang River basin, China: A multi-scale analysis, *Science of the total environment*, *551*, 205-216.

Donnenfeld, Z., Crookes, C. and Hedden, S. 2018. *A delicate balance: Water scarcity in South Africa*, Institute for Security Studies, Southern Africa Report, South Africa.

Driver, A., Nel, J.L., Snaddon, K., Murry, K., Roux, D.J, Hill, L., Swartz, E.R., Manuel, J. and Funke, N. 2011. Implementation Manual for the Freshwater Ecosystem Priority Areas, Water Research Commission, Report No. 1807/1/11, Pretoria.

Du Plessis, A., 2023. *South Africa's Water Predicament: Freshwater's Unceasing Decline* (Vol. 101), Springer Nature, Switzerland.

DWAF, 1996. South African Water Quality Guidelines volume 7 Aquatic Ecosystems: Second Edition, Pretoria, South Africa.

DWAF, 2008. Series 2A Guidelines for Water Management for Mine Residue Deposits, Best practice guidelines for water resource protection in the South African Mining Industry, Directorate: Resource Protection and Waste, Pretoria.

DWS, 2023. The National Water Resources Strategy Third Edition (NWRS-3) March 2023, Pretoria, South Africa.

Erasmus, J.H., Malherbe, W., Zimmermann, S., Lorenz, A.W., Nachev, M., Wepener, V., Sures, B. and Smit, N.J., 2020. Metal accumulation in riverine macroinvertebrates from a platinum mining region, *Science of the Total Environment*, *703*, 1-13.

Feld, C.K., Segurado, P. and Gutierrez-Canovas, C., 2016. Analysing the impact of multiple stressors in aquatic biomonitoring data: A ‘cookbook’with applications in R, *Science of the Total Environment*, *573*, 1320-1339.

Foord, S.H. and Fouché, P.S.O., 2016. Response of instream animal communities to a short-term extreme event and to longer-term cumulative impacts in a strategic water resource area, South Africa, *African Journal of Aquatic Science*, *4*, 29-40.

Förstner, U., 1979. ‘Metal Pollution Assessment from Sediment Analysis’, in Förstner, U, Wittmann, G.T.W (eds.) *Metal pollution in the aquatic environment*, pp. 110 – 196, Springer-Verlag, Berlin Heidelberg

Frost and Sullivan, 2010. Eutrophication Research Impact Assessment, Water Research Commission, Report No. TT 461/10, Pretoria.

Funk, C., Peterson, P., Landsfeld, M., Pedreros, D., Verdin, J., Shukla, S., Husak, G., Rowland, J., Harrison, L., Hoell, A. and Michaelsen, J., 2015. The climate hazards infrared precipitation with stations—a new environmental record for monitoring extremes. Scientific data, 2(1), 1-21.

Gqomfa, B., Maphanga, T. and Shale, K., 2022. The impact of informal settlement on water quality of Diep River in Dunoon, *Sustainable Water Resources Management*, *8*(27), 1-18.

Griffin, N.J., 2017. The rise and fall of dissolved phosphate in South African rivers, *South African Journal of Science*, *113*(11/12), 1-7.

Grizzetti, B., Lanzanova, D., Liquete, C., Reynaud, A. and Cardoso, A.C., 2016. Assessing water ecosystem services for water resource management, *Environmental Science & Policy*, *61*, 194-203.

Gurrieri, J.T., 1998. Distribution of metals in water and sediment and effects on aquatic biota in the upper Stillwater River basin, Montana, *Journal of Geochemical Exploration*, *64*, 83-100.

Hesslein, R.H., Capel, M.J., Fox, D.E. and Hallard, K.A., 1991. Stable isotopes of sulfur, carbon, and nitrogen as indicators of trophic level and fish migration in the lower Mackenzie River basin, Canada, *Canadian Journal of Fisheries and Aquatic Sciences*, *48*, 2258-2265.

Hill, J.M, Kaehler, S., Hill, M.P. and Coetzee, J., 2011. *A stable isotope approach for the early detection and identification of N loading in aquatic ecosystems*, Water Research Commission, Report No. KV 280/11, Pretoria.

Jackson, M., Woodford, D. and Weyl, O., 2016. Linking key environmental stressors with the delivery of provisioning ecosystem services in the freshwaters of southern Africa, *Geo: Geography and Environment*, 3(2), 1-12.

Jackson, M.C., Fourie, H.E., Dalu, T., Woodford, D.J., Wasserman, R.J., Zengeya, T.A., Ellender, B.R., Kimberg, P.K., Jordaan, M.S., Chimimba, C.T. and Weyl, O.L., 2020. Food web properties vary with climate and land use in South African streams, *Functional Ecology*, *34*, 1653-1665.

King, J. and Pienaar, H., 2011. *Sustainable use of South Africa's inland waters: a situation assessment of resource directed measures 12 years after the 1998 National Water Act*, Water Research Commission, Report No. TT 491/11, Pretoria.

King, R.S., Baker, M.E., Whigham, D.F., Weller, D.E., Jordan, T.E., Kazyak, P.F. and Hurd, M.K., 2005. Spatial considerations for linking watershed land cover to ecological indicators in streams, *Ecological applications*, *15*, 137-153.

Kleynhans, C.J., Louw, M.D., Thirion, C., Rossouw, N.J. and Rowntree, K., 2007. River EcoClassification–Manual for EcoStatus Determination, *Department of Water Affairs and Forestry, Pretoria, South Africa*.

Kleynhans, C.J., Thirion, C. and Moolman, J., 2005. *A Level I River Ecoregion classification System for South Africa, Lesotho and Swaziland*, Report No. N/0000/00/REQ0104, Resource Quality Services, Department of Water Affairs and Forestry, Pretoria, South Africa.

Kodikara, K.A.S., Lewandowski, S., De Silva, P.M.C.S., Gunarathna, S.D., Madarasinghe, S.K., Ranasinghe, P., Jayatissa, L.P. and Dahdouh-Guebas, F., 2022. Heavy metal pollution in selected upland tributaries of Sri Lanka: comprehension towards the localization of sources of pollution, *Journal of water and health*, *20*, 505-517.

Laha, F., Gashi, F., Frančišković-Bilinski, S., Bilinski, H. and Çadraku, H., 2022. Geospatial distribution of heavy metals in sediments of water sources in the Drini i Bardhë river basin (Kosovo) using XRF technique, *Sustainable Water Resources Management*, *8*(31), 1-16.

Levin, J.C., Woodford, D.J., Woodborn, S., Curtis, C.J. 2023. *Assessing water user impacts on eco-hydrology using stable isotopes*, Water Research Commission, Report No. 3079/1/23, Pretoria.

Li, M., Wiedmann, T. and Hadjikakou, M., 2019. Towards meaningful consumption-based planetary boundary indicators: The phosphorus exceedance footprint, *Global Environmental Change*, *54*, 227-238.

Madikizela, L.M., Chimuka, L. and Ncube, S., 2023. Metal pollution source apportionment in two important Rivers of Eastern Cape Province, South Africa: a case study of Bizana and Mthatha Rivers, *Environmental Forensics*, *24*(1-2), 71-84.

Matumba, J., 2019. 'Water security: Is South Africa optimally pursuing its options', in Mambretti, S. and Garcia, J.L.M.I. (eds.), *Water and Society 2019*, pp 47-54, WIT Press Southampton, Boston.

Mello, K.D., Valente, R.A., Randhir, T.O., dos Santos, A.C.A. and Vettorazzi, C.A., 2018. Effects of land use and land cover on water quality of low-order streams in Southeastern Brazil: Watershed versus riparian zone, *Catena*, *167*, 130-138.

Motitsoe, S.N., Hill, J.M., Coetzee, J.A. and Hill, M.P., 2022. Invasive alien aquatic plant species management drives aquatic ecosystem community recovery: An exploration using stable isotope analysis, *Biological Control*, *173*, 1-12.

Motitsoe, S.N., Hill, M.P., Avery, T.S. and Hill, J.M., 2020. A new approach to the biological monitoring of freshwater systems: Mapping nutrient loading in two South African rivers, a case study, *Water Research*, *171*, 1-12.

Mudge, S.M., 2008. 'Approaching Environmental Forensics', In Mudge, S.M. (ed.) *Methods in Environmental Forensics*, pp. 1-15, Taylor & Francis Group, Florida, USA.

Namugize, J.N., Jewitt, G. and Graham, M., 2018. Effects of land use and land cover changes on water quality in the uMngeni river catchment, South Africa, *Physics and Chemistry of the Earth, Parts a/b/c*, *105*, 247-264.

Nkosi, M., Mathivha, F.I. and Odiyo, J.O., 2021. Impact of land management on water resources, a South African context, *Sustainability*, *13,* 1-32.

Ouma, K.O., Shane, A. and Syampungani, S., 2022. Aquatic ecological risk of heavy-metal pollution associated with degraded mining landscapes of the Southern Africa River Basins: A review, *Minerals*, *12*, 1-41.

Paul, M.J. and Meyer, J.L., 2001. Streams in the urban landscape, *Annual review of Ecology and Systematics*, *32*, 333-365.

Petrisor, I.G. (ed.), 2014. *Environmental forensics fundamentals: A practical guide*, Taylor and Francis Group, Florida, USA.

Pollard, S. and Du Toit, D., 2011. *Towards the Sustainability of Freshwater Systems in South Africa: An Exploration of Factors that Enable or Constrain Meeting the Ecological Reserve Within the Context of Integrated Resources Management in the Catchments of the Lowveld,* Water Research Commission, Report No. TT 477/10, Pretoria.

Pool-Stanvliet, R., 2013. A history of the UNESCO Man and the Biosphere Programme in South Africa, *South African Journal of Science*, *1*09(9-10), 1-6.

Richardson, K., Steffen, W., Lucht, W., Bendtsen, J., Cornell, S.E., Donges, J.F., Drüke, M., Fetzer, I., Bala, G., von Bloh, W. and Feulner, G., 2023. Earth beyond six of nine planetary boundaries, *Science advances*, *9*, 1-16.

Sappa, G., Ergul, S. and Ferranti, F., 2013. Geochemical evolution of groundwater in carbonate aquifers of southern Latium region, central Italy, *Acque Sotterranee-Italian Journal of Groundwater*, *2*(1), 9-15.

Schreiner, B., 2013. Viewpoint—Why has the South African National Water Act been so difficult to implement, *Water Alternatives*, *6*, 239-245.

Selwe, K.P., Thorn, J.P., Desrousseaux, A.O., Dessent, C.E. and Sallach, J.B., 2022. Emerging contaminant exposure to aquatic systems in the Southern African Development Community, *Environmental Toxicology and Chemistry*, *41*(2), 382-395.

Shen, Z., Hou, X., Li, W., Aini, G., Chen, L. and Gong, Y., 2015. Impact of landscape pattern at multiple spatial scales on water quality: A case study in a typical urbanised watershed in China, *Ecological Indicators*, *48*, 417-427.

South African Weather Service (SAWS). Climate data 2007 to 2022 of A21K, from http://www.weathersa.co.za/climate.

van Wyk, E., Breen, C.M., Roux, D.J., Rogers, K.H., Sherwill, T. and van Wilgen, B.W., 2006. The ecological reserve: towards a common understanding for river management in South Africa, *Water SA*, *32*(3), 403-409.

Von der Meden, C.E.O., Palmer, C.g., Daves-Coleman, H.D., and Gola, N.P., 2005. Environmental water quality in Makana municipality, Eastern Cape, South Africa: A case study of local government responsibility for water resource management (unpublished).

Vörösmarty, C.J., McIntyre, P.B., Gessner, M.O., Dudgeon, D., Prusevich, A., Green, P., Glidden, S., Bunn, S.E., Sullivan, C.A., Liermann, C.R. and Davies, P.M., 2010. Global threats to human water security and river biodiversity, *Nature*, *467*, 555-561.

Wayland, M. and Hobson, K.A., 2001. Stable carbon, nitrogen, and sulfur isotope ratios in riparian food webs on rivers receiving sewage and pulp-mill effluents, *Canadian journal of zoology*, *79*, 5-15.

Wepener, V., Dlamini, P., O'Brien, G.C. and Malherbe, W., 2015. *Development of a relative risk assessment framework to assess multiple stressors in the Klip River System*, Water Research Commission, Report No. 2204/1/15, Pretoria.

Xu, H., Tan, X., Liang, J., Cui, Y. and Gao, Q., 2022. Impact of agricultural non-point source pollution on river water quality: evidence from China, *Frontiers in Ecology and Evolution*, *10*, 1-11.

Zhang, J., Li, S., Dong, R., Jiang, C. and Ni, M., 2019. Influences of land use metrics at multi-spatial scales on seasonal water quality: a case study of river systems in the Three Gorges Reservoir Area, China, *Journal of Cleaner Production*, *206*, 76-85.

Chapter 2 – A multi-spatial scale assessment of land-use stress on water quality in headwater streams in the Platinum Belt, South Africa

2.1. Abstract

River water quality is affected by various stressors (land-uses) operating at different hydrological spatial scales. Few studies have employed a multi-scaled analyses to differentiate effects of natural grasslands and woodlands, agriculture, impoundments, urban and mining stressors on headwater streams. Using a multi-scaled modelling approach, this study disentangled the distinct spatial signatures and mechanistic effects of specific stressors and topographic drivers on individual water quality parameters in tributaries of the Gwathle River Catchment in the Platinum Belt of South Africa. Water samples were collected on six occasions from 15 sites on three rivers over 12-months. Physio-chemical parameters as well as major anions, cations and metals were measured. Five key water quality parameters were identified using principal components analysis: sulfate, ammonium, copper, turbidity, and pH to characterise catchment water quality conditions. Using class-level composition (PLAND) and connectedness (COHESION) metrics together with topographic data, generalised linear mixed models were developed at multiple scales (sub-basin, cumulative catchment, riparian buffers) to identify the most parsimonious model with the dominant drivers of each water quality parameter. Ammonium concentrations were best explained by urban stress, Cu increased with mining and agriculture, turbidity increased with elevation heterogeneity, agriculture, urbanisation and fallow lands all at the sub-basin scale. River pH was positively predicted for by slope heterogeneity, mining cover and impoundment connectivity at the catchment scale. Sulfate increased with mining and agriculture composition in the cumulative 100 m riparian buffer. Hierarchical cluster analysis of water quality and scale-dependent parsimonious drivers separated the river sites into three distinct groups distinguishing pristine, moderately impacted, and heavily mined sites. By demonstrating stressor- and scale-dependent water quality responses, this multi-scale nested modelling approach reveals the importance of developing adaptive, targeted management plans at hydrologically meaningful scales to sustain water quality amid intensifying land use.

2.2. Introduction

Headwater streams are crucial for supplying appropriate water quality to support aquatic and adjacent terrestrial ecological functionality, while also ensuring socio-economic development. They provide refugia and dispersal corridors for aquatic biodiversity, ensure hydrological connectivity for the storage, processing and energy transfer downstream; all thereby supporting lowland aquatic ecosystem integrity (Wallace and Eggert, 2015). These streams are inherently coupled to the terrestrial biosphere, being reliant on allochthonous energy subsidies from run-off and the surrounding riparian zone (Vannote et al., 1980). Their high stream edge to surface area ratio, however, makes them susceptible to surrounding land-use activities, particularly those that generate mobile pollutants (Richardson and Danehy, 2007). Due to their comparatively smaller size relative to lowland systems, headwater streams are also often unprotected, with few resources allocated to their conservation in developing countries (Richardson and Danehy, 2006; Wallace and Eggert, 2015).

Surface water quality is influenced by natural processes and anthropogenic land-use activities (stressors). In undisturbed catchments, rivers contain seasonally-influenced dissolved substances, such as phosphorus, that support essential biogeochemical cycles and rarely constitute water quality concerns (Boyd, 2019). Globally, anthropogenic stressors modify surface water quality via point and/or diffuse pollution sources. As a result, the relationship between land-use and surface water quality has been investigated extensively (Johnson et al., 1997). Commercial agriculture and livestock farming are leading contributors to sediment loading as well as nitrogenous nutrient input in rivers worldwide through diffuse and point-source pollution inputs (Saleh et al., 2000). Urban settlements also contribute diffuse pollution, through storm water infrastructure and septic tank systems. Poorly maintained domestic bulk wastewater distribution networks and treatment facilities can become point sources of metals and nutrients entering aquatic systems (Paul and Meyer, 2001; Carey et al., 2013). Additional point source and diffuse pollutants are derived from industry and mining, originating from waste storage facilities as well as effluent discharges increasing concentrations of a wide range of pollutants (Erasmus et al., 2020).

To improve catchment water quality management of headwater streams, it is essential to assess the spatial pattern-process relationship between stressors and adjacent water quality (Shehab et al., 2021). Much of the research linking stressors to surface water quality has been conducted on lowland rivers in developed nations (Zhou et al., 2012; Xu et al., 2020; Liu et al., 2021), with fewer on headwater streams in developing nations (Ding et al., 2018). In assessing the effects of stressors on river water quality, the class-level composition metric, being the percentage cover of each land cover class (PLAND), is often integrated with additional class-level metrics, including those assessing connectivity (Ding et al., 2016; Giri and Qui, 2016; Li et al., 2022). Using such, studies have determined that the predictive relationship between stressors at different spatial scales and aquatic water quality is often catchment and study specific (Allan, 2004).

Past investigations using a range of physico-chemical water quality determinants have identified the catchment scale to best explain water quality variability (Zhou et al., 2012), while other research indicated finer scales (e.g. sub-basin and riparian buffer) (Tran et al., 2010; Ding et al., 2016). For example, nutrient loading and retention has been found to occur at catchment scale (King et al., 2005; Ding et al., 2016; Xu et al., 2020), while across narrower extents rivers can exhibit natural filtering capacities and remove nutrients (Shen et al., 2015; Zhang et al., 2019). Few spatially-aligned studies have, however, examined multi-stressor interactions with mining activities on water quality in headwater streams, particularly within South African catchments. For example, chrome and platinum mining, which provide critical foreign currency revenue for the South African economy (Oranje et al., 2021), are major sources of mobile pollution that can interact with other stressors to influence aquatic water quality. Assessing metal mining contaminants in combination with other determinants like nutrients and sediment, can thus provide an important perspective on integrated stressor exposures in streams draining these heavily industrialized regions of the country.

While past studies sought optimal single scales for water quality management (Zhang et al., 2020), certain water quality parameters may respond to heterogeneous drivers operating at different spatial extents, necessitating multi-scaled modelling and management approaches tailored to the processes governing individual parameters (de Mello et al., 2019; Wang et al., 2023). A multi-scale multi-parameter approach can capture the true complexity of multi-scale processes influencing river water quality. Importantly, this provides the ability to elucidate the distinct spatial signatures and mechanistic controls of specific stressors as well as catchment processes on individual water quality parameters. Such an approach can allow the development of more adaptive, targeted and scale-dependent management plans for specific problematic water quality parameters while providing a more nuanced understand of the interplay with and various controls on river water quality.

The Gwathle River Catchment in the North West Province of South Africa, situated within the western lobe of South Africa's intensively mined Platinum Belt (Oranje et al., 2021), offers the ideal case study to assess the relationship between stressors and river water quality responses using different class-level metrics and potentially confounding topographic factors at the sub-basin, cumulative basin, as well as differing riparian scales. This catchment represents a natural experiment with longitudinally stepped mixed land-use activities drained by three low-order rivers, including fallow-land, agriculture, urban and mining activities. All water-usage activities associated with these stressors produce specific and often predictable step-changes on surface water quality through point and/or diffuse source inputs. This allows for individual stressors to be identified and untangled from one another within mixed-use catchments such as this.

This study sought to disentangle and identify dominant drivers influencing specific water quality responses across a land-use intensification gradient using a multi-scaled approach across sub-basin, cumulative, and riparian scales. Sub-basin scales are of particular interest to water resource management in South Africa, where multiple approaches to defining sub-quaternary catchment units have previously been employed for more effective hydrological modelling and water resource conservation (Driver et al., 2011; Nel et al., 2011; Maherry et al., 2013). The research objectives are to 1) determine the key water quality parameters that best characterise the surface water quality conditions of the Gwathle Catchment, 2) assess at which spatial scale water quality responses are best predicted at, as a function of class-level metrics and topographic factors, and 3) assess the spatial similarities between river sites using spatially-explicit predictors and water quality variables.

2.3. Materials and methods

2.3.1. Study area

The Gwathle River Catchment (Quaternary Catchment A21K), part of the larger Limpopo Water Management Area, drains the northern slopes of the Magaliesberg Mountain range between the towns of Rustenburg and Mooinooi, before its confluence with the Crocodile (West) River at Roodekoppies Dam in the North West Province, South Africa. The catchment has minimum and maximum elevations of 986 m and 1843 m respectively. The semiarid catchment receives on average 629 mm of rainfall per year with the typical wet season being between November-March (wettest January) and the dry season between April-October (Funk et al., 2015). The average monthly air temperatures range between 4.94°C and 31.76°C, with June and February being the coolest and warmest months respectively (SAWS, 2023). The western part of the catchment is drained by the third-order Sterkstroom (sites STK1-7), and the eastern part by the third order Maretlwane (sites MRT1-7), before the two form a confluence with the fourth order Gwathle River (site GWT1) (**Figure 2-1**).

The rivers fall within two aquatic ecoregions (level 1), the Western Bankenveld and Bushveld Basin. Level 1 ecoregions in South Africa are broad-scale spatial units delineated based on similarities in geology, geomorphology, climate, and ecology, to simplify and contextualize assessments of river ecosystem characteristics and water resource management (Kleynhans et al., 2005). The upland reaches of the catchment are partially contained within the Magaliesberg Biosphere Reserve; an area designated for ecotourism and sustainable development under the UNESCO Man and Biosphere Programme (Pool-Stanvliet, 2013). The catchment lies on the western lobe of the Bushveld Igneous Complex, important for the platinum group elements (PGE) mining industry (Thormann et al., 2017) (**Figure 2-1** and **Figure 2-2**). The catchment is exposed to a stepped progression of stressors from the pristine headwater reaches, followed by commercial irrigated agriculture and livestock rearing (fallow-land), urban and informal settlements, chrome and platinum mining as well as mine supportive industry activities (e.g. smelters). The predominant land cover classes are natural grasslands (67.6%), followed by agricultural lands (22.0%), mining activities (4.4%) and informal-formal urban cover (4.4%).

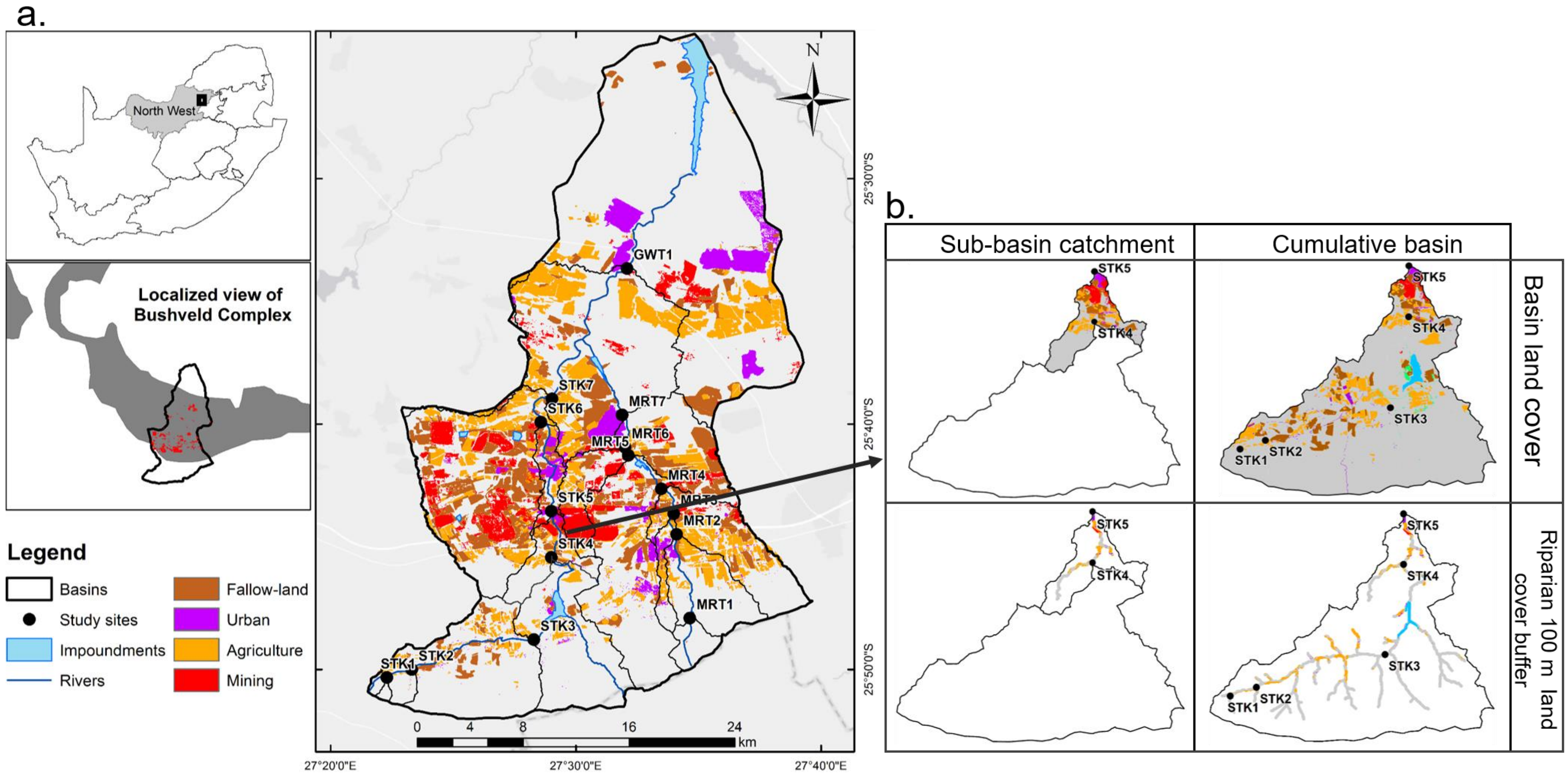

Figure 2-1: The distribution of (a.) study sites across the Sterkstroom (STK), Maretlwane (MRT) and Gwathle (GWT) rivers draining an intensification gradient including natural (greyed area within), urban, agriculture and mining stressors in the Gwathle study catchment which lays across the Bushveld Complex. A diagram representing the four assessed spatial scales (b.) of sub-basin catchment, cumulative catchment as well as the riparian sub-basin 100 m buffer and riparian cumulative 100 m buffer spatial scales.

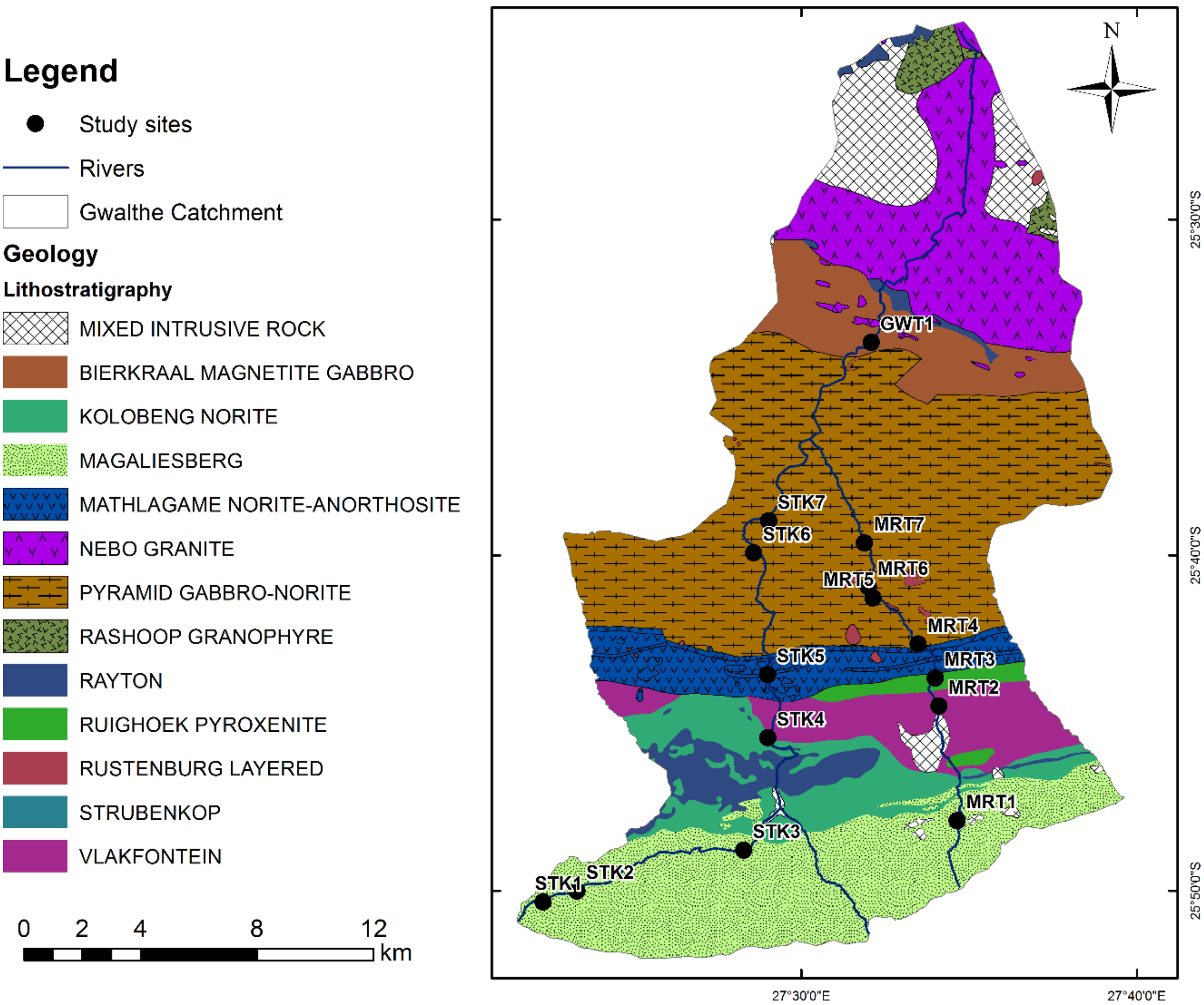

Figure 2-2: Map of the Gwathle study catchment geology (lithostratigraphy) with respect to the position of the Sterkstroom (STK), Maretlwane (MRT) and Gwathle (GWT) river study sites (Council for Geoscience, 2017). The main formations include Magaliesberg (Part of the Transvaal sequence) quartzites and shales, as well as Pyramid Gabbo-Norite (part of the Rusternburg Layered Suite) composed of pyroxenite, gabbro and norite cumulative rock layers (Mitchell, 1990).

2.3.2. Physico-chemical field sampling

Physico-chemical water quality data were collected during six separate sampling events, capturing individual points in time of wet, intermediate, and dry seasons, between May 2021 and March 2022. A total of 15 river sites were strategically selected, with seven on the Sterkstroom, seven on the Maretlwane and one on the Gwathle river below the confluence of the two main tributaries. Sites were placed immediately up- and down-stream of different land-use activities to capture these unique stressors. At each sampling event, electrical conductivity (µS/cm), total dissolved solids (mg/L), pH (units), dissolved oxygen (mg/L), temperature (°C) were recorded every 30 seconds for five minutes *in-situ*, using a YSI-Professional Plus Handheld Multi-parameter meter. All probes were calibrated prior to field sampling as outlined by the manufactures specifications. River water clarity (turbidity) was measured in triplicate at each site using a portable Hanna turbidity meter (HI98703-02).

For the chemical analyses, 400 mL water samples were collected from the top 30 cm of active river channel and filtered through Supor® 0.45µm 47 mm filters using a Thermo Scientific Nalgene reusable filter unit. Filtrate was stored in two separate one-litre acid rinsed polyethylene bottles and kept in a cold storage until transported to the laboratories for further analyses (Akyildiz and Duran, 2021). Once at the laboratory, the sample was analysed for Cl^-, SO_4-S (sulfate), NO_3^--N (nitrate), NO_2^--N (nitrite), PO_4^{3-}-P (ortho-phosphate), NH_3-N (ammonia) and NH_4^+-N (ammonium) using a Aquakem/Discrete Analyser (photometric analyser).

Major cations and trace metals were analysed using an Agilent 7800x inductively coupled plasma mass spectrometry (ICP-MS) with concentrations measured against external matrix-matched standards. Total dissolved solids were determined using a Thermo Scientific ORION STAR A322. Samples with dissolved solids exceeding 120 mg/L were then diluted with milipore water. Each sample had 0.1 m/L of ultrapure acid (HNO_3) added to 10 mL of filtrate. The limitations posed by limit of detection (LOD) to further statistical analyses were overcome by using a substitution method, whereby the LOD was replaced by an estimate of its division by two; following the assumption where data are uniformly distributed (Croghan et al., 2003).

2.3.3. Key land-cover class (stressor) determination

The landscape stressor data (land-cover) was obtained using the South African National Land Cover (SANLC) 2020 dataset released in June 2021 (GeoTerraImage, 2021). The dataset was generated using ~20 m multi-seasonal Sentinel-2 satellite imagery and has a Kappa Index above 85 and an overall map accuracy greater than 85%. The Land-cover data were then interpreted using ArcGIS 10.5. The level 1 national database contains 73 land-cover classes, of which 53 classes occur within the bounds of the study catchment. The level 1 classes were reduced and reclassified into six key natural and stressor categories including (1) natural – woodland, shrubland and grassland, (2) cultivated land – all commercial annual crops, (3) fallow-land –

altered range land for cattle grazing, (4) urban – residential formal and informal, commercial and smallholdings, (5) mining – extraction pits and tailing storage facilities and finally (6) dams – in-channel weirs and storage dams.

2.3.4. Study area and spatial-scale delineation

The river catchment, together with the investigated rivers, were delineated from the 30 m Shuttle Radar Topography Mission (STRM) digital elevation model (DEM) using the ArcSWAT (Soil & Water Assessment Tool) extension module in the ArcGIS software package (ESRI) (Farr and Kobrick, 2000). Prior to their delineation the DEM sinks were filled using the Spatial Analysis toolbox in ArcGIS. The spatially explicit nature of this study, was so that the stressor effects in the Gwathle Catchment on the aquatic ecosystems, could be assessed at a (1) cumulative catchment scale (i.e. draining entirely of one point upstream), (2) sub-basin and at (3) cumulative riparian and (4) sub-basin riparian scales (**Table 2-1**).

For the sub-basin scale, the extent was defined from the location study site (outlet location) and its upstream drainage area until the prior site (immediately upstream). The cumulative catchment extents of each study site were defined from the outlet location of each study site, and includes the catchments/riparian zones of sites located upstream, thus creating a nested design (Xu et al., 2021). Each of the sub- and cumulative catchments were delineated using the Spatial Analyst tools in ArcGIS 10.5. The riparian buffers at the cumulative- and sub-basin scales were computed at 100 m using the Analyst Toolbox in ArcGIS 10.5. The 100 m buffer was selected based on the well-researched recommendation of at least a 50 m developmental buffer for South African 1:500 000 mountain streams for most land-cover practices and features, which has been demonstrated to effectively mitigate sedimentation and reduce macronutrients in high-risk scenarios (Berliner and Desmet, 2007; Macfarlane and Bredin, 2017). The extended buffer, of 100 m, allows for the capture of stressors adjacent to the riparian zone. The reclassified landscape stressor layers were clipped to each of the new spatial layers (i.e. scales) using the ArcGIS Data Management Tool.

Table 2-1: The four spatial scales of water quality assessment and their descriptions.

Spatial scale		Description
1	Cumulative scale	The total upstream catchment area draining to a single downstream study site
2	Sub-basin scale	The area draining between the downstream and immediate upstream site
3	Riparian cumulative 100 m buffer	A 100 m riparian buffer draining the total upstream area to a single downstream study site
4	Riparian sub-basin 100 m buffer	A 100 m riparian buffer draining the area between the downstream and immediate upstream study sites

2.3.5. Environmental driver determination

A combination of potential driver variables were used in the analysis to determine the most parsimonious drivers of catchment aquatic water quality (**Table 2-2**). For the topographic features, the mean and standard deviation for elevation and slope for each of the sites respective four spatial scales were calculated in ArcGIS 10.5 using the conversion from raster to point tool and the Spatial Analyst Toolbox respectively. These variables exert strong controls on hydrologic flows and connectivity between upland areas and downstream water bodies, mediating impacts on aquatic ecosystems (Allan, 2004; Thompson et al., 2011; Ding et al., 2016). Using the SANLC dataset two class-level metrics, measuring composition and connectivity; PLAND (i.e., % landcover) and COHESION (i.e., connectedness to patches with the same landcover class) respectively were analysed in the computer software, FRAGSTATS 4.2, for each of the six stressors in their four respective spatial scales (**Table 2-2**; McGarigal et al., 2002; Shi et al., 2017). Two class-level metrics were selected for as they provide spatial characteristics of each land cover class crucial for relating landscape structure to aquatic integrity while avoiding excessive redundancy (Uuemma et al., 2006).

Table 2-2: A summarized view of the specific stressor classes assessed, as well as the class-level metrics and topographic factors determined, with a description for each.

Variables		**Description**
Stressor classes	Agriculture	Agricultural land, containing irrigated and rain-fed cropland
	Fallow-land	Fallow-land used for cattle grazing and in crop rotation
	Urban	Settlement and commercial activities, both for the formal and informal
	Dams	On-stream impoundments, including dams and shallow weirs used for various purposes e.g. agriculture and mining
	Mining	Mine inclusive features, including tailing storage facilities (wet and dry), mining pits/strips and related industries (e.g. smelters)
	Natural	Natural land-cover inclusive of forests, rocky outcrops, grassland and shrubs
Class-level metrics	Percentage of landscape (PLAND - composition)	Percentage of the landscape belonging to a particular class
	Patch cohesion index (COHESION - connectedness)	Characterises the connectedness of the patches belonging to a particular class
Topographic factors	Mean slope	The average slope of the assessed spatial scale measured in degrees
	Slope standard deviation	The standard deviation of the slope at the assessed spatial scale
	Mean elevation	The average elevation of the assessed spatial scale measured in meters
	Elevation standard deviation	The standard deviation of the elevation at the assessed spatial scale

2.3.6. Statistical analysis

Principal Component Analysis (PCA) was employed as a dimensional reduction technique, as well as to visualise spatially explicit patterns among the data. The analysis reduced the high number of correlated water quality parameters to a few variables that best explain the catchment's overall river water quality variability in R (R Core Team, 2023). Prior to the analysis, data assumptions were tested using the Kaiser-Meyer-Olkin (KMO) and the Bartlett tests (Zhang et al., 2016). To avoid misinterpretations accompanied by variables of different units, the variables were standardized through z-scale transformation and centered. The Kaiser's rule was adhered to, in identifying the principal components for further use (Kaiser, 1960). One key uncorrelated, but significant contributing water quality parameter of the highest loading from each of the retained principal components was identified using the dimdesc function in the FactoMineR package, for use in further analysis (Lê et al., 2008).

Following the retention of the final water quality parameters as response variables, multi-spatial-scale generalised linear mixed effects models (GLMMs) were utilized to elucidate the dominant explanatory driver(s) of water quality within the catchment. Given the hierarchical data structure with river sites nested within repeated measurements over time, the utilization of GLMMs enabled the incorporation of temporal and spatial effects, thus facilitating a robust analysis tailored to the complexities of the dataset. The predictor datasets, consisting of the FRAGSTATS class-level metrics for each of the six stressor classes and topographic factors, at the four spatial scales, were independently assessed for multicollinearity prior to model fitting. Variables where $r > 0.7$ were removed using the findCorrelation function in the caret package, before scale-specific model fitting, thus reducing model interpretability and overfitting issues (Kuhn et al., 2020). The glmer function from the lme4 package was used to fit the full GLMMs for each response variable at the different scales, and the scales respective predictors as main effects with sample season and site as random effects (Bates et al., 2014). A Gamma distribution with a log link, was fit to each model due to the continuous, skewed nature of the water quality response variables.

With the GLMMs created for each of the key water quality variables (responses) variables across the four spatial scales, a total of 20 models were fitted (Zuur et al., 2009). The most parsimonious GLMM for each response variable at each of the four scales was obtained through the stepwise dredge function in the MuMIN package (Barton, 2010). The stepwise analysis, based on Akaike's Information Criterion corrected for small sample size (AICc), allowed for the simplest yet most informative model to be identified that included predictors best explaining the responses variability. The final model selection, to determine at which spatial scale each response variable is best predicted, was determined by selecting the most parsimonious model among the four spatial scales with the lowest AICc. The goodness of fit for the final models was determined using the marginal R^2 ($R^2_{GLMM(m)}$; the variance explained for by the fixed factors) and the conditional R^2 ($R^2_{GLMM(c)}$; the variance explained by both fixed and random factors) coefficients using the `r.squaredGLMM` function in the MuMIN package (Barton, 2010; Wanderi et al., 2022).

To isolate and visually assess the relationship between each water quality response variable and their most important predictor identified in the respective GLMM, reduced parsimonious models were created excluding the important variable while retaining the other predictors to account for their influence (Mashal et al., 2002). The log-transformed residuals of the reduced models were plotted against the respective important predictor with a trend line fit using ggplot2 (Wickham, 2016). Agglomerative hierarchical cluster analysis (HCA) was performed to assess environmental similarities among the river study sites. The analysis considered the five water quality response variables as well as the continuous class-level and topographic explanatory factors selected from the final fitted GLMM models. The analysis utilized the Euclidean distance metric and the suitable Wards clustering algorithm for the data determined using `agnes` and `map_dbl` functions from the cluster and purrr packages respectively (Maechler et al., 2022; Wickham, 2023). The optimal number of clusters (i.e. groups) for the cluster analysis was determined using the total within sum of squares (WSS) in the Factoextra R package (Kassambara and Mundt, 2020). The resulting groups paired with respective sites, along with the response variables, the class-level metrics and topographic factors were represented for visual purposes on a final summary PCA biplot to visually discern drivers of the groupings.

2.4. Results

2.4.1. Class-level land use and topographic patterns between scales

The composition (percentage) of the agriculture, fallow-land, urban and mining predictors, tended to show higher proportions in the smaller headwater sub-basins and sub-basin riparian buffers than in the cumulative catchment and cumulative riparian buffers. The percentage of dam and natural land coverage conversely increased as the cumulative catchment and riparian scales increased area coverage. On average, the cohesion of agriculture and dams was higher with the cumulative catchment and cumulative riparian scales draining larger regions while decreasing with smaller scales draining less area. Both topographic factors including elevation and slope on average were higher in the cumulative catchment and riparian scales, decreasing as scale become smaller. Elevation and slope, however, on average remained higher in the mountainous sites' respective spatial scales.

2.4.2. Key response variable determination

The PCA analysis highlighted the high multi-collinearity between the water quality parameters measured across the Gwathle Catchment (**Figure 2-3**). From the ordination the first principal component (PC1) accounted for most the datasets variation with 57.2% followed by PC2 with 17.4%. The first PC is the axes in which the sites are mostly separated according to land-use effects on water quality. Specifically sites in the positive pole of PC1 were characterised by higher sulfates, electrical conductivity and major cations (e.g. Na^{+}, Mg^{+}), and are those positioned further down the mountainous catchment experiencing increased agricultural, cattle rearing and mining activities. Conversely those sites further up the catchment, experiencing small scale farming and a limited residential footprint, are negatively associated with these indicators. Having retained five principal components, accounting for 93% of the datasets cumulative variance, following the Kaiser's rule, a reduced set of five water quality parameters, one from each PC (highest loading), were determined to be key variables that best characterise the overall water quality variation of the Gwathle river catchment during the study period. These included sulfate (mg/L), ammonium (mg/N-L), copper (ppb), turbidity (NTU) and pH (units). These five variables would become the responses used in further model fitting and thereby achieving the first objective. The loadings for the PCA are presented in **Figure S2-1**.

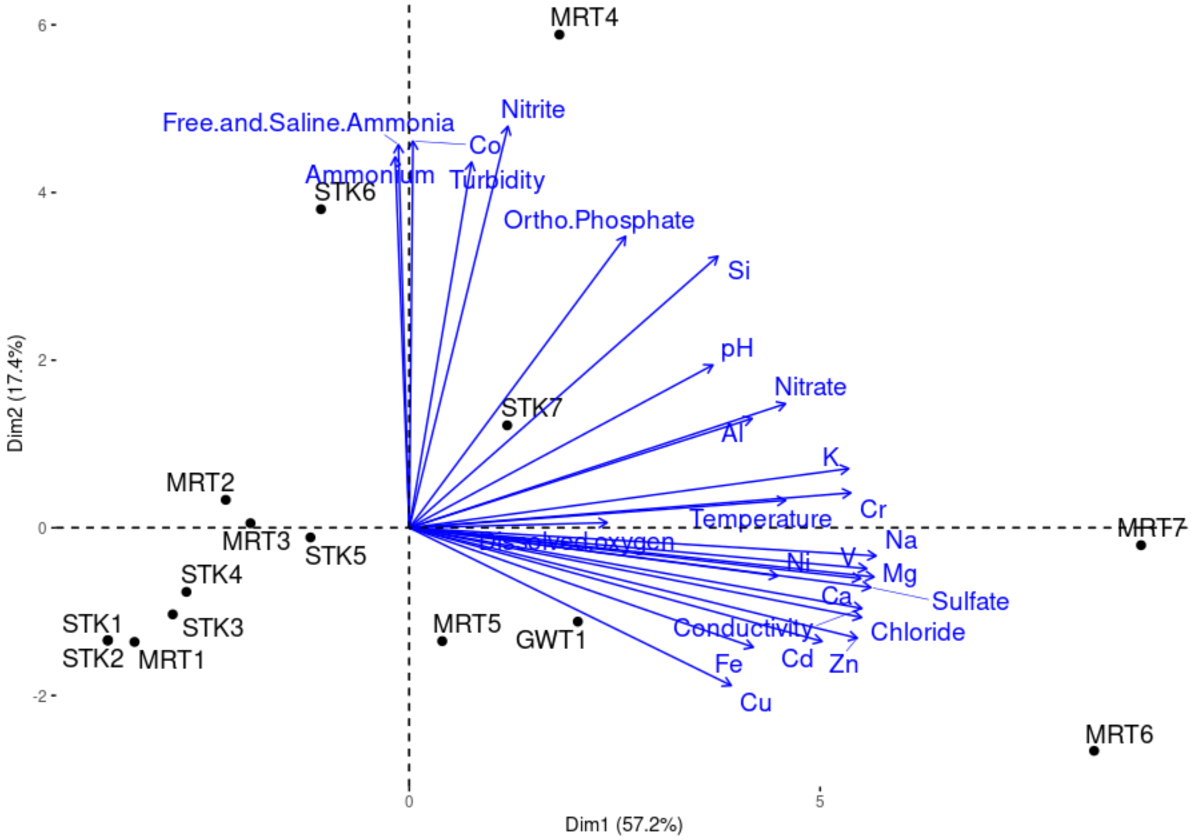

Figure 2-3: A principal component analysis bi-plot showing the separation of individual study sites through their association with mean annual water quality parameters.

2.4.3. Optimal spatial scale for the catchment water quality prediction

Following the stepwise model selection to derive the most parsimonious models, it was determined that three of the four assessed spatial scales were important in predicting key water quality response variables. The final fitted models with the predictor variables are presented in

Table 2-3, with the relationship between the water quality response variable and the models' most important predictor variables at their respective spatial scale presented in **Table 2-4**. At the sub-basin scale, ammonium, copper and turbidity were most accurately predicted. While at the cumulative catchment scale, river pH, and at the cumulative 100 m riparian buffer scale, sulfate concentrations, were most accurately predicted respectively. In the models with multiple determinants, mining land cover was the most important variable predicting elevated copper, pH and sulfate levels across the basin, while turbidity was strongly associated with the proportion of agricultural land cover at the sub-basin scale (**Table 2-4**). The visual relationships between each key water quality parameter and their corresponding most important (scale aligned) predictor from the model outputs are presented in **Figure 2-4**.

Table 2-3: The five most parsimonious generalised mixed effects models for each of the five water quality response variables the spatial-scale they best predicted at as well as each models respective explanatory/predictive variable(s).

Spatial Scale	**Sub-basins**			**Cumulative basin**	**Cumulative 100 m riparian buffer**
Response	**Ammonium**	**Copper**	**Turbidity**	**pH**	**Sulfate**
Model predictors	• PLAND Urban	• COHESION agriculture • COHESION dams • PLAND fallow-land • PLAND mining	• Elevation (SD) • PLAND agriculture • PLAND urban • PLAND fallow-land	• COHESION dams • Slope (SD) • PLAND mining	• PLAND agriculture • PLAND mining
Model intercept	-2.18(±0.29)-7.41***	2.61(±0.36)7.79***	-1.49(±0.47)-3.19**	1.40(±0.11)12.64***	1.28(±0.39)3.28**
	Model Selection	**Model Selection**	**Model Selection**	**Model Selection**	**Model Selection**
weight	0.05	0.05	0.18	0.19	0.03
AICc	-126.07	758.21	655.92	166.31	786.81
BIC	-114.35	779.0	674.0	182.3	804.4
	Goodness of fit	**Goodness of fit**	**Goodness of fit**	**Goodness of fit**	**Goodness of fit**
$R^2_{GLMM(m)}$	0.11	0.21	0.72	0.60	0.66
$R^2_{GLMM(c)}$	0.51	0.36	0.78	0.70	0.80
	Random effects	**Random effects**	**Random effects**	**Random effects**	**Random effects**
Site (SD)	0.66	0.01	0.39	0.04	0.60
Season (SD)	0.45	0.51	0.15	0.02	0.36
Residuals (SD)	0.89	1.04	0.83	0.08	0.85

Table 2-4: The model average parameter estimates for each variable in the fitted models, as well as the variables importance representing the proportional effect of each variable in explaining the response variable. The greyed cells indicate the row the with predictor variable that has the greatest importance in each of the fitted models. Variables with asterisk (*) are significant at the 95% level.

Parsimonious models spatial scale	Response	variable	Variable estimate	Lower 95% CI	Upper 95% CI	Variable importance
Sub-basin scale	Ammonium	PLAND urban*	0.05	0.01	0.10	1.00
	Copper	COHESION agriculture*	0.01	0.00	0.02	0.25
		COHESION dams	-0.01	-0.02	0.00	0.25
		PLAND fallow-land*	-0.06	-0.11	-0.02	0.23
		PLAND mining *	0.07	0.03	0.11	0.27
	Turbidity	Elevation (SD)*	0.02	0.01	0.02	0.23
		PLAND agriculture*	0.14	0.10	0.17	0.27
		PLAND urban*	0.04	0.00	0.07	0.24
		PLAND fallow-land*	0.08	0.04	0.12	0.25
Cumulative scale	pH	COHESION dams*	0.01	0.00	0.00	0.32
		Slope (SD)*	0.09	0.05	0.13	0.35
		PLAND mining*	0.01	0.00	0.02	0.32
Cumulative 100 m riparian scale	Sulfate	PLAND agriculture*	0.09	0.03	0.15	0.41
		PLAND mining*	0.45	0.33	0.57	0.59

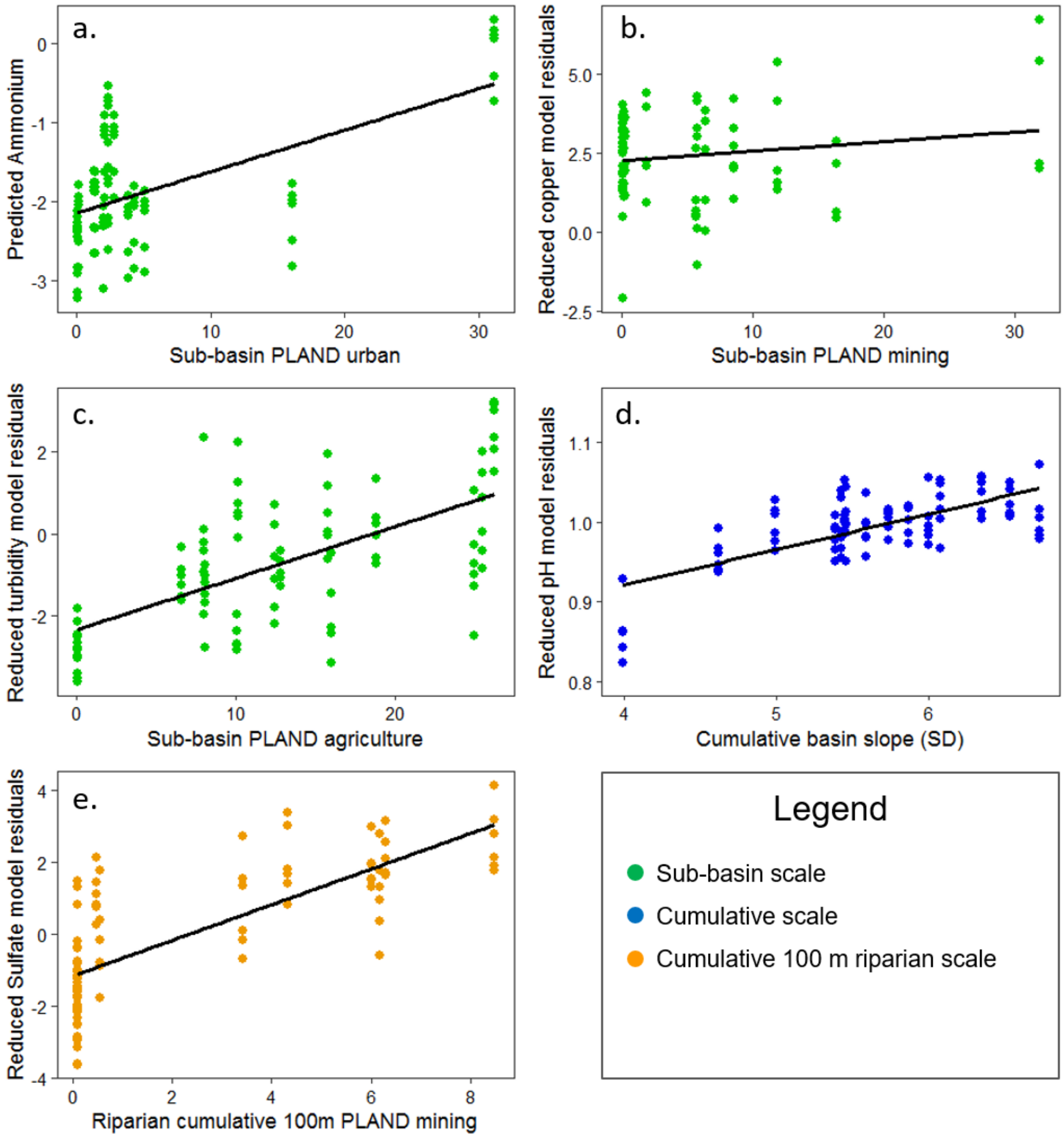

Figure 2-4: Figures b – e presents the visual relationships between each key water quality response variable and the most important predictor of each as identified in each respective generalised linear mixed effects model. Each figure represents the log-transformed residuals of the reduced parsimonious models plotted against the important predictor of each respective model. For figure a, no less important predictors were included in the parsimonious model, thus the predicted values from the full model were plotted against the expected values to provide a visual assessment of the relationship between response and predictor.

2.4.4. Water quality responses to land-use metrics

For ammonium, the percentage of urban areas in the sub-basin exhibited a statistically significant positive relationship, where a 1% increase predicted ~5.50% rise in ammonium concentrations. Copper concentrations were predicted to increase by

~6.35% and 1.36% for every 1-unit rise in mining PLAND of mining and COHESION of agriculture respectively, which both displayed significant positive associations with copper. In contrast, PLAND of fallow-land displayed a significantly negative relationship, with a 1% increase predicting a ~4.20% decrease in copper concentrations in the sub-basin. Both COHESION of dams and PLAND urban displayed negative relationships with copper concentrations with a 1-unit change leading to decrease by ~0.86% and 2.84% respectively.

Also at the sub-basin scale, turbidity was significantly predicted by class-level metrics and a topographic factor. Specifically, PLAND agriculture, PLAND fallow-land and PLAND urban, three class-level metrics, exhibited significant positive relationships with turbidity. For every 1% increase in each of the three latter metrics it was predicted that there was an associated increase of approximately 14.83%, 7.95% and 3.82% in turbidity respectively. Furthermore, the topographic factor elevation (SD) had a statistically significant positive effect on turbidity. For every +1 standard deviation increase in elevation at the sub-basin scale, turbidity was predicted to rise by ~1.57%.

At the cumulative basin scale, river pH was most accurately predicted. Two class level metrics, PLAND mining and COHESION dams were significant positive predictors for river pH in the catchment, where a 1-unit increase led to a 0.80% and 0.20% increase in river pH respectively. Determined as the most important predictor, the slope (SD) topographic factor, was also a significant positive predictor of pH, whereby an increase of 9.46% in pH was experienced following every +1 standard deviation change in slope heterogeneity at the cumulative basin scale.

At the cumulative 100 m riparian buffer scale, the prediction of sulfate (mg/L) concentrations was most accurate. Notably, both PLAND agriculture and PLAND mining emerged as significant predictors, demonstrating their strong influence on sulfate levels. For every 1% increase in agricultural and mining land cover, there was an associated increase of approximately 9.40% and 56.20% in sulfate concentration respectively. These findings emphasize the significant roles of agricultural and mining activities in shaping sulfate levels within the riparian buffer zone.

2.4.5. Cluster analysis and patterns

The sampled river study sites were grouped into three meaningful clusters, denoted A, B and C, determined from the HCA analysis. Integrated into a PCA for visual purposes together with the five water quality response variables and their respective parsimonious model predictors (e.g. PLAND etc.), the three groupings were clearly distinguishable across PC1 (**Figure 2-5**). In group A, the two pristine study sites were grouped together, followed by sites with experiencing lower-land-use stress in group B, and finally sites experiencing a range of the latter land-use activities with the addition of intensive mining activities in group C.

Observing the water quality parameters, the pristine sites in group A were characterised particularly by lower pH as well as reduced turbidity, anion and metal concentrations compared to sites in the other groups, see supplementary **Table S2-2**. Pertaining to the land-cover metrics, the class experienced low level agricultural, limited urban land-cover as well as few to no impoundments.

The study sites in group B, downstream from group A, were characterised by higher differences in elevation standard deviation between the study sites (in the sub-basins), owing to this group being located both within and downstream of the slopes of the Magaliesburg mountain range. The group was also characterised by low copper and sulfate concentrations due to no mining activities present in the sites sub-basin nor in the cumulative 100 m riparian buffers (**Figure 2-5**; **Table S2-2**). The group did experience higher ammonium concentrations associated with higher urban and agricultural land-cover as well as rising pH levels as the COHESION of dams also rose.

Sites in group C, were characterised by lower standard deviation of elevation, owing to being located on the foothills (flatlands) of the Magaliesburg mountain range. They were also characterised by higher pH levels, associated with increased patch connectivity of dams in the cumulative basins. In addition, these sites experienced greater ammonium concentrations and turbidity levels, associated with higher PLAND urban land cover in the sub-basins. The sites were also characterised by higher copper and sulfate concentrations associated with increases in the PLAND mining land cover in the sub-basins and the cumulative 100 m riparian buffers. The PCA loadings are presented in **Table S2-3**.

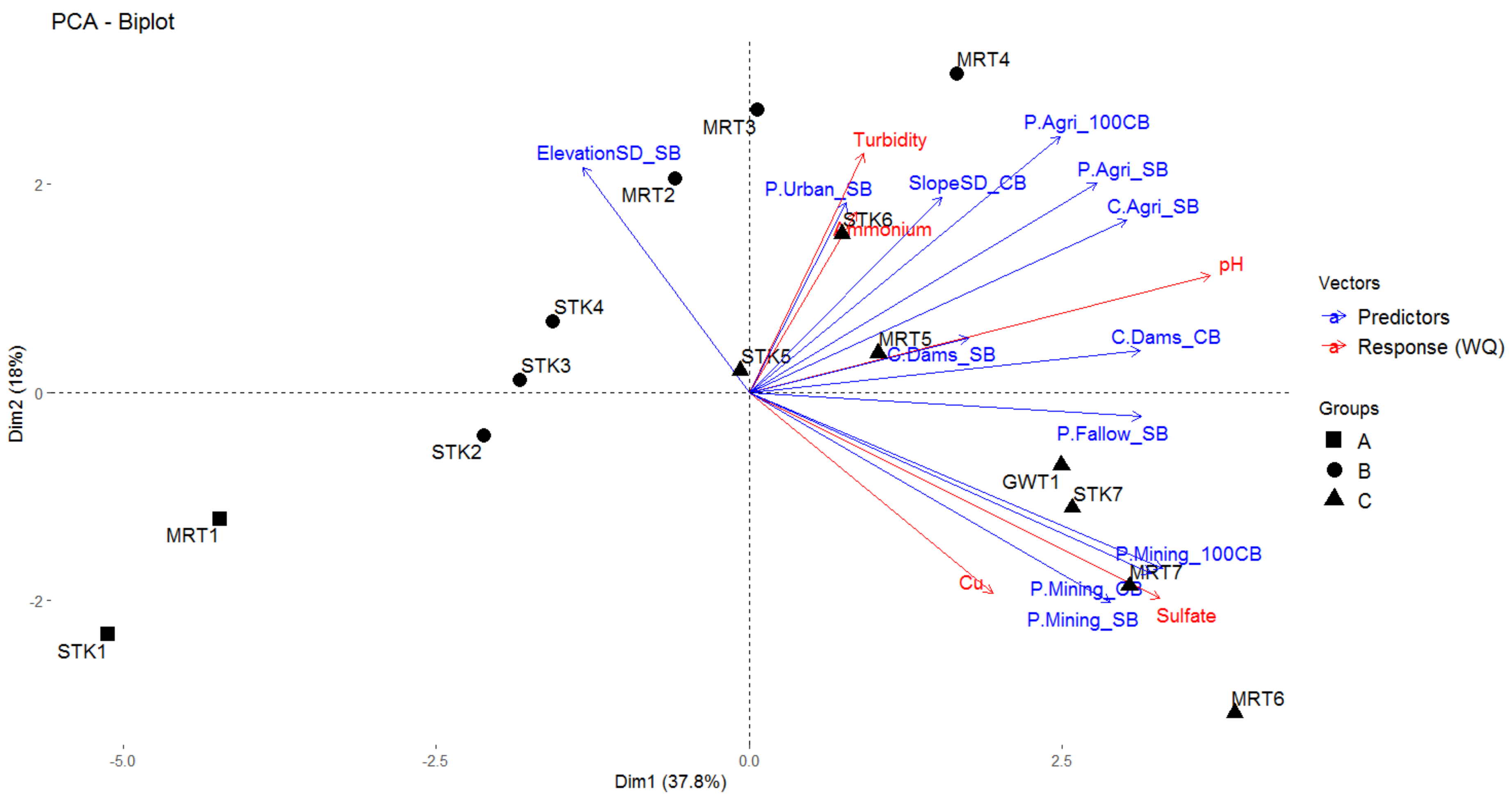

Figure 2-5: A biplot with the sites clustered into three separate groups based upon all five river water quality (WQ) responses (red) as well as their respective parsimonious model responses to assess drivers of spatial change observed among the study sites. The FRAGSTATS derived predictors retained in the statistical models are denoted using the following abbreviations in the figure: P. = percentage of landscape (PLAND), C. = patch cohesion index (COHESION), Agri = agriculture, SD = standard deviation, SB = sub-basin, CB = cumulative-basin, 100CB = 100 m cumulative riparian buffer.

2.5. Discussion

2.5.1. Scale-dependent relationships between land-use stressors and water quality

The parsimonious GLMM models derived from stepwise model selection indicated that water quality parameters, for the most part, responded best to land-use configurations (PLAND and COHESION) and less so to topographical factors (elevation and slope), owing to a higher frequency of the former in the fitted models. In the sub-basin scale, ammonium was significantly associated with positive increases in PLAND urban areas, which is consistent with previous findings linking increased urbanisation to ammonium loading in rivers (Drury et al., 2013; Levin et al., 2019).

The biological uptake and cycling characteristics of ammonium over relatively short distances supports its optimal prediction at the sub-basin scale, when influenced by urban effects (**Figure 2-4**). For example, localized inputs of ammonium may become largely dissipated at larger scales due to the rapid biological uptake by plants and microorganisms within a few hundred meters (Peterson et al., 2001), as well as rapid nitrification to nitrate which can occur at localized well-oxygenated scales (Kemp and Dodds, 2002).

The built-up urban areas within the Gwathle catchment are primarily characterised by large expanses of both formal and informal residential development with some commercial districts. The urbanized impervious surfaces are known to provide an efficient pathway for mobile pollutants to enter rivers during rainfall events, leading to deteriorated urban river water quality (Paul and Meyer, 2001). This includes ammonium-rich grey-water entering rivers due to the use of urban-lawn fertilizers, ammonium rich detergents and pet waste (Carey et al., 2013). In addition, sewerage infrastructure servicing urban areas in developing nations are often characterised by ill-maintained waste-water treatment works as well as blocked or leaky sewer systems allowing for raw sewage, high in ammonium, to be introduced into the aquatic environment (Carey et al., 2013; Levin et al., 2019). The informal areas in the catchment, however, frequently lack connections to the municipal sewerage network, leading communities to resort to bucket and pit latrine alternatives (Gqomfa et al., 2022). Anaerobic conditions inside filled pit latrines favour the conversion of nitrogenous compounds to ammonium, which can enter nearby systems via leachate or run-off during rainfall events. With inadequate wastewater infrastructure, ammonium-rich greywater can also be improperly disposed of on road surfaces, later entering the river as pollution (Gqomfa et al., 2022).

Copper was best predicted for at sub-basin scale. It was strongly associated with positive increases in the agricultural land-use connectivity (COHESION) as well as percent mining coverage, where PLAND mining had the highest variable importance in the fitted model (**Figure 2-4**). In contrast, higher dam connectivity (COHESION), as well as the percent of fallow-land were negatively associated with copper. Although research exploring drivers of *in-situ* copper concentrations at differing spatial scales is limited, findings do support the sub-basin scale model prediction, where spikes in copper near pollution point-sources such as mines have been found to rapidly dilute downstream (Navarro et al., 2008). Mining activities, including the extraction of Bushveld Complex platinum-group element (PGE) ore deposits, do contribute to riverine trace metal concentrations (Erasmus et al., 2020). Gangue rock, a characteristic component of the PGE deposits, is commonly associated with copper-bearing sulfide minerals (Thormann et al., 2017). The extensive strip and pit mining activities in the catchment thus likely result in oxidation of improperly stored PGE-gangue minerals in tailing storage facilities, generating metalliferous drainage rich in dissolved copper (Mungall, 2014).

Globally, links have been identified between high agricultural land-cover (connectivity) and increased riverine trace metal concentrations. Copper-based bactericides and fungicides are commonly applied to cherry and blueberry plantations, such as those present in the upper catchment (Carroll et al., 2010; Oliver et al., 2022). A large proportion of such crop-applied chemicals, however, end up in soils (Aikpokpodion et al., 2010), and with high connectivity of agricultural land, characterised by modified hydrological pathways, it is likely that there is rapid and high copper-concentrated runoff, aided by copper desorption, into nearby streams.

The negative association between high dam connectivity across sub-basins and copper concentrations, suggests that impoundments act as pollution sinks, trapping trace metals at finer catchment scales. This entrapment is supported by geochemical processes, where copper binds to the high sediment organic matter (e.g. fulvic acids) in dams through complexation reactions, producing stable Cu-ligand complexes, reducing potential desorption back into the water column (Shank et al., 2004; Tadini et al., 2020). In addition, anaerobic/anoxic sediments further promote Cu retention, since the lower redox potential under such conditions, lead to further Cu sorption (Sharma et al., 2022). Copper also decreased with respect to higher fallow land cover at the sub-basin scale. While no direct literature comparisons have made between sources of copper in agriculturally cultivated versus fallow-lands, it is possible that leaving fields uncultivated for certain periods of time, raising fallow-land coverage, can mitigate possible prior copper runoff into adjacent streams as less chemical ladened materials are applied to or on the land.

There was a significant positive association between the three PLAND class-level metrics, being agriculture, urban and fallow-land on riverine turbidity at the sub-basin scale; with the agricultural predictor having the highest variable importance in the model (**Figure 2-4**). It can be suggested that the turbidity input and removal processes operating at the sub-basin scale are more frequently predicted for than other scales. For example, local agricultural expansion and associated tillage practices, expose sediments and accelerates soil erosion; facilitated by wind and run-off, leading to sediment loading of nearby rivers (Jones et al., 2001). Turbidity is also considered an indicator of catchment hardening, as impervious surfaces associated with urban development reduce infiltration, thereby providing an effective storm water pathway for mobile anthropogenic waste and sediments to enter nearby streams (Levin et al., 2019).

Fallow-land and crop rotational areas can experience extensive cattle grazing activities, thereby also contributing to increased river turbidity. Over-grazing can de-vegetate land expanses near rivers, reducing infiltration capacity and increasing runoff of loose sediment into nearby streams (Zaimes et al., 2004). In addition, cattle access to the rivers from adjacent grazing-land, deliver a major source of particulate organic matter through defecation while extensive trampling leads to erosional riparian and terrestrial landforms such as gullies, that concentrate overland flow and sediment into rivers (Belsky et al., 1999; Davies-Colley et al., 2004). Additionally, variation in elevation was a positive predictor of river turbidity, serving as an effective indicator of topographical heterogeneity in the Gwathle catchment. The diversity of catchments' slopes likely creates dynamic hydrologic connections throughout the watershed, delivering greater sediment loads into the rivers (Bracken and Croke, 2007).

At the cumulative catchment scale, the longitudinal rise in river pH across the Gwathle catchment was predicted for by the COHESION of dams, slope and mining. Besides for one deep water dam, the catchment has many smaller, shallow on-stream weirs and agricultural dams. The positive association between COHESION of dams and pH, indicates that the series of smaller dams had an overriding positive effect on downstream river pH, compared to the potential pH reducing effects of a single deep dam (Wang et al., 2015). Shallow impoundments allow for high CO_2 concentrations to build up in the inundated zones via microbial and soil respiration as well as through enhanced dissolution of atmospheric CO_2 following the large water-air surface area (Kemenes et al., 2007). Under shallow, light-permitting conditions, enhanced photosynthesis can absorb high CO_2 concentrations and increase pH downstream (Wang et al., 2015).

Downstream mining activities on the catchment lowlands, with low variation in slope, also increase river pH (**Figure 2-4**). The slope (SD) may, in this case, act as a proxy for the catchments heterogeneous geology that may pose a confounding role in pH patterns. The quartzite- dominated mountain slopes may provide low acid buffering from soil material and plant activity, and although chemically inert. In the lowlands, as the rivers flow into the mafic rocks of norite and gabbro that are enriched in Ca, Mg and Fe, sources of basic cations that can buffer and neutralize acidic inputs (Cawthorn, 2010; Mungall, 2014; **Figure 2-2**).

Characteristic of the western lobe of the Platinum Belt are large pollution control dams (PCDs) supporting platinum and vanadium mining operations. There is substantial evidence from this study to support pollution leaching from these reservoirs, permeating into the adjacent environment before entering surface water, with other regionally relevant studies also identifying pollution leaching into ground and surface water (Skinner, 2018). Although high mine-derived sulfate concentrations are usually linked to acid mine drainage in rivers where gold and coal mining occurs, the opposite is found to be true in the Gwathle catchment like others with platinum, vanadium and chrome mines (McCarthy, 2011). The platinum group elements (PGE) mining belt, within the Gwathle catchment, is characterised by alkaline Gabbro and Norite rock materials (**Figure 2-2**). Both are mafic to ultramafic igneous rocks with mineral compositions generally high in alkaline metals such as calcium and magnesium (Cawthorn, 2010). These rocks might host carbonate minerals such as calcite or dolomite, which possess inherent pH-buffering properties, potentially leading to elevated pH (Mungall, 2014). Furthermore, the composition of these rocks may include additional distinct minerals, such as calcium-rich plagioclase feldspars (e.g. anorthite) and pyroxenes (Cawthorn, 2010). Upon dissolution in water, such minerals release alkaline ions that can effectively counteract the acidic effect of decant water, while raising the pH.

Sulfate was the only water quality parameter best predicted for at the riparian 100 m cumulative buffer scale (**Figure 2-4**). Within these boundaries, percentage mining and agricultural land-cover were positively associated with sulfate, indicating contributions from point- and diffuse sources. The effectiveness of the buffer for predicting the anion is supported by its integration of multiple processes governing the fate and transport of sulfate inputs from such sources across successive riparian zones. These include the hydrological connectivity regulating delivery of such inputs from adjacent mining facilities and agricultural activities to streams, soil retention and microbial transformations moderating export (e.g. in wetland soils) enabling the cumulative riparian assessment to capture major river-scape interactions and patterns in the anion (Li et al., 2009; Ledesma et al., 2016). Other major anions (e.g. nitrite) have also shown strong positive associations with land-cover activities within similar sized riparian buffers (Li et al., 2009; Li et al., 2022).

With western lobe PGE being highly concentrated in sulfide grains, the extensive mining activities within the catchment are the major point-source contributor of sulfates in the Gwathle catchment (Cawthorn, 2010; Thormann et al., 2017). The sulfide minerals form part of the original composition of mafic and ultramafic igneous rocks such as norite, gabbros and pyroxenites that form the PGE ore bodies (Schouwstra and Kinloch, 2000; Cawthorn, 2010). Common sulfide minerals in these deposits include pyrrhotite, pentlandite, and chalcopyrite (Thormann et al., 2017). During mining and extraction activities, the crushing and grinding of the PGE-bearing sulfide ores exposes an abundance of fresh reactive mineral surfaces to oxidation (Alpers and Blowes, 1994; Schouwstra and Kinloch, 2000). These reactive minerals come into contact with oxygenated water, releasing highly mobile dissolved sulfate, which then becomes collected and stored in large evaporation PCDs adjacent to tailing dumps and near the 100 m riparian buffer.

Upon permeating into the environment from unmaintained solid and liquid mine-waste storage facilities, the sulfate-rich mine water is then transported via small tributaries and decants into the major tributaries of the Gwathle Catchment. Notably, the presence of large tailing storage facilities (e.g. evaporative dams) were largely uncaptured in the GIS analysis by the cumulative 100 m buffer zones. This is owing to such facilities largely being aligned with the national regulations; stating no mine deposit, dam or reservoir may be positioned within the 1:100-year flood-line or within a 100 m horizontal distance from a watercourse (DWAF, 2007). However, residual supporting mine classified infrastructure was captured, and served as a proxy indicator for such sulfate generating and storage features, resulting in its land-cover being a significant contributor to the parsimonious model. In addition, small-scaled unregulated artisanal mining operations target PGE (chromite) outcrops and process the ore within the Sterkstroom and Maretlwane rivers riparian zones. These activities occur within the riparian cumulative 100 m buffer zone, and thus may provide additional point-sources of sulfate entering the river system.

Percentage agricultural land-cover was also a significant predictor of sulfate in the parsimonious model at the cumulative 100 m riparian scale. Such land-cover and its' associated activities have been linked with elevated sulfate levels in adjacent rivers globally, through various pathways (Liu and Han, 2020). Vast expanses of the Gwathle catchment area are occupied by a variety of irrigated and rain-fed agricultural crops; many of which are planted adjacent to the rivers. The application of agrochemicals, including sulfur containing inorganic fertilizers (e.g. ammonium sulfate [$(NH_4)_2SO_4$] and potassium sulfate; K_2SO_4) as well as fungicides (e.g. copper sulfate; $CuSO_4$) dissociate in water and oxidize in soil releasing SO_4^{2}, with the potential for diffuse sulfate pollution to enter rivers via erosional processes (Lodhi et al., 2006; Silva et al., 2018; Lwimbo et al., 2019; Zak et al., 2021). By identifying the key water quality parameters and their dominant landscape predictors at their respective spatial scales, objective two was fulfilled.

2.5.2. Spatial variations in water quality in response to land-use and topographic effects

This study assessed multiple river sites, traversing the Magaliesberg uplands to the lowlands of the Gwathle Catchment. The spatially explicit, nested nature of the study sites captured for different land-use stressors, allowing for the relationship between spatial scales, water quality, class-level metrics and topographical factors to be assessed. Integrating the outputs of an HCA analysis with a PCA, allows us to not only assess similarities between river sites, but visualise and summarize the key drivers of catchment water quality conditions and patterns.

The HCA analysis clustered the river study sites into three distinct groups based on similarities in the sites' respective water quality responses, as well as associated class-level metrics and topographic factors. Following PCA analysis, these groups were best distinguished across PC1, accounting for most of the datasets variation (36.2%). The pristine sites, located in the quarzitic Magaliesberg mountain headwaters, were characterised by only natural land-cover, with no stressor land-cover types. The sites were defined by the low pH river conditions ($\bar{x}$ = 6.50 pH units), as well as natural physico-chemistry. The low pH of these sites is likely influenced by vegetation type (ferns), dissolved organic carbon from soils, atmospheric deposition of acids (surrounding smelters) as well as the underlying quarzitic sandstone geology (Arunachalam et al., 1999; Mompati et al., 2022).

The second group, consisting of the intermediately impacted river sites were characterised by higher standard deviations of elevation ($\bar{x}$ = 114.33) at the sub-basin spatial scale. This group was also associated with built-up urban areas (PLAND urban), on-stream impoundments (COHESION dams) and agricultural activities. Consistent with these mixed land uses, the cluster exhibited elevated turbidity, ammonium concentrations, and pH levels compared to the pristine group (Levin et al., 2019). The nutrient enrichment is attributable to the well-researched effects of both urban and agricultural land covers as sources of nutrient pollution to aquatic systems. The third and final cluster was characterised by extensive mining related activities, indicated by percentages of mining land cover in both the sub-basin as well as the riparian 100 m cumulative buffer. Among the water quality parameters, Cu as well as sulfate exhibited marked increases coinciding with mining activities within the Bushveld complex (Thormann et al., 2017; Erasmus et al., 2020). Having identified the similarities in the sampled river sites among the three clusters, objective three was achieved.

2.5.3. Implications of scale-specific assessment of land-use effects for catchment management

The step changes in land-cover across the Gwathle River Catchment during this study, have indicated that water quality parameters respond best at differing scales of spatial-assessment. It became clear that the macronutrient ammonium, the trace metal Cu, as well as river turbidity were best predicted for at sub-basin scale. This suggests that targeting management efforts at the sub-basin level may be more effective, compared to current South African legislated mitigation measures, such as the 50 m riparian buffers for 1:500 000 mountain streams, in controlling and improving water quality conditions for these parameters (Berliner and Desmet, 2007).

Catchment management agencies together with municipal stakeholders need to regulate urban derived nutrient inputs regardless of their proximity to rivers. This is due to the improper disposal of ammonium rich compounds as well as poorly maintained and inadequate wastewater infrastructure in the immediate drainage area, contributing to aquatic nutrient loading. During this investigation free ammonia concentrations exceeded the chronic effect value (0.015 mg/L; DWAF, 1996) at urban impacted study sites, whereas the upper headwaters (inside the partially-protected Magaliesberg Biosphere Reserve) likely act as refugia from such toxic downstream inputs, especially for mobile organisms like aquatic insects and fish (Pringle, 2001; Orlinskiy et al., 2015). At the ammonia concentrations observed at the urban sites, fishes experience acute toxicity effects, impeding reproductive success, impaired growth and morphological development (DWAF, 1996). Targeted corrective measures are required and can be aided by implementing monitoring programs at the sub-basin spatial scale to identify priority hotspots for ammonium and ammonia pollution to limit aquatic ecosystem effects.

Urban, agricultural and mining activities should also be monitored at the sub-basin scale for the discharge of trace metal compounds to alleviate contamination in aquatic ecosystems. Being used in various sectors, for a variety of applications, Cu among other metal pollutants is widespread in other river catchments in South Africa, resulting in their bio-accumulation into the aquatic food web (Erasmus et al., 2020). Certain aquatic species have shown sensitivities to elevated concentrations of the trace metals, where acute toxicity for Cu reported in fishes at concentrations as low as 0.01 – 0.02 mg/L (NAS, 1977; DWAF, 1996). In this research, mining-affected study sites (e.g. MRT6) experienced Cu concentrations exceeding 0.17 mg/L. The National Water Act of South Africa (Act 26 of 1998), requires mining corporations to have effective water monitoring systems, which includes providing routine monitoring of effluents from storage facilities e.g. spills (DWAF, 2007). The monitoring is necessary to identify deviation from compliance, to implement appropriate remedial actions as well as for regulatory enforcement purposes (DWAF, 2007).

The cumulative basin scale was effective at assessing changes in river pH where increased presence of mine- and dam- related stressors had a cumulative downstream influence. The catchments heterogeneous geology likely confounds distinguishing natural versus human effects on pH. Catchment management authorities should consider the cumulative scale when assessing the water quality implications of removing or adding impoundments to a river basin. In contrast, riparian buffer extents, specifically the riparian 100 m cumulative buffer, may better capture localized mining inputs across a river basin.

Sulfate is a key indicator of mining stress (strongly correlated with mine-related effluents) in the Gwathle River Catchment (**Figure 2-5**). The high concentrations are indicative of the poor operation or maintenance of tailing storage facilities (e.g. settling or evaporation PCDs), where underdrainage and seepage control measures are required by law to mitigate river pollution (DWAF, 2007). Without adequate controls on seepage/leaching of mine derived mobile pollution from the storage facilities, pollution readily enters the main stem rivers within the catchment. Although spillage and/or leaching from PCDs is a possibility during storm events, this study found seepage and/or leaching from certain facilities occurred in both dry and wet seasons and, thus, urgent corrective actions are required to mitigate this chronic pollution of the surrounding freshwater resources. During the dry season sample, three river study sites downstream of PCD related inputs, experienced sulfate concentrations in excess of 500 mg/L.

2.6. Conclusions

This study highlights the importance of a multi-spatial-scale approach in managing river water quality across an intensification gradient in a developing catchment. The investigation revealed that no single scale model optimally predicted all water quality drivers. Holistic management is thus needed at different extents to capture and disentangle complex land-cover and ecohydrological interactions influencing each constituent, to develop and inform adaptive spatially-optimized management plans. The sub-basin scale was shown in this case to better capture the stepwise intensification of stressors among three of the five water quality response variables, and should be considered in future landscape assessments of water-quality stress. For resource managers to track and forecast water quality threats across the land-use intensification gradient, a comprehensive river water quality monitoring network at ecologically meaningful scales would best target and identify pollution hotspots, allowing for focused corrective measures and enforcement. The synergistic integration of monitoring river water quality parameters across multiple spatial extents offers the most promising path for sustaining water quality amidst catchment intensification. Future research can include additional landscape metrics like edge density and/or shape complexity to provide supplemental context on land-water interactions beyond the current set.

2.6.1. Acknowledgements

This Chapter was authored by Jonathan Levin, with material contributions Darragh Woodford and Chris Curtis. This research was funded by the Water Research Commission. All fieldwork was conducted under a North West Province research permit (NW 17458/03/2020). The authors thank Mark Ashfield and Gert Eastes for access to sampling sites on their properties, and Chevonne Reynolds and Jason Marshal for advice on the statistical analysis.

2.6.2. References

Aikpokpodion, P. E., L. Lajide, and A. F. Aiyesanmi., 2010. Heavy metals contamination in fungicide treated cocoa plantations in Cross River state, Nigeria, *American-Eurasian Journal of Agricultural & Environmental Sciences*, 8(3), 268-274.

Akyildiz, G.K. and Duran, M., 2021. Evaluation of the impact of heterogeneous environmental pollutants on benthic macroinvertebrates and water quality by long-term monitoring of the buyuk menderes river basin, *Environmental Monitoring and Assessment*, *193*(5), 1-23.

Allan, J.D., 2004. Landscapes and riverscapes: the influence of land use on stream ecosystems, *Annual Review of Ecology, Evolution, and Systematics*, *35*, 257-284.

Arunachalam, K., Arunachalam, A. and Melkania, N.P., 1999. Influence of soil properties on microbial populations, activity and biomass in humid subtropical mountainous ecosystems of India. *Biology and Fertility of Soils*, *30*, 217-223.

Barton, K., 2010. MuMIn: multi-model inference. R package version 0.13. 17. *http://CRAN. R-project. org/package= MuMIn*.

Bates, D., Mächler, M., Bolker, B. and Walker, S., 2014, Fitting linear mixed-effects models using lme, *arXiv preprint arXiv:1406.5823*.

Belsky, A.J., Matzke, A. and Uselman, S., 1999. Survey of livestock influences on stream and riparian ecosystems in the western United States, *Journal of Soil and water Conservation*, *54*(1), 419-431.

Berliner D., and Desmet P. 2007. Eastern Cape Biodiversity Conservation Plan: Technical Report. Department of Water Affairs and Forestry (DWAF), Project No. 2005-012. Pretoria.

Boyd, C.E., 2019. *Water quality: an introduction*. Springer International Publishing, Switzerland.

Bracken, L.J. and Croke, J., 2007. The concept of hydrological connectivity and its contribution to understanding runoff-dominated geomorphic systems, *Hydrological Processes: An International Journal*, *21*(13), 1749-1763.

Carey, R.O., Hochmuth, G.J., Martinez, C.J., Boyer, T.H., Dukes, M.D., Toor, G.S. and Cisar, J.L., 2013. Evaluating nutrient impacts in urban watersheds: Challenges and research opportunities, *Environmental Pollution*, *173*, 138-149.

Carroll, J., Robinson, T., Burr, T., Hoying, S. and Cox, K., 2010. Evaluation of pruning techniques and bactericides to manage bacterial canker of sweet cherry, *New York Fruit Quarterly*, *18*, 9-15.

Cawthorn, R.G., 2010. The platinum group element deposits of the Bushveld Complex in South Africa, *Platinum Metals Review*, *54*(4), 205-215.

Croghan, C.A.P.P.E. and Egeghy, P.P., 2003. Methods of dealing with values below the limit of detection using SAS, *Southern SAS User Group*, *22*(24), 22-24.

Davies-Colley, R.J., Nagels, J.W., Smith, R.A., Young, R.G. and Phillips, C.J., 2004. Water quality impact of a dairy cow herd crossing a stream, *New Zealand Journal of Marine and Freshwater Research*, *38*(4), 569-576.

de Mello, K., Valente, R.A., Randhir, T.O., dos Santos, A.C.A. and Vettorazzi, C.A., 2018. Effects of land use and land cover on water quality of low-order streams in Southeastern Brazil: Watershed versus riparian zone, *Catena*, *167*, 130-138.

Ding, J., Jiang, Y., Liu, Q., Hou, Z., Liao, J., Fu, L. and Peng, Q., 2016. Influences of the land use pattern on water quality in low-order streams of the Dongjiang River basin, China: A multi-scale analysis, *Science of the Total Environment*, *551*, 205-216.

Driver, A., Nel, J.L., Snaddon, K., Murray, K., Roux, D.J., Hill, L., Swartz, E.R., Manuel, J. and Funke, N., 2011. Implementation manual for freshwater ecosystem priority areas. Report for the Water Research Commission No. 1801/1/11. Water Research Commission, Pretoria, South Africa.

Drury, B., Rosi-Marshall, E. and Kelly, J.J., 2013. Wastewater treatment effluent reduces the abundance and diversity of benthic bacterial communities in urban and suburban rivers, *Applied and environmental microbiology*, *79*(6), 1897-1905.

DWAF, 1996. South African Water Quality Guidelines volume 7 Aquatic Ecosystems: Second Edition, Pretoria, South Africa.

DWAF, 2007. Pollution Control Dams: Best practice guidelines for water resource protection in the South African mining industry, Department: Water Affairs and Forestry.

Erasmus, J.H., Malherbe, W., Zimmermann, S., Lorenz, A.W., Nachev, M., Wepener, V., Sures, B. and Smit, N.J., 2020. Metal accumulation in riverine macroinvertebrates from a platinum mining region, *Science of the Total Environment*, *703*, 1-13.

Farr, T. G., and M. Kobrick, 2000, Shuttle Radar Topography Mission produces a wealth of data, Eos Trans, AGU, 81, 583-583

Funk, C., Peterson, P., Landsfeld, M., Pedreros, D., Verdin, J., Shukla, S., Husak, G., Rowland, J., Harrison, L., Hoell, A. and Michaelsen, J., 2015. The climate hazards infrared precipitation with stations—a new environmental record for monitoring extremes, *Scientific data*, *2*(1), 1-21.

Geoterraimage, 2021. *2020 South Africa National Land-Cover Dataset*, Geoterraimage, viewed 10 February 2022, from https://egis.environment.gov.za/sa_national_land_cover_datasets.

Giri, S. and Qiu, Z., 2016. Understanding the relationship of land uses and water quality in Twenty First Century: A review, *Journal of environmental management*, *173*, 41-48.

Gqomfa, B., Maphanga, T. and Shale, K., 2022. The impact of informal settlement on water quality of Diep River in Dunoon, *Sustainable Water Resources Management*, *8*(27), 1-18.

Johnson, L., Richards, C., Host, G. and Arthur, J., 1997. Landscape influences on water chemistry in Midwestern stream ecosystems, *Freshwater biology*, *37*(1), 193-208.

Jones, K.B., Neale, A.C., Nash, M.S., Van Remortel, R.D., Wickham, J.D., Riitters, K.H. and O'neill, R.V., 2001. Predicting nutrient and sediment loadings to streams from landscape metrics: a multiple watershed study from the United States Mid-Atlantic Region, *Landscape Ecology*, *16*, 301-312.

Kaiser, H. F. 1960. The application of electronic computers to factor analysis, *Educational and Psychological Measurement*, 20, 141–151.

Kassambara A, Mundt F (2020). factoextra: Extract and Visualize the Results of Multivariate Data Analyses, R package version 1.0.7.

Kemenes, A., Forsberg, B.R. and Melack, J.M., 2011. CO2 emissions from a tropical hydroelectric reservoir (Balbina, Brazil), *Journal of Geophysical Research: Biogeosciences*, *116*(G3).

Kemp, M.J. and Dodds, W.K., 2002. The influence of ammonium, nitrate, and dissolved oxygen concentrations on uptake, nitrification, and denitrification rates associated with prairie stream substrata, *Limnology and Oceanography*, *47*(5), 1380-1393.

Kleynhans, CJ, Thirion, C and Moolman, J. 2005. *A Level I River Ecoregion Classification System for South Africa, Lesotho and Swaziland*, Resource Quality Services, Department of Water Affairs and Forestry, Pretoria, South Africa, Report No. N/0000/00/REQ0104.

King, R.S., Baker, M.E., Whigham, D.F., Weller, D.E., Jordan, T.E., Kazyak, P.F. and Hurd, M.K., 2005. Spatial considerations for linking watershed land cover to ecological indicators in streams, *Ecological applications*, *15*(1), 137-153.

Kuhn, M., Wing, J., Weston, S., Williams, A., Keefer, C., Engelhardt, A., Cooper, T., Mayer, Z., Kenkel, B. and Team, R.C., 2020. Package 'caret', *The R Journal*, *223*(7), 1-224.

Lê, S., Josse, J. and Husson, F., 2008. FactoMineR: An R package for multivariate analysis, *Journal of statistical software*, *25*, 1-18.

Ledesma, J.L., Futter, M.N., Laudon, H., Evans, C.D. and Köhler, S.J., 2016. Boreal forest riparian zones regulate stream sulfate and dissolved organic carbon. *Science of the Total Environment*, *560*, 110-122.

Levin, J.C., Woodford, D.J. and Snow, G.C., 2019. Evaluating the effectiveness of freshwater fishes as bio-indicators for urban impacts in the Crocodile (West) catchment, South Africa, *Water SA*, *45*(3), 477-486.

Li, S., Gu, S., Tan, X. and Zhang, Q., 2009. Water quality in the upper Han River basin, China: the impacts of land use/land cover in riparian buffer zone, *Journal of hazardous materials*, *165*(1-3), 317-324.

Li, S., Zhang, J., Jiang, P. and Zhang, L., 2022. Linking land use with riverine water quality: A multi-spatial scale analysis relating to various riparian strips, *Frontiers in Environmental Science*, *10*, 1-15.

Liu, J. and Han, G., 2020. Major ions and $\delta^{34}S$ SO_4 in Jiulongjiang River water: Investigating the relationships between natural chemical weathering and human perturbations, *Science of the Total Environment*, *724*, 1-12.

Liu, J., Xu, J., Zhang, X., Liang, Z. and Rao, K., 2021. Nonlinearity and threshold effects of landscape pattern on water quality in a rapidly urbanized headwater watershed in China, *Ecological indicators*, *124*, 1-10.

Liu, J., Zhang, D., Tang, Q., Xu, H., Huang, S., Shang, D. and Liu, R., 2021. Water quality assessment and source identification of the Shuangji River (China) using multivariate statistical methods, *PloS one*, *16*(1), 1-6.

Lodhi, H.S., Khan, M.A., Verma, R.S. and Sharma, U.D., 2006. Acute toxicity of copper sulphate to fresh water prawns, *Journal of Environmental Biology*, *27*(3), 585-588.

Macfarlane D., and Bredin I. 2017. Buffer Zone Guidelines for Rivers, Wetlands and Estuaries Part 1: Technical Manual. Water Research Commission Report No. TT715-1-17. Produced as part of Project No. K5/2463 entitled *Testing the preliminary guidelines for the determination of buffer zones for rivers, wetlands and estuaries*.

Maechler, M., 2018. Cluster: cluster analysis basics and extensions, *R package version 2.0. 7–1*.

Maherry, A. M., Horan, M. J. C., Smith-Adao, L. B., van Deventer, H., Nel, J. L., Schulze, R. E., and Kunz, R. P. 2013. Delineating river network quinary catchments for South Africa and allocating associated daily hydrological information, WRC Report No. 2020/1/12, Water Research Commission, Gezina.

Maier, W.D., Smithies, R.H., Spaggiari, C.V., Barnes, S.J., Kirkland, C.L., Yang, S., Lahaye, Y., Kiddie, O. and MacRae, C., 2016. Petrogenesis and Ni–Cu sulphide potential of mafic–ultramafic rocks in the Mesoproterozoic Fraser Zone within the Albany–Fraser Orogen, Western Australia, *Precambrian Research*, *281*, 27-46.

Marshal, J.P., Krausman, P.R., Bleich, V.C., Ballard, W.B. and McKeever, J.S., 2002. Rainfall, El Nino, and dynamics of mule deer in the Sonoran Desert, California, *The Journal of wildlife management*, 1283-1289.

McCarthy, T.S., 2011. The impact of acid mine drainage in South Africa, *South African Journal of Science*, *107*(5/6), 1-7.

McGarigal, K., Cushman, S.A., Neel, M.C. and Ene, E., 2002. *FRAGSTATS: spatial pattern analysis program for categorical maps*, Computer software, University of Massachusetts, Amherst. Available from: www.umass. edu/landeco/research/fragstats/fragstats.

Mitchell, A.A., 1990. The stratigraphy, petrography and mineralogy of the Main Zone of the northwestern Bushveld Complex, *South African Journal of Geology*, *93*(4), 818-831.

Mompati, M.K., Piketh, S.J., Aas, W., Van Zyl, P.G., Pienaar, J.J. and Curtis, C.J., 2022. Rainwater Chemistry and Total Deposition of Acidity from the Northern Savanna to the Southern Coastal Fynbos of South Africa, *Water, Air, & Soil Pollution*, *233*(7), 275.

Mungall, J.E., 2014. 13.8 Geochemistry of Magmatic Ore Deposits. In: Turekian, K.K. and Holland, H.D (eds) Treatise on Geochemistry 2nd Edition, Elsevier Science, 195-218.

NAS, 1977. Copper. National Research Council, National Academy of Sciences, Washington DC.

Navarro, M.C., Pérez-Sirvent, C., Martínez-Sánchez, M.J., Vidal, J., Tovar, P.J. and Bech, J., 2008. Abandoned mine sites as a source of contamination by heavy metals: a case study in a semi-arid zone, *Journal of Geochemical exploration*, *96*(2-3), 183-193.

Nel, J. L., Strydom, W. F., Maherry, A., Petersen, C., Hill, L., Roux, D. J., Nienaber, S., van Deventer, H., Swartz, E., & Smith-Adao, L. B. 2011. Atlas of freshwater ecosystem priority areas in South Africa: Maps to support sustainable development of water resources, WRC Report No. TT500/11, Water Research Commission, Gezina.

Oliver, J.E., Cline, B. and Curry, S., 2022. Evaluating organic fungicides for control of blueberry diseases in the southeastern US Progress Report, Projects 2022 R-02 and 2022 R-03.

Oranje, M., Nel, V., van Huyssteen, E., and Maritz, J. 2021. A Brief History of Platinum Mining with a Focus on the Rustenburg Region. In: Marais L., Campbell, M., Denoon-Stevens S., van Rooyen D. (eds.) Mining and community in the South African platinum belt a decade after Marikana. Nova Science Publishers, New York. 11-38.

Orlinskiy, P., Münze, R., Beketov, M., Gunold, R., Paschke, A., Knillmann, S., & Liess, M. 2015. Forested headwaters mitigate pesticide effects on macroinvertebrate communities in streams: Mechanisms and quantification, *Science of the Total Environment*, *524–525*, 115–123.

Paul, M.J. and Meyer, J.L., 2001. Streams in the urban landscape, *Annual review of Ecology and Systematics*, *32*(1), 333-365.

Peterson, B.J., Wollheim, W.M., Mulholland, P.J., Webster, J.R., Meyer, J.L., Tank, J.L., Marti, E., Bowden, W.B., Valett, H.M., Hershey, A.E. and McDowell, W.H., 2001. Control of nitrogen export from watersheds by headwater streams, *Science*, *292*(5514), 86-90.

Pool-Stanvliet, R., 2013. A history of the UNESCO Man and the Biosphere Programme in South Africa, *South African Journal of Science*, *1*09(9-10), 1-6.

Pringle, C. M. 2001. Hydrologic connectivity and the management of biological reserves: A global perspective, *Ecological Applications*, *11*(4), 981–998.

R Core Team. 2023. R: A Language and Environment for Statistical Computing. R Foundation for Statistical Computing, Vienna, Austria.

Richardson, J.S. and Danehy, R.J., 2007. A synthesis of the ecology of headwater streams and their riparian zones in temperate forests, *Forest Science*, *53*(2), 131-147.

Saleh, A., Arnold, J.G., Gassman, P.W.A., Hauck, L.M., Rosenthal, W.D., Williams, J.R. and McFarland, A.M.S., 2000. Application of SWAT for the upper North Bosque River watershed, *Transactions of the ASAE*, *43*(5), 1077-1087.

SAWS, 2023. South African Weather Service, precipitation data for the Gwathle Catchment

Schouwstra, R.P., Kinloch, E.D. and Lee, C.A., 2000. A short geological review of the Bushveld Complex, *Platinum Metals Review*, *44*(1), 33-39.

Shank, G.C., Skrabal, S.A., Whitehead, R.F. and Kieber, R.J., 2004. Strong copper complexation in an organic-rich estuary: the importance of allochthonous dissolved organic matter, *Marine Chemistry*, *88*(1-2), 21-39.

Sharma, N., Wang, Z., Catalano, J.G. and Giammar, D.E., 2022. Dynamic responses of trace metal bioaccessibility to fluctuating redox conditions in wetland soils and stream sediments, *ACS Earth and Space Chemistry*, *6*(5), 1331-1344.

Shehab, Z., Jamil, N.R., Aris, A.Z. and Shafie, N.S., 2021. Spatial variation impact of landscape patterns and land use on water quality across an urbanized watershed in Bentong, Malaysia, *Ecological indicators*, *122*, 1-12.

Shen, Z., Hou, X., Li, W., Aini, G., Chen, L. and Gong, Y., 2015. Impact of landscape pattern at multiple spatial scales on water quality: A case study in a typical urbanised watershed in China, *Ecological Indicators*, *48*, 417-427.

Shi, P., Zhang, Y., Li, Z., Li, P. and Xu, G., 2017. Influence of land use and land cover patterns on seasonal water quality at multi-spatial scales, *Catena*, *151*, 182-190.

Silva, V., Marques, C.R., Campos, I., Vidal, T., Keizer, J.J., Goncalves, F. and Abrantes, N., 2018. Combined effect of copper sulfate and water temperature on key freshwater trophic levels–approaching potential climatic change scenarios, *Ecotoxicology and environmental safety*, *148*, 384-392.

Skinner, S.J.W., 2018. Platinum Tailings Review-A comparison of the water quality in the tailings dam to the surrounding groundwater, *IMWA*, 733-737.

Tadini, A.M., Mounier, S. and Milori, D.M.B.P., 2020. Modeling the quenching of fluorescence from organic matter in Amazonian soils, *Science of the total environment*, *698*, 1-9.

Thompson, S.E., Harman, C.J., Troch, P.A., Brooks, P.D. and Sivapalan, M., 2011. Spatial scale dependence of ecohydrologically mediated water balance partitioning: A synthesis framework for catchment ecohydrology, *Water Resources Research*, *47*(10), 1-20.

Thormann, L., Buchspies, B., Mbohwa, C. and Kaltschmitt, M., 2017. PGE production in southern Africa, part I: production and market trends, *Minerals*, *7*(11), 1-22.

Tran, C.P., Bode, R.W., Smith, A.J. and Kleppel, G.S., 2010. Land-use proximity as a basis for assessing stream water quality in New York State (USA), *Ecological Indicators*, *10*(3), 727-733.

Uuemaa, E., Roosaare, J. and Mander, Ü., 2007. Landscape metrics as indicators of river water quality at catchment scale, *Hydrology Research*, *38*(2), 125-138.

Vannote, R.L., Minshall, G.W., Cummins, K.W., Sedell, J.R. and Cushing, C.E., 1980. The river continuum concept, *Canadian journal of fisheries and aquatic sciences*, *37*(1), 130-137.

Wallace, J.B. and Eggert, S.L., 2015. Terrestrial and longitudinal linkages of headwater streams, *Southeastern Naturalist*, *14*(7), 65-86.

Wanderi, E.W., Gettel, G.M., Singer, G.A. and Masese, F.O., 2022. Drivers of water quality in Afromontane-savanna rivers, *Frontiers in Environmental Science*, *10*, 1-20.

Wang, B., Liu, C.Q., Wang, F., Liu, X.L. and Wang, Z.L., 2015. A decrease in pH downstream from the hydroelectric dam in relation to the carbon biogeochemical cycle, *Environmental Earth Sciences*, *73*, 5299-5306.

Wang, Y., Song, Z., Bai, H., Tong, H., Chen, Y., Wei, Y., Wang, X. and Yang, S., 2023. Scale effects of land use on river water quality: a case study of the Tuojiang River Basin, China, *Environmental Science and Pollution Research*, 30(16), 48002-48020.

Wickham, H., 2016. ggplot2: Elegant Graphics for Data Analysis. Springer-Verlag New York.

Wickham, H., and Henry, L. 2023. Purrr: Functional programming tools, R package version 1.0.1.

Xu, Q., Wang, P., Shu, W., Ding, M. and Zhang, H., 2021. Influence of landscape structures on river water quality at multiple spatial scales: A case study of the Yuan river watershed, China, *Ecological Indicators*, *121*, 1-11.

Xu, S., Li, S.L., Zhong, J. and Li, C., 2020. Spatial scale effects of the variable relationships between landscape pattern and water quality: Example from an agricultural karst river basin, Southwestern China. Agriculture, *Ecosystems & Environment*, 300, 1-13.

Zaimes, G.N., 2004. *Riparian land-use impacts on stream and gully bank soil and phosphorus losses with an emphasis on grazing practices*, Doctoral dissertation, Lowa State University.

Zak, D., Hupfer, M., Cabezas, A., Jurasinski, G., Audet, J., Kleeberg, A., McInnes, R., Kristiansen, S.M., Petersen, R.J., Liu, H. and Goldhammer, T., 2021. Sulphate in freshwater ecosystems: A review of sources, biogeochemical cycles, ecotoxicological effects and bioremediation, *Earth-Science Reviews*, 212, 1-23.

Zhang, J., Li, S., Dong, R., Jiang, C. and Ni, M., 2019. Influences of land use metrics at multi-spatial scales on seasonal water quality: a case study of river systems in the Three Gorges Reservoir Area, China, *Journal of Cleaner Production*, 206, 76-85.

Zhou, T., Wu, J. and Peng, S., 2012. Assessing the effects of landscape pattern on river water quality at multiple scales: a case study of the Dongjiang River watershed, China, *Ecological Indicators*, *23*, 166-175.

Zuur, A.F., Ieno, E.N., Walker, N.J., Saveliev, A.A. and Smith, G.M., 2009. Mixed effects models and extensions in ecology with R. Springer, New York.

2.6.3. Supplementary material

Table S2-1: Loadings of the experimental variables used in the principal components analysis presented in Figure 2-6.

Variable	PC1	PC2	PC3	PC4	PC5
Conductivity	0.96	-0.17	0.17	-0.08	-0.02
Dissolved oxygen	0.42	0.01	-0.49	0.39	-0.48
pH	0.65	0.34	-0.05	0.06	-0.56
Temperature	0.80	0.06	0.48	-0.07	-0.07
Turbidity	0.13	0.76	0.26	0.55	0.12
Chloride	0.96	-0.19	-0.12	-0.06	0.10
Sulfate	0.98	-0.12	0.00	-0.03	0.03
Nitrate	0.80	0.26	-0.29	-0.09	-0.23
Nitrite	0.21	0.84	0.28	0.19	-0.03
Ortho-Phosphate	0.46	0.61	-0.53	-0.15	0.26
Free and Saline Ammonia	-0.02	0.80	0.08	-0.57	0.02
Ammonium	-0.03	0.77	0.06	-0.60	0.02
Al	0.73	0.23	-0.48	0.17	0.38
V	0.97	-0.09	-0.11	-0.06	0.08
Cr	0.94	0.07	0.20	0.14	0.18
Fe	0.73	-0.25	0.19	0.02	0.05
Ni	0.79	-0.10	-0.52	0.05	0.24
Co	0.01	0.81	0.26	0.38	0.32
Cu	0.69	-0.33	0.53	0.02	-0.03
Zn	0.95	-0.23	0.17	-0.06	0.04
Cd	0.88	-0.24	0.29	-0.03	0.14
Ca	0.96	-0.11	-0.16	-0.10	0.04
Si	0.66	0.57	-0.05	0.06	-0.40
Na	0.99	-0.06	0.02	-0.01	0.03
Mg	0.99	-0.10	-0.02	-0.03	0.04
K	0.94	0.12	0.15	-0.10	-0.18

Table S2-2: The average and standard deviation (SD) of concentrations of the five river water quality responses as well as the average (mean) and standard deviation (SD) of the FRAGSTATS class-level metrics and topographical factors/determinants retained following the model fitting. Where for the predictors, P. = percentage of landscape (PLAND) for a given land use class and C. = patch cohesion index (COHESION) for a land use class. The SB = sub-basin, CB = cumulative-basin and 100cm = the 100m cumulative riparian buffer.

Group	Statistics	Responses									
		Sulfate	Ammonium	Cu	Turbidity	pH					
A	Mean	2.67	0.07	14.10	1.01	6.50					
	SD	0.24	0.01	0.58	0.15	1.22					
B	Mean	23.97	0.24	22.54	103.48	7.94					
	SD	31.51	0.18	5.33	192.27	0.69					
C	Mean	156.84	0.32	48.96	17.92	8.63					
	SD	109.80	0.46	74.56	4.80	0.23					
Group	**Statistics**	**Predictors**									
		P.urban SB	**C.Agri SB**	**C.Dams SB**	**P.Fallow SB**	**P.Mining SB**	**ElevationSD SB**	**C.Dams CB**	**SlopeSD CB**	**P.Agri 100CB**	**P.Mining 100CB**
A	Mean	0.00	0.00	0.00	0.00	0.00	77.44	0.00	5.25	0.00	0.00
	SD	0.00	0.00	0.00	0.00	0.00	26.32	0.00	1.03	0.00	0.00
B	Mean	3.93	96.95	55.52	5.44	0.99	114.33	68.42	5.57	13.49	0.55
	SD	6.00	1.07	33.09	4.60	2.30	25.40	16.49	1.07	6.70	1.35
C	Mean	7.17	96.58	68.22	16.22	11.72	61.88	94.84	5.55	10.37	4.51
	SD	10.60	1.41	21.98	6.71	9.99	51.18	2.39	0.23	2.94	3.05

Table S2-3: Loadings of the 15 experimental variables used, with five water quality response variables (italics) and 10 class-level metrics and topographical factors (grey).

Variable	PC1	PC2	PC3	PC4	PC5
Sulfate	*0.62*	*0.26*	*0.02*	*0.00*	*0.01*
Ammonium	*0.07*	*0.30*	*0.27*	*0.20*	*0.01*
Cu	*0.23*	*0.35*	*0.07*	*0.01*	*0.20*
Turbidity	*0.04*	*0.19*	*0.28*	*0.10*	*0.16*
pH	*0.78*	*0.06*	*0.04*	*0.00*	*0.00*
P.Urban_SB	0.05	0.30	0.26	0.22	0.10
C.Agri_SB	0.56	0.17	0.00	0.17	0.03
C.Dams_SB	0.19	0.07	0.11	0.48	0.01
P.Fallow_SB	0.62	0.00	0.10	0.08	0.08
P.Mining_SB	0.53	0.29	0.00	0.02	0.01
ElevationSD_SB	0.09	0.21	0.30	0.20	0.00
C.Dams_CB	0.62	0.03	0.10	0.20	0.03
SlopeSD_CB	0.13	0.11	0.35	0.12	0.02
P.Agri_100CB	0.34	0.20	0.30	0.00	0.04
P.Mining_100CB	0.59	0.16	0.00	0.00	0.18

Table S2-4: The month year and season of each sampling regime

Month	Year	Season
May	2021	Wet
June	2021	Intermediate
August	2021	Dry
October	2021	Dry
January	2022	wet
March	2023	wet

Table S2-5: Physico-chemical river water quality averages and standard deviations over the six sampling seasons

Sites	Measure	Conductivity (µS/cm)	DO (mg/L)	pH	Temp (°C)	Turbidity (NTU)	Chloride (mg/L)	Sulfate (mg/L-S)	Nitrate (mg/L-N)	Nitrite (mg/L-N)	Ortho Phosphate (mg/L-P)	Free and Saline Ammonia (mg/L-N)	Ammonium (mg/L-N)
STK1	Mean	18.32	6.45	5.64	17.36	0.91	1.17	2.50	0.15	0.03	0.07	0.08	0.08
	SD	4.58	0.53	0.18	2.46	0.82	0.41	1.52	0.14	0.00	0.03	0.03	0.03
STK2	Mean	31.40	5.47	7.14	15.92	2.03	1.33	2.33	0.12	0.03	0.08	0.12	0.12
	SD	9.94	0.55	2.05	3.39	0.86	0.52	1.37	0.08	0.00	0.06	0.14	0.14
STK3	Mean	40.23	7.92	7.46	16.22	5.40	9.33	18.83	0.95	0.03	0.06	0.15	0.15
	SD	3.28	0.74	0.19	3.68	1.86	17.48	42.22	2.03	0.00	0.03	0.17	0.17
STK4	Mean	83.43	6.82	7.59	17.24	7.62	4.50	3.50	0.25	0.03	0.09	0.15	0.15
	SD	43.96	1.36	0.24	4.50	3.67	2.51	0.55	0.16	0.00	0.06	0.13	0.13
STK5	Mean	301.08	8.60	8.64	17.92	11.46	13.33	27.33	9.90	0.06	0.08	0.10	0.09
	SD	186.05	1.07	0.22	4.46	3.95	8.62	21.26	10.29	0.07	0.06	0.05	0.06
STK6	Mean	323.38	6.69	8.24	17.67	25.60	17.50	26.17	6.17	0.15	0.20	1.43	1.32
	SD	104.24	1.58	0.23	4.92	20.74	6.89	8.59	6.92	0.10	0.16	1.57	1.48
STK7	Mean	827.64	6.88	8.51	18.07	17.76	97.00	135.00	9.42	0.29	0.12	0.46	0.43
	SD	538.93	1.41	0.19	5.03	15.31	89.35	98.70	6.54	0.35	0.09	0.71	0.68
MRT1	Mean	23.21	7.42	7.36	16.30	1.12	1.33	2.83	0.14	0.03	0.07	0.07	0.07
	SD	6.18	0.86	0.28	2.97	0.73	0.52	0.98	0.15	0.00	0.03	0.03	0.03
MRT2	Mean	179.90	6.50	7.96	17.42	27.47	13.00	15.33	0.83	0.05	0.12	0.36	0.34
	SD	84.45	1.20	0.27	5.69	13.49	7.82	10.31	0.81	0.07	0.07	0.40	0.41
MRT3	Mean	198.47	7.97	8.53	15.60	87.93	14.33	17.17	1.22	0.06	0.12	0.10	0.09
	SD	84.35	1.33	0.17	4.61	123.73	7.66	9.47	1.20	0.07	0.07	0.05	0.06
MRT4	Mean	570.75	7.31	8.96	18.88	490.42	39.83	86.67	6.50	0.47	0.18	0.68	0.57
	SD	330.55	0.61	0.17	4.49	421.33	27.60	68.72	5.69	0.46	0.18	0.58	0.49
MRT5	Mean	1000.57	7.48	8.51	18.38	20.71	118.17	171.33	2.29	0.03	0.07	0.10	0.10
	SD	974.51	1.66	0.23	6.22	23.27	160.85	182.34	2.41	0.00	0.03	0.05	0.05
MRT6	Mean	2680.68	7.30	8.74	21.61	12.64	264.20	288.20	7.76	0.08	0.06	0.08	0.08
	SD	1692.43	2.56	0.15	3.62	5.94	211.11	215.70	10.53	0.12	0.02	0.03	0.03
MRT7	Mean	1907.42	8.64	8.81	18.45	19.32	323.67	300.00	14.78	0.05	0.28	0.14	0.14
	SD	1292.36	1.60	0.11	5.69	19.21	293.97	209.12	10.22	0.03	0.23	0.18	0.18
GWT1	Mean	955.03	7.26	8.94	18.47	17.96	127.83	149.83	5.98	0.04	0.07	0.12	0.10
	SD	395.14	2.16	0.30	5.21	24.09	71.31	57.47	2.71	0.02	0.03	0.07	0.05

Table S2-5 continued

Sites	Measure	Al (ppb)	V (ppb)	Cr (ppb)	Mn (ppb)	Fe (ppb)	Ni (ppb)	Co (ppb)	Cu (ppb)	Zn (ppb)	Cd (ppb)	Pb (ppb)	U (ppb)	Ca (ppb)	Si (ppb)	Na (ppb)	Mg (ppb)	K (ppb)
STK1	Mean	17.43	1.01	1.13	15.82	12.95	3.05	0.50	14.51	36.08	1.02	3.24	0.68	872.22	127.63	54.31	367.96	153.52
	SD	10.45	1.17	0.90	5.06	16.47	1.11	1.11	13.35	19.07	1.15	5.42	1.26	197.00	47.78	26.74	64.71	70.42
STK2	Mean	6.33	0.78	0.86	10.81	106.09	3.03	0.10	17.46	49.78	0.63	0.59	0.18	1413.91	314.59	59.46	787.62	206.56
	SD	5.59	0.17	0.48	3.64	75.78	1.08	0.11	10.40	18.58	0.31	0.88	0.07	428.76	101.67	25.00	238.60	66.18
STK3	Mean	11.06	0.76	0.97	15.87	78.75	5.67	0.07	23.26	59.46	0.57	2.70	0.16	2721.35	1628.93	116.23	1591.94	503.40
	SD	16.01	0.11	0.27	2.66	46.87	8.16	0.17	16.75	27.63	0.33	4.09	0.07	439.27	871.40	21.81	245.76	91.44
STK4	Mean	8.25	1.16	0.72	89.08	160.18	3.18	0.12	21.20	50.41	0.54	7.00	0.15	5607.34	2078.67	138.33	3200.80	718.52
	SD	9.21	0.39	0.35	104.12	92.78	0.67	0.26	15.65	36.94	0.23	7.46	0.08	3315.96	814.27	48.48	1671.98	300.80
STK5	Mean	1.64	2.83	0.72	21.36	38.11	3.31	0.06	23.12	61.90	0.49	1.34	0.21	14250.88	3529.60	702.24	10501.17	1095.38
	SD	2.57	1.82	0.59	13.73	46.53	1.95	0.10	23.43	64.99	0.26	2.90	0.14	10047.68	1031.58	736.50	8190.31	524.40
STK6	Mean	26.76	5.31	1.50	146.43	72.08	5.05	0.49	4.61	70.81	0.83	14.96	0.45	21051.90	3219.14	926.25	10312.59	1703.86
	SD	29.75	1.65	0.42	211.16	55.40	1.67	0.46	5.18	34.58	0.59	36.22	0.26	9082.94	1088.95	406.34	3499.15	705.31
STK7	Mean	20.94	16.04	1.96	47.31	86.01	12.17	0.00	5.99	150.84	0.85	0.00	0.71	63057.98	3693.64	2302.97	38321.63	2552.36
	SD	32.55	11.91	0.94	57.60	30.65	10.54	0.00	7.34	172.74	0.88	0.00	0.55	45382.90	1242.48	1542.98	26317.74	1449.06
MRT1	Mean	13.25	0.69	1.03	12.15	41.16	2.59	0.06	13.68	30.09	0.73	8.34	0.17	1706.46	532.23	75.84	782.44	272.22
	SD	11.28	0.29	0.41	6.14	41.18	1.06	0.08	10.64	7.97	0.54	19.65	0.07	864.12	473.31	40.23	199.75	259.65
MRT2	Mean	16.29	4.00	1.08	40.59	27.58	4.49	0.25	21.88	53.64	0.60	2.15	0.19	8180.01	2760.95	541.06	6677.25	954.15
	SD	19.73	1.45	0.41	38.05	38.37	2.20	0.31	21.58	22.25	0.29	3.13	0.07	4015.92	617.47	307.62	3083.94	429.47
MRT3	Mean	8.72	4.79	1.19	25.81	33.90	17.81	0.20	18.90	49.13	0.59	2.40	0.24	9740.55	2977.14	669.44	7131.17	1243.47
	SD	10.75	2.12	0.25	42.19	63.59	33.22	0.22	13.06	16.58	0.18	4.08	0.05	5346.00	800.52	456.35	3403.08	643.95
MRT4	Mean	111.35	10.06	5.39	69.17	194.98	13.22	1.74	32.55	127.09	1.32	16.72	0.74	27074.58	4761.86	2304.27	27461.10	2260.22
	SD	101.83	4.34	4.25	49.79	202.66	6.49	3.32	30.48	63.82	1.09	32.77	0.43	17569.27	2015.90	1719.34	21316.53	1279.96
MRT5	Mean	16.80	16.11	2.33	226.55	499.64	42.21	0.00	17.45	213.21	1.15	17.05	0.88	63812.68	2898.03	3673.40	51244.95	2745.99
	SD	22.89	20.10	1.20	402.22	985.09	48.23	0.00	19.80	115.04	1.22	40.26	0.93	53667.53	1014.38	3574.79	62677.77	1637.96
MRT6	Mean	40.11	32.41	7.98	258.98	540.91	38.64	0.00	214.49	549.10	4.83	17.14	2.67	105157.85	3648.46	5880.70	89815.73	3904.37
	SD	53.69	20.68	4.64	439.97	419.90	16.73	0.00	353.06	239.69	2.53	35.16	1.93	73008.43	1148.01	3932.49	71804.61	1620.78
MRT7	Mean	266.85	40.88	6.82	64.81	397.69	136.76	0.13	50.03	407.62	2.97	0.51	1.72	146169.93	4140.16	5951.50	96053.52	3175.91
	SD	449.41	29.57	4.59	37.73	337.76	137.46	0.31	83.02	281.76	1.52	1.25	0.95	112848.30	1433.78	4541.98	86878.59	1167.99
GWT1	Mean	51.07	19.96	3.57	59.88	215.15	13.56	0.16	27.01	218.14	2.12	11.29	1.00	71820.79	1898.41	2823.69	42038.96	2601.32
	SD	48.83	7.95	1.36	61.55	93.81	3.30	0.38	33.41	122.00	1.38	18.70	0.52	34893.95	1055.18	1203.94	20459.75	1032.10

Table S2-6: Land-cover data used to assess land-use stressors at four spatial scales, where abbreviated The FRAGSTATS and topographic predictors are denoted using the following abbreviations: P. = percentage of landscape (PLAND), C. = patch cohesion index (COHESION), Agri = agriculture, SD = standard deviation, SB = sub-basin, CB = cumulative-basin, 100CB = 100m cumulative riparian buffer.

Sub-basin scale																
Sites	**P.Agri**	**C.Agri**	**P.Urban**	**C.Urban**	**P.Fallow**	**C.Fallow**	**P.Dams**	**C.Dams**	**P.Mining**	**C.Mining**	**P.Natural**	**C.Natural**	**Mean slope (degree)**	**Slope SD**	**Mean elevation**	**Elevation SD**
STK1	0.00	0.00	0.00	0.00	0.00	0.00	0.00	0.00	0.00	0.00	100.00	100.00	9.65	4.52	1664.65	58.83
STK2	9.97	96.74	0.11	24.06	0.75	92.28	0.07	73.81	0.00	0.00	89.10	99.93	7.63	3.72	1567.98	76.56
STK3	7.98	94.93	1.20	77.35	7.90	96.31	0.02	49.84	0.00	0.00	82.90	99.96	7.23	5.00	1491.71	112.76
STK4	6.50	96.99	1.28	84.15	1.54	95.66	2.30	98.19	0.06	83.11	88.33	99.98	7.66	5.76	1466.00	151.47
STK5	12.67	95.22	3.81	92.31	13.05	96.65	0.05	51.42	8.48	98.00	61.93	99.48	5.60	5.55	1312.67	97.54
STK6	10.02	94.92	31.05	98.02	21.23	97.08	0.21	74.71	5.59	90.86	31.90	97.62	1.91	1.94	1187.23	19.25
STK7	15.67	97.18	1.97	91.25	23.95	98.50	0.07	73.82	16.30	98.03	42.05	99.58	3.20	4.91	1224.41	70.36
MRT1	0.00	0.00	0.00	0.00	0.00	0.00	0.00	0.00	0.00	0.00	100.00	100.00	10.90	5.98	1581.16	96.05
MRT2	18.72	97.57	2.68	91.83	2.24	95.75	0.02	65.72	0.00	0.00	76.34	99.87	7.19	6.58	1356.13	117.16
MRT3	25.36	97.64	16.04	97.00	8.02	94.78	0.00	0.00	0.21	81.41	50.38	98.03	4.46	4.16	1296.29	99.73
MRT4	26.07	97.83	2.26	82.09	12.20	97.49	0.05	45.58	5.67	95.62	53.75	99.40	4.48	5.65	1295.54	128.32
MRT5	7.88	96.00	5.03	95.38	9.99	97.43	0.45	94.51	6.30	97.28	70.35	99.88	5.23	5.41	1322.17	158.43
MRT6	15.86	96.37	1.90	82.60	12.39	97.02	0.02	45.65	31.78	98.50	38.05	99.14	2.41	3.29	1195.52	31.32
MRT7	12.34	97.34	2.28	95.89	24.25	98.62	0.01	42.80	11.77	97.34	49.35	99.50	2.73	4.42	1175.40	25.22
GWT1	24.83	99.02	4.18	97.96	8.66	98.66	0.24	94.62	1.81	91.29	60.27	99.83	2.39	3.49	1134.44	31.01

Table S2-6 continued

Cumulative scale															
Sites	**P.Agri**	**C.Agri**	**P.Urban**	**C.Urban**	**P.Fallow**	**C.Fallow**	**P.Dams**	**C.Dams**	**P.Mining**	**C.Mining**	**P.Natural**	**C.Natural**	**Mean slope (degree)**	**Slope SD**	**Mean elevation**	**Elevation SD**
STK1	0.00	0.00	0.00	0.00	0.00	0.00	0.00	0.00	0.00	0.00	100.00	100.00	9.65	4.52	1664.65	58.83
STK2	8.72	96.70	0.09	24.05	0.66	92.24	0.06	73.78	0.00	0.00	90.47	99.93	7.88	3.89	1580.13	81.17
STK3	8.04	95.58	1.09	77.19	7.13	96.34	0.03	57.38	0.00	0.00	83.71	99.97	7.31	4.89	1501.70	113.19
STK4	7.39	96.31	1.17	80.85	4.69	96.21	1.01	97.78	0.05	83.95	85.70	99.98	7.46	5.29	1486.05	132.05
STK5	7.99	96.10	1.48	85.11	5.65	96.26	0.90	97.60	1.05	97.37	82.92	99.96	7.24	5.35	1465.86	140.12
STK6	8.15	96.01	3.59	93.75	6.80	96.45	0.85	97.32	1.37	96.70	79.25	99.93	6.86	5.36	1445.73	153.06
STK7	11.17	96.71	2.94	94.14	13.69	98.31	0.54	96.42	7.38	98.00	64.28	99.88	5.39	5.49	1356.73	166.67
MRT1	0.00	0.00	0.00	0.00	0.00	0.00	0.00	0.00	0.00	0.00	100.00	100.00	10.90	5.98	1581.16	96.05
MRT2	14.80	97.46	2.15	91.88	1.79	95.70	0.02	65.70	0.00	0.00	81.25	99.90	7.97	6.63	1403.23	145.56
MRT3	16.37	97.80	4.31	96.48	2.77	95.71	0.01	65.68	0.10	87.67	76.43	99.80	7.43	6.44	1386.70	144.77
MRT4	20.98	98.02	3.40	93.99	7.24	97.24	0.03	50.20	2.70	95.41	65.64	99.86	6.04	6.25	1343.49	144.36
MRT5	15.13	97.72	4.12	95.20	8.48	97.35	0.22	92.72	4.32	96.65	67.72	99.91	5.67	5.90	1333.87	151.20
MRT6	15.18	97.60	3.86	94.84	8.94	97.33	0.20	92.42	7.28	97.91	64.53	99.90	5.32	5.77	1318.99	149.48
MRT7	14.71	97.56	3.57	94.89	11.66	97.88	0.17	92.11	8.10	97.83	61.80	99.90	4.86	5.64	1293.24	146.61
GWT1	15.24	97.91	3.43	95.38	11.93	98.19	0.34	95.31	11.93	98.19	62.56	99.94	4.58	5.33	1288.25	164.01

Table S2-6 continued

Riparian sub-basin 100 m buffer																	
Sites	**P.Agri**	**C.Agri**	**P.Urban**	**C.Urban**	**P.Fallow**	**C.Fallow**	**P.Dams**	**C.Dams**	**P.Mining**	**C.Mining**	**P.Natural**	**C.Natural**	**Mean slope (degree)**	**Slope SD**	**Mean elevation**	**Elevation SD**
STK1	0	0	0	0	0.00	0.00	0.00	0.00	0	0	100.00	100.00	12.59	5.47	1589.61	45.07
STK2	9.85	84.72	0.30	20.36	0.00	0.00	0.00	0.00	0	0	89.86	99.86	6.84	4.00	1480.65	29.84
STK3	8.83	91.26	0.33	45.37	11.21	94.19	0.08	54.66	0	0	79.55	98.77	7.21	5.31	1403.87	60.34
STK4	4.07	88.73	1.03	71.69	1.91	92.98	12.38	98.34	0	0	80.60	99.09	7.38	6.76	1351.61	76.39
STK5	14.01	89.35	4.53	84.29	16.30	93.00	0.20	51.42	3.37	92.58	61.60	98.09	4.50	3.50	1268.54	67.80
STK6	2.68	87.77	26.18	96.05	6.96	86.81	0.30	74.36	0	0	63.88	97.98	2.73	1.66	1179.12	16.75
STK7	8.02	90.98	0.12	29.34	25.63	95.20	0.18	73.01	20.17	94.75	45.88	97.12	2.69	4.48	1189.31	27.39
MRT1	0	0	0	0	0.00	0.00	0	0	0	0	100	100	10.38	7.06	1490.41	61.33
MRT2	21.75	94.98	3.25	93.45	6.22	92.30	0.01	0.00	0	0	68.77	98.65	5.93	6.56	1267.39	56.71
MRT3	37.50	95.49	19.59	94.21	17.08	94.17	0.00	0.00	0.03	0.00	25.81	91.65	1.98	1.50	1218.40	26.53
MRT4	19.27	91.63	2.75	85.28	17.94	95.23	0.13	51.39	7.09	87.86	52.82	95.77	2.47	2.28	1234.93	52.94
MRT5	6.67	88.47	3.86	87.53	15.50	95.28	1.92	94.04	5.25	93.94	66.80	98.89	4.24	5.18	1250.15	86.07
MRT6	7.33	91.53	0.06	21.94	4.96	87.79	0	0	25.03	97.46	62.63	98.72	2.16	1.96	1176.09	27.73
MRT7	5.04	87.65	0.24	50.53	25.03	97.46	0.04	50.50	6.63	93.00	62.96	98.75	1.78	2.95	1151.71	18.51
GWT1	13.92	94.84	2.67	95.92	9.09	96.55	0.99	92.98	0.11	55.10	73.23	99.51	1.80	1.73	1113.30	23.07

Table S2-6 continued

Riparian cumulative 100 m buffer																
Sites	**P.Agri**	**C.Agri**	**P.Urban**	**C.Urban**	**P.Fallow**	**C.Fallow**	**P.Dams**	**C.Dams**	**P.Mining**	**C.Mining**	**P.Natural**	**C.Natural**	**Mean slope (degree)**	**Slope SD**	**Mean elevation**	**Elevation SD**
STK1	0.00	0.00	0.00	0.00	0.00	0.00	0.00	0.00	0.00	0.00	100.00	100.00	12.59	5.47	1589.61	45.07
STK2	7.47	84.55	0.22	20.30	0.00	0.00	0.00	0.00	0.00	0.00	92.30	99.90	8.33	5.11	1507.13	57.84
STK3	8.53	90.45	0.32	44.19	9.98	93.83	0.07	54.64	0.00	0.00	81.09	98.83	7.34	5.29	1415.98	68.60
STK4	6.82	90.16	0.62	64.86	6.67	93.95	4.94	97.88	0.00	0.00	80.95	98.93	7.35	5.91	1390.41	78.36
STK5	7.61	89.59	1.09	73.75	7.99	93.22	4.36	97.75	0.45	91.64	78.50	98.84	6.98	5.74	1374.77	87.22
STK6	7.20	89.55	3.45	90.59	7.90	92.67	3.92	97.60	0.37	91.48	77.16	98.69	6.58	5.63	1356.14	101.05
STK7	7.53	90.14	2.07	89.66	15.15	94.51	2.44	97.16	8.37	94.41	64.43	98.20	5.00	5.53	1288.48	114.37
MRT1	0.00	0.00	0.00	0.00	0.00	0.00	0.00	0.00	0.00	0.00	100.00	100.00	10.38	7.06	1490.41	61.33
MRT2	16.18	94.87	2.26	92.90	4.65	92.76	0.01	0.00	0.00	0.00	76.90	99.28	7.06	6.97	1323.67	112.84
MRT3	21.40	94.69	7.22	93.43	7.74	92.68	0.01	0.00	0.00	0.00	63.64	98.74	5.74	6.44	1296.52	108.33
MRT4	20.51	93.44	5.16	91.06	12.52	94.62	0.06	48.86	3.32	87.33	58.42	97.60	4.21	5.21	1267.76	92.19
MRT5	14.03	92.45	4.48	89.80	13.84	94.75	0.94	93.11	4.23	90.92	62.47	98.20	4.22	5.20	1259.39	89.75
MRT6	13.42	92.35	4.12	89.57	13.17	94.56	0.86	93.07	6.08	93.34	62.36	98.27	4.03	5.03	1251.98	89.24
MRT7	12.20	92.04	3.61	89.40	14.67	94.33	0.74	92.92	6.20	93.23	62.58	98.39	3.71	4.85	1237.82	90.02
GWT1	10.60	92.28	2.76	90.45	13.74	94.59	1.51	95.90	5.90	93.77	65.49	98.56	3.88	4.89	1234.48	113.50

Chapter 3 – Pollutant source identification in a platinum belt headwater catchment: A comparative geospatial assessment of dissolved and sediment-bound metals

3.1. Abstract

Land-use stressors contribute to trace metal accumulation in both water and sediment of aquatic ecosystems. However, South African national river health assessments currently rely solely on dissolved metal monitoring, overlooking the potential of sediment analysis as a cost-effective, time-integrated complement to overcome potential limitations of water sampling. For this study water and sediment samples were collected in the dry and wet seasons from 14 river study sites in the Gwathle River Catchment in the Platinum Belt of South Africa. Using a multi-spatial scale approach, this study assessed the ability of chromium (Cr) and zinc (Zn), both analysed using separate analytical techniques being inductively coupled plasma mass spectrometry ICP-MS for dissolved and energy dispersive X-ray fluorescence (EDXRF) sediment media, to disentangle catchment stressors. In addition, the complementarity and agreement (evaluating concordance) of each metal sampled from its respective media to consistently track terrestrial stressor effects along river continua were analysed. Seasonal analyses revealed significantly higher dissolved Cr in the dry season, while no significant differences were observed for dissolved Zn. In addition, there were no significant seasonal differences in either sediment-bound Cr or Zn. Statistical modelling revealed that dissolved Cr and sediment-bound Cr are best predicted by cumulative mining impacts, whereas dissolved Zn with sub-basin lithology and sediment Zn with combined urban and lithological factors. Spatial concordance analysis revealed substantial agreement between water and sediment Cr signals along land-use intensification gradient, suggesting its conservative geochemistry enables effective multi-media source tracking. Conversely, Zn showed negligible phase concordance, indicating dissimilar dissolved versus particulate behaviour. The strong performance of Cr across water and sediment suggests that paired sampling comprehensively traces pollution along an intensification gradient. Notably, metal accumulation in sediments provides a stable, integrative record, potentially reducing logistical burdens of transient water sampling. The incorporation of EDXRF sediment monitoring would enhance river health programs, delineating persistent catchment contamination cost-effectively. Establishing a national sediment monitoring protocol to complement water analysis can optimize the detection of metal pollution and guide targeted mitigation, thereby achieving water quality objectives.

3.2. Introduction

Societies and ecosystems depend on headwater streams for the provision of clean water. The integrity of these systems, however, faces a multitude of threats from the inputs of nutrients, sediments, organic and inorganic chemicals that degrade river water quality worldwide (Vörösmarty et al., 2010). Of the inorganic chemical contaminants and trace metals constitute a major hazard to global freshwater quality, posing risks to human and ecosystem health (Nriagu and Pacyna, 1988; Kolarova and Napiórkowski, 2021). Though lithogenic in origin, metals such as Cu, Fe, Zn and Ni can accumulate to toxic levels in aquatic ecosystems in response to human activities (i.e. stressors) (Jaishankar et al., 2014). Yet these same metals at low levels are requisite constituents for aquatic flora and fauna (Laha et al., 2022). An array of stressors, often associated with improper waste management strategies, introduce metal pollution to river systems; these include mining, industrial effluents, automotive discharges, agriculture, and domestic sources (Förstner and Wittmann, 2012).

With multiple inorganic pollution sources, recent investigations have reported a rise in aquatic metal pollution globally (Kodikara et al., 2022), with heightened attention among researchers highlighting the alarming extent of metal pollution in South African aquatic systems (Dalu et al., 2017; Erasmus et al., 2020). Such pollution threatens the preservation of ecosystem integrity and, thus, is a major challenge for freshwater resource management, governance and policy (Balaram et al., 2023). This is owing to the non-degradable and persistent nature of metals in water and riverine sediments having the potential to lead to food web biomagnification through dietary uptake, absorption and uptake across gills of aquatic biota (Gurrieri, 1985; Amundsen et al., 1997). Prolonged exposure can result in acute adverse health effects at higher aquatic trophic levels, with the potential to damage organs, disrupt metabolic functions, and thus disrupt aquatic ecosystem functionality which has cascading effects downstream (Singh and Kalamdhad, 2011).

While high-order rivers generally experience a higher number of stressors, accumulating contaminants from larger catchments, headwater streams with fewer stressors have a small surface-edge ratio, making these streams particularly vulnerable to metal contamination (Siziba et al., 2021). This is especially true for streams within the South African Bushveld Igneous Complex (BIC), which experience extensive mining activities and their supportive industries (Almécija et al., 2017). The South African BIC contains approximately 80% of the global platinum group elements (PGE) metal deposits and is a source of Pt, Pd, Ru, and Ir to name a few (Crowson, 2001; Thormann et al., 2017). The PGE-rich layers are also strongly associated with chromitite rock, which contains elevated Cr as well as Cu-Ni (Barnes and Maier, 2002). Identifying metal pollution sources can assist resource managers to elucidate with greater specificity the contributing sources and pathways of contaminants into headwaters to guide targeted mitigation efforts (Albuquerque et al., 2021; Laha et al., 2022; Balaram et al., 2023). The complex topography of these headwaters, their smaller size, and restricted accessibility also make these streams challenging to monitor on a continuous basis.

In the last four decades, inductively coupled plasma mass spectrometry (ICP-MS), has become a prevalent technique globally for rapidly monitoring dissolved metals in river water samples (Yuan et al., 2004; Balaram et al., 2023). It offers a highly sensitive approach to detect transient (snapshot) signals of dissolved metals in aquatic environments, that can discern between key anthropogenic stressor inputs (Gafur et al., 2018; Erasmus et al., 2020; Kodikara et al., 2022). Due to being a relatively rapid and sensitive technique, ICP-MS is commonly used in South Africa to assess dissolved metals in aqueous river samples. The technique is routinely employed in management at both catchment and national scales, contributing information towards national river health monitoring programmes for adaptive management and policy, while also being used for academic research purposes (Atangana and Oberholster, 2021). In addition, this analytical technique has proved effective at assessing metal pollution and associating such to spatial stressor patterns in heterogeneous South African catchments (Marara and Palamuleni, 2020).

Energy dispersive X-ray fluorescence (EDXRF) technique has the capability to rapidly screen metal pollution in riverine sediments, identifying contamination sources across heterogeneous catchments. The ability of streambed particulates to sorb trace metals, binding them within organic matter and oxide fractions (Wang et al., 1997; Devesa-Rey et al., 2010), along with depositional processes buffering deeper sediment layers from high flows (Ciszewski and Grygar, 2016), enables these sediments to serve as time-integrated reservoirs of landscape metal contamination (Förstner and Müller, 1981). Although sediment-bound trace metals can be analysed rapidly, sediment it is not yet integrated into any South African catchment and national river health programs for trace metal monitoring. Through their time-integrated nature, sediment may complement water sampling, providing a comprehensive portrayal of catchment contamination. International studies have employed the XRF technique in freshwater ecosystem studies (Mahommed and Makundi, 2002; Loannides et al., 2015), particularly on benthic river sediments (Islam et al., 2016; Laha et al., 2022) as a means to link the pollution to the stressor (Hurley et al., 2017; Albuquerque et al., 2021). Far fewer peer-reviewed studies have examined its potential to discern sources of stress in South African mixed-use river catchments.

The ability of each sample type (i.e. water and sediment) to identify transient versus residual sources of metal pollution (stressors) in a multi-user catchment, may depend on the spatial scale of the stressors assessed in relation to the study site. This is because natural, spatially variable ecohydrological controls on effluent transport can be further modified by catchment-scale human activities (King et al., 2005; Shen et al., 2015). For example, the transient dissolved metal signals may dissipate unequally between sampling points along a river continuum due to variable precipitation and surface-ground water interactions, human dewatering activities, sedimentation and biological uptake patterns (Bridgestock et al., 2022; Fernández-Auso et al., 2023). In contrast, the sediment-bound metals may be affected by various transport dynamics (e.g. water velocity), sediment and organic loading, as well as streambed heterogeneity (Förstner and Müller, 1981). A multi-spatial scale assessment is thus essential when assessing potential agreement between sample (i.e. media) types (i.e. similar spatial detection patterns), as the spatial variability of the ecohydrological processes may strongly influence the relative detectability of dissolved and sediment-bound metal between study sites, thereby affecting the relative utility of the two.

This study aimed to track the movement of pollutants across a catchment by conducting a comparative geospatial assessment of dissolved and sediment-bound metals. Comparative analysis between dissolved and sediment-bound metals was used to assess their effectiveness and complementarity in tracking metal pollution in aquatic ecosystems across a land-use intensification gradient. The specific objectives were to: 1) assess wet and dry seasonal variation in metal concentrations in both sample types (water and sediment), 2) identify at which spatial scale each sample type best predicts trace metal concentrations as a function of land-use and geology, 3) evaluate agreement and consistency between the sample types parsimonious statistical model outputs. Meeting these objectives would elucidate the complementary strengths of the two sample types for discernment of anthropogenic metal pollution sources and inform water resource managers of potential scenarios where its suitable to employ each in particular combinations.

3.1. Methodology

3.2.1. Study area

The Gwathle River Catchment (Quaternary catchment A21K) is part of the larger Limpopo Water Management Area and drains the northern slopes of the Magaliesberg Mountain range between the towns of Rustenburg and Mooinooi, in the North West Province, South Africa. The catchment receives on average, ~629 mm of rainfall per year, with the typical wet season being between November to March and the dry between April to October (Funk et al., 2015). The minimum and maximum air temperatures range between 4.94°C and 31.76°C, with June and February being the coolest and warmest months, respectively (SAWS, 2023). Three rivers drain the catchment. Two are third-order rivers, being the Sterkstroom (sites STK1-7) drained to the West and the Maretlwane (sites MRT1-7) to the East, before forming a confluence to form the fourth order Gwathle River draining South into Roodekoppies Dam (**Figure 1-1**).

The catchment experiences a stepped progression of stressors from the pristine headwater reaches, beginning with commercial irrigated agriculture and livestock rearing, followed by urban and informal settlements, chromium and platinum mining as well as mine supportive industry activities, including smelters (**Figure 1-1**), with the study sites stressor details presented in **Table 3-2** (placed in Results). The upland quarzitic and minor-shale reaches of the catchment (**Figure 2-2**) are partially contained within the Magaliesberg Biosphere Reserve; an area designated for ecotourism and sustainable development under the UNESCO Man and Biosphere Programme (Pool-Stanvliet, 2013). The lowland reaches traverse the Western lobe of the Bushveld Igneous Complex, and in particular both the Merensky Reef and the Upper Group 1 and 2 layers, which together form the most continuous layer among the Complex and contain the world’s richest PGE deposits (Von Gruenewaldt et al., 1986).

This Complex provides ~75% of global platinum production and ~50% of the global chromite production (Almécija et al., 2017). The Lower Group 6 (LG-6) layer in the Western Limb is the most exploited chromitite layer and has a Cr_2O_3 content of 46-47% (Von Gruenewaldt et al., 1986; Schürmann et al., 1998). In addition, chromium content of chromitite layers are known to decrease upwards, while vanadium increases with concentration of two wt.-% V_2O_5 (Schürmann et al., 1998; Nikonow et al., 2023). The mafic-ultramafic layered intrusion in the lowlands of the study area contains gabbro and norite rock layers interspersed with anorthosite bands, among other lithological units (**Figure 2-2**; excluding the GWT1 site from this chapter).

3.2.2. Land-cover class (stressor) determination

The stressor (land-use) data for the study area were obtained from the 2020 South African National Land Cover dataset (SANLC; GeoTerraImage, 2021). This ~20 m resolution product was derived from Sentinel-2 satellite imagery using a robust classification approach, resulting in high accuracy (Kappa Index >0.85). To characterise key catchment stressors, level 1 land-use classes within the Gwathle catchment were reclassified into three aggregated stressor categories: (1) cultivated land (commercial and annual crops), (2) urban (residential, smallholdings and commercial areas), and (3) mining (extraction pits as well as wet and dry tailings facilities). These aggregated stressor classes representing major catchment stressors were processed using ArcGIS 10.5 software. Thereafter, the class-level Percentage of Landscape (PLAND) metric was derived in the computer software FRAGSTATS 4.2 (McGarigal et al., 2002), indicating each stressor's proportion at the respective hydrological spatial scales.

3.2.3. Spatial scale delineation

The spatial design of this study enabled stressor effects on the aquatic ecosystems to be assessed at a (1) sub-basin scale as well as the (2) cumulative basin scale. For the sub-basin scale, each basin's extent was defined by the location of its respective study site (outlet location) and that of the study site immediately upstream on the same river. The cumulative catchment extent for each study site was defined from the outlet location of each study site, whereby including the rivers entire upstream catchment area, resulting in a nested hierarchy with the downstream sites reflecting the sum of the upstream sub-basins. Each sub-basin and cumulative basin was delineated using the Spatial Analyst tools in ArcGIS 10.5. The reclassified landscape stressor layers from the SANLC were clipped to each of the new spatial layers (i.e. scales) using the ArcGIS Data Management Tool to obtain spatial scales containing the proportions of the different stressors.

3.2.4. Catchment geology

As the study area falls within the Bushveld Igneous Complex, there are mafic and ultramafic intrusions, referred to as the Rusternburg Layered Suite, containing concentrated mineralization that outcrop at or near the surface across portions of the catchment (Barnes and Maier, 2002; Cawthorn, 2010). For example, the Middle Group chromitite layers, also consisting of pyroxenite, norite, anorthosite are well developed just north of the towns of Mooinooi and Marikana, leading to outcrops on old fallow and agricultural lands as well as in the riparian zones of the Sterkstroom and Maretlwane rivers (Von Gruenewald et al., 1986). Background weathering and erosion processes of ore-bearing lithologies, particularly by river water, have been identified in a neighboring river catchment to contribute to PGE concentrations in benthic river sediment (Almécija et al., 2017). To therefore account for these potentially confounding natural contributions in the statistical modelling and isolate the effects of stressor activities on metal concentrations in solution and deposited, lithostratigraphic geological data was obtained for each spatial scale using the South Africa 250k Litho-Chronostratigraphic layer in ArcGIS 10.5 (Council for Geoscience, 2017).

3.2.5. Sample collection and analytical procedure

A total of 14 river sampling sites were established across the catchment, with seven on the Sterkstroom River and seven on the Maretlwane River, with the aim of capturing a range of natural and stressor variability, including informal-formal urban, agriculture and mining stressors in a stepped progression from upstream to downstream. Each sampling site along the two investigated rivers was visited and samples were collected in April 2021 for the wet season and September 2021 for the dry season.

Water samples were collected from the top 30 cm of the active river channel at each site (Akyildiz and Duran, 2021). Samples were filtered through Supor® 0.45 µm filters using a Thermo Scientific Nalgene reusable filter unit and stored in 200 mL acid-rinsed polyethylene bottles. Samples were kept in cold storage and transported to the laboratory for further analysis. Analysis focused on V, Cr, Ni and Zn as these metals are found naturally enriched in the Bushveld Igneous Complex and represent common stressor pollutants associated with mining activities (Almécija et al., 2017). Metal concentrations were analysed using ICP-MS (Agilent 7800x), with concentrations measured against external reference standards. A Thermo Scientific ORION STAR A322 was used to assess if samples had total dissolved solids exceeding 120 mg/L. If so, these samples were diluted with Millipore water, before all samples were acidified with ultrapure HNO_3. The analytical precision of the ICP-MS results are presented in **Table 3-1**.

For sediment, two to three replicate samples were collected ~10 m apart, where permitting, to account for potential within-reach heterogeneity in grain size and varied depositional processes influencing metal accumulation at each sampling site. To minimise potential PGE inputs from vehicle exhaust catalytic converters, samples were collected > 10 m away from roads (Almécija et al., 2017). Sediment samples were collected from the top 5 cm of the river benthos using a square graduated plastic shovel, best representing the recent surface deposition and greatest influence from potential stressor sources of trace metals (Laha et al., 2022). The sediment replicates were collected and stored separately in unused labelled polyethylene plastic bags and stored frozen until further laboratory possessing.

In the laboratory, the sediment samples were defrosted and wet sieved with deionized water using a 125 µm metal soil sieve (Rocha et al., 2015). The <125 µm fraction was then homogenized into fine powder using a ball mill. Homogenized powders were placed into pre-weighed crucibles and combusted at ~550 °C for four hours to remove organic matter. Combusted powders were transferred to clean polyethylene sample cups and analysed for major oxides (SiO_2, Al_2O_3, $Fe2O_3$, CaO, K_2O, TiO_2) and trace elements (V, Cr, Ni and Zn) were measured by X-ray fluorescence spectrometry (XRF) using a Bruker Ranger S2 instrument, with the analytical precision of the results presented in **Table 3-1**. The instrument was calibrated using a suite of geologic reference materials, including both locally-sourced rock standards as well as standards from the U.S. Geological Survey, including Andesite Geochemical Standard and Granodiorite Geochemical Standard. Concentrations were typically within 10% of accepted values.

Table 3-1: The analytical precision of the ICP-MS and EDXRF trace metal results. Andesite Geochemical Standard (AGV-2) and Granodiorite Geochemical Standard (GSP-2) were the two reference materials used to evaluate the analytical precision of the EDXRF results.

Method	Precision	Cr	Zn	V	Ni
ICP-MS	%RSD	4.29	2.38	5.11	4.27
EDXRF	% RSD AGV-2	2.20	0.40	1.60	3.80
	% RSD GSP-2	1.60	1.50	0.60	3.00

3.2.6. Data processing

To account for differences in sediment mineralogy and grain size between sites, metal enrichment factors (EF) were calculated using titanium oxide (TiO_2) as a conservative background or baseline reference material, collected from local pristine river sediment samples (Abrahim and Parker, 2008). The standardization approach was achieved using the following equation:

$$EF = (\text{Metal}/TiO_2)_{\text{sample}} / (\text{Metal}/TiO_2)_{\text{reference}}$$

Standardizing to enrichment factors using local background values minimises variability unrelated to pollution, enabling comparisons of metal contamination signals across river sites with diverse streambed composition to discern metal pollution signals across the river continua (Barbieri, 2016; Gregory et al., 2019).

3.2.7. Statistical analysis

To reduce potential redundancy in comparative analyses, multi-collinearity among each of the trace metals within their respective techniques was removed using the `findCorrelation` function in the R caret package (where $r > 7$), in R version 4.3.1 (Kuhn, 2008; R Core Team, 2023). Spearman rank correlation matrices were computed using the Hmisc package (Harrell and Dupont, 2023) to identify the retained trace metals that were highly correlated with the excluded metals. To assess the seasonal variability in trace metal concentrations between the wet and dry seasonal flows, analysis of variance (ANOVA) tests were performed on generalised linear mixed effect models (GLMMs) for each technique-derived trace metal with ‘site’ as a random effect. The GLMMs were constructed using the lme4 R package (Bates et al., 2015).

gamma distribution with log-link function was specified due to the positive, skewed distribution of trace metal data.

To determine at which spatial scale each sample medium (water and sediment) best predicts trace metal concentrations as a function of land-use (i.e. capturing stressor effects) across the intensification gradient, the uncorrelated trace metal concentrations from ICP-MS and EDXRF were modelled using GLMMs. The GLMMs offer the appropriate approach given the non-normal distribution of trace metal data while accounting for the nested sampling by site (i.e. for the cumulative scale analysis). Metal concentrations were modelled as a function of each stressors proportion (%cultivated, %urban, %mining) at the respective spatial scale assessed. Geological type was added to account for potentially confounding lithostratigraphic factors, season as a fixed effect, and site as a random effect; all with additive terms.

Separate spatially explicit GLMMs were constructed at both sub-basin and cumulative basin scales for Cr and Zn from each sample medium (water and sediment), generating a total of eight GLMMs (see **Figure 3-1** for the simplified analysis workflow for one metal). The most parsimonious model for each of the eight GLMMs (the simplest model with the best fit) was sought using the dredge function from the MuMIN package (Barton, 2010). Comparing between candidate parsimonious models for each media-derived metal at their respective spatial scales, the simplest yet most informative model was selected and retained based on the lowest Akaike's Information Criterion with small-sample correction (AICc) value. This thereby indicating the spatial scale at which the stress(ors) and/or confounding lithology best drives variation in each media-derived metal (**Figure 3-1**). This process resulted in two retained parsimonious models for each metal (i.e. one model retained per media), resulting in four total models retained models for the two metals (Cr and Zn). The goodness of fit for the retained models were then determined using the marginal R^2 ($R^2_{GLMM(m)}$; the variance explained for by the fixed factors) and the conditional R^2 ($R^2_{GLMM(c)}$; the variance explained by both fixed and random factors) coefficients using the `r.squaredGLMM` function in the MuMIN package (Wanderi et al., 2022).

To elucidate spatial trends (i.e., spatial detection patterns relative to stressor locations) and visualise agreement between the like-trace metals analysed via the two analytical techniques, predicted values (estimates of concentration and EF) from the parsimonious GLMMs were averaged across seasons. These averaged values were then graphically depicted on line graphs with dual y-axes, one for each metal for each river continuum. Arrows were annotated on the line graphs to denote the location of stressors upstream of sampling sites relative to trace metal fluctuations. Using the retained GLMM model predictions in visual and statistical analysis (**Figure 3-1**) is advantageous, as it minimises the influence of confounding factors, as well as site-specific variability and differences in sampling seasons between sample types. This approach ultimately harmonizes the data enabling the comparison of estimated values from the two different analytical techniques along the river continua (Gelman and Hill, 2006).

Concordance correlation coefficient analysis (Lin, 1989) was performed to assess agreement and consistency quantitatively (evaluates congruence) between predicted values of the same metal derived from water versus sediment samples (**Figure 3-1**). As a reproducibility index, the analysis provides information on both precision and accuracy to determine whether the two sample types produce consistent estimates of trace metal trends along the river continua (Lin, 1989). The concordance correlation coefficient (CCC) assesses correlation and bias, where ρ = 1 would indicate both techniques capture similar longitudinal trends ('almost perfect concordance'), while lower values suggest larger discrepancies (Landis and Koch, 1977).

The average difference between ($\bar{d}$) the two trace metals from the two sample types as well as the standard deviation of the differences between the two sample types (ΔSD) were assessed. A smaller $\bar{d}$ and closer ΔSD range reflect a stronger absolute agreement between the analytical techniques (Stevenson et al., 2023). A bias correction factor (C_b) was reported, as it measures the deviation of the best-fit line from the ideal 45° line of perfect concordance, where values range from 0 to 1, where 1 indicates no deviation (Lin, 1989). The scale shift (υ) measure, indicates if one method is consistently higher/lower than the other, where a positive value indicates the one method is consistently higher and a negative value, indicating consistently lower.

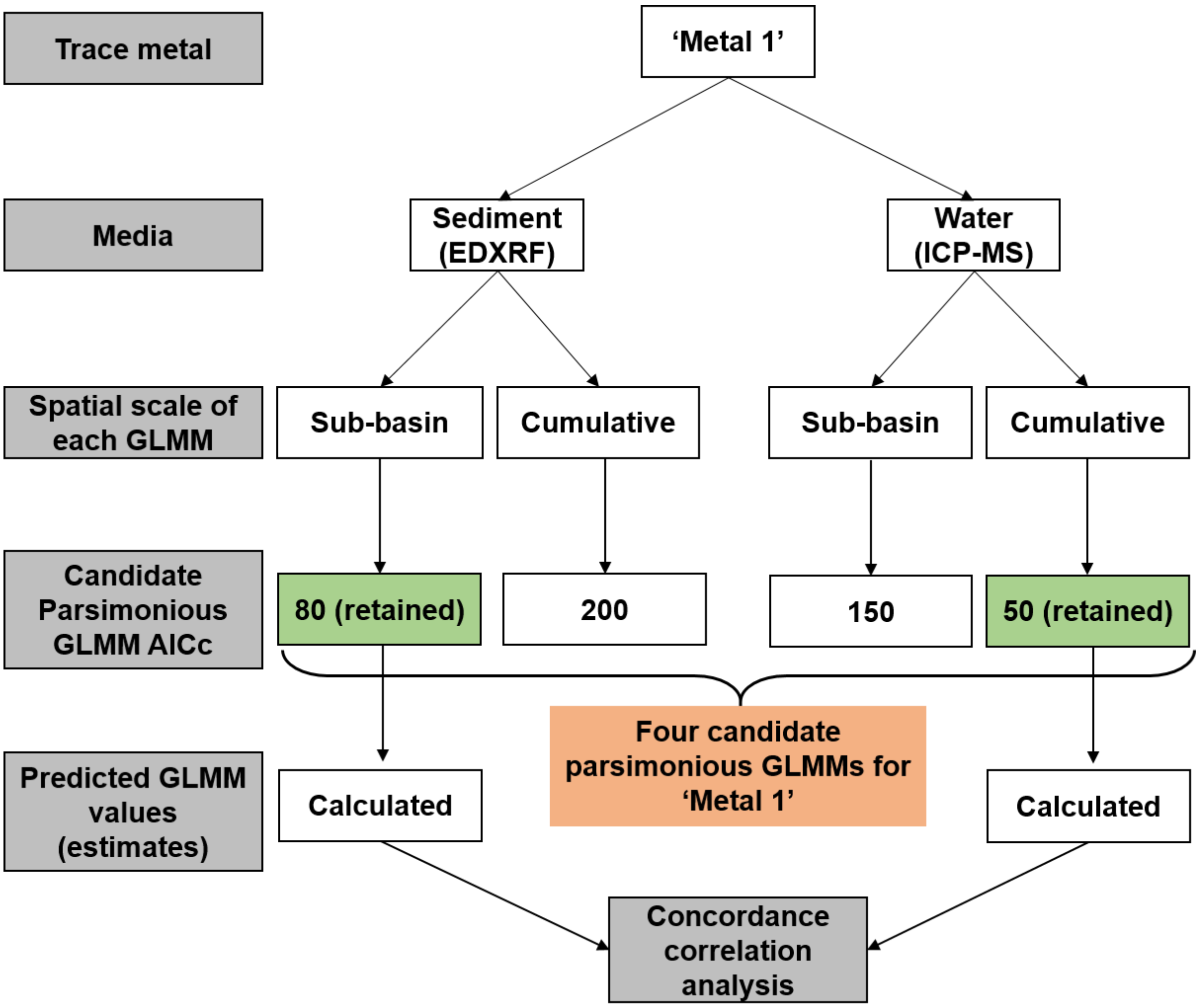

Figure 3-1: Simplified analysis workflow used to derive four candidate parsimonious generalised linear mixed effects models (GLMMs) per trace metal (orange shaded block) from sediment and water, analysed via EDXRF and ICP-MS, respectively. The parsimonious candidate model for each media was developed using stressor and lithology data at each of the sub-basin and cumulative basin scales. The most informative parsimonious model for each media, with the lowest AICc value (i.e., 80 for sub-basin and 50 for cumulative basin), was retained (green block, where values within are hypothetical). With two trace metals being assessed in this investigation, a total of four final parsimonious models were retained. From the retained GLMMs, predicted values (i.e., estimated concentrations and enrichment factors) were computed and used in concordance correlation analysis.

3.3. Results

Following correlation analysis among metals in both sample types, Cr and Zn were retained for further investigation, as they demonstrated the lowest correlation coefficients compared to other metal pairs in both water (**Table 3-3**) and sediment (**Table 3-4**) media. These two metals act as effective indicators best representing the datasets variance for both water and sediment, and thus were applied in further comparative analysis. Analysis of variance (ANOVA) on the dissolved metal GLMMs revealed significantly higher Cr in the dry season (chi = 12.96, p < 0.01), while no significant differences were recorded for Zn (chi = 2.89, p = 0.09); although higher concentrations were recorded in the dry season. Analysis of variance on the sediment-bound metals GLMMs, indicated no significant differences in standardized EF of Cr (chi = 2.89, p = 0.09) nor Zn (chi = 0.25, p = 0.61) between seasons, although the dry season did record higher EF values in both metals (**Table 3-2**). The non-standardized trace metal EDXRF results (ppm) are presented in **Table S3-1**.

Following the GLMM analysis, four of the eight models were retained based on best-fit i.e. lowest AICc, and presented in **Table 3-5**. Model selection identified mining and geology as the most parsimonious predictors of increased dissolved Cr at the cumulative basin scale, while agriculture, mining, and lithology together best predicted increases in dissolved Zn at the sub-basin scale (**Table 3-5**). Among the predictive variables in the dissolved metal models, mining was the most important contributor in the Cr (cumulative basin scale) model, while lithology was the most important for the Zn (sub-basin scale) model (**Table 3-6**). The GLMM analysis for the sediment-bound metals identified that mining and lithology at the cumulative basin scale were associated with increased Cr, while urban stress and lithology also at the cumulative basin scale were associated with negligibly higher Zn (**Table 3-5**). The mining variable was also the most important variable in the prediction of sediment-bound Cr, while lithology was negligibly higher than the urban stress in predicting sediment-bound Zn (**Table 3-6**). The parameter estimates of each explanatory variable in the parsimonious models are presented in **Table 3-6**.

The parsimonious dissolved Zn model at the sub-basin scale demonstrated a higher conditional R^2 ($R^2_{GLMM(c)}$ = 0.88) compared to the sediment-bound Zn model at the cumulative scale ($R^2_{GLMM(c)}$ = 0.58). In contrast, for Cr, the parsimonious sediment-derived model showed improved model fit ($R^2_{GLMM(c)}$ = 0.95) over the dissolved Cr model ($R^2_{GLMM(c)}$ = 0.70), both at the cumulative basin scale (**Table 3-5**). These results suggest that the effectiveness of different sampling media in explaining metal variability depends on the specific metal and the spatial scale of analysis. For Zn, dissolved sampling better captured variability at sub-basin scales, while for Cr, sediment sampling proved more effective at explaining variability at cumulative basin scale.

Line graphs generated from the predicted values of the retained parsimonious GLMMs (over the two seasons), indicated that the comparative trends for Cr between the two sample types across each river showed general agreement (**Figure 3-2**). This is confirmed by the concordance correlation coefficient of ρ = 0.67 (95% CI: 0.40 to 0.83), indicating a substantial positive agreement, with uncertainty ranging from fair to almost perfect (Landis and Koch, 1977). The scale shift of υ = 0.92 suggests that the predictions for dissolved metals were slightly lower on average compared to the sediment-derived predictions. The bias-correction factor C_b value of 0.98 indicates very minimal deviation on average from the best-fit line between the dissolved and sediment-bound metal predictions, and thus a good overall correlation.

There was a comparatively greater divergence between water and sediment Zn predicted values, with a noticeable separation of the trend lines (**Figure 3-2**). The concordance correlation coefficient ρ = 0 (95% CI: 0 to 0), confirms this indicating no agreement between the two sample types. The scale shift was also negligible at υ = 0, suggesting neither method yielded consistently higher nor lower values and C_b = 0 indicates complete deviation from the best-fit line, rather than running parallel. Overall, the CCC analysis indicates very poor agreement between the Zn water and sediment models, with complete inconsistency, as opposed to the Cr water and sediment models, which presented substantial agreement.

Table 3-2: Study sites with their stressor descriptions at the two spatial scales assessed as well as the dissolved and sediment-bound metal data collected over the wet and dry seasons.

Study site	Latitude	Longitude	Possible pollution sources		Season	Dissolved metals				Sediment-bound metals			
			Sub-basin stressor(s)	Cumulative stressor(s)		Cr (ppb)	Zn (ppb)	V (ppb)	Ni (ppb)	Cr-EF	Zn-EF	V-EF	Ni-EF
STK1	-25.838786	27.37161	None	None	Wet	0.83	25.76	0.63	2.45	0.47	0.02	0.03	0.03
					Dry	0.84	24.65	0.61	2.69	0.48	0.01	0.03	0.02
STK2	-25.833387	27.388428	Agriculture	Agriculture	Wet	0.05	41.26	0.58	1.77	0.29	0.01	0.02	0.01
					Dry	0.98	31.87	1.02	2.87	0.24	0.01	0.02	0.01
STK3	-25.81307	27.47133	Agriculture	Agriculture	Wet	0.13	30.39	0.67	3.57	0.20	0.01	0.02	0.02
					Dry	0.98	44.50	1.75	3.89	0.25	0.01	0.03	0.02
STK4	-25.757205	27.483254	Agriculture	Agriculture	Wet	0.30	82.28	1.87	2.27	0.11	0.01	0.03	0.02
					Dry	0.98	43.82	3.13	5.40	0.13	0.01	0.03	0.03
STK5	-25.725874	27.483245	Mining	Agriculture, Mining	Wet	1.09	61.54	6.53	4.91	2.40	0.01	0.03	0.04
					Dry	3.74	500.03	38.32	32.74	2.98	0.01	0.04	0.05
STK6	-25.665385	27.476215	Urban	Agriculture, Mining, Urban	Wet	1.02	36.47	0.83	2.02	0.56	0.01	0.03	0.02
					Dry	1.08	68.3	0.88	2.59	0.38	0.00	0.02	0.01
STK7	-25.649581	27.483748	Agriculture	Agriculture, Mining, Urban	Wet	1.03	90.44	4.84	4.27	0.21	0.01	0.02	0.02
					Dry	1.76	45.78	8.04	7.43	0.24	0.01	0.03	0.02
MRT1	-25.798461	27.577297	None	None	Wet	0.70	24.05	0.51	1.59	0.42	0.02	0.03	0.03
					Dry	0.94	28.57	0.77	3.07	0.45	0.02	0.03	0.03
MRT2	-25.741539	27.568359	Agriculture, Urban	Urban, Agriculture	Wet	0.76	71.86	4.23	3.05	0.23	0.01	0.02	0.04
					Dry	0.92	38.99	6.15	5.77	0.32	0.02	0.02	0.04
MRT3	-25.727593	27.566446	Agriculture	Urban, Agriculture	Wet	0.78	32.82	3.95	2.79	3.76	0.01	0.03	0.04
					Dry	1.40	65.28	8.37	8.85	2.67	0.01	0.03	0.04
MRT4	-25.710699	27.558002	Mining	Urban, Agriculture, Mining	Wet	7.66	118.1	11.57	14.77	7.05	0.02	0.04	0.05
					Dry	5.18	156.97	9.23	13.56	11.71	0.02	0.05	0.09
MRT5	-25.687824	27.535524	Mining	Urban, Agriculture, Mining	Wet	1.62	185.38	7.05	36.56	2.92	0.01	0.03	0.04
					Dry	4.59	384.03	56.84	50.94	3.95	0.01	0.04	0.04
MRT6	-25.682372	27.533205	Mining	Urban, Agriculture, Mining	Wet	Not sampled							
					Dry	11.83	878.09	51.84	54.07	8.47	0.02	0.06	0.05
MRT7	-25.660467	27.531345	Urban	Urban, Agriculture, Mining	Wet	4.61	376.96	22.62	191.36	1.80	0.01	0.04	0.04
					Dry	15.52	799.14	98.37	105.06	1.56	0.01	0.04	0.04

Table 3-3: Correlation matrix of four trace metals analysed from water samples (dissolved), where Cr (ppb) and Zn (ppb) were retained for further analysis.

	V (ppb)	Cr (ppb)	Ni (ppb)	Zn (ppb)
V (ppb)	1	0.85*	0.91*	0.88*
Cr (ppb)		1	0.84*	0.76*
Ni (ppb)			1	0.77*
Zn (ppb)				1

Table 3-4: Correlation matrix of the four trace metals analysed from sediment (benthic), where Cr (EF) and Zn (EF) were least correlated and retained for further analysis.

	V (EF)	Cr (EF)	Ni (EF)	Zn (EF)
V (EF)	1	0.74*	0.7*	0.34*
Cr (EF)		1	0.75*	0.31*
Ni (EF)			1	0.46*
Zn (EF)				1

Table 3-5: Four parsimonious generalised mixed effects models for each Cr and Zn response variables the at the respective spatial-scale they best predicted at. Each model includes the models explanatory stressor and geology. The (*) indicates the level of significance.

Sample type	**Water (dissolved)**		**Sediment (benthic)**	
Optimal scale	**Cumulative**	**Sub-basins**	**Cumulative**	
Response	**Cr**	**Zn**	**Cr**	**Zn**
Model predictors	• Mining • Vlakfontein	• Mining • Rayton • Ruighoek-Pryoxenite • Rustenberg layered	• Mining • Pyramid • gabbo-Norite	• Urban • Vlakfontein
Model intercept	-0.87(0.21)-4.16***	3.35(0.12)27.91***	-0.80(0.23)-3.49***	-3.71(0.06)-58.36***
	Model Selection	**Model Selection**	**Model Selection**	**Model Selection**
weight	0.12	0.34	0.10	0.086
AICc	80.95	290.25	12.12	-214.25
BIC	84.5	293.4	13.66	-210.6
	Goodness of fit	**Goodness of fit**	**Goodness of fit**	**Goodness of fit**
$R^2_{GLMM(m)}$	0.64	0.87	0.70	0.47
$R^2_{GLMM(c)}$	0.70	0.88	0.95	0.58
	Random effects	**Random effects**	**Random effects**	**Random effects**
Site (SD)	0.34	0.00	0.64	0.08
Residuals (SD)	0.49	0.39	0.28	0.15

Table 3-6: The conditional model parameter estimates for each variable in the parsimonious models, with the relative importance score for each variable. Greyed boxes indicating the variable with the greatest importance in the model, expressed as a rounded-up proportion.

Models spatial scale	Response	Variable	Variable estimate	Lower 95% CI	Upper 95% CI	Variable importance
Cumulative	Dissolved Chromium	Mining	0.20	0.10	0.30	0.52
		Vlakfontein	0.04	0.01	0.07	0.48
Sub-basin	Dissolved Zinc	Mining	0.09	0.07	0.11	0.21
		Rayton	0.05	0.03	0.07	0.21
		Ruighoek Pyroxenite	0.09	0.05	0.13	0.21
		Rustenberg Layered	0.62	0.45	0.80	0.36
Cumulative	Sediment Chromium	Mining	0.64	0.61	1.16	0.59
		Pyramid Gabbo Norite	0.28	-0.37	-0.18	0.41
	Sediment Zinc	Urban	0.02	-0.04	-0.01	0.50
		Vlakfontein	0.03	0.00	0.01	0.50

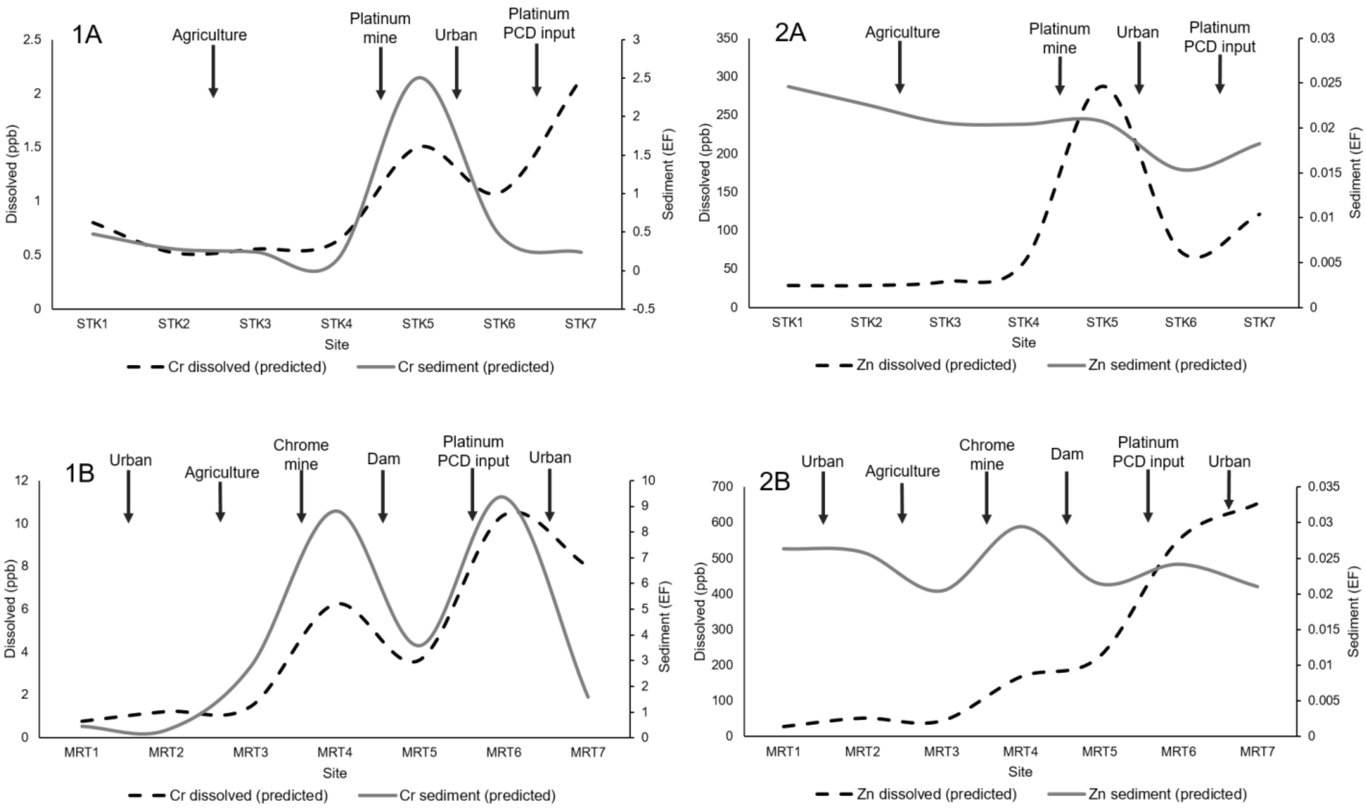

Figure 3-2: Comparative line graphs depicting predicted (estimated; see Figure 3-2) Cr (1) and Zn (2) from the respective final parsimonious generalised linear mixed effect models from the water (black-dotted line) and sediment (grey-solid line) media along the (A) Sterkstroom (STK) and (B) Maretlwane (MRT) rivers. Arrows indicate locations of known stressor introductions between sampling sites to enable visual assessment of coincident fluctuations in dissolved and sediment-bound metal concentrations.

3.4. Discussion

3.4.1. Seasonal differences in water and sediment Cr and Zn

The differential seasonal variation between the metals analysed in water versus sediment provides insight into these media constraints and the environmental processes driving metal concentrations. For the dissolved metal analysis, Cr exhibited statistically higher concentrations in the dry as opposed to the wet season, while Zn did not demonstrate significant seasonal variation, although it still recorded higher concentrations in the dry season. The significant seasonal variation in Cr is supported by local literature (Dalu et al., 2017) and is likely driven by changes in solubility and geochemical mobility of Cr between wet and dry hydrological conditions (Saalidong et al., 2022). Specifically, lower flow volumes in the dry season reduce dilution effects, spiking concentrations of mining effluents entering via pathways like leaching. This is reflected in the higher recorded Cr levels during low flows compared to the wet season, where together with base flow, rainfall and landscape runoff increase dilution (Almécija et al., 2017; Marara and Palamuleni, 2020). The transient nature of dissolved metals makes water concentrations more variable in response to hydrological shifts (Beck et al., 1991).

The non-significant seasonal fluctuations in dissolved Zn concentrations align with other local investigations of mixed-use river catchments that likewise found minimal variability between wet and dry periods (Edokpayi et al., 2016). This finding suggests a similar proportional pollutant input across the intensification gradient (Louis et al., 2014) and/or cyclic effects of eutrophication in the dry season (Jin et al., 2019; Sharma et al., 2022). While oxic conditions favour Zn adsorption to Fe/Mn oxides in sediments during the wet season, this adsorption does not necessarily decrease dissolved Zn concentrations, as high river flows dilute Zn inputs before substantial adsorption can occur. However, once adsorbed during high oxygen conditions, the Zn remains immobilized on the sediments and is not released back into the water column (Jin et al., 2019; Sharma et al., 2022). Therefore, wet season dissolved Zn levels reflect a balance of dilution counteracting any potential decrease from Zn adsorption under oxic conditions.

The dry season eutrophication conditions may create anoxic conditions at night that induce redox-driven release of mobile Zn(II) from sediments through reductive dissolution of Fe/Mn oxides (Jin et al., 2019; Sharma et al., 2022). Zinc is, however, then adsorbed back to Fe/Mn oxides during the dry season daytime when algal photosynthesis restores oxic conditions. Therefore, the opposing effects of dilution versus sediment release in the summer and winter seasons, respectively, balance out to yield similar Zn levels in both seasons.

Neither sediment-bound Cr nor Zn indicated any significant difference between seasons, although both recorded marginally higher concentrations in the dry season. The relative stability of the metals in the sediment is likely attributed to both the time-integrated nature of the sediment through deposition, potentially dampening episodic pollution (Ciszewski and Grygar, 2016; Addo-Bediako et al., 2021), as well as various ongoing hydrodynamic, chemical and biological processes that cause the steady release of metals (Singh et al., 2005). This contrasts with the water chemistry where the aqueous samples provided snapshots that are subjected to transient fluctuations and effective at detecting episodic pollution, but sensitive to local scale hydrological effects (Beck et al., 1991; Kodikara et al., 2022). The relatively stable sediment-bound trace metal signals can reflect consistent, long-term metal loading as opposed to *in-situ* samples, which are sensitive to short-term fluctuations.

3.4.2. Spatial scale influences and predictive drivers

3.4.2.1. Dissolved trace metals

Assessing the spatial scale at which trace metals from each sample type were best predicted showed distinctions between the dissolved phases. Dissolved Cr displayed a broad, cumulative-scale accumulation pattern that was best predicted by a higher proportion of mining stress and lithogenic sources. Studies in the neighboring catchment support these findings, indicating higher Cr concentrations after mining-related activities (Almécija et al., 2017). Among the predictive variables in the dissolved Cr model, mining contributed the most to its variability (**Table 3-6**). Dissolved Zn, however, was best predicted by more localized sub-basin scale mining influences (Gozzard et al., 2011) and various lithogenic sources, with the lithogenic sources contributing the greatest to the model (**Table 3-6**). The dissolved trace metal models' spatial scale-dependency for Cr and Zn may likely result from their respective inherent aqueous chemistries and associated transport pathways from systemic mining inputs and background erosional processes.

Among the model variables, percentage cumulative mining was the predominant predictor of increasing dissolved Cr, while the inclusion of the Vlakfontein lithology in the model may stem simply from spatial associations rather than direct mineralogical contributions and associated Cr release. The Vlakfontein lithology contains little chromite, with these quartzitic areas surrounding one Cr-linked mining operation in the study catchment. Mafic and ultramafic rocks, however, such as those present in the Bushveld Igneous complex, are extensively mined as they are a major source of Cr(III) in river catchments (D'Arcy et al., 2016). The Cr(VI) oxyanions are the predominant Cr species in relatively pH-neutral conditions and are highly mobile (D'Arcy et al., 2016). The negative charges associated with dissolved Cr(VI) oxyanions (e.g. chromate and dichromate) cause resistance to instream hydrolysis and precipitation reactions, thus limits sorption to streambed surfaces and allowing conservative downstream transport (Gorny et al., 2016). This highly mobile Cr(VI) likely integrates contamination signals from broad-scale lithologic and mining (stressor) as water transits the cumulative river network, supporting the cumulative spatial scale finding (**Table 3-6**).

Conversely, dissolved Zn can complex with organic matter and sorb to suspended particles as previously observed (Louis et al., 2014; Jin et al., 2019). The current findings, showing dissolved zinc was best predicted at the sub-basin scale (between study sites), support its limited downstream transport potential, with local scale attenuation also observed by Gozzard et al. (2011) in a mining-stressed catchment. This suggests free Zn^{2+} is readily removed via sorption during downstream transport, yielding a sub-basin scale signal that decays between the study sites within an otherwise nested study design. Additional complexes that may promote Zn sorptive removal include ternary complexes with Fe/Al oxides and carbonates (Bradl, 2004; Gozzard et al., 2011). The prevalence of Zn attenuation processes like sorption and complexation aid its particulate uptake and local-scale patterns, rather than broad cumulative downstream transport. However, shifting redox conditions can potentially mobilize particle-bound zinc through reductive dissolution (Jin et al., 2019), acting against Zn sorptive removal tendencies. Overall, the multiple Zn uptake pathways revealed by the sub-basin scale predictions, highlight the relative instability and limited cumulative behaviour of dissolved Zn in the sampled rivers.

3.4.2.2. Sediment trace metals

Unlike the spatial scale-dependent patterns observed in the dissolved models, the sediment-bound metal models showed cumulative scale factors that best explained both Cr and Zn trends. The cumulative downstream accumulation of Cr in sediments likely stems from stable complexation with other metal oxyhydroxides (e.g. iron and manganese), resistance to reductive dissolution, and lower mobility of Cr(III) forms (D'Arcy et al., 2016; Richard and Bourg, 1991). This is likely attributed to Cr entering the river systems from background weathering processes (Almécija et al., 2017), as well as the evident mining-derived, Cr-rich mineral (processed ore) and water (pollution control dam) related effluents entering the rivers.

Chromium was positively associated with a greater proportion of cumulative mining stress and a specific lithogenic source, Pyramid Gabbro-Norite (pyroxenite-gabbro-norite) (**Table 3-5**). Mines in Western Limb largely exploit the Upper Group (e.g. UG-1 & UG-2; Cr_2O_3 = ~43%) and Middle Group reefs (including MG-1; Cr_2O_3 = ~46%) (Schürmann et al., 1998) of the Upper and Lower Critical Zones of the Rustenburg Layered Suite for chromium ores (Von Gruenewaldt et al., 1986). The Main Zone consisting of Pyramid Gabbro-Norite unit is stratigraphically above these layers and is absent of chromite, but is extracted to access the deeper chromitites (Mitchell, 1990; Barnes and Maier, 2002), supporting its inclusion in the model and the rationale as to why the mining variable (like with dissolved Cr) remained the most important predictor in the Cr in sediment model at the cumulative scale (**Table 3-6**).

The sediment-bound Zn was positively associated with higher urbanisation and Vlakfontein lithography in the cumulative catchment, with the underlying lithogenic source, like with the dissolved Zn, being the most important contributor although only by 0.05% compared to urban stressor sources. This suggests an almost equal importance (contribution) of both predictors to the instream sediment-bound Zn findings (variability). Zinc in sediment exhibits a weak, yet strong enough affinity for binding to sediment components to allow for a cumulative scale retention capacity, as identified from the parsimonious Zn-sediment model (**Table 3-5**). The affinity for binding to sediment in oxic river systems includes binding to organic matter, adsorption by Fe/Mn oxides and clay minerals, creating stable complexes (Louis et al., 2014; Jin et al., 2019). It does, however, remain somewhat prone to release under certain conditions, for example through biological uptake, reductive dissolution of manganese oxides and competitive desorption processes (Roussiez et al., 2013).

The relationship observed between positive Zn in sediment and greater urban stress within the catchment (**Table 3-6**) is supported by other metal-sediment aligned study findings (Louis et al., 2014; Dias-Ferreira et al., 2016). Such patterns may arise from Zn inputs from roofing materials, domestic wastewater effluents and other urban-related run-off as well as the inherent geochemical attributes controlling its attenuation in the streambed (Louis et al., 2014). However, the inclusion of the Vlakfontein lithology in the statistical model warrants further examination as no studies have documented major/minor zinc ores hosted within it, particularly within in the South African Bushveld Igneous Complex. The spatial coincidence of Vlakfontein with some urban centers (i.e. Mooinooi and Tharisa Township) may exaggerate its statistical importance for zinc input and/or the potential for geologic zinc input through increased physical erosion driven by urban activities.

Although Vlakfontein formations do not necessarily harbor economic PGE mineralization in the region, they are known to consist of non-mineralized quartzite's and shales. A potential explanation is that the quartzite's within this formation may contain accessory sulfide mineralization in small amounts. Late-stage quartzite is known to contain, for example Sphalerite, a zinc sulfide mineral and a source of geogenic zinc (Moore and Reid, 1988). While typically not major Zn hosts, Sphalerite and other Zn-bearing sulfides have been documented in minor quantities within non-mineralized quartzite units (Moore and Reid, 1988; Pašava, 1993). Furthermore, Vlakfontein's interbedded shale layers may provide additional potential for strata-bound sphalerite mineralization, known to concentrate Zn-Pb sulfide mineralization along bedding planes (Broadbent et al., 1998). Urban activities may enhance physical weathering of these minerals leading to increased geogenic zinc mobilization into storm water systems and rivers.

3.4.3. Agreement between sample types

In comparing pollution signals between both sample types (water and sediment; see **Figure 3-2**), in the CCC analysis, Cr displayed substantial positive agreement (ρ = 0.67) between the analysed water and sediment media (Landis and Koch, 1977). The substantial CCC concordance observed for Cr, having been analysed by the independent ICP-MS and EDXRF techniques, substantiates its inherent conservative geochemistry in river systems. This may reflect processes such as dominance of Cr(VI) species in the dissolved phase persisting through anionic complexes, while particulate Cr(III) is stabilized through associations with mineral oxides (Richard and Bourg, 1991; D'Arcy et al., 2016; Gorny et al., 2016). However, explicit investigation of speciation and phase partitioning is still needed to substantiate the specific modes driving observed agreement for Cr across analytical methods within this catchment. The agreement between both sample types in relation to cumulative stressors, is a positive outcome in the capacity of both monitoring methods to detect broader river continuum pollution patterns.

On the other hand, negligible concordance between dissolved Zn from aqueous samples and sediment-bound Zn, is indicative of no agreement between the sample media (**Figure 3-2**). This outcome implies that Zn behaves differently in water versus sediment (differential phase partitioning and mobility; Jin et al., 2019). For the dissolved phase, Zn largely forms complexes with organic and inorganic ligands, only weakly sorbing to suspended particles, thus limiting its downstream accumulation (Louis et al., 2014; Jin et al., 2019). In contrast, zinc in sediment exhibits a weak, yet strong enough cumulative scale retention capacity, remaining somewhat prone to release under certain chemical conditions. The sediment derived-Zn trend therefore better reflected spatial stressor dynamics compared to aqueous derived-Zn along the two river continua (**Figure 3-2**).

3.4.4. Key findings

This study revealed distinct spatial behaviours can occur between dissolved and sediment-bound metals in mixed land-use catchments. Dissolved Cr demonstrated persistent cumulative downstream transport. In contrast, dissolved zinc showed a weaker downstream cumulative transport relationship, being best predicted at the sub-basin scale. The greater instability of the dissolved Zn model (sub-basin scale), as indicated by its higher AICc value (AICc = 290.25) compared to the dissolved Cr model (cumulative basin scale) (AICc = 80.95; **Table 3-5**), may be attributed to more localized complexation and particulate uptake processes, yielding stronger sub-basin scale patterns over that of cumulative patterns. Both dissolved Cr and Zn were best predicted by mining activities at their respective scales as well as lithogenic sources.

Sediment-bound Cr, exhibited pronounced downstream accumulations, integrating upstream pollution legacies over time. Such lead to sediment-Cr enrichment factors exceeding 1.5 on multiple occasions at STK5 as well as between MRT3 and MRT7 for both seasons, indicative of significant stressor-derived inputs, in this case primarily mining activities (Garcia-Ordiales et al., 2014). The sediment-bound Zn, however, did not exhibit as pronounced downstream accumulation, while too being best predicted at the cumulative scale. None of the sediment-bound Zn enrichment factors exceeded 1.5 and, thus, were not significantly different from background levels showing low or poor stressor enrichment (Garcia-Ordiales et al., 2014). Therefore, in the Gwathle Catchment, sediment-bound Cr proves to be a more robust indicator of mining stress compared to sediment-bound Zn in the Gwathle Catchment.

Pertaining to the agreement between sample types, dissolved and sediment-bound Cr showed strong concordance, suggesting sediment-bound Cr may serve as an effective proxy for transient dissolved Cr contamination in a mining-intensive catchment, while also capturing legacy pollution inputs. The dissolved Zn and sediment-bound Zn, however, indicated negligible concordance. This indicates that dissolved Zn likely better reflects immediate, short-term pollution inputs that may not be captured by the longer-term depositional nature of metals in streambed sediments. Such an assessment of agreement between sample types and across different trace metals highlights the importance of considering a multi-media, multi-element analysis for comprehensive freshwater pollution tracking.

3.4.5. Management implications

Currently, the analysis of dissolved metals via ICP-MS is the primary monitoring approach used to assess metal pollution in South African national river health assessments. Although only considering Cr and Zn, this study suggests that incorporating routine sediment sampling could provide invaluable long-term legacy metal pollution tracking with minimal logistical constraints, owing to the time-integrated nature of sediment-bound metals, particularly for Cr. Dissolved sampling gives high-quality temporal snapshots to detect pollution and guide short-term decisions. Sediment-bound metals, however, integrate their concentrations over time and space, offering a more feasible way to map broad, longitudinal pollution legacies and their connections to upstream stressors at the catchment scale, given South Africa's vast river networks and logistical constraints.

Sediment-bound metals analysed via EDXRF provide a pragmatic, rapid, and cost-effective screening tool to profile metal distributions despite capacity constraints, allowing large-scale assessments that identify hotspots, guide remediation, and evaluate cumulative impacts with limited sampling requirements (Hurley et al., 2017). Overall leveraging such mixed-media approaches is key for balanced water quality tracking in South Africa and overcoming each approach’s potential shortfalls in freshwater resource management (DWAF, 2004). This study proves that integrating routine sediment sampling could provide river health monitoring assessments with invaluable integrated spatial perspectives on legacy pollution, critical for targeted improvement toward achieving national water quality priorities (DWA, 2023).

Overall, these findings highlight the value of paired water and sediment sampling, particularly for Cr, to track stressor-related trace metal inputs into aquatic ecosystems. It also emphasizes the effectiveness of sediment-bound metal analysis, using a rapid and cost-efficient method of EDXRF (compared to ICP-MS) to effectively identify accumulated (legacy) pollution from different stressors within a multi-user catchment. This study reveals an opportunity to expand this research to further assess the concordance of additional metals in both media which can be used to inform catchment management agencies when to adopt each in particular scenarios (e.g. to identify certain catchment stressors). It also demonstrates the potential to develop national, affordable sediment monitoring protocols (separate from the national protocol used for dissolved metals; DWAF, 2004), to identify sources of aquatic ecosystem stress. In the South African context, adding routine and cost-effective sediment metals analysis such as EDXRF could provide invaluable long-term pollution mapping to guide national water quality priorities and strategies.

3.5. Conclusion

This comparative geospatial assessment demonstrated differential utility between water and sediment sampling for tracking metals from catchment stressors along a land-use intensification gradient. The behaviourally conservative Cr, exhibited consistent signals (substantial concordance) for both water and sediment media, which were best predicted at the cumulative scale for both. Further spatio-temporal research is needed to explore concordance for other conservative trace metals in connecting water and sediment derived metals to common catchment stressors. This finding, however, does suggest that sediment analysis, via rapid and cost-effective EDXRF, can serve as an effective complementary tool for use in routine river health monitoring as it provides time-integrated signals for behaviourally conservative metals. Such multi-phase sampling can provide a holistic approach to aquatic stress tracing, particularly when dissolved samples only provide a temporal snapshot that may require more frequent sampling as opposed to the time-integrated nature of benthic sediments. For reactive trace metals that undergo biogeochemical transformations such as Zn, each matrix offers distinct forensic evidence. This is with dissolved Zn being best predicted at the sub-basin scale mining, while Zn-sediment was best predicted at cumulative scale by lithogenic factors and urban stress; with both media having negligible concordance in tracking stressors across the land-use intensification gradient.

While current South African water quality monitoring programs and protocols emphasizes the collection of snapshot dissolved measurements, this study shows benthic sediments harbor invaluable complementary signatures of mining-related stress. As an additional or complementary tool to the national trace metal water sample analysis, sediment samples provide a pragmatic spatially-integrated ‘screening’ tool given potential capacity constraints for local and/or national water quality monitoring programs. It allows rapid profiling of metal distribution and contamination in sediments across large areas providing important insight for management actions (Hurley et al. 1996). Such capability for cost-effective, integrated assessments makes sediments and their analysis through EDXRF advantageous in South Africa for identifying pollution hotspots/risks, guiding targeted remediation, and evaluating cumulative pollution impact. A paired water and sediment approach maximises insights, but standalone sediment samples delivered valuable spatial perspectives on sediment pollution with limited sampling frequency constraints that would otherwise be unattainable.

3.5.1. Acknowledgements

This Chapter was authored by Jonathan Levin, with material contributions from Mark Humphries, Chris Curtis and Darragh Woodford. We are thank Patrick Lacey and Mandlenkosi Nkala (University of KwaZulu-Natal) for assisting in the collection of the field samples. We thank Marc for also providing the necessary training and laboratory resources to allow for sample analysis in the Environmental Geochemistry Laboratory (University of the Witwatersrand). We thank Nompendulo Khoza (University of the Witwatersrand) who assisted in the laboratory to ensure the samples were prepared on schedule. We are grateful to Gert Easters of Cherry Ridge (Pty), Mark Ashfield at the Maretlwane Wilderness School and staff at the Utopia Nature Resort for access to river sites for the purpose of data collection. We thank Chevonne Reynolds for providing statistical support (University of the Witwatersrand). All fieldwork was conducted under a North West Province research permit (NW 17458/03/2020).

3.5.2. Reference list

Addo-Bediako, A., Nukeri, S. and Kekana, M., 2021. Heavy metal and metalloid contamination in the sediments of the Spekboom River, South Africa, *Applied Water Science*, *11*, 1-9.

Abrahim, G.M.S. and Parker, R.J., 2008. Assessment of heavy metal enrichment factors and the degree of contamination in marine sediments from Tamaki Estuary, Auckland, New Zealand, *Environmental monitoring and assessment*, *136*(1), 227-238.

Akyildiz, G.K. and Duran, M., 2021. Evaluation of the impact of heterogeneous environmental pollutants on benthic macroinvertebrates and water quality by long-term monitoring of the buyuk menderes river basin, *Environmental Monitoring and Assessment*, *193*(5), 1-23.

Albuquerque, P.T., Fredou, T., Barcellos, R.L., Melo, J.T., Arruda, G.N. and De França, E.J., 2022. Anthropogenic influences on sedimentary geochemistry of Itapessoca Estuarine Complex, Pernambuco, Brazil, *Environmental monitoring and assessment*, *194*(1), 1-18.

Almécija, C., Cobelo-García, A., Wepener, V. and Prego, R., 2017. Platinum group elements in stream sediments of mining zones: The Hex River (Bushveld Igneous Complex, South Africa), *Journal of African Earth Sciences*, *129*, 934-943.

Amundsen, P.A., Staldvik, F.J., Lukin, A.A., Kashulin, N.A., Popova, O.A. and Reshetnikov, Y.S., 1997. Heavy metal contamination in freshwater fish from the border region between Norway and Russia. *Science of the Total Environment*, *201*(3), 211-224.

Atangana, E. and Oberholster, P.J., 2021. Using heavy metal pollution indices to assess water quality of surface and groundwater on catchment levels in South Africa, *Journal of African Earth Sciences*, *182*, 1-12.

Balaram, V., Copia, L., Kumar, U.S., Miller, J. and Chidambaram, S., 2023. Pollution of water resources and application of ICP-MS techniques for monitoring and management–A comprehensive review, *Geosystems and Geoenvironment*, 1-24.

Barbieri, M., 2016. The importance of enrichment factor (EF) and geoaccumulation index (Igeo) to evaluate the soil contamination, *Journal of Geology & Geophysics*, *5*(1), 1-4.

Barnes, S.J. and Maier, W.D., 2002. Platinum-group elements and microstructures of normal Merensky reef from Impala Platinum Mines, Bushveld Complex, *Journal of Petrology*, *43*(1), 103-128.

Barton, K., 2010. MuMIn: multi-model inference. R package version 0.13.17 <http://CRAN. R-project. org/package= MuMIn>.

Bates, D., Mächler, M., Bolker, B. and Walker, S., 2014. Fitting linear mixed-effects models using lme4, *arXiv preprint arXiv:1406.5823*.

Beck, M.B., Adeloye, A.J., Finney, B.A. and Lessard, P., 1991. Operational water quality management: transient events and seasonal variability, *Water Science and Technology*, *24*(6), 257-265.

Bradl, H.B., 2004. Adsorption of heavy metal ions on soils and soils constituents, *Journal of Colloid and Interface Science*, *277*(1), 1-18.

Bridgestock, L., Henderson, G.M., Holdship, P., Khaing, A.M., Naing, T.T., Myint, T.A., Htun, W.W., Khant, W., Thu, W.M., Chi, M.A.N. and Baronas, J.J., 2022. Dissolved trace element concentrations and fluxes in the Irrawaddy, Salween, Sittaung and Kaladan Rivers, *Science of the Total Environment*, *841*, 1-13.

Broadbent, G.C., Myers, R.E. and Wright, J.V., 1998. Geology and origin of shale-hosted Zn-Pb-Ag mineralization at the Century deposit, northwest Queensland, Australia, *Economic Geology*, *93*(8), 1264-1294.

Cawthorn, R.G., 2010. The platinum group element deposits of the Bushveld Complex in South Africa, *Platinum Metals Review*, *54*(4), 205-215.

Chetty, S., Pillay, L. and Humphries, M.S., 2021. Gold mining's toxic legacy: Pollutant transport and accumulation in the Klip River catchment, Johannesburg, *South African Journal of Science*, *117*(7-8), 1-11.

Ciszewski, D. and Grygar, T.M., 2016. A review of flood-related storage and remobilization of heavy metal pollutants in river systems, *Water, Air, & Soil Pollution*, *227*, 1-19.

Council for Geoscience, *2017. South Africa 250k Litho-Chronostratigraphic layer (complete coverage), Council for Geoscience,* Pretoria. Available from https://maps.geoscience.org.za

D’Arcy, J., Babechuk, M.G., Døssing, L.N., Gaucher, C. and Frei, R., 2016. Processes controlling the chromium isotopic composition of river water: Constraints from basaltic river catchments, *Geochimica et Cosmochimica Acta*, *186*, 296-315.

Dalu, T., Wasserman, R.J., Tonkin, J.D., Mwedzi, T., Magoro, M.L. and Weyl, O.L., 2017. Water or sediment? Partitioning the role of water column and sediment chemistry as drivers of macroinvertebrate communities in an austral South African stream, *Science of the Total Environment*, *607*, 317-325.

Devesa-Rey, R., Díaz-Fierros, F. and Barral, M.T., 2010. Trace metals in river bed sediments: An assessment of their partitioning and bioavailability by using multivariate exploratory analysis, *Journal of Environmental Management*, *91*(12), 2471-2477.

Dias-Ferreira, C., Pato, R.L., Varejão, J.B., Tavares, A.O. and Ferreira, A.J., 2016. Heavy metal and PCB spatial distribution pattern in sediments within an urban catchment—contribution of historical pollution sources, *Journal of soils and sediments*, *16*, 2594-2605.

DWAF, 2004. *Water Resource Quality Monitoring Volume 1 – sampling protocol for Inorganic chemical analysis*, Resource Quality Services Department of Water Affairs, Pretoria, South Africa.

DWS, 2023. *The National Water Resources Strategy Third Edition (NWRS-3) March 2023*, Department of Water and Sanitation, Pretoria, South Africa.

Edokpayi, J.N., Odiyo, J.O., Popoola, O.E. and Msagati, T.A., 2016. Assessment of trace metals contamination of surface water and sediment: a case study of Mvudi River, South Africa, *Sustainability*, *8*(2), 1-13.

Erasmus, J.H., Malherbe, W., Zimmermann, S., Lorenz, A.W., Nachev, M., Wepener, V., Sures, B. and Smit, N.J., 2020. Metal accumulation in riverine macroinvertebrates from a platinum mining region, *Science of the Total Environment*, *703*, 1-13.

Fernández-Ayuso, A., Kohfahl, C., Aguilera, H., Rodríguez-Rodríguez, M., Ruiz-Bermudo, F., Serrano-Hidalgo, C. and Romero-Álvarez, C., 2023. Control of trace metal distribution and variability in an interdunal wetland, *Science of The Total Environment*, *857*, 1-12.

Förstner, U. and Müller, G., 1981. Concentrations of heavy metals and polycyclic aromatic hydrocarbons in river sediments: geochemical background, man's influence and environmental impact, *GeoJournal*, *5*, 417-432.

Förstner, U. and Wittmann, G.T., 2012. *Metal pollution in the aquatic environment,* Springer Science & Business Media.

Funk, C., Peterson, P., Landsfeld, M., Pedreros, D., Verdin, J., Shukla, S., Husak, G., Rowland, J., Harrison, L., Hoell, A. and Michaelsen, J., 2015. The climate hazards infrared precipitation with stations—a new environmental record for monitoring extremes. Scientific data, 2(1), 1-21.

Gafur, N.A., Sakakibara, M., Sano, S. and Sera, K., 2018. A case study of heavy metal pollution in water of Bone River by Artisanal Small-Scale Gold Mine Activities in Eastern Part of Gorontalo, Indonesia, *Water*, *10*(11), 1-10.

Garcia-Ordiales, E., Loredo, J., Esbrí, J.M., Lominchar, M.A., Millan, R. and Higueras, P., 2014. Stream bottom sediments as a means to assess metal contamination in the historic mining district of Almadén (Spain), *International Journal of Mining, Reclamation and Environment*, *28*(6), 357-376.

Gelman, A. and Hill, J., 2006. *Data analysis using regression and multilevel/hierarchical models*, Cambridge university press.

Geoterraimage, 2021. *2020 South Africa National Land-Cover Dataset*, Geoterraimage, viewed 10 February 2022, from https://egis.environment.gov.za/sa_national_land_cover_datasets.

Gorny, J., Billon, G., Noiriel, C., Dumoulin, D., Lesven, L. and Madé, B., 2016. Chromium behavior in aquatic environments: a review, *Environmental Reviews*, *24*(4), 503-516.

Gozzard, E., Mayes, W.M., Potter, H.A.B. and Jarvis, A.P., 2011. Seasonal and spatial variation of diffuse (non-point) source zinc pollution in a historically metal mined river catchment, UK. *Environmental Pollution*, *159*(10), 3113-3122.

Gregory, B.R., Patterson, R.T., Reinhardt, E.G., Galloway, J.M. and Roe, H.M., 2019. An evaluation of methodologies for calibrating Itrax X-ray fluorescence counts with ICP-MS concentration data for discrete sediment samples, *Chemical Geology*, *521*, 12-27.

Gurrieri, J.T., 1998. Distribution of metals in water and sediment and effects on aquatic biota in the upper Stillwater River basin, Montana, *Journal of Geochemical Exploration*, *64*(1-3), 83-100.

Harrell, F.E. and Dupont, C., 2023. Hmisc: Harrell miscellaneous. R package version 5.1-1.

Hurley, R.R., Rothwell, J.J. and Woodward, J.C., 2017. Metal contamination of bed sediments in the Irwell and Upper Mersey catchments, northwest England: exploring the legacy of industry and urban growth, *Journal of Soils and Sediments*, *17*, 2648-2665.

Islam, S.M.D., Bhuiyan, M.A.H., Rume, T. and Mohinuzzaman, M., 2016. Assessing heavy metal contamination in the bottom sediments of Shitalakhya River, Bangladesh; using pollution evaluation indices and geo-spatial analysis, *2*(3), 299 – 312.

Jaishankar, M., Tseten, T., Anbalagan, N., Mathew, B.B. and Beeregowda, K.N., 2014. Toxicity, mechanism and health effects of some heavy metals, *Interdisciplinary Toxicology*, *7*(2), 60-72.

Jin, Z., Ding, S., Sun, Q., Gao, S., Fu, Z., Gong, M., Lin, J., Wang, D. and Wang, Y., 2019. High resolution spatiotemporal sampling as a tool for comprehensive assessment of zinc mobility and pollution in sediments of a eutrophic lake, *Journal of hazardous materials*, *364*, 182-191.

King, R.S., Baker, M.E., Whigham, D.F., Weller, D.E., Jordan, T.E., Kazyak, P.F. and Hurd, M.K., 2005. Spatial considerations for linking watershed land cover to ecological indicators in streams, *Ecological applications*, *15*(1), 137-153.

Kodikara, K.A.S., Lewandowski, S., De Silva, P.M.C.S., Gunarathna, S.D., Madarasinghe, S.K., Ranasinghe, P., Jayatissa, L.P. and Dahdouh-Guebas, F., 2022. Heavy metal pollution in selected upland tributaries of Sri Lanka: comprehension towards the localization of sources of pollution, *Journal of Water and Health*, *20*(3), 505-517.

Kolarova, N. and Napiórkowski, P., 2021. Trace elements in aquatic environment. Origin, distribution, assessment and toxicity effect for the aquatic biota, *Ecohydrology & Hydrobiology*, *21*(4), 655-668

Kuhn, M., 2008. Building predictive models in R using the caret package, *Journal of statistical software*, *28*, 1-26.

Laha, F., Gashi, F., Frančišković-Bilinski, S., Bilinski, H. and Çadraku, H., 2022. Geospatial distribution of heavy metals in sediments of water sources in the Drini i Bardhë river basin (Kosovo) using XRF technique, *Sustainable Water Resources Management*, *8*(1), 1-16.

Landis, J.R. and Koch, G.G., 1977. The measurement of observer agreement for categorical data, *Biometrics*, 159-174.

Lin, K.L., 1989. A concordance correlation coefficient to evaluate reproducibility, *Biometrics*, 255-268.

Loannides, K., Stamoulis, K., Papachristodoulou, C., Tziamou, E., Markantonaki, C. and Tsodoulos, I., 2015. Distribution of heavy metals in sediment cores of Lake Pamvotis (Greece): a pollution and potential risk assessment, *Environmental Monitoring and Assessment*, *187*, 1-16.

Loannides, K., Stamoulis, K., Papachristodoulou, C., Tziamou, E., Markantonaki, C. and Tsodoulos, I., 2015. Distribution of heavy metals in sediment cores of Lake Pamvotis (Greece): a pollution and potential risk assessment, *Environmental Monitoring and Assessment*, *187*, 1-16.

Louis, Y., Pernet-Coudrier, B. and Varrault, G., 2014. Implications of effluent organic matter and its hydrophilic fraction on zinc (II) complexation in rivers under strong urban pressure: Aromaticity as an inaccurate indicator of DOM–metal binding, *Science of the Total Environment*, *490*, 830-837.

Mahommed, N.K. and Makundi, I.N., 2002. Optimization of EDXRF for the study of heavy metal pollution of Lake Victoria, *Tanzania Journal of Science*, *28*(1), 7-24.

Marara, T. and Palamuleni, L.G., 2020. A spatiotemporal analysis of water quality characteristics in the Klip river catchment, South Africa, *Environmental Monitoring and Assessment*, *192*(9), 1-28.

McGarigal, K., Cushman, S.A., Neel, M.C. and Ene, E., 2002. *FRAGSTATS: spatial pattern analysis program for categorical maps*, Computer software, University of Massachusetts, Amherst. Available from: www.umass. edu/landeco/research/fragstats/fragstats.

Mitchell, A.A., 1990. The stratigraphy, petrography and mineralogy of the Main Zone of the northwestern Bushveld Complex, *South African Journal of Geology*, *93*(4), 818-831.

Moore, J.M. and Reid, A.M., 1988. Implications of sphalerite inclusions in gahnite from the Namaqualand Metamorphic Complex, South Africa, *The Canadian Mineralogist*, *26*(2), 293-300.

Nikonow, W., Rammlmair, D. and Meima, J.A., 2023. Continuous element mapping of drill cores from the Bushveld Complex, SA using LIBS and µEDXRF, *Society for Geology Applied to Mineral Deposits*, 57 - 60.

Nriagu, J.O. and Pacyna, J.M., 1988. Quantitative assessment of worldwide contamination of air, water and soils by trace metals, *Nature*, *333*, 134-139.

P. Crowson, *Minerals Handbook 2000–01: Statistics and Analyses of the World's Minerals Industry*, Mining Journal Books Ltd, Edenbridge, Kent, UK, 2001.

Pašava, J., 1993. Anoxic sediments—an important environment for PGE; an overview, *Ore Geology Reviews*, *8*(5), 425-445.

Pool-Stanvliet, R., 2013. A history of the UNESCO Man and the Biosphere Programme in South Africa, *South African Journal of Science*, *109*(9), 1-6.

R Core Team. 2023. R: A Language and Environment for Statistical Computing, R Foundation for Statistical Computing, Vienna, Austria.

Richard, F.C. and Bourg, A.C., 1991. Aqueous geochemistry of chromium: a review, *Water research*, *25*(7), 807-816.

Rocha, F.R., Silva, P.S.C., Castro, L.M., Bordon, I.C.C.L., Oliveira, S.M.B. and Favaro, D.I.T., 2015. NAA and XRF technique bottom sediment assessment for major and trace elements: Tietê River, São Paulo State, Brazil, *Journal of Radioanalytical and Nuclear Chemistry*, *306*(3), 655-665.

Roussiez, V., Probst, A. and Probst, J.L., 2013. Significance of floods in metal dynamics and export in a small agricultural catchment, *Journal of hydrology*, *499*, 71-81.

Saalidong, B.M., Aram, S.A., Otu, S. and Lartey, P.O., 2022. Examining the dynamics of the relationship between water pH and other water quality parameters in ground and surface water systems, *PloS one*, *17*(1), 1-17.

Schűrmann, L.W., Grabe, P.J. and Steenkamp, C.J., 1998. 'Chromium', in Wilson, M.G.C. and Anhaeusser, C.R. (eds.), *Chromium mineral resources of South Africa: Handbook*, Council for Geoscience, pp. 740.

Sharma, N., Wang, Z., Catalano, J.G. and Giammar, D.E., 2022. Dynamic responses of trace metal bioaccessibility to fluctuating redox conditions in wetland soils and stream sediments, *ACS Earth and Space Chemistry*, *6*(5), 1331-1344.

Shen, Z., Hou, X., Li, W., Aini, G., Chen, L. and Gong, Y., 2015. Impact of landscape pattern at multiple spatial scales on water quality: A case study in a typical urbanised watershed in China, *Ecological Indicators*, *48*, 417-427.

Singh, J. and Kalamdhad, A.S., 2011. Effects of heavy metals on soil, plants, human health and aquatic life, *International Journal of Research in Chemistry and Environment*, *1*(2), 15-21.

Singh, K.P., Mohan, D., Singh, V.K. and Malik, A., 2005. Studies on distribution and fractionation of heavy metals in Gomti river sediments—a tributary of the Ganges, India, *Journal of Hydrology*, *312*(1-4), 14-27.

Siziba, N., Mwedzi, T. and Muisa, N., 2021. Assessment of nutrient enrichment and heavy metal pollution of headwater streams of Bulawayo, Zimbabwe, *Physics and Chemistry of the Earth*, *122*, 1-8.

South African Weather Service (SAWS). Climate data 2007 to 2022 of A21K, from http://www.weathersa.co.za/climate.

Thormann, L., Buchspies, B., Mbohwa, C. and Kaltschmitt, M., 2017. PGE production in southern Africa, part I: production and market trends, *Minerals*, *7*(11), 1-22.

Von Gruenewaldt, G., Hatton, C.J. and Merkle, R.K.W., 1986. Platinum-group element-chromitite associations in the Bushveld Complex, *Economic Geology*, *81*(5), 1067-1079.

Vörösmarty, C.J., McIntyre, P.B., Gessner, M.O., Dudgeon, D., Prusevich, A., Green, P., Glidden, S., Bunn, S.E., Sullivan, C.A., Liermann, C.R. and Davies, P.M., 2010. Global threats to human water security and river biodiversity, N*ature*, *467*, 555-561.

Wanderi, E.W., Gettel, G.M., Singer, G.A. and Masese, F.O., 2022. Drivers of water quality in Afromontane-savanna rivers, *Frontiers in Environmental Science*, *10*, 1-20.

Wang, F., Chen, J. and Forsling, W., 1997. Modeling sorption of trace metals on natural sediments by surface complexation model, *Environmental science & technology*, *31*(2), 448-453.

Yuan, C.G., Shi, J.B., He, B., Liu, J.F., Liang, L.N. and Jiang, G.B., 2004. Speciation of heavy metals in marine sediments from the East China Sea by ICP-MS with sequential extraction, *Environment international*, *30*(6), 769-783.

3.5.3. Supplementary material

Table S3-1: The non-standardized EDXRF derived trace metal data (ppm) together with the reference for standardization to enrichment factor (TiO_2).

Sample Identifier	Site name	Season	Date analysed	TiO2 (%)	Ni (PPM)	Zn (PPM)	V (PPM)	Cr (PPM)
25266	STK1	Wet	2/16/2022 12:32	1.05	155	103	203	2567
25264	STK1	Wet	2/16/2022 12:16	0.97	141	111	175	2618
25263	STK1	Wet	2/16/2022 12:07	1.20	130	84	159	2165
25301	STK1	Dry	2/21/2022 10:30	0.69	110	68	134	3112
25260	STK2	Wet	2/16/2022 11:42	0.53	50	31	86	1508
25258	STK2	Wet	2/16/2022 11:26	0.52	61	34	82	1057
25259	STK2	Wet	2/16/2022 11:34	0.51	47	26	76	978
25306	STK2	Dry	2/21/2022 11:11	0.65	57	36	103	1849
25311	STK2	Dry	2/21/2022 11:52	1.00	124	72	164	1637
25316	STK2	Dry	2/21/2022 12:34	0.63	65	39	109	1208
25321	STK3	Dry	2/21/2022 13:16	0.81	136	85	161	1274
25326	STK3	Dry	2/21/2022 13:58	0.81	106	68	120	1377
25331	STK3	Dry	2/21/2022 14:49	0.78	124	81	143	1445
25257	STK3	Wet	2/16/2022 11:17	0.70	93	65	122	968
25265	STK3	Wet	2/16/2022 12:24	0.77	103	67	135	1039
25262	STK3	Wet	2/16/2022 11:59	0.82	113	70	138	1250
25261	STK4	Wet	2/16/2022 11:51	0.86	124	40	145	517
25268	STK4	Wet	2/16/2022 12:50	0.89	95	35	141	658
25269	STK4	Wet	2/16/2022 12:58	0.84	136	45	143	559
25345	STK4	Dry	2/24/2022 12:13	1.08	142	37	163	710
25347	STK4	Dry	2/24/2022 12:30	0.97	127	42	150	550
25349	STK4	Dry	2/24/2022 12:47	1.19	156	37	183	922
25270	STK5	Wet	2/16/2022 13:06	0.84	228	74	190	13963
25271	STK5	Wet	2/16/2022 13:15	0.74	226	67	163	12426
25272	STK5	Wet	2/16/2022 13:23	0.77	229	65	167	13183
25351	STK5	Dry	2/24/2022 13:04	0.82	288	78	197	14694
25353	STK5	Dry	2/24/2022 13:20	0.87	280	74	198	16048
25355	STK5	Dry	2/24/2022 13:37	0.99	285	77	235	18331
25328	STK6	Dry	2/21/2022 14:14	0.56	70	27	84	2085
25273	STK6	Wet	2/16/2022 13:31	1.15	112	53	176	3214
25274	STK6	Wet	2/16/2022 13:39	0.95	133	72	162	2604
25275	STK6	Wet	2/16/2022 13:48	1.15	99	47	177	3401
25277	STK7	Wet	2/16/2022 14:05	0.70	124	43	119	841
25276	STK7	Wet	2/16/2022 13:56	0.78	119	41	120	1268
25278	STK7	Wet	2/16/2022 14:13	0.84	97	38	121	1304
25348	STK7	Dry	2/24/2022 12:38	1.22	109	37	181	1378
25350	STK7	Dry	2/24/2022 12:55	1.03	103	34	161	1067
25352	STK7	Dry	2/24/2022 13:12	1.17	108	38	185	1528
25303	GWT1	Wet	2/21/2022 10:46	1.61	93	34	251	887
25308	GWT1	Wet	2/21/2022 11:28	1.23	35	26	121	336
25313	GWT1	Wet	2/21/2022 12:09	2.13	115	39	396	1577
25354	GWT1	Dry	2/24/2022 13:28	1.36	145	48	247	803
25356	GWT1	Dry	2/24/2022 13:45	2.11	109	39	340	994
25358	GWT1	Dry	2/24/2022 14:02	2.45	102	37	397	1113

Table S3-1 Cont.

Sample Identifier	Site name	Season	Date analysed	TiO_2 (%)	Ni (PPM)	Zn (PPM)	V (PPM)	Cr (PPM)
25333	MRT1	Dry	2/21/2022 15:06	0.76	103	63	134	2723
25300	MRT1	Dry	2/21/2022 10:21	0.90	186	120	159	2230
25280	MRT1	Wet	2/16/2022 14:30	0.81	147	84	151	2329
25281	MRT1	Wet	2/16/2022 14:38	0.90	171	99	164	2304
25283	MRT1	Wet	2/16/2022 14:46	0.89	166	95	158	2313
25304	MRT2	Dry	2/21/2022 10:54	0.64	253	109	95	1617
25323	MRT2	Wet	2/21/2022 13:32	0.47	226	48	66	940
25309	MRT2	Dry	2/21/2022 11:35	0.58	252	102	95	1753
25314	MRT2	Dry	2/21/2022 12:17	0.60	205	73	91	1944
25284	MRT2	Wet	2/16/2022 14:54	0.67	194	43	101	1243
25285	MRT2	Wet	2/16/2022 15:03	0.58	210	54	90	1597
25319	MRT3	Dry	2/21/2022 12:59	0.65	238	79	155	16576
25318	MRT3	Wet	2/21/2022 12:51	0.60	179	48	106	9288
25324	MRT3	Dry	2/21/2022 13:41	0.74	197	61	151	15398
25329	MRT3	Dry	2/21/2022 14:32	0.73	197	62	145	12033
25286	MRT3	Wet	2/16/2022 15:12	0.78	219	69	179	21718
25279	MRT3	Wet	2/16/2022 14:21	0.98	205	76	235	30836
25296	MRT4	Dry	2/21/2022 9:56	0.62	255	81	170	26763
25334	MRT4	Dry	2/21/2022 15:14	0.67	530	124	297	64065
25302	MRT4	Wet	2/21/2022 10:38	0.96	220	98	271	49606
25299	MRT4	Dry	2/21/2022 10:13	0.79	454	128	312	67421
25307	MRT4	Wet	2/21/2022 11:19	0.69	287	101	220	39629
25305	MRT4	Dry	2/21/2022 11:03	0.66	483	119	294	61249
25310	MRT5	Dry	2/21/2022 11:43	0.84	256	60	171	12720
25312	MRT5	Dry	2/21/2022 12:00	0.85	226	55	159	12944
25317	MRT5	Wet	2/21/2022 12:42	1.13	264	73	257	28919
25315	MRT5	Dry	2/21/2022 12:26	0.72	236	53	139	7139
25322	MRT5	Wet	2/21/2022 13:24	0.75	213	47	128	6362
25320	MRT5	Dry	2/21/2022 13:08	0.76	232	54	143	7614
25335	MRT5	Dry	2/21/2022 15:23	1.75	283	104	440	58958
25325	MRT6	Dry	2/21/2022 13:49	1.46	273	93	351	46282
25330	MRT6	Dry	2/21/2022 14:41	1.46	281	92	362	46621
25327	MRT7	Wet	2/21/2022 14:06	1.57	219	59	278	12787
25332	MRT7	Wet	2/21/2022 14:58	1.45	209	54	242	10546
25297	MRT7	Wet	2/21/2022 10:05	1.03	205	52	161	6346
25357	MRT7	Dry	2/24/2022 13:53	1.14	228	57	188	7554
25359	MRT7	Dry	2/24/2022 14:11	1.32	240	60	213	8591
25346	MRT7	Dry	2/24/2022 12:22	1.58	226	57	239	9474

Chapter 4 – Stable sulfur isotopes from fish tissue as an ecotoxicological tracer of riverine stressors along a land-use intensification gradient in the Platinum Belt, South Africa

4.1. Abstract

Aquatic ecosystems experience sulfur loading from multiple terrestrial land-use sources (stressors) and atmospheric deposition, leading to potential ecological impairments. Stable sulfur isotope ratios ($\delta^{34}S$), which compare the relative abundance of ^{34}S to ^{32}S in a sample, can be used to trace the sources and transformations of sulfur in the environment. There is limited scientific understanding of how fish tissue $\delta^{34}S$ responds to a range of potentially interacting terrestrial stressors along land-use intensification gradients (urban, agriculture and mining), while also accounting for confounding atmospheric $SO_{2(g)}$ effects. This study employed a multi-scaled modelling approach to assess the relative effects of these stressors on fish tissue $\delta^{34}S$ values, with the aim to develop a tool for disentangling their distinct effects in river systems. Fish tissue samples were collected from 14 sites across two rivers during wet and dry seasons in the Gwathle River Catchment, in South Africa's Platinum Belt. The proportion of each terrestrial stressor was quantified at both sub-basin and cumulative basin scales, revealing similar stressor proportions, except for significantly higher cumulative agricultural coverage on the Maretlwane River. Among the water quality parameters measured concurrently with tissue sampling, total dissolved solids (TDS) emerged as a key indicator of catchment land-use intensification, significantly predicting fish tissue $\delta^{34}S$ values. Biplots of TDS and $\delta^{34}S$ showed clustering of river sites experiencing specific stressors. Generalised linear mixed-effects models (GLMMs) revealed that sub-basin agricultural activity led to relatively enriched fish tissue $\delta^{34}S$, and cumulative basin-scale mining resulted in depleted $\delta^{34}S$ values. It is likely that sulfur-containing fertilizers and livestock manure, which contain S-products enriched in ^{34}S relative to natural inputs, enter aquatic ecosystems through leaching and run-off. Discharged mine tailings into the aquatic ecosystem, may experience in-channel bacterial sulfate reduction producing S-products depleted in $\delta^{34}S$, while mine waste water seepage into adjacent mediated wetlands, may result in simultaneous sulfur transformations influenced by aquatic macrophytes, also producing S-products depleted in $\delta^{34}S$. Atmospheric $SO_{2(g)}$ did not significant influence fish tissue $\delta^{34}S$ variability, being overwhelmed by agricultural and mining stressors. This research presents a potential environmental forensic tool for disentangling complex catchment stressors, identifying likely sulfur polluters, and informing adaptive management strategies for area-specific remediation.

4.2. Introduction

Sulfur occurs and cycles naturally within aquatic ecosystems, playing a vital role in supporting their functionality (Takahashi et al., 2011), however, sulfur pollution from land-use activities (stressors) can disrupt biogeochemical cycles and impair aquatic ecosystem integrity (Mitchell and Likens, 2011). Elevated aquatic sulfur may alter multiple ecohydrological processes including weathering, disrupt the turnover of key aquatic constituents such as N, P and Fe (Zak et al., 2021), as well as modify dissolved inorganic carbon availability (Eimers et al., 2008). It has also been linked to the production of methylmercury, a bioaccumulative neurotoxin that can threaten fish-consuming organisms (Bates et al., 2002; Clayden et al., 2016). Additionally, elevated sulfate levels can cause toxicity in aquatic invertebrates, leading to reduced biodiversity (Soucek et al., 2005). Aquatic producers and consumers, including fishes, accumulate distinct stable sulfur isotope ratios reflecting the pollution inputs along land-use intensification gradients (Clayden et al., 2016), characterised by the increasing presence and influence of anthropogenic stressors. By integrating these signals in aquatic food webs, sulfur-stable isotopes can serve as ecotoxicological tracers of particular riverine stressors affecting ecosystems across different pollution gradients.

Sulfur in aquatic ecosystems is present in various chemical forms, including dissolved sulfate (SO_4^{2-}) and sulfide (S^{2-}) species. These sulfur species originate from an array of natural and anthropogenic point and nonpoint sources within a watershed. Even in relatively undisturbed catchments, instream sulfur variability occurs due to seasonal hydrological conditions, geological weathering, sulfide oxidation, organic matter breakdown and atmospheric deposition (Mitchell et al., 1998). During the industrial revolution, the combustion of S-rich fossil fuels substantially increased atmospheric-S loading in freshwater systems (Rice et al., 2014). In the last 30 years, however, the enactment of air quality regulations on sulfur emissions has led to less acidic deposition and initial chemical recovery in some Northern Hemisphere watersheds (Fölster and Wilander, 2002; Mitchell and Likens, 2011; Aas et al., 2019), while developing countries like South Africa, remain major atmospheric-S contributors (Aas et al., 2019; Shikwambana et al., 2020). This is particularly due to ore roasting (smelting) and coal combustion, which can directly deposit or run-off into aquatic ecosystems (Koptsik and Alewell, 2007; Mitchell and Likens, 2011; Rice et al., 2014).

There are a variety of additional, terrestrial sources of inorganic and organic sulfur compounds in aquatic ecosystems. Such include raw and treated sewage (SO_4^{2-}), the manufacture and application of agrochemicals ($CuSO_4$ and $(NH_4)^2SO_4$), domestic and industrial detergents (SO_4^{2-}), as well as mine water decant (SO_4^{2-} and FeS_2) (Lodhi et al., 2006; Hosono et al., 2007; Ochieng et al., 2010; Dubinsky et al., 2020). Different atmospheric and terrestrial S-sources can present distinct $\delta^{34}S$ signatures which can be used to pinpoint pollution inputs and thus the various sources of aquatic ecosystem stress (Nielsen, 1974; Cravotta, 2002; Morrissey et al., 2013). Isotopes are variants of the same chemical element with the same number of protons but different numbers of neutrons, resulting in different atomic masses (Kennedy and Krouse, 1990). The $\delta^{34}S$ values is the $^{34}S/^{32}S$ abundance ratios compared to the same ratio in the standard reference material, troilite (FeS) (Kennedy and Krouse, 1990).

Atmospheric research has demonstrated that industrial precipitation tends to have more depleted wide-ranging sulfur isotope ratios in dissolved sulfate ($\delta^{34}S_{SO4}$) due to distinctive fractionation effects during fuel combustion, contrasting with narrower, enriched values in non-industrial areas (Nakai and Jensen, 1967; Nielsen, 1974; Zhang et al., 2002). Smelting activities produce relatively depleted rainfall $\delta^{34}S_{SO4}$, with such areas demonstrating homogeneous $\delta^{34}S_{SO4}$ signatures, when compared to precipitation solely influenced by vehicle emissions (Grey and Jensen, 1972). Subsequent atmospheric deposition introduces these sulfur compounds into aquatic systems (Giesler et al., 2009), where assimilation by biota can reflect the sourced isotopic signal (Kennedy and Krouse, 1990).

Foundational terrestrial-source characterisation on dissolved $\delta^{34}S_{SO4}$ has also demonstrated distinctive signatures. Synthetic solid fertilizers have values characteristically enriched ($\bar{x}$=8.22, σ= 6.61) relative to natural fertilizers such as cow manure ($\bar{x}$=4.21, σ=0.67), whereas aerated sewage is relatively depleted ($\bar{x}$=4.97, σ=1.11) compared to septic tank effluent ($\bar{x}$=9.20, σ=0.28) (Cravotta, 2002). With diverse atmospheric and terrestrial sulfur sources potentially affecting aquatic ecosystems, distinguishing S-contributions in mixed-use watersheds is key for targeted mitigation of aquatic contamination. The lack of research linking stressor-tissue $\delta^{34}S$ responses will allow such foundational work on $\delta^{34}S_{SO4\ to}$ provide insight into interpreting tissue $\delta^{34}S$ responses; with tissue $\delta^{34}S$ responses linked directly to differences in sulfur speciation and fractionation.

The cycling and fractionation of terrestrially derived sulfur can lead to distinctive sulfur isotope rations ($\delta^{34}S$) in the tissues of aquatic consumers, such as fish, that can be used to spatially disentangle specific stressor-related pollution sources in aquatic ecosystems (Trust and Fry, 1992; Dubinsky et al., 2020). Sulfide oxidation can produce sulfate depleted in $\delta^{34}S$ if reversible equilibrium fractionation dominates (Cravotta, 2002; Turchyn et al., 2013), whereas, processes like microbial sulfate reduction preferentially use the lighter ^{32}S isotope, enriching residual sulfate ^{34}S, while the sulfide product is depleted in $\delta^{34}S$ (Fry et al., 1988; Habicht and Canfield, 1997). For example, aquatic primary producers, in their S-assimilation pathway, reduce inorganic sulfate (primary S-source) to sulfide enriched in ^{32}S, which is then incorporated into their tissues as sulfur-containing amino acids (Bowen, 1960; Takahashi et al., 2011).

Aquatic consumers, being unable to metabolize inorganic sulfate directly, assimilate their sulfur requirements from the primary producers, with a negligible fractionation between subsequent trophic levels within the aquatic food web (Kennedy and Krouse, 1990). Furthermore, the majority of the terrestrial DOM exported to aquatic ecosystems closely reflects the SO_4^{2-} input source(s), from which it was derived e.g. atmospheric S-deposition (Giesler et al., 2009). This is because, during aerobic conditions, the S-uptake (SO_4^{2-}) by microbes and plants associated with organic matter formation (by mineralization) experiences only a minor fractionation of 1-2‰ in SOM-$\delta^{34}S$ values (Giesler et al., 2009).

Recent aquatic-stress tracing studies using sulfur stable isotopes have paired $\delta^{34}S_{SO4}$ with oxygen isotope ratios in dissolved sulfate ($\delta^{18}O_{SO4}$), (i.e. transient or spot water analyses) to discern aquatic contributors (Hosono et al., 2007; Zhang et al., 2020; Liu and Han, 2020). Aquatic tissues may, however, be a better option, offering a measure of $\delta^{34}S$ assimilation over time, which can be effective for long-term pollution monitoring and tracing (Hesslein et al., 1991; Wayland and Hobson, 2001). Although tissue $\delta^{34}S$ is widely used in aquatic food web studies to track the consumption of food sources (Ofukany et al., 2014; Srayko et al., 2023), few studies have used it to distinguish key industrial and sewage pollution sources in rivers (Wayland and Hobson, 2001; Morrissey et al., 2013). Furthermore, no South African aquatic research, other than using $\delta^{34}S$ to account for variable catchment geology (Woodborne et al., 2012), has used it to disentangle sources of river stress. Thus, the assessment of fish tissue $\delta^{34}S$

as an ecotoxicological tracer of multiple interactive stressors (agricultural, urban and mining), while accounting for confounding atmospheric $SO_{2(g)}$ effects, has not yet been attempted within local nor international river catchments.

The Gwathle Catchment within South Africa's economically vital Bushveld Igneous Complex (BIC), colloquially referred to as the Platinum Belt, has a progression of natural, agricultural, urban and mining stressors. Synonymous with extensive mining activity, the BIC hosts the Merensky Reef and UG-2 Chromitite layer; significant global sources of platinum group elements (PGE) and chrome mineralization (Cawthorn, 2010; Almécija et al., 2017). The Merensky Reef is composed of orthopyroxene, and the UG-2 chromitite layers, which include cooperite (PtS) and laurite (RuS_2); both rich in sulfides and thus serve as potential sources of sulfur to the surrounding environment (Magalhães et al., 2018). Previous research in the Western Lobe using drill core samples, indicated that the Merensky Reef had $\delta^{34}S$ values of 1.7 ± 0.6‰ ($\Delta^{33}S$ value of 0.12 ± 0.02‰; 1 σ), while UG-2 chromitite layers have relatively uniform $\delta^{34}S$ values of 2.7 ± 0.3‰ ($\Delta^{33}S$ from 0.10‰ to 0.12‰; within 1σ), with both stratigraphic layers having statistically indistinguishable $\delta^{34}S$ values (Penniston-Dorland et al., 2008; Penniston-Dorland et al., 2012; Magalhães et al., 2018). Sulfide oxidation, weathering, and microbial cycling can, however, modify initial mineral $\delta^{34}S$ values before the mine-derived sulfur reaches aquatic ecosystems (Meier et al., 2004; Schippers, 2004).

While studies have used aquatic tissue $\delta^{34}S$ in an attempt to distinguish between pollution sources, its application for tracing and disentangling mining-derived pollution along river continua within a multi-stressor catchment remains unexplored. This research aims to disentangle the effects of key aquatic stressors in the Gwathle Catchment, using aquatic fish tissue $\delta^{34}S$. The objectives are to 1) characterise the catchment's proportional stressor coverage and the key catchment water quality parameters relative to fish tissue $\delta^{34}S$, 2) assess the ability of a key catchment water quality indicator and fish tissue $\delta^{34}S$ to identify pollution hotspots and disentangle stressor sources in a catchment subject to multiple stressors, over a pollution gradient, 3) assess stepwise and cumulative trends in $\delta^{34}S$ for each river, 4) determine key land-use stressors that best predict and describe $\delta^{34}S$ variation at sub-basin and cumulative basin scales while accounting for atmospheric $SO_{2(g)}$ effects. By pioneering the use of fish tissue $\delta^{34}S$ to disentangle multiple sulfur pollution sources in an African watershed, this study develops an innovative, time-integrated tracing tool to inform river pollution mitigation strategies and improve aquatic health in understudied regions facing complex stressors, which will be relevant worldwide.

4.3. Materials and Methods

4.3.1. Study area

The Gwathle River Catchment (Quaternary Catchment A21K) is situated within South Africa's Limpopo Basin, draining northern slopes of the Magaliesberg Mountains between Rustenburg and Mooinooi before its confluence with the Crocodile (West) River at Roodekoppies Dam in North West Province. The semi-arid catchment receives a mean annual precipitation of 629 mm, with a wet season from November-March peaking in January, and a dry season from April-October (Funk et al., 2015). Mean monthly temperatures range from 4.94 – 31.76°C, with June and February being coolest and warmest months, respectively (SAWS, 2023). The catchment's Western Sterkstroom (site codes: STK1-7) and Eastern Maretlwane (site codes: MRT1-7) are third-order tributaries (**Figure 1-1**).

The rivers occur within the Western Bankenveld and Bushveld Basin aquatic ecoregions, with the southern section’s falling within the Magaliesberg Biosphere Reserve under the UNESO Man and the Biosphere Programme, focused on sustainable development and eco-tourism (Pool-Stanvliet, 2013). The catchment overlaps the PGE-rich Western Lobe of the Bushveld Complex, which is vital for mining and contains extensive sulfur-bearing mineral layers, such as pyrrhotite, within its mafic-ultramafic intrusions including gabbro-norite units (**Figure 2-2**) (see Thormann et al. 2017). Natural weathering of S-containing mineral deposits can provide a geological source of sulfur to nearby water systems (Berner, 1971), while excavating activities (e.g. mining, see **Chapter 3**) and subsequent atmospheric exposure, accelerates erosion and aquatic contamination.

Within the catchment, the pristine headwater conditions transition downstream to agriculture, informal and formal settlements and towns, mining as well as in-catchment smelting operations (**Figure 1-1** and **Figure S4-2**), with additional smelting facilities situated external to the watershed; to the West and East. Major land covers are natural grassland (67.6%), agriculture (22.0%), mining (4.4%) and urban/informal areas (4.4%).

4.3.2. The quantification of key land-cover stressors

Land-cover data, used to quantify landscape stressors, were derived from the South African National Land Cover (SANLC) 2020 dataset (GeoTerraImage, 2021). This recent release uses ~20 m resolution Sentinel-2 satellite imagery, achieving over 85% mapping accuracy and a Kappa Index above 85. The dataset contains 73 level 1 land-cover classes of which 53 are within the bounds of the study catchment. Using ArcGIS 10.5, the necessary level 1 classes were reduced (aggregated) to one natural cover class (woodland, shrubland and grassland) and four key anthropogenic stressor classes, being (1) cultivated commercial farmland; (2) fallow-land (rangeland) for cattle grazing and rearing, (3) urban residential and commercial infrastructure, formal and informal and (4) mining activities including pits and waste storage facilities, including waste rock dumps.

4.3.3. Study catchment delineation and multi-scale land-use analysis

Delineation of the river networks was achieved using the 30 m resolution Shuttle Radar Topography Mission digital elevation model (DEM) in the ArcSWAT module within ArcGIS, after filling sinks in the raw data (Farr and Kobrick, 2000). A total of 14 river sites were selected from the two tributaries, the Sterkstroom and Maretlwane rivers. Both tributaries contained the highest replication of stressors within the catchment and thus, seven sites were chosen along each (**Figure 1-1**, excluding the GWT1 study site). Sites were selected immediately up- and down-stream of different land-use activities along the continuum to capture distinct stressors, thus creating the nested study design. The scale-specific drainage areas were also extracted with the ArcSWAT module to enable spatially explicit stressor analysis at: (1) individual sub-basins defined between monitoring sites, and the (2) sites cumulative basins (**Table 4-1**).

The sub-basin boundaries were set between sequential study sites to characterise incremental upstream stressor contributions and capture spatial-dependent processes within. Cumulative catchments for each location encompassed the study site’s total upstream area, including all nested sub-basins, capturing cumulative processing effects. The National land cover layers were clipped to the two respective spatial scales using ArcGIS 10.5 Data Management and Spatial Analyst tools before stressor quantification at each spatial scale. Using the SANLC dataset the proportion of the natural class and four stressor classes within their respective spatial scales was quantified using the Percentage of Landscape (PLAND) metric in FRAGSTATS 4.2 (McGarigal et al., 2002; Shi et al., 2017).

Table 4-1: The two hydrological spatial scales used in the assessment of river water quality and statistical modelling with descriptions of each scale.

	Spatial scale	Description
1	Cumulative scale	The total upstream catchment area draining to a single downstream study site
2	Sub-basin scale	The area draining between the downstream and immediate upstream site

4.3.4. Extraction of atmospheric $SO_{2(g)}$ data

There is local and international evidence to support the effects of atmospheric wet and dry S-deposition influencing the chemistry of aquatic ecosystems at differing spatio-temporal scales (Giesler et al., 2009; Mitchell and Likens, 2011; Dunnink et al., 2016). With the catchment positioned within the intensively mined Bushveld Igneous Complex, where the PGE minerals are present in sulfides (Cawthorn, 2010; Thormann et al., 2017), it is likely that the multiple mining complexes and associated sulfide roasting within the smelters exposes the catchment to relatively high concentrations of atmospheric $SO_{2(g)}$ compared to local unindustrialised and unmined catchments (Nielsen, 1973; Shikwambana et al., 2020). Given the strong relationship between organic-S soil concentrations and proximity to smelters (Koptsik and Alewell, 2007), as well as the variable $\delta^{34}S$ values associated with fossil fuel combustion and mining smelters (Nielsen, 1974), it is crucial to account for the confounding effects of atmospheric $SO_{2(g)}$ emissions on fish $\delta^{34}S$ values when attempting to disentangle terrestrial catchment stressors in a spatial assessment. For this study, it is assumed that the seasonal concentrations of atmospheric $SO_{2(g)}$ may influence fish tissue $\delta^{34}S$ variation, irrespective of any unknowing changes to atmospheric $SO_{2(g)}$ isotopic composition.

The Sentinel-5P (near-real-time) NRTI $SO_{2(g)}$ platform, containing the Troposphere Monitoring Instrument (TROPOMI) from the Copernicus mission, is dedicated to monitoring atmospheric conditions and is widely used for high spatio-temporal atmospheric air quality monitoring in South Africa and abroad (Shikwambana et al., 2020). The instrument has a temporal resolution of one day and a spatial resolution of

~3.5 x 5 km; allowing for the detection of small natural and stressor $SO_{2(g)}$ plumes (Romahn et al., 2023). The data are presented as $SO_{2(g)}$ vertical column density (VCD) in mol/m^2 units, where the slant column density (SCD) is first retrieved and then converted to VCD using an air mass factor (AMF) that accounts for atmospheric and surface conditions as well as $SO_{2(g)}$ vertical profiles (Cofano et al., 2021; Romahn et al., 2023). This thereby standardising the data values and thus enabling the fair comparison of pixel $SO_{2(g)}$ values at differing localities (pixels) (Romahn et al., 2023).

Google Earth Engine atmospheric $SO_{2(g)}$ was extracted monthly for each study site's assessed spatial scale (i.e. sub-basin scale and cumulative basin scale), between January 2019 and December 2021 to capture long-term seasonal $SO_{2(g)}$ variability and aquatic exposure (**Figure S4-1** and **Figure S4-2**). This is because experimental research has shown that the turnover rates of $\delta^{34}S$ in fish muscle tissue are highly dependent on the weight and species of the fish following exposure to sulfur sources (Charest, 2015). Due to the atmospheric $SO_{2(g)}$ variability, two seasonal $SO_{2(g)}$ metrics including the average and standard deviation (heterogeneity) were determined. These two metrics were determined for each site's respective spatial scale during the dry and wet seasons, coinciding with the seasons of tissue $\delta^{34}S$ field data collection (**Table S4-2**). The wet season atmospheric $SO_{2(g)}$ data was captured from January to April and October to December, while the dry season $SO_{2(g)}$ was captured from May to September (**Figure S4-1**). The resulting wet and dry atmospheric seasonal $SO_{2(g)}$ data (at their respective spatial scales) were then paired with their seasonal fish tissue $\delta^{34}S$ data in further statistical analyses.

4.3.5. Physico-chemical field sampling

Water quality data were collected during wet (March 2021) and dry (September 2021) months concurrent with fish tissue sampling to characterise the contemporary physico-chemical conditions. Total dissolved solids (g/L), pH (units), dissolved oxygen (mg/L) and temperature (°C) were logged at 30-second intervals for five-minutes with a YSI-Professional Plus Handheld Multi-parameter meter calibrated pre-sampling to manufacturers specifications. Turbidity was measured in triplicate via a Hanna portable meter (HI98703-02). For major ions and metals, 400 mL were filtered through Supor® 0.45µm 47 mm filters using a Thermo Scientific Nalgene reusable filter unit and stored in one-litre acid-rinsed polyethylene bottles which were placed on ice until analysis (Akyildiz and Duran, 2021). Once at the laboratory, the samples were analysed for SO_4-S (sulfate), NO_3^--N (nitrate), NO_2^--N (nitrite), PO_4^{3-}-P (ortho-phosphate), NH_3-N (ammonia) and NH_4^+-N (ammonium) using an Aquakem/Discrete Analyser (photometric analyser).

Major cations and trace metals were analysed using an Agilent 7800x inductively coupled plasma mass spectrometry (ICP-MS) with concentrations measured against external matrix-matched standards. Following dilutions, each sample had 0.1 m/L of ultrapure acid (HNO_3) added to 10 mL of filtrate to disassociate precipitates. Analytes below detection limits were estimated at half detection limits to enable statistical continuity rather than omission (Croghan et al., 2003). These field and laboratory procedures provided complementary snapshots of seasonal water quality dynamics.

4.3.6. Sulfur stable isotope collection and analysis

To capture the tertiary aquatic consumer group at each river site, fish (or anuran tadpoles in their absence) were sampled by single-pass electrofishing for five minutes using a Halltech HT-2000 battery backpack electrofisher. The applied voltage ranged from 100 to 750 V with a frequency of 80 Hz. Anuran tadpoles were collected at fishless sites as they represent an important vertebrate primary consumer in streams. A 50 m representative river reach was selected prior to sampling at each site, which had at least three of the instream geomorphic habitat units recognized by the Rapid Habitat Assessment Method (Kleynhas and Louw, 2007). By selecting reaches with a diversity of habitat types (e.g. riffles, runs and pools), the sampling aimed to maximise capture efficiency across species with different habitat preferences. Additionally, block nets were stationed below riffles during electrofishing. This barrier capture method prevented fast-swimming species from evading the sampling area before they could be netted, further improving overall catch efficiency.

Where possible, a minimum of five to ten specimens per species were collected at a site to ensure sufficient replication. If one or two specimens of a particular species were collected at a site, they were released, unless no other species in high enough abundance were present. Due to the inconsistent presence of fish species between river sites and their differing abundances, no particular species with a specific feeding trait (e.g., insectivorous was selected. Instead, a diversity of species was collected to ensure data availability across all sites. Upon collection, all indigenous vertebrates larger than 6 cm were euthanized in a 120 mg/L solution of clove oil (eugenol) following the protocol outlined by Bennett et al. (2016). A block of muscle tissue from the right flank of the specimen was then removed for $\delta^{34}S$ analysis, while ensuring that no skin nor scales were present on the sample before storage. All samples were stored in labelled DNA and RNA free Eppendorf® microcentrifuge tubes and placed in a mobile Camp Master freezer at -20°C before being transported to the laboratory for further processing.

In the laboratory, all tissue samples were defrosted in a fridge over 12-hours before being thoroughly rinsed with deionized water to remove any remaining residual contaminants. The rinsed tissue samples were placed on sterile watch glasses and dried at 60°C for 48 hours to achieve a constant weight, after which the samples were homogenized using a sterile percaline mortar and pestle (Jackson et al., 2020). The samples were then transferred into completely sterile Ultra-Pure elemental tin capsules, where they were weighted between 3.8 and 4.2 mg on a five-place decimal Mettler Toledo-XP6 balance. The solid $\delta^{34}S$ samples were analysed using an Elementar vario ISOTOPE cube elemental analyser (Elementar Analysensysteme GmbH, Langenselbold, Germany) interfaced to an Elementar PrecisION isotope ratio mass spectrometer (Cheadle Hulme, Cheadle, England) at the Stable Isotope Facility at the University of California, Davis.

Samples were combusted at 1150°C in a reactor packed with tungsten oxide. Immediately following combustion, sample gases are reduced with elemental copper at 880°C and subsequently passed through a buffering reactor filled with quartz chips held at 900°C. Resulting SO_2 and CO_2 are separated by adsorption columns, allowing for full separation and peak focusing. Following separation, the SO_2 adsorption trap is heated, and the sample SO_2 passes directly to the IRMS for measurement. The lab references were calibrated against international reference materials, including: IAEA-S-1, IAEA-S-2, IAEA-S-3, NBS-127, IAEA-SO-5, and IAEA-SO-6. The final delta (δ) values are expressed relative to Vienna Cañon Diablo Trolite (VCDT) (Ofukany et al., 2014). The quality assurance reference materials included Taurine, Whale Baleen, Cysteine and the quality control reference materials included Hair, Mahi-Mahi Muscle. The final isotope ratios were expressed in delta notation using parts per mille scale (‰), were defined by equation 1, where X = ^{34}S and R represents $^{34}S/^{32}S$. The precision of the sulfur stable isotope analysis was ± 0.47‰ (mean SD for reference material replicates), and the mean absolute accuracy for calibrated reference materials was within ± 0.38‰.

Equation 1: $\delta X(‰) = [(R_{sample} – R_{standard})/R_{standard} – 1] \times 1000$

4.3.7. Statistical analysis

To enable cross-site comparison of $\delta^{34}S$ values and assess relative enrichment and depletion associated with downstream stepped-stressor activities, all statistical analyses were performed on pristine-corrected $\delta^{34}S$ values. These values were calculated by subtracting the mean $\delta^{34}S$ value of each downstream site from the mean $\delta^{34}S$ value of its respective pristine site (MRT1 for the Maretlwane River and STK2 for the Sterkstroom River; as reference sites) for each season. This standardization approach effectively sets the pristine sites to zero, allowing for a clear interpretation of the relative effect of stressors on $\delta^{34}S$ values along the river continua.

To assess any significant differences in the proportion of stressor land-cover (%) for the two river watersheds with the greatest replication (i.e. STK and MRT), an Analysis of Variance (ANOVA) was performed using the stressor proportions from each of the river's sub-basins in R. A single Principal Component Analysis (PCA) was performed in the R to identify the key water quality indicator of catchment land-use intensification and the potential drivers (covariates) of the $\delta^{34}S$ values and heterogeneity (SD) across the sampled rivers for the two seasons (R Core Team, 2023). Prior to the analysis using the factoextra and FactoMineR packages in R, variables with differing units underwent z-score standardization to allow for appropriate statistical interpretation (Lê et al., 2008; Kassamara and Mundt, 2020). To identify the key water quality parameters characterising the river water quality over the two seasons, variables with the highest loading from the first three Principal Components (PCs) were identified using the `dimdesc` function in the FactoMineR package.

Following the non-normally distributed nature of the fish tissue $\delta^{34}S$ values and the residuals (p = 0.01; Anderson-Darling Test) in linear models, the relationship between the water quality parameter with the highest loading in PC1 and the $\delta^{34}S$ (mean) values were assessed using a generalised linear mixed-effects model (GLMM), using the lmer4 package in R (Bates et al., 2014). Given the negatively skewed distribution of the response variable, the family Gamma with a log-link function was applied in the GLMM. To evaluate the potential for rapidly distinguishing river-stressor aligned spatial patterns along the catchment's land-use intensification gradient, dual variable scatter plots were generated comparing the key water quality parameter from PC1 (serving as an indicator for catchment intensification) to the pristine-corrected fish $\delta^{34}S$ values. The response, fish $\delta^{34}S$ mean values (by site and season), were plotted as the dependent variable with standard deviation bars to convey variability. This analysis sought to identify potential spatial groupings that would provide insight into the effectiveness of the dual parameter technique to disentangle meaningful $\delta^{34}S$-stressor associations.

To elucidate potential stepwise as well as cumulative effects and trends on $\delta^{34}S$ values as additional stressors enter each river system, river-specific scatter plots were constructed depicting sample sites sequentially along the x-axis and tissue $\delta^{34}S$ as the dependent variable. Comparing longitudinal $\delta^{34}S$ profiles between rivers can reveal locations where different stressors enter the system, influencing the downstream isotopic signal and thus overarching trends. Because riverine sulfate has shown to be a predictor of $\delta^{34}S$ values following terrestrial stressor inputs (Yucel et al., 2016) similar and separate scatter plots were created for each river's seasonally respective SO_4^{2-} concentrations.

Multi-scale GLMMs were developed to identify dominant stressor variables, driving relative fish tissue $\delta^{34}S$ variability within the catchment at the two hydrological spatial scales (i.e. sub-basin scale and cumulative basin scale; **Table 4-1**). The non-parametric $\delta^{34}S$ (mean) response variable as well as the nested nature of the data (i.e. cumulative basin scale) with repeated measurements through time allowed for the GLMMs to provide a suitable approach to investigate the spatial multivariate air-land-water complexities on the receiving riverine fish $\delta^{34}S$ values (Zuur et al., 2009). The predictive variables included the FRAGSTAT-derived class-level PLAND metric for the natural and stressor classes (e.g. agriculture) as well as the mean and heterogeneity metrics for atmospheric $SO_{2(g)}$ (mol/m^2) during the respective season of $\delta^{34}S$ sampling, to account for potential confounding effects. All predictors were included as additive terms in the models without interactions to examine the individual effects of each.

Full models were fitted with predictive variables across the two spatial scales to assess scale-dependent stressors (and processes) influencing shifts in fish-tissue $\delta^{34}S$ values. Two full GLMMs were fit, one for each spatial scale, using the `glmer` function from the lme4 package (Bates et al., 2014). All candidate predictors, of the respective spatial scales, were fit as main effects including the rivers sampled, with “Season” as the random effect. The categorical “River” variable was included as a fixed effect to isolate the unique stressors in each river on $\delta^{34}S$ variability. Each model was again fitted using a Gamma distribution with a log-link function owing to the continuous, skewed nature of the $\delta^{34}S$ values.

Full models with all candidate predictors were initially fitted to observe the coefficients and any statistical significance for the explanatory variables. Once observed, the most parsimonious model, balancing model performance and complexity, was determined through a systematic stepwise elimination of parameters using the `dredge` function in the MuMIN package (Barton, 2023). The stepwise dredge analysis uses Akaike’s Information Criterion corrected for small sample size (AICc) to identify the most parsimonious yet informative fitted model, including the top predictor terms that maximised clarification of variation in the response variable, $\delta^{34}S$ (Burnham and Anderson, 2004). The best-fitted model, based on AICc, was identified using the `get.model` function from the MuMIn package. The final fitted model’s goodness of fit was assessed using the marginal R^2 ($R^2_{GLMM(m)}$; the variance explained for by the fixed factors) and the conditional R^2 ($R^2_{GLMM(c)}$; the variance explained by both fixed and random factors) coefficients using the `r.squaredGLMM` function in the MuMIN package (Wanderi et al., 2022; Barton, 2023).

4.4. Results

4.4.1. Comparative stressor proportion across the studied rivers

Eight separate one-way ANOVAs, testing the differences in stressor (i.e., urban, agriculture, fallow-land, and mining) proportions at the sub-basin and cumulative-basin scales for each of the two rivers, indicated no significant differences ($p > 0.05$; **Figure 4-1** and **Figure 4-2**), except agricultural coverage at the cumulative-basin scale, where the Maretlwane watershed had significantly higher agricultural coverage than the Sterkstroom watershed (df = 12, F = 5.49, $p = 0.04$). Overall, spatial proportions of the major stressors were similar for the two primary tributary catchments, exhibiting comparably similar magnitudes of watershed land-use modifications.

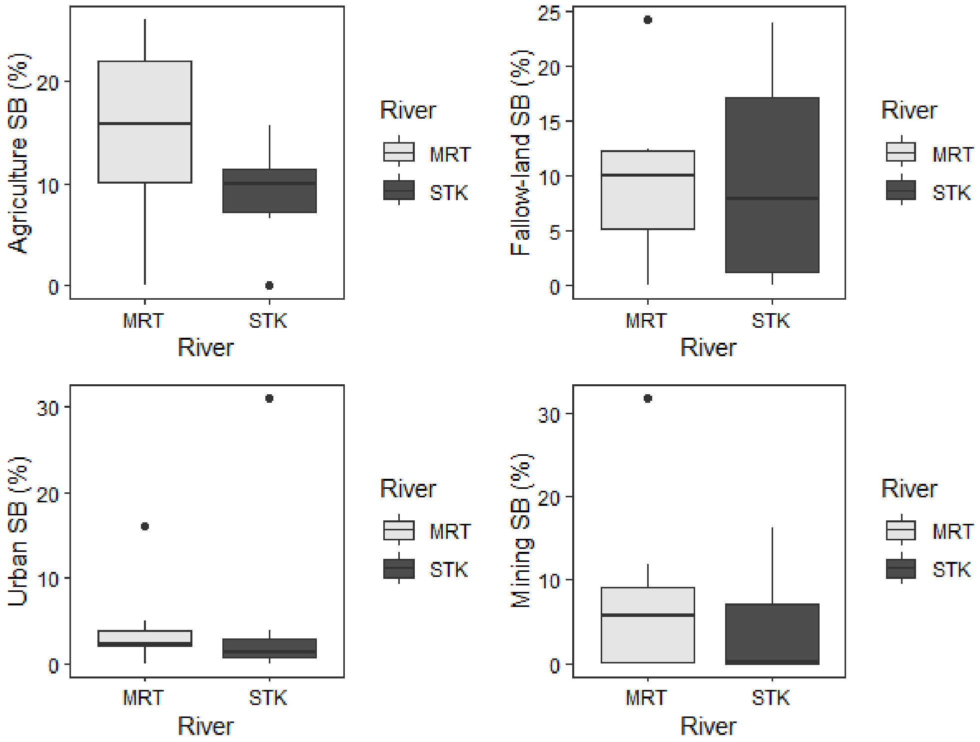

Figure 4-1: Comparison of the proportions of the four key land cover stressors between the Maretlwane (MRT) and Sterkstroom (STK) rivers at the sub-basin scale, indicating no significant differences in stressor coverage between the rivers.

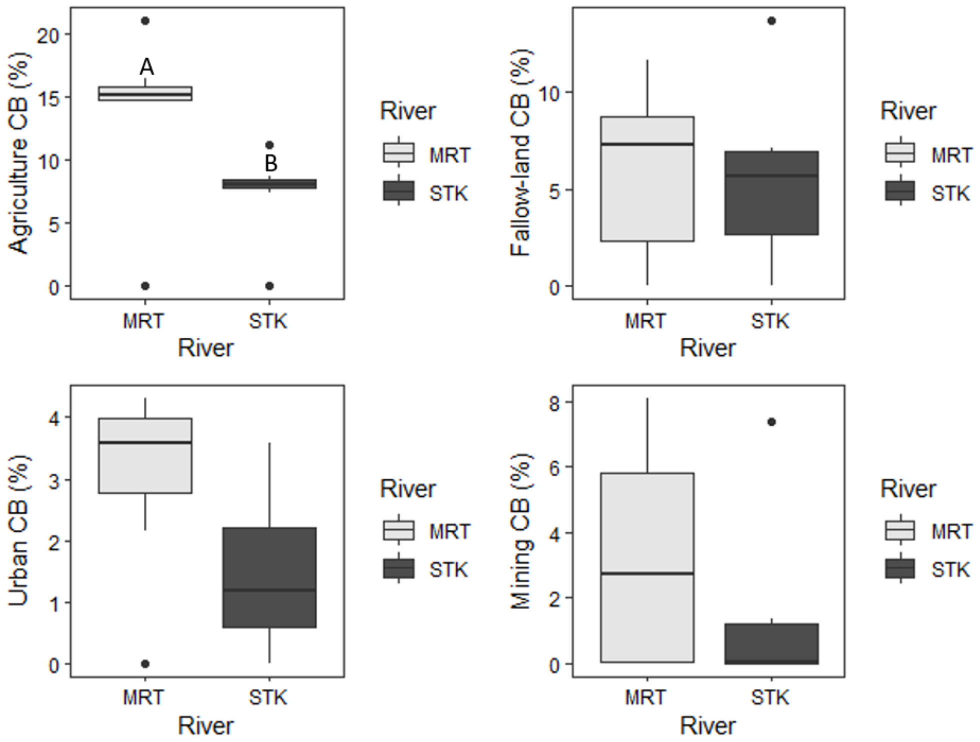

Figure 4-2: Comparison of the proportions of the four key land cover stressors between the Maretlwane (MRT) and Sterkstroom (STK) rivers at the cumulative basin scale, with agricultural coverage differing significantly ($p = 0.04$; ANOVA) between the two rivers. The annotated superscripts, "A" and "B" indicate a significant difference between the two rivers.

4.4.2. Key water quality characteristics between catchments

The first Principal Component (eigenvalue of 7.25), accounted for 34.54% of the total variance in the multivariate water quality dataset. This indicates that over one-third of the overall data variability was encapsulated within the initially extracted component axis **(Figure 4-3)**. Additional variability from PC2 and PC3 accounted for 12.25% and 10.56% respectively, with the three leading principal components capturing 57.34% of the cumulative system-wide variance over the two seasons. The three variables with the highest and most significant loadings from the respective principal components were total dissolved solids (TDS; g/L), orthophosphate (mg/L-P) and ammonium (mg/L-N) respectively (**Table S4-1**). Therefore, TDS represents a key water quality variable that acts as a proxy for catchment land-use intensification.

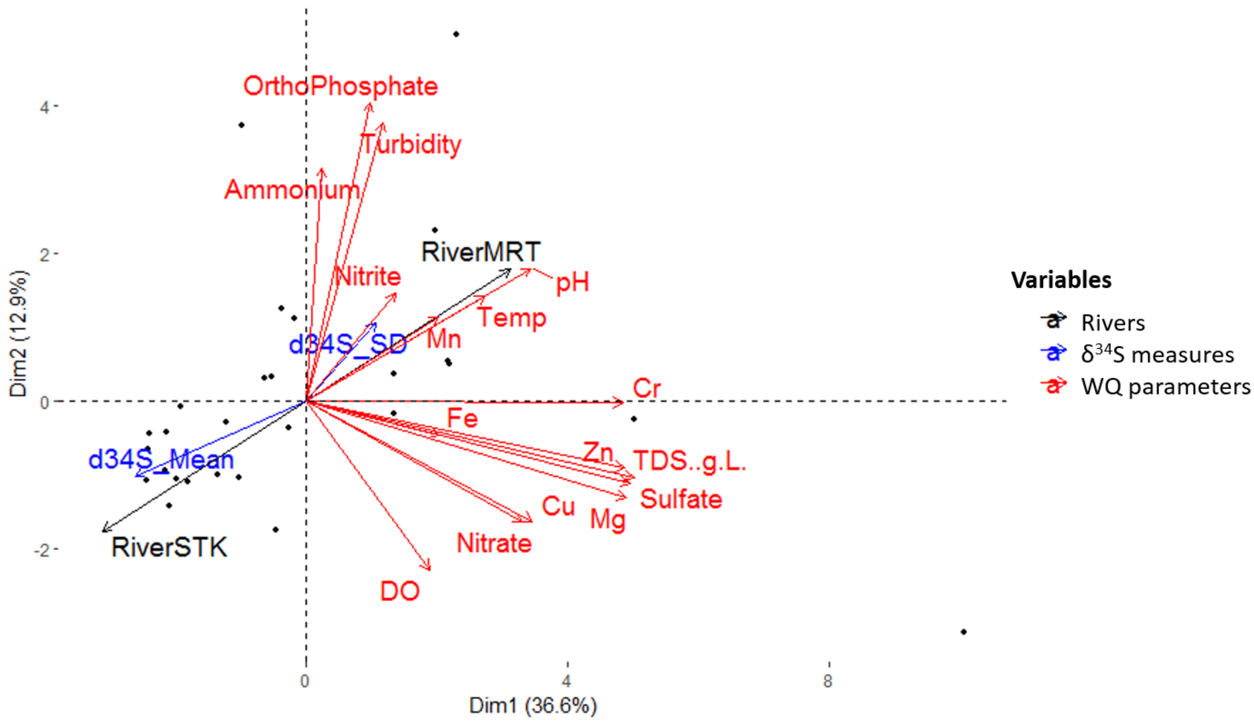

Figure 4-3: A Principal component analysis characterising the wet and dry seasonal variability in $\delta^{34}S$ ratios as corrected mean and standard deviation (SD) vectors, as well as the various water quality (WQ) parameters; collected at the time of tissue sampling across the two investigated rivers the Sterkstroom (STK) and Maretlwane (MRT).

4.4.3. Predictive relationship between TDS and $\delta^{34}S$

The mean fish $\delta^{34}S$, presents a significant loading onto PC1, indicating a shared but inverse loading result with the highest loading variable of PC1, being TDS (g/L), followed by sulfate, which had a significant positive correlation with TDS ($r = 0.99$, $p < 0.01$). Using a GLMM to investigate how well TDS (g/L) predicts fish $\delta^{34}S$ isotopic values, revealed that TDS (g/L) was a significant negative predictor of tissue $\delta^{34}S$ ($p = 0.04$), where a one-unit increase in TDS (g/L) corresponds to an estimated 13.36% decrease in the fish $\delta^{34}S$ values in units per mille (coefficient = -0.14) (2.50% CI: -0.27 and 97.50% CI: -0.01). Total dissolved solids also accounted for 14% of the fish $\delta^{34}S$ variability ($R^2_{GLMM(m)} = 0.14$; $R^2_{GLMM(c)} = 0.14$) across the three river systems sampled during the two seasons.

4.4.4. Analysis of TDS and $\delta^{34}S$ to disentangling catchment stressors

Using TDS (g/L) as the independent variable and corrected $\delta^{34}S$ (‰) values as the dependent variable in biplots revealed visual clustering among sampling sites on each river, based on relative enrichment and depletion patterns. Sites STK3 and STK6, were enriched and grouped across both seasons (**Figure 4-4a**). The STK3 site experienced intensive upstream agricultural activities in the upstream valley (Buffelspoort Valley), while STK6 experienced upstream formal and informal urban settlement effects (i.e. Marikana Township).

The study sites STK4 and STK7 also grouped together, being enriched relative to pristine conditions. The STK4 study site experiences upstream agricultural impoundment effects, while STK7 receives inputs from a wetland draining from a mining (platinum) pollution control dam (PCD) and effluent from surrounding agricultural activities (**Figure 1-1**). The high spatial separation between the two STK5 sites from the two seasons, as well as from the other sites prevented their grouping (**Figure 4-4a**). The STK5 was depleted (-0.8‰ ± 3.6SD) in the wet season and conversely for the dry season which was relatively enriched (2.4‰ ± 1.1SD). The STK5 site is subjected to both upstream informal urbanisation as well as active platinum mining effects with tailings (solid) storage facilities in close proximity to the site.

The dual assessment of TDS (g/L) and $\delta^{34}S$ (‰) biplots for the Maretlwane River also revealed distinct visual clustering among sampled sites across the seasons relative to pristine conditions (**Figure 4-4b**). The sites MRT2 and MRT3 for both seasons were enriched and clustered together (~1.5‰ wet; dry, ~5.1‰). The MRT2 site is downstream of the town of Mooinooi, with extensive impervious surfaces and storm-water drainage networks as well as an active wastewater treatment works (WWTW). Comparatively, the MRT3 site is downstream of cattle and irrigated cropland.

The $\delta^{34}S$ of the MRT4 site during the wet season was enriched (1.3‰ ± 1.9SD) and isolated on the biplot. Conversely, the MRT4 site in the dry season had depleted $\delta^{34}S$ values (-3.9‰ ± 0.8SD) and grouped with the MRT5 dry and wet season samples (-3.8‰ and -5.9‰), as well as MRT7 in the dry season (-1.7‰ ± 0.5SD) (**Figure 4-4b**). MRT4 is downstream of an active commercial chrome mine, which during this investigation, discharged processed mineral tailings (silt) into the river. The sites MRT5 and MRT6 (-1.5‰ ± 1.1SD) are both downstream of the same legacy platinum PCDs and waste rock dumps. The MRT7 site receives urban runoff as well as effluent from legacy platinum PCDs upstream (**Figure 1-1**). In the wet season, MRT6 and MRT7 both have similar $\delta^{34}S$ values and both receive wet seasonal legacy platinum mine-related inputs via mediated wetlands, from separate PCDs.

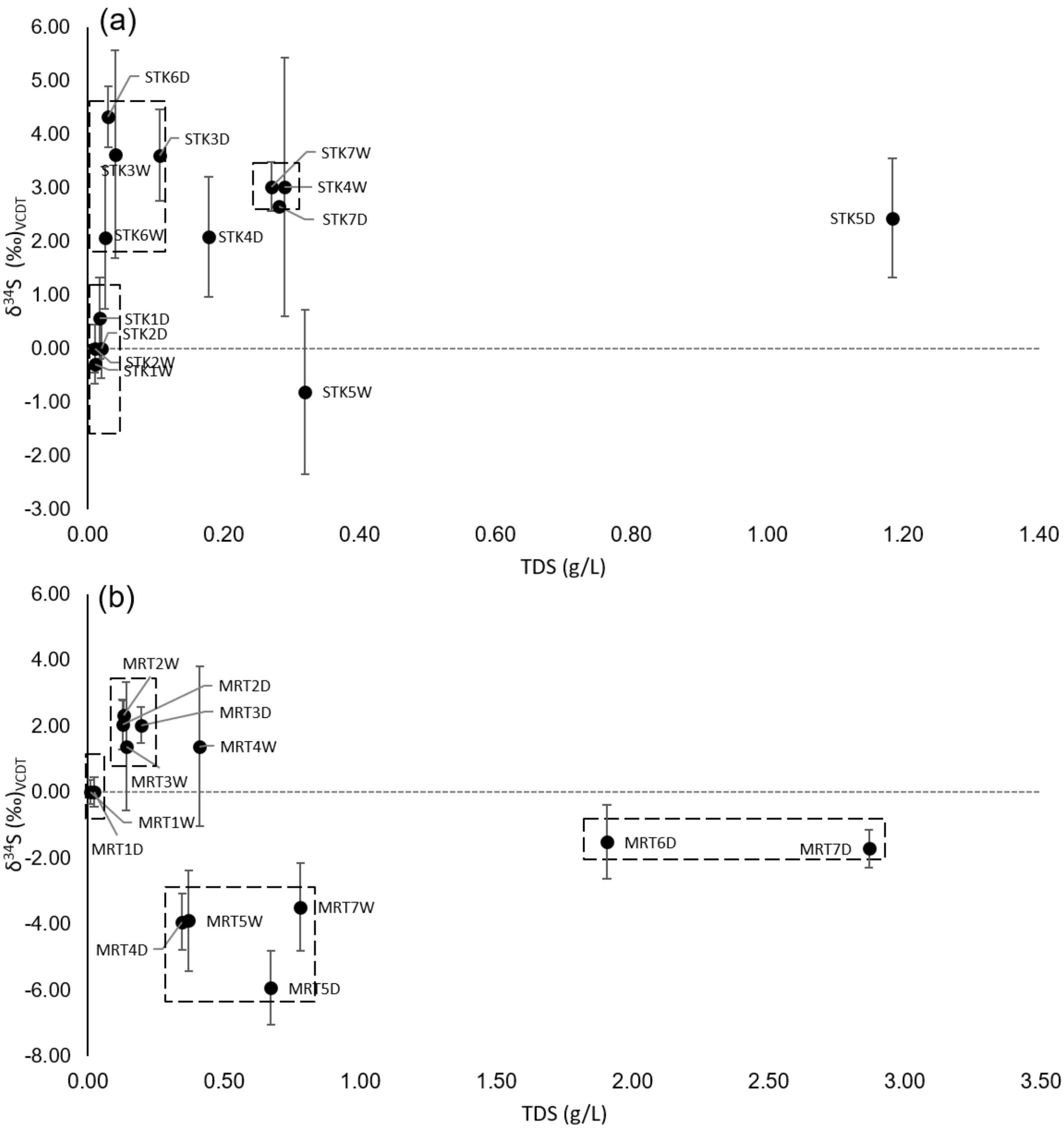

Figure 4-4: The distribution and clustering of river study sites sampled in the a) Sterkstroom (STK) and b) Maretlwane (MRT) rivers, based on the average $\delta^{34}S$ (‰ ± SD) and TDS (g/L) values. Sites sampled in the wet season are suffixed with a W and sites sampled in the dry season are suffixed with a D.

4.4.5. Longitudinal trends in SO_4^{2-} across each river

Although TDS had the top loading in PC1 and strongly correlated with sulfate ($r = 0.99$, $p < 0.01$), sulfate itself is a key water quality parameter known to directly influence dissolved $\delta^{34}S$ values across a range of stressors (Yucel et al., 2016). Trends in sulfate can thus provide important seasonal insight into stressor effects on receiving river water quality and changes in fish tissue $\delta^{34}S$. Trends in sulfate concentrations increased in a linear fashion over the wet and dry seasons for both the Sterkstroom and Maretlwane rivers. Along the Sterkstroom, sulfate concentrations were generally lower in the dry versus wet season samples, except for the large spike (outlier) at STK7 downstream of platinum mine inputs (302 mg/L-S) (**Figure 4-5a**). This single outlier obscured the typical dry season linear trend line and led to a steeper gradient being observed.

The largest changes in the wet season were seen at STK3 below the agricultural valley, at STK5 after the platinum mine and at STK6 after the town of Marikana. Their dry season equivalents were all lower in concentrations than the wet season samples, except STK7 after the legacy platinum PCD's inputs. In contrast to Sterkstroom, the Maretlwane River SO_4^{2-} concentrations were the highest in the dry season, particularly for the last three sites on the river continuum (**Figure 4-5a**). The greatest change along the river, however, was the wet season sample at the MRT4 site after the active chrome mine; which discharges mineral tailings and enters the river. After that site, the remaining downstream sites characterised by legacy platinum PCD effects, had the highest concentrations in the dry season (**Figure 4-5b**).

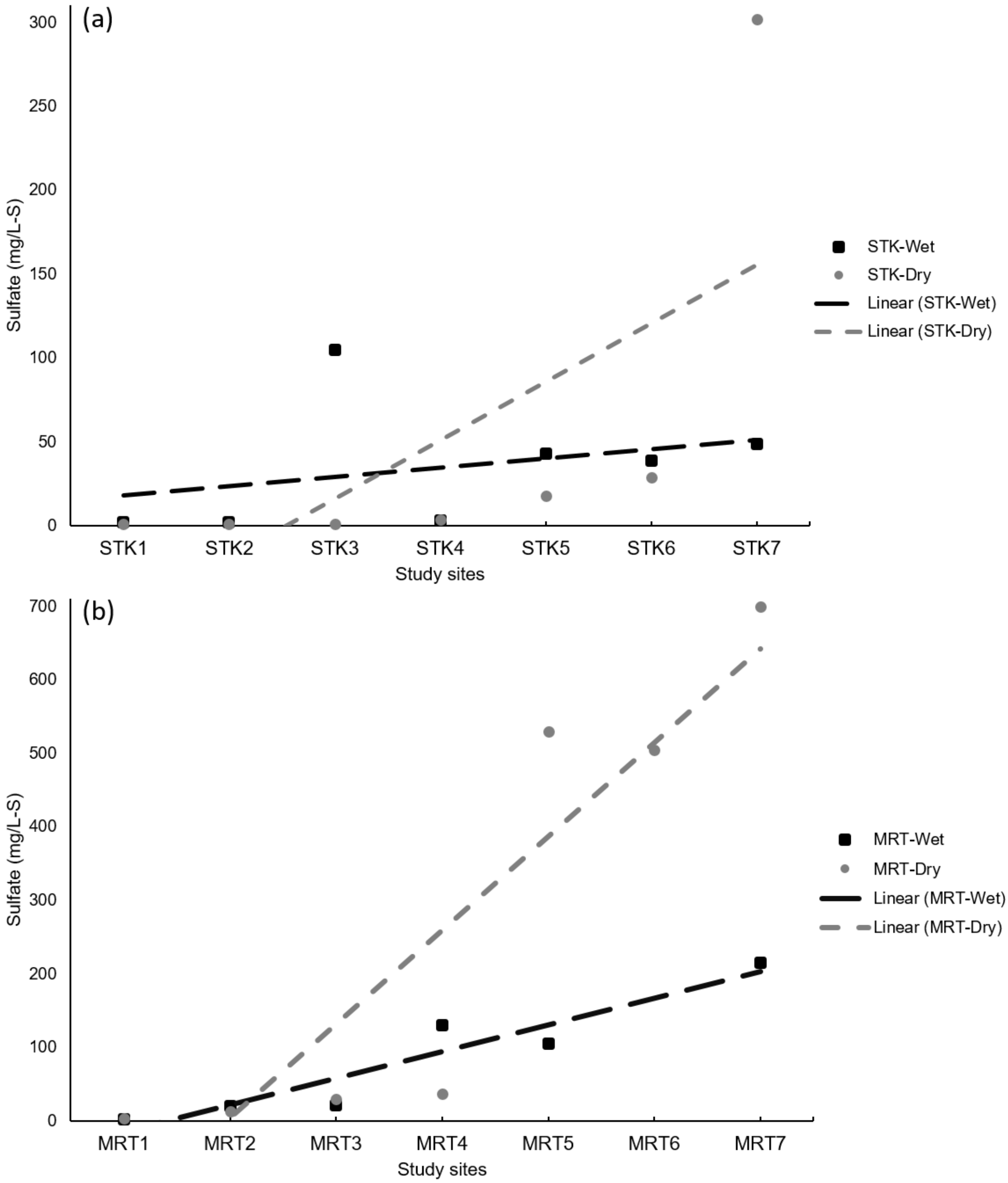

Figure 4-5: Longitudinal trends in sulfate (mg/L-S) concentrations along the a) Sterkstroom (STK) and b) Mareltwane (MRT) rivers during both wet and dry seasons.

4.4.6. Longitudinal trends in $\delta^{34}S$ across each river

Longitudinal patterns in the tissue $\delta^{34}S$ values during both the wet and dry seasons showed an overall trend in enrichment in the Sterkstroom River, relative to pristine conditions. On average, the dry season Sterkstroom values were relatively enriched (2.2‰ ± 0.4SD) compared to the wet season, which were relatively depleted (1.5‰ ± 1.2SD) (**Figure 4-6a**). Comparatively, the longitudinal patterns in seasonal $\delta^{34}S$ values of fish tissue across the Maretlwane River revealed an overall trend of depletion down the river continuum.

Fish in the Maretlwane River had mean $\delta^{34}S$ values that were relatively enriched in the wet season (-0.4‰ ± 0.7SD), compared to the dry season $\delta^{34}S$ (-1.3‰ ± 0.3SD) (**Figure 4-6b**). A t-test with equal variance conducted on the corrected $\delta^{34}S$ (relative to pristine conditions) values collected during both seasons for the two rivers, indicated a significant difference in the $\delta^{34}S$ values between the Sterkstroom and Maretlwane rivers ($t = 3.17$, $df = 25$, $p < 0.01$), with the Maretlwane being significantly depleted in $\delta^{34}S$ compared to the Sterkstroom.

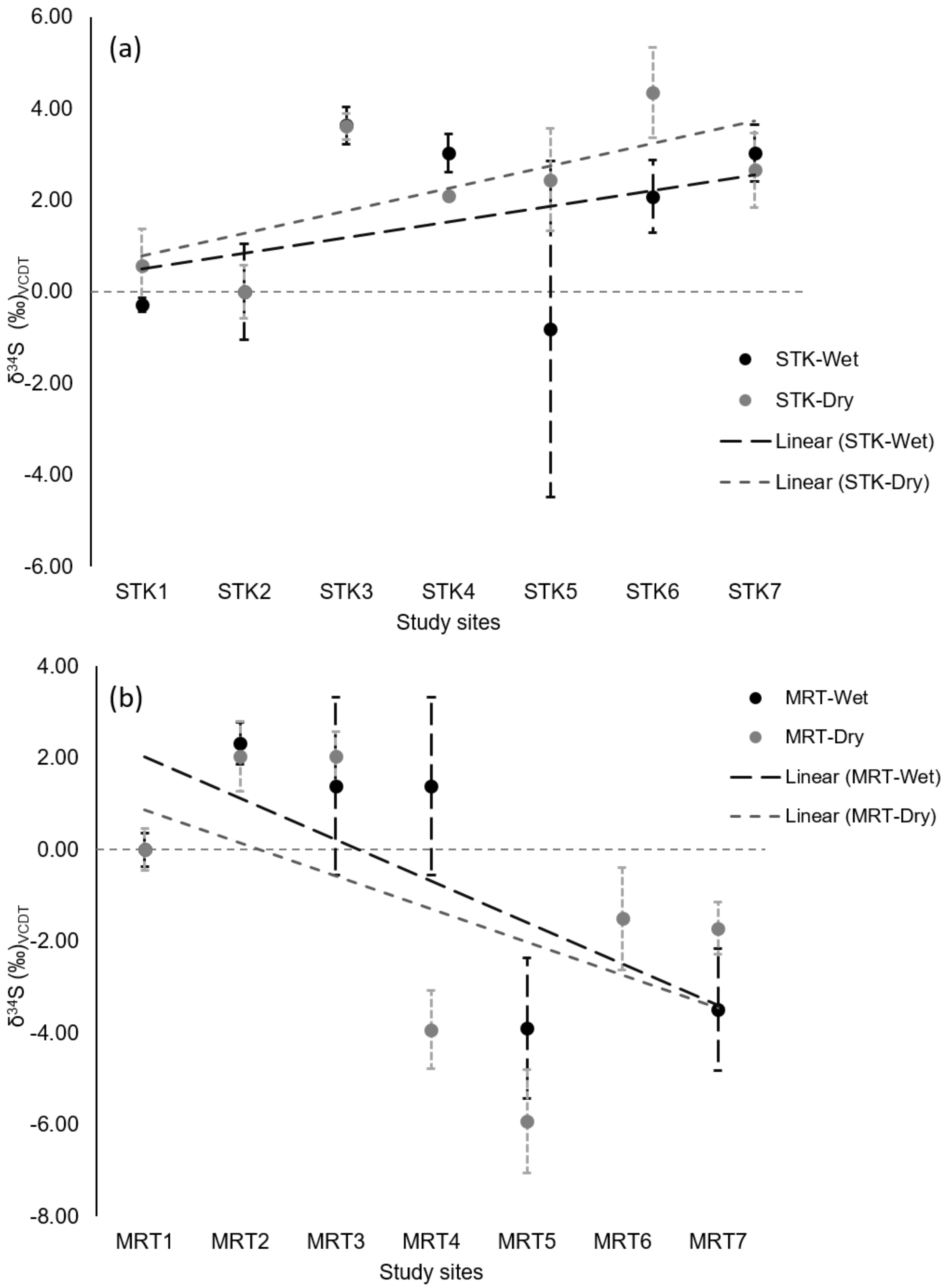

Figure 4-6: Longitudinal trends in mean pristine-corrected fish tissue $\delta^{34}S$ values (‰ ± SD) at each sample site along the a) Sterkstroom (STK) and b) Maretlwane (MRT) rivers during both wet and dry seasons.

4.4.7. Key stressor predictors of $\delta^{34}S$ and their respective spatial scales

Although both the Sterkstroom and Maretlwane watersheds share similar proportionate stressor coverage, there are significant differences in fish $\delta^{34}S$ values between the two rivers. To account for these differences, GLMMs were constructed with “River” as a categorical fixed effect and "Season" as a random effect to capture any additional seasonality effects on $\delta^{34}S$ values. Isolating the river’s influences, allows for a better understanding of their unique effects and a more accurate and nuanced understanding of how stressors from each respective river drive variations in the fish $\delta^{34}S$ values.

4.4.7.1. Sub-basin scale

Full candidate GLMM models, fitted for each spatial scale, were assessed separately. The sub-basin scale full candidate model, which included the atmospheric $SO_{2(g)}$ average and heterogeneity confounding variables, indicated that only the percentage of agriculture was a statistically significant predictor of $\delta^{34}S$ (p = 0.04), while “River” was also significant (p = 0.01). Following the automatic stepwise model selection to derive the most informative parsimonious sub-basin scale model, it was determined that tissue $\delta^{34}S$ variation was best predicted by percentage mining and percentage agriculture at the sub-basin scale as well as the river system, with the latter two predictive variables being statistically significant in the model (p = 0.03; p < 0.01 respectively) (**Table 4-2**).

The effects of mining, urbanisation, impoundments and atmospheric sulfur dioxide (mean and heterogeneity) at the sub-basin scale did not show detectable effects on the response variable $\delta^{34}S$, and thus, were not captured in the final parsimonious model selection. Among the retained variables, sub-basin mining exhibited a non-significant negative trend (p = 0.09; coef = -0.01), indicating relative shifts towards more depleted $\delta^{34}S$ values with increasing mining land use proportions. For every 1% increase in sub-basin mining coverage, the $\delta^{34}S$ values were depleted by an estimated 0.93% in units per mille. This indicates for example, an upstream sites $\bar{x}$ fish $\delta^{34}S$ = 0.5‰, then the downstream sites sub-basin has a 1% increase in mining cover, therefore new estimated downstream $\bar{x}$ fish $\delta^{34}S$ = 0.5‰ – 0.93%). Agriculture at the sub-basin scale, however, had a significant positive effect on $\delta^{34}S$ (p = 0.03; coef = 0.01), indicating relative shifts towards the enrichment of $\delta^{34}S$ with greater sub-basin coverage and was the most important stressor predictor in the final model (**Table 4-3**). It is estimated that for 1% rise in sub-basin agricultural cover, tissue-derived $\delta^{34}S$, in units per mille, was enriched by 1.23%.

4.4.7.2. Cumulative basin scale

At the cumulative basin scale, the full candidate GLMM presented no significant predictive variables ($p > 0.05$). The stepwise model selection revealed that variation in tissue $\delta^{34}S$ values across the two river continua were best predicted by percentage fallow-land and percentage mining cover at the cumulative scale as well as the river system (**Table 4-2**). Among the predictors, fallow-land had a non-significant yet positive effect, indicating relative shift towards the enrichment of fish $\delta^{34}S$ values (p = 0.18, coef = 0.03). It was estimated that for every 1% increase in cumulative basin scale fallow-land cover, there was a 2.97% enrichment in fish tissue $\delta^{34}S$, in units per mille. Conversely, cumulative mining cover was the most important stressor predictor in the final model (**Table 4-3**). It had significant negative effect, indicating a relative shift towards more depleted $\delta^{34}S$ values (p = 0.04, coef = -0.07), with a 1% increase in cumulative mining coverage resulting in an estimated 6.36% depletion in fish tissue $\delta^{34}S$, in units per mille.

Table 4-2: The two parsimonious generalised linear mixed-effects models for tissue $\delta^{34}S$ modelled at the two spatial scales with their respective predictors.

Response ($\delta^{34}S$ in ‰)	**Spatial Scale**	
	Sub-basin	**Cumulative-basin**
Parsimonious Model predictors	• Agriculture (%) • Mining (%) • River	• Fallow-land (%) • Mining (%) • River
Model intercept	2.20(±0.21)10.69***	2.92(±0.24)12.42***
	Model Selection	**Model Selection**
weight	0.06	0.06
AICc	149.04	149.27
BIC	153.30	153.50
	Goodness of fit	**Goodness of fit**
$R^2_{GLMM(m)}$	0.43	0.43
$R^2_{GLMM(c)}$	0.43	0.43
	Random effects	**Random effects**
Season (SD)	0.00	0.00
Residuals (SD)	0.19	0.19

Table 4-3: The model average parameter estimates for each variable in the two spatially aligned models as well as the variable's importance, represented as a proportion, in explaining tissue δ^{34}S variability across the catchment. The greyed cell indicates the stressor (land-use) variable that was most important in the final parsimonious model selection, where the asterisk (*) indicates significance at the 95% level.

Parsimonious models spatial scale	variable	Variable estimate	Lower 95% CI	Upper 95% CI	Variable importance
Sub-basin scale	PLAND Agriculture*	0.01	0.01	0.02	**0.13**
	PLAND Mining	-0.01	-0.02	0.01	0.11
	MRT-River*	-0.13	-0.47	0.21	0.04
	STK-River	0.21	-0.16	0.57	0.07
Cumulative scale	PLAND Fallow-land	0.03	-0.01	0.07	0.06
	PLAND Mining*	-0.07	-0.13	-0.01	**0.10**
	MRT-River*	-0.69	-1.15	-0.23	0.14
	STK-River	-0.52	-1.04	0.01	0.09

4.5. Discussion

4.5.1. Discerning aquatic stressors: dual total dissolved solids and δ34S approach

As the top-loading parameter in the PCA, total dissolved solids (TDS) serve as an effective integrated indicator of spatio-temporal water chemistry variation and thus, proxy for catchment land-use intensification. It is rapidly measured without the specialised analyses often required for other constituents, such as sulfate, which correlated strongly with TDS and which displayed redundancy in explaining the collective river water quality shifts. The measurement of TDS is a key water quality parameter for aquatic ecosystem health as elevated levels have the potential to modify ecological functionality (e.g. community composition) and various aquatic ecosystem processes (e.g. nutrient cycling) (Nielsen et al., 2003; Castillo et al., 2018). It can also indicate the presence of toxic metals as well as elevated constituents that can remobilize such metals from sediments (Addo et al., 2011; Berger et al., 2018). Importantly, it is an effective indicator of stepwise change across watershed stressors, with significant variations having been reported in rivers experiencing natural, urban and commercial effects (Fashae et al., 2019) as well as indicating mining activities (Merriam et al., 2022), thereby effectively capturing socio-economic catchment drivers.

The significant inverse relationship observed between TDS and tissue $\delta^{34}S$ indicates that when used together, they can discern stepwise stressor inputs incrementally along a river continuum. From the TDS-$\delta^{34}S$ biplots, there were distinct clusters observed between sites experiencing certain stressors as also identified by previous studies using transient TDS-$\delta^{34}S_{SO4}$ biplots (Zhang et al., 2020). For instance, sites subjected to agriculture and urban stressors, including STK3 and STK6, clustered together, as did MRT3 and MRT2 in both seasons (**Figure 4-4**). This was also true for study sites that experienced both active and legacy mining-related stressor effects (i.e. MRT4 to MRT7), leading to mineral-rich discharges as well as leaching and outflows from platinum pollution control dams (PCD) or tailing facilities into the river. Stressor activities, including agriculture, urbanisation and mining are major sources of both TDS and sulfate (Bashkova et al., 2001; Zhang et al., 2020).

4.5.2. Enrichment of fish tissue $\delta^{34}S$

Along the Sterkstroom River continuum, STK3 located below an agricultural valley, was the first major change in tissue $\delta^{34}S$ values (**Figure 4-6**). This is indicated by enrichment of $\delta^{34}S$ in fish tissue relative to pristine conditions ($\bar{x}$ = 3.6‰) in both seasons, with higher sulfate concentrations recorded in the wet season (**Figure 4-5a**), likely due to irrigation and precipitation run-off (Jadhav and Jadhav, 2017; Liu and Han, 2021). The STK6 site below the urban (informal and formal) Marikana township, particularly in the dry season, also presented a highly enriched $\delta^{34}S$ ($\bar{x}$ = 4.3‰), in resident fishes, with similar sulfate concentrations reported in both seasons (**Figure 4-5**). There is limited scientific literature available on responses of aquatic tissue-derived $\delta^{34}S$, especially that of tertiary consumers to terrestrial stressors. However, studies documenting shifts in dissolved $\delta^{34}S_{SO4}$ across land-use stressor gradients can provide useful qualitative insights into relative enrichment and depletion ranges expected in water.

Studies on sulfur-containing synthetic fertilizers and livestock manure have found substantial variability in $\delta^{34}S_{SO4}$, but are generally enriched in ^{34}S relative to natural inputs (Hosono et al., 2007; Wang and Zhang, 2019). Specifically, synthetic fertilizer $\delta^{34}S_{SO4}$ values present an average of +4.7‰ ranging from -6.5‰ to +21.4‰ globally, with ammonium sulfate among the most depleted formulations, compared to compound fertilizers. Livestock manures also cover a wide range from -0.9‰ to +8.5‰

but typically fall between 0‰ and +6‰ (Cravotta 1997; Otero et al., 2004; Wang and Zhang, 2019; Jakóbczyk-Karpierz and Ślósarczyk, 2022). Despite their overlap, manure $\delta^{34}S_{SO4}$ profiles remain distinct from the broader fertilizer isotope ratios (i.e. envelope), indicative of narrower positive $\delta^{34}S_{SO4}$ values (Jakóbczyk-Karpierz and Ślósarczyk, 2022). Agricultural fertilizers, livestock manure, and their transformation byproducts represent ^{34}S-enriched point sources to river systems, that can bioaccumulate and spiral upwards through aquatic food webs (Anderson and Cabana, 2006).

Urban-treated wastewater is a major source of anthropogenic effluent entering global aquatic ecosystems and similar to fertilizers and manures, has enriched $\delta^{34}S_{SO4}$ values with a global average of +7.4‰ (Wang and Zhang, 2019). Some research on the effect of wastewater treatment plants on aquatic tissue $\delta^{34}S$ values in highly diluted systems has reported slight (arguably negligible) enrichment downstream, compared to other sources such as industrial waste (Wayland and Hobson, 2000). Previous work on $\delta^{34}S_{SO4}$, however, has found that treated sewage has predominately positive $\delta^{34}S_{SO4}$ values, with values ranging from -0.4‰ to +6.4‰ (Cravotta, 1997; Jakóbczyk-Karpierz and Ślósarczyk, 2022). Untreated sewage, however, from $\delta^{34}S_{SO4}$ studies is characterised by wider, generally more enriched $\delta^{34}S_{SO4}$ ranges, with studies identifying ranges of +0.4‰ to +13.2‰ (Otero et al., 2007; Bottrell et al., 2008; Jakóbczyk-Karpierz and Ślósarczyk, 2022). Among the study sites, MRT2 is known to receive treated sewage from an active wastewater treatment works, as opposed to STK6 which may receive leaked untreated sewage inputs from the Marikana Township. Urban areas, such as STK6 and MRT2 (**Figure 4-6**), are also a key source of domestic detergents, too characterised by enriched $\delta^{34}S_{SO4}$ values, with a global mean of +7.3‰ and values ranging -3.2‰ to 22.8‰ (Otero et al., 2004; Wang and Zhang, 2019).

4.5.3. Depletion of fish tissue $\delta^{34}S$

Along the Sterkstroom River, fish tissue from the site STK5 in the wet season was relatively depleted in $\delta^{34}S$, with values ranging from -4.5‰ to + 2.9‰, whereas in the dry season, it was enriched between +1.3‰ to +3.6‰ relative to pristine conditions (**Figure 4-6a**). Although this site is downstream of a large commercial platinum mine, there was no visual indication of surface-liquid waste emanating from any mine waste rock dumps. It can, however, be suggested that wet seasonal run-off and associated leachate from the surrounding these active dumps, which store processed ore from sulfide-bearing lithologies, can enter freshwater systems (Cawthorn, 2010; Thormann et al., 2017). This can be corroborated by the elevated sulfate concentrations detected at the site during the wet season sample when leaching may be most prevalent, while there were lower concentrations in the dry season sample (**Figure 4-5a**), suggesting less mining-related effluents entering the rivers. The waste rock dump facilities associated with mining in the catchment contain crushed rock rich in sulfide minerals that may support both oxic and anoxic isotope-selective processes fractionating sulfur isotopes.

In the oxic surface layers, exposure to atmospheric oxygen and water can potentially support microbially-mediated oxidation of sulfide minerals to aqueous sulfate. The microbially-catalyzed sulfide oxidation, enhanced by the cycling of metals such as iron that act as powerful oxidants, leads to sulfur isotope fractionation, primarily driven by kinetic isotope effects that preferentially release ^{32}S enriched sulfate, i.e. depleted in $\delta^{34}S$ (Chambers and Trudinger, 1979; Nordstrom and Southam, 1997; Yucel et al., 2016). In the deeper anoxic layers of the waste rock dumps, dissimilatory bacterial sulfate reduction can occur, provided there is a supply of organic matter and sulfate, which can be derived from the percolation of sulfate-rich water from surface oxidation processes and waste material. This process leads to the enrichment of residual sulfate in ^{34}S, while the sulfide end products are depleted in ^{34}S (Habicht and Canfield, 1997).

The combined effects of microbial sulfide oxidation and bacterial sulfate reduction in the waste rock dumps can lead to the formation of ^{34}S depleted S-minerals which are capable of then leaching into nearby rivers when mobilized in the wet season. Through the preferential assimilation of depleted $\delta^{34}S$ sulfur products, this isotopic signature is transferred from aquatic primary producers to tertiary consumers (Novák et al., 2001; Novák et al., 2005). During the dry season, however, with less mining-related effluents (run-off and leachate) depleted in $\delta^{34}S$ entering the river, this likely leads to relatively enriched $\delta^{34}S$ fish tissue in the dry season. This would closely reflect more expected downstream biogeochemical fractionation enrichment pathways associated with sulfur trophic transfer via assimilation of S derived from lesser mine-stressed rivers (Kennedy and Krouse, 1990; Srayko et al., 2023).

Among the Maretlwane River sites, there is a clustering of the active mining affected MRT4D site with the legacy mining sites MRT5D, MRT5W and MRT7W, all of which are characterised by depleted $\delta^{34}S$ values relative to pristine conditions (**Figure 4-4b**). Although both MRT4 sites demonstrated a depletion in $\delta^{34}S$, MRT4D demonstrated the first most distinct change along the continuum (**Figure 4-6**). The site is located ~1.5 km downstream of a large commercial chrome mine which was identified to be a significant source of fine tailings sediment that enters the river channel. The fine silt smothers the downstream river benthos for hundreds of meters upstream of the sampling site. With a peak in wet seasonal sulfate concentrations (**Figure 4-5b**), mine is likely introducing a mobile sulfur source to the river; following the continuous chromium ore processing and discharging of the pulverized waste rock, which then enters the river.

Initial oxidation of the pulverized rock sulfur through air and water exposure during on-land ore processing, produces fractionated sulfur products depleted in $\delta^{34}S$ that likely enter the river channel with the discharged tailings. During dry seasonal low-flow conditions, anaerobic microsites may develop within the accumulated stagnant fine tailings within the river, creating a conducive environment for significant dissimilatory bacterial sulfate reduction (Novak et al., 2005). Consequently, sulfate reducers discriminate against ^{34}S during sulfate reduction, leading to the enrichment of residual sulfate in ^{34}S, while the sulfide end products (e.g. H_2S) are depleted in ^{34}S (Leavitt et al., 2014). These isotopically light sulfur compounds (sulfide) are, as mentioned, preferentially assimilated by primary producers, aligning with kinetic and thermodynamic benefits and leaving behind residual sulfate enriched in ^{34}S (Novak et al., 2001; Novak et al., 2005). It is therefore possible that wet seasonal river flows, leading to the greater dilution as well as disrupting anaerobic microsites and therefore dissimilatory sulfate reduction within the fine in-stream tailings, may lead to the relatively enriched $\delta^{34}S$ fish values compared to the dry season (**Figure 4-6**).

The legacy mining-affected sites, MRT5 and MRT7, grouped with the active mining at MRT4, clearly present depleted $\delta^{34}S$ values in fish tissue (**Figure 4-4b**). Both legacy mining stressed sites receive mine-related decant (leachate and/or overflows) from two separate large platinum PCDs, as indicated by the elevated sulfate concentrations in both wet and dry seasons at each site (**Figure 4-5b**). The large PCDs facilitate stagnant conditions within, which may lead to anaerobic microsites and/or sediments.

Together with the run-off of sulfate-rich minerals and organic matter (acting as the electron donor) from the adjacent waste rock dumps, it is likely for dissimilatory sulfate reduction to occur within the PCDs (Novak et al., 2005). At the MRT5 site, the leached decant enters short, non-vegetated drainage channels before flowing into the Maretlwane main stem. It is thus likely that leached sulfur compounds, including sulfides (depleted in ^{34}S) and sulfates (enriched in ^{34}S) as a result of the dissimilatory sulfate-reduction, enter the river soon after from the PCD, resulting in sulfur compounds that are highly depleted and then assimilated to be reflected in the fish-tissue.

Unlike MRT5, the legacy mining sites MRT6 and MRT7 receive (mining) effluent via wetland (vegetated) channels of similar lengths, before decanting into the main stem Maretlwane. Although both MRT6 and MRT7 receive inputs from separate legacy platinum PCDs, both sites record similar (clustered together; **Figure 4-4b**) mean $\delta^{34}S$ values in the dry season (-1.5‰ and -1.7‰). In addition, both MRT5 (with no mediating wetland) and MRT6 (with a mediating wetland) receive inputs from the same PCD, although MRT5 with direct PCD-related inputs, experienced far more depleted $\delta^{34}S$ values in the same season (-5.9‰; dry season) compared to MRT6 (**Figure 4-6b**). This suggests additional processes within the wetland streams draining PCD effluents are modifying the $\delta^{34}S$ values of S-compounds before being assimilated by consumers at the MRT6 and MRT7 sites, together with potential dilution effects.

The cycling of sulfur can also be altered through the release of organic carbon as well as oxygen from the roots of the wetland macrophytes. This sets up conditions for various, potentially simultaneous, sulfur transformations that can amplify isotopic differences between sulfur species (Wu et al., 2011). Within the wetlands, bacterial sulfate reduction can occur, converting sulfate to sulfide in a process that enriches residual sulfate in ^{34}S while depleting the resulting sulfide in ^{34}S with little isotope effect on the sulfide (Giesler et al., 2009; Wu et al., 2011). However, the oxygen release from the macrophytes can facilitate re-oxidation of the ^{34}S-depleted sulfide back into elemental sulfur and isotopically light sulfate (enriched in ^{32}S). Furthermore, plant roots can also facilitate sulfur disproportionation, whereby elemental sulfur gets disproportionated into sulfate enriched in ^{34}S and sulfides that are relatively depleted in ^{34}S (Wu et al., 2011). These processes, particularly the re-oxidation of ^{34}S-depleted sulfide and the disproportionation of elemental sulfur, can lead to the production of sulfur species that are enriched in ^{34}S compared to the original sulfur entering the wetland from the PCD.

While aquatic primary consumers generally tend to preferentially assimilate lighter isotopes, such as ^{32}S, over heavier isotopes like ^{34}S (Novak et al., 2001), the preferential assimilation of ^{32}S depends on the availability of different sulfur species in the environment (Hesslein et al., 1991). In the case of the fish downstream of the wetland, they are likely assimilating the available sulfur species, which may happen to be enriched in ^{34}S as a result of the upstream wetland processes. Aided by dilution effects, this can result in the more enriched $\delta^{34}S$ values observed in the fish tissues downstream of the PCD mediated wetland inputs, compared to the relatively depleted $\delta^{34}S$ values in fish tissues directly downstream from the more direct-PCD input. As far as we are aware, this is the first study to investigate the effects of chrome as well as platinum mining inputs on aquatic-tissue $\delta^{34}S$. Yet the highly depleted sulfur isotope values associated with the mining stressors have nonetheless been corroborated by some $\delta^{34}S_{SO4}$ (dissolved) research on coal mining (Yucel et al., 2016) and not by others using $\delta^{34}S_{SO4}$ and aquatic invertebrates (Otero and Soler, 2002; Corson, 2017).

4.5.4. Longitudinal trends in seasonal fish tissue $\delta^{34}S$ between rivers

Other than agricultural cover being significantly higher in the Maretlwanes cumulative basin scale, the stressor proportions are similar between the two watersheds. The opposing $\delta^{34}S$ trends among the Sterkstroom and Maretlwane Rivers, however, suggest substantial river-specific differences in the relative magnitude of source contributions (**Figure 4-6**). The enrichment in Sterkstroom River fish tissue implies a greater overriding role for agricultural (chemical fertilizers and manure) as well as urban waste inputs (sewage and detergents) which are enriched in $\delta^{34}S$ (Cravotta et al. 2002; Trust and Fry 1992). It is possible that environmentally compliant mining operations and containment facilities within the Sterkstrooms watershed may limit potentially depleting mining effects (i.e. less depleted $\delta^{34}S$ S-pool), from associated liquid wastes, on the fish-$\delta^{34}S$ values in this system.

The tissue $\delta^{34}S$ values between the seasonal samples from the Sterkstroom River indicated that the dry season sample was on average more enriched compared to the wet season (**Figure 4-6a**). This may be due to seasonal low flow conditions, exacerbated by evaporative water loss and biological uptake, leading to concentrating effects of agricultural chemicals/by-products (e.g. fertilizers and manure) as well as urban waste (stormwater detergents and sewage spills). Upon entering the river as either point or diffuse sources, this would lead to spikes in tissue $\delta^{34}S$ enrichment, as opposed to the wet season where the pollutants may be more diluted upon entering the river, but still overwhelm the effects of the other stressors, such as mining.

Conversely, the more depleted $\delta^{34}S$ values in the Maretlwane River likely arise from the watershed mining activities overwhelming any agricultural or urban sulfur inputs (**Figure 4-6b**). This likely arises in part from the sequenced mining intensification along the river continuum, potentially exacerbating cumulative impacts. For instance, mining in the Maretlwane cumulative catchments steadily increases at each site from 0.10% at MRT3 to 8.10% at MRT7. The heightened dry season depletion and high sulfate concentrations at the mining sites suggest mine drainage generation and sulfide mineral oxidative weathering reactions are disproportionately contributing ^{34}S-depleted sulfur products under concentrated low flow conditions. During the dry season, however, sites experiencing PCD wetland mediated inputs were notably $\delta^{34}S$ enriched, indicating additional $\delta^{34}S$ fractionation processes occurring within the nearby wetlands before entering the main stem (see Wu et al. 2011).

Due to the decreased dry season connectivity between the PCD-wetland-river, it appears biochemical fractionation processes within the mediated wetlands, such as re-oxidation from the macrophyte roots, may transform initially negative S-products in $\delta^{34}S$ enriched residual sulfate in the as well as sulfide with relatively depleted $\delta^{34}S$ (e.g. STK6 and MRT7) (Giesler et al., 2008; Wu et al., 2011). These processes may dominate as residence time within the wetland is prolonged due to the lower dry seasonal wetland flows, compared to during the wet seasonal higher flows, which would result in shorter residence times. Such may also explain the clustering and slight enrichment of both MRT6 and MRT7 $\delta^{34}S$ values in the dry season (**Figure 4-4b and Figure 4-6b**). Consequently, the sulfur species available for assimilation by aquatic organisms, including fish, downstream of the mediated wetlands may be enriched in ^{34}S during the dry season.

Determining the proportional contributions of proposed PCD inputs into the environment as well as the contributing effects of mediated wetland inputs on the PCD-derived S-compound $\delta^{34}S$ values, i.e. hydrological concentrating effects and *in-situ* fractionation pathways, warrant future research of flow regimes in both seasons. This additional research is needed to quantify the responsible fractionation mechanisms and isolate the distinct influences on sulfur cycling associated with aquatic biota. This study is the first to trace chrome tailings-derived and platinum PCD sulfur isotopes into aquatic consumer tissues and, thus, there is no prior research from which to directly compare these seasonal findings. The pronounced seasonal tissue-derived $\delta^{34}S$ depletions along the Maretlwane River, however, illustrate the significance of mining's dominance within the mosaic of mixed land uses, overwhelming other stressors such as agriculture and urbanisation (**Table 4-3**).

4.5.5. Stressors acting on different spatial scales driving tissue-derived $\delta^{34}S$ variation

At the sub-basin scale, the proportion of agricultural land-use emerged as the most important, significant positive predictor of consumer $\delta^{34}S$ values (p = 0.03), enriching isotopic ratios by an estimated +1.2% in part per mille for every 1% rise in agricultural sub-basin coverage. This effect outweighed the non-significant sub-basin depletion linked to mining expansion (p = 0.09), likely reflecting the enrichment of bioavailable S-compounds from agrochemical usage. Agricultural fertilizers contain relatively enriched-S (Cravotta et al. 2022), that can propagate through fluvial networks via primary consumer uptake and trophic transfer. This thereby bioaccumulating in tertiary consumers as observed in other aquatic food web studies assessing tissue-derived $\delta^{15}N$ along agricultural gradients (Lee et al., 2018).

On the other hand, the depleting effects of mining activities on $\delta^{34}S$ did not contribute as substantially to the fish-tissue $\delta^{34}S$ variations at the sub-basin scale. This suggests that less continuous mining coverage, as observed along the Sterkstroom River, may lead to lesser depleting effects on fish $\delta^{34}S$. Such my limit sulfur mobilization from ores within sub-basins, thereby restricting significant detectable mining impacts on fish tissue $\delta^{34}S$ at the sub-basin scale. Overall, increasing proximal agricultural intensity appears to be the most influential stressor to enrich tertiary consumer sulfur isotope ratios within the sub-basins of the Gwathle catchment.

In contrast to the sub-basin scale, mining stressors at the cumulative catchment scale exhibited a significant negative relative influence on fish tissue $\delta^{34}S$ signatures (p = 0.04), where tissue $\delta^{34}S$ in part per mil, is estimated to be depleted by 6.4%, per 1%

increase in cumulative mining cover. This implies upstream release and transport of $\delta^{34}S$ depleted particulate and dissolved sulfur from tailing storage facilities and PCDs downstream for biotic assimilation. Once fractionated by *in-situ* oxidative or reductive processes, the bioavailable dissolved sulfate pool exhibits advanced $\delta^{34}S$ depletion (Nordstrom and Southam, 1997; Leavitt et al., 2014), available for primary consumer uptake and trophic transfer to upper consumers. On the cumulative basin scale, the inverse relationship between mining cover and $\delta^{34}S$ indicates continuous stepped mining stressors accompanied by poorer waste containment practices, which may be overwhelming localized containment and remediation efforts. This allows greater volumes of $\delta^{34}S$ depleted sulfur species to be transported downstream into broader river networks.

Conversely, fallow-land characterised by cattle rearing and grazing activities, had a positive yet non-significant effect at the cumulative basin scale. This finding suggests the possible input of oxidized organic rich material contributing to aquatic S-pools enriched in $\delta^{34}S$ entering the aquatic ecosystems (Mayer et al., 1995; Jakóbczyk-Karpierz and Ślósarczyk 2022). The cumulative model indicated the disproportionate depletion in Maretlwane fish tissue, despite similar stressor proportions with the Sterkstroom river. This indicates that sequential placement of the stressors, particularly the mining activities along the Maretlwane River, result in dominant mining-related sulfur contributions that significantly overwhelm other cumulative stressor signals including urban, agricultural and atmospheric $SO_{2(g)}$ effects.

4.5.6. Management implications

In accordance with Section 21(g) of the South African National Water Act (Act 36 of 1998), any polluted water that leaks or is deposited into a water-body is considered waste and must be prevented. National legislation allows for Resource Directed Measures (RDM), to protect and manage environmental effects on river systems clear ecological goals (quantify and quality) for the water resource, as supported for by Sourced Directed Controls (SDCs) (DWA, 2008). The SDCs involve identifying and thereby controlling pollution at its source to prevent the spread of contaminants and minimise negative effects on water resources. The work undertaken in this chapter demonstrated the that pairing rapidly obtained TDS data with fish tissue $\delta^{34}S$ in biplots as well as performing spatio-temporal statistical approaches (GLMMs) using fish tissue $\delta^{34}S$ response data, to effectively distinguish between agricultural and mining stressors (pollution) in river systems and along a land-use intensification gradient. This research presents a potential environmental forensic tool for use as a SDC to disentangle complex, interacting catchment stressors where each may act as a potential polluter. Such a tool would better inform-adaptive catchment management strategies to implement suitable area-specific remediation actions.

To mitigate the significant $\delta^{34}S$ enrichment effects associated with agricultural runoff at the sub-basin level, improved nutrient management practices could be implemented by farmers as practiced within designated Biosphere Reserve transition zones, located in the Southern section of the catchment. Drawing from the UNESCO Man and Biosphere Programme framework, sustainable agricultural techniques encouraged in these areas, like precision farming, vegetative buffer strips, and improved-till management, could reduce downstream transport of nutrients into waterways (Sharpley et al., 1994; Lowrance et al., 1997). Additionally, the National Water Act provides for compulsory licensing of agriculturally related return flows, allowing for enforceable good practice standards regarding fertilizer application (Day and Davies, 2023).

Regarding the cumulative basin scale mining impacts, there are national legislative acts as well as accompanying best practice guidelines to inform the construction and operation of waste facilities to prevent pollution to the surrounding environment (see DWAF, 2008). To uphold such legislation and mitigate mining induced pollution on aquatic ecosystems, mining companies, through their surveillance teams, are obligated to perform routine inspections and scheduled rehabilitation of damaged or leaking containment facilities (e.g. through adding additional geosynthesic liners) (Kossoff et al., 2014). Implementing corrective agricultural and mine land management activities, would limit downstream assimilation of sulfur compounds by river biota.

In modelling the stressors-spatial relationships driving fish tissue $\delta^{34}S$ variation, while also accounting for the atmospheric $SO_{2(g)}$ spatio-temporal effects, atmospheric $SO_{2(g)}$ was not identified as a key predictor of the $\delta^{34}S$, at either the sub-basin scale or cumulative basin scale. This suggests that agricultural stress at the sub-basin scale (significant positive $\delta^{34}S$ effect) as well as mining stress (significant negative $\delta^{34}S$ effect) at the cumulative basin scale both overwhelm (obscure) any significant effects of atmospheric $SO_{2(g)}$ on $\delta^{34}S$ of the fish tissue. It is likely that atmospheric $SO_{2(g)}$ does contribute to aquatic tissue $\delta^{34}S$, however, further investigative specific aquatic-atmosphere studies are required to assess its relative contributions/effects on fish tissue $\delta^{34}S$ in this, and other catchments.

From this study, it was clear there was spatio-temporal heterogeneity among atmospheric $SO_{2(g)}$ VCD in the catchment, likely driven by the location of ore extraction and processing (smelters) facilities (**Figure S4-1** and **Figure S4-2**). The South Africa's National Environmental Management: Air Quality Act (No. 39 of 2004), identifies atmospheric $SO_{2(g)}$ emissions as a national pollutant of concern, that require local and regional management and regulates national emissions (DEA, 2018). Local mining activities are by law required to reduce dust Act through dust suppression activities. In addition, from April 2015, the Act requires that all metallurgical industries, including mine smelters, operate with appropriate abatement technologies thereby achieving the Minimum Emission Standards. In cases where there is high sulfide roasting, suitable $SO_{2(g)}$ abatement systems are required to be installed, some may include dry or wet alkali scrubbers as well as electric furnace primary gas cleaning (Scheepers, 2017). To ensure locally implemented measures are limiting atmospheric sulfur deposition in the catchment, further research could assess the changes in the relative spatio-temporal contributions of dry and wet atmospheric sulfur deposition, pre- and post-implementation, thereby also accounting for outside inputs.

Across South Africa, wet and dry atmospheric $SO_{2(g)}$ deposition rates are driven by meteorology and land use activities (Zunckel et al., 1999; Zunckel et al., 2000). Previous research has shown that in the Highveld region, where the Gwathle Catchment is situated, wet deposition of atmospheric $SO_{2(g)}$ likely plays a more significant role than dry deposition (Zunckel et al., 2000). This results in episodic events of higher concentrated atmospheric sulfur entering the river systems, contrasting with lower concentrations, but still steadier deposition that occurs over the drier periods. While studies have independently characterised aerosol $\delta^{34}S$ values within industrialized areas (Guo et al., 2010), others have done so in precipitation (Nielsen, 1973; Zhang et al., 2002) while both accounting for their respective fractionation pathways. No one study, in an industrialized area has, however, integrated the two to explore potentially unique effects of wet versus dry $\delta^{34}S$ deposition of each on aquatic ecosystems.

4.6. Conclusion

The pairing of fish tissue $\delta^{34}S$ values with TDS concentrations is effective for distinguishing stepwise stressor effects along river continua. Additionally, the multi-scale spatial modelling assessment permitted the disentangling of sub-basin versus cumulative basin scale stressor impacts on aquatic ecosystems. The integration of fish tissue $\delta^{34}S$ thus has the potential to act as a complimentary ecotoxicological tracer tool for improving freshwater resource management in South Africa, via the effective tracing and differentiating of multi-stressor effects operating at multiple scales, to best capture complex pollution input patterns. Fish tissue $\delta^{34}S$ analysis provides a time-integrated measure (of ecologically available sulfur) that is more sensitive to multiple aquatic stressors compared to other water quality tracers and time-integrated metals. While other water quality tracers can demonstrate large variations over multiple samples (**Chapter 2**) and time-integrated metals, specifically conservative chrome, only show one key catchment driver being mining (**Chapter 3**), tissue $\delta^{34}S$, offers a more comprehensive understanding of the impacts of various stressors on the aquatic ecosystem.

As South Africa seeks to balance developmental pressures with ecological sustainability, this time-integrated stable isotope monitoring tool could complement existing abiotic and biotic monitoring indices. It would aid in diagnosing specific stressor sources arising from situations such as incremental agricultural encroachment or cumulative mining discharges. Additional local source characterisation research can be conducted where absolute $\delta^{34}S_{SO4}$ values from potential pollutants (e.g. fertilizer) can be better paired with aquatic (fish) tissue $\delta^{34}S$ responses rather than performing a multi-spatial scale relative assessment. This chapter's findings showcase that fish-tissue $\delta^{34}S$, assessed through space and time, can separate stressor signals over meaningful management spatial scales, making it well-suited for watersheds facing mixed land and water resource demands. With further testing across ecoregions, the approach may evolve into a standardised biomonitoring protocol for watershed pollution source apportionment to better inform regulatory strategies at catchment level.

Using fish tissue $\delta^{34}S$ as a tracer of pollution sources and stressors provides crucial information on drivers of ecosystem change. However, to fully understand ecological consequences, we need tools to evaluate how these drivers alter aquatic ecosystem function and food web dynamics. Commonly used $\delta^{13}C$ and $\delta^{15}N$, used in aquatic food web structure and function assessments can provide these functional insights into energy flow and trophic structure that complement $\delta^{34}S$ pollution source inputs. Combining this multi-isotope toolkit has the potential to functionally fingerprint aquatic ecosystems while connecting stressor sources with their respective biological responses across spatial scales. This could become a powerful biomonitoring approach for watershed management in South Africa and globally. The next steps should explore integrating $\delta^{13}C$ and $\delta^{15}N$ alongside $\delta^{34}S$ in target rivers across land-use gradients to quantify these stressors to aquatic integrity relationships.

4.6.1. Acknowledgements

This Chapter was authored by Jonathan Levin, with material contributions from Stephan Woodborne, Chris Curtis, Jaclyn Hill and Darragh Woodford. We thank Mandlenkosi Nkala and Nompendulo Khoza for assisting the processing of the tissue samples. Jaclyn also assisted in the logistics of samples between South Africa and the isotope laboratory for analysis in the USA. We thank Chris Yarnes and James Farlin at the University of California, Davis Stable Isotope Facility for processing the isotope samples. All fieldwork was conducted under a North West Province research permit (NW 17458/03/2020). Tissue samples were collected under a University of the Witwatersrand Animal Research Ethics Committee Clearance Certificate No. 2021/03/05/A. The authors thank Mark Ashfield and Gert Eastes for access to sampling sites on their properties, and Chevonne Reynolds for statistical analysis advice. A big thank you to Rene Shields at Milorho Lodge ensuring the necessary back-up energy solutions to securely store collected stable isotope samples.

4.6.2. References

Aas, W., Mortier, A., Bowersox, V., Cherian, R., Faluvegi, G., Fagerli, H., Hand, J., Klimont, Z., Galy-Lacaux, C., Lehmann, C.M. and Myhre, C.L., 2019. Global and regional trends of atmospheric sulfur, *Scientific Reports*, *9*(953), 1-11.

Addo, M.A., Okley, G.M., Affum, H.A., Acquah, S., Gbadago, J.K., Senu, J.K. and Botwe, B.O., 2011. Water quality and level of some heavy metals in water and sediments of Kpeshie Lagoon, La-Accra, Ghana, *Research Journal of Environmental and Earth Sciences*, *3*(5), 487-497.

Almécija, C., Cobelo-García, A., Wepener, V. and Prego, R., 2017. Platinum group elements in stream sediments of mining zones: the Hex River (Bushveld Igneous Complex, South Africa), *Journal of African Earth Sciences*, *129*, 934-943.

Anderson, C. and Cabana, G., 2006. Does $\delta^{15}N$ in river food webs reflect the intensity and origin of N loads from the watershed?, *Science of the Total Environment*, *367*, 968-978.

Barton K., 2023. _MuMIn: Multi-Model Inference_. R package version 1.47.5 <https://CRAN.R-project.org/package=MuMIn>.

Bashkova, S., Bagreev, A., Locke, D.C. and Bandosz, T.J., 2001. Adsorption of SO2 on sewage sludge-derived materials, *Environmental science & technology*, *35*(15), 3263-3269.

Bates, A.L., Orem, W.H., Harvey, J.W. and Spiker, E.C., 2002. Tracing sources of sulfur in the Florida Everglades, *Journal of Environmental Quality*, *31*(1), 287-299.

Bates, D., Mächler, M., Bolker, B. and Walker, S., 2014. Fitting linear mixed-effects models using lme4. arXiv preprint arXiv:1406.5823.

Bennett, R.H., Ellender, B.R., Mäkinen, T., Miya, T., Pattrick, P., Wasserman, R.J., Woodford, D.J. and Weyl, O.L., 2016. Ethical considerations for field research on fishes, *Koedoe*, *58*(1), 1-15.

Berger, E., Frör, O. and Schäfer, R.B., 2018. Salinity impacts on river ecosystem processes: a critical mini-review, *Philosophical Transactions of the Royal Society B*, *374*, 1-10.

Berner, R.A., 1971. Worldwide sulfur pollution of rivers, *Journal of Geophysical Research*, *76*(27), 6597-6600.

Bottrell, S., Tellam, J., Bartlett, R. and Hughes, A., 2008. Isotopic composition of sulfate as a tracer of natural and anthropogenic influences on groundwater geochemistry in an urban sandstone aquifer, Birmingham, UK, *Applied Geochemistry*, *23*(8), 2382-2394.

Bowen, H.J.M., 1960. Biological fractionation of isotopes, *The International Journal of Applied Radiation and Isotopes*, *7*(4), 261-272.

Burnham, K. and Anderson, D., 2004. *Model selection and multi-model inference, Second Edition,* Springer-Verlag, New York.

Castillo, A.M., Sharpe, D.M., Ghalambor, C.K. and De León, L.F., 2018. Exploring the effects of salinization on trophic diversity in freshwater ecosystems: a quantitative review, *Hydrobiologia*, *807*, 1-17.

Cawthorn, R.G., 2010. The platinum group element deposits of the Bushveld Complex in South Africa, *Platinum Metals Review*, *54*(4), 205-215.

Chambers, L.A. and Trudinger, P.A., 1979. Microbiological fractionation of stable sulfur isotopes: a review and critique, *Geomicrobiology Journal*, *1*(3), 249-293.

Charest, M., 2015. 'Turnover rates and trophic discrimination factors of $\delta^{34}S$ in brook trout, Salvelinus fontinalis', M.Sc. thesis, Dept. Graduate Academic Unit of Biology, University of New Brunswick.

Clayden, M.G., Lescord, G.L., Kidd, K.A., Wang, X., Muir, D.C. and O'Driscoll, N.J., 2017. Using sulfur stable isotopes to assess mercury bioaccumulation and biomagnification in temperate lake food webs, *Environmental Toxicology and Chemistry*, *36*(3), 661-670.

Cofano, A., Cigna, F., Santamaria Amato, L., Siciliani de Cumis, M. and Tapete, D., 2021. Exploiting Sentinel-5P TROPOMI and ground sensor data for the detection of volcanic SO2 plumes and activity in 2018–2021 at Stromboli, Italy, *Sensors*, *21*, 1-23.

Corson, K.B., 2017. 'Coal ash derived sulfur and mercury in the Dan River Invertebrate food web', M.Sc. thesis, The Graduate School, The University of North Carolina at Greensboro.

Cravotta, C.A., 2002. *Use of stable isotopes of carbon, nitrogen, and sulfur to identify sources of nitrogen in surface waters in the Lower Susquehanna River Basin, Pennsylvania*, U.S. Geological Survey Water-supply paper No. 2497, Pennsylvania Department of Environmental Protection, US Government Printing Office.

Croghan, C.A.P.P.E. and Egeghy, P.P., 2003. Methods of dealing with values below the limit of detection using SAS, *Southern SAS User Group*, *22*(24), 1-5.

Day, J. and Davies, B., 2013. *Vanishing Waters – Third Revised Edition*, Water Research Commission, Pretoria.

DEA, 2018. National environmental Management: Air Quality Act, 2004 (Act No. 39 of 2004) – the 2017 National framework for air quality management in the Republic of South Africa, Report No. 41996, Department of Environmental Affairs, Pretoria.

Dubinsky, A.J., Wilks, R.P. and Buhay, W.M., 2020. Confirming the source of high-sulfate concentrations in Dead Horse Creek, Winkler, Manitoba, Canada, using a dual-isotope Bayesian probability mixing model, *Water, Air, & Soil Pollution*, *231*, 1-14.

Dunnink, J.A., Curtis, C.J., Beukes, J.P., Van Zyl, P.G. and Swartz, J., 2016. The sensitivity of Afromontane tarns in the Maloti-Drakensberg region of South Africa and Lesotho to acidic deposition, *African Journal of Aquatic Science*, *41*(4), 413-426.

Eimers, M.C., Watmough, S.A., Buttle, J.M. and Dillon, P.J., 2008. Examination of the potential relationship between droughts, sulphate and dissolved organic carbon at a wetland-draining stream, *Global Change Biology*, *14*(4), 938-948.

Farr, T. G., and M. Kobrick, 2000, Shuttle Radar Topography Mission produces a wealth of data, Eos Trans, AGU, 81, 583-583

Fashae, A.O., Abiola Ayorinde, H., Oludapo Olusola, A. and Oluseyi Obateru, R., 2019. Landuse and surface water quality in an emerging urban city, *Applied Water Science*, *9*, 1-12.

Fölster, J. and Wilander, A., 2002. Recovery from acidification in Swedish forest streams, *Environmental Pollution*, *117*(3), 379-389.

Fry, B., Gest, H. and Hayes, J., 1988. 34S/32S fractionation in sulfur cycles catalyzed by anaerobic bacteria, *Applied and Environmental Microbiology*, *54*(1), 250-256.

Funk, C., Peterson, P., Landsfeld, M., Pedreros, D., Verdin, J., Shukla, S., Husak, G., Rowland, J., Harrison, L., Hoell, A. and Michaelsen, J., 2015. The climate hazards infrared precipitation with stations—a new environmental record for monitoring extremes, *Scientific data*, *2*(1), 1-21.

Geoterraimage, 2021. 2020 South Africa National Land-Cover Dataset, Geoterraimage, viewed 10 February 2022, from https://egis.environment.gov.za/sa_national_land_cover_datasets.

Giesler, R., Bjorkvald, L., Laudon, H. and Morth, C.M., 2009. Spatial and seasonal variations in stream water δ34S-dissolved organic matter in Northern Sweden, *Environmental science & technology*, *43*(2), 447-452.

Grey, D.C. and Jensen, M.L., 1972. Bacteriogenic sulfur in air pollution, *Science*, *177*(4054), 1099-1100.

Habicht, K.S. and Canfield, D.E., 1997. Sulfur isotope fractionation during bacterial sulfate reduction in organic-rich sediments, *Geochimica et Cosmochimica Acta*, *61*(24), 5351-5361.

Hesslein, R.H., Capel, M.J., Fox, D.E. and Hallard, K.A., 1991. Stable isotopes of sulfur, carbon, and nitrogen as indicators of trophic level and fish migration in the lower Mackenzie River basin, Canada, *Canadian Journal of Fisheries and Aquatic Sciences*, *48*(11), 2258-2265.

Hosono, T., Nakano, T., Igeta, A., Tayasu, I., Tanaka, T. and Yachi, S., 2007. Impact of fertilizer on a small watershed of Lake Biwa: Use of sulfur and strontium isotopes in environmental diagnosis, *Science of the Total Environment*, *384*(1-3), 342-354.

Jackson, M.C., Fourie, H.E., Dalu, T., Woodford, D.J., Wasserman, R.J., Zengeya, T.A., Ellender, B.R., Kimberg, P.K., Jordaan, M.S., Chimimba, C.T. and Weyl, O.L., 2020. Food web properties vary with climate and land use in South African streams, *Functional Ecology*, *34*(8), 1653-1665.

Jadhav, S.D. and Jadhav, M.S., 2017. Study of sulphate concentration of Pavana River at Pune: A case study, *IJCS*, *5*(2), 198-200.

Jakóbczyk-Karpierz, S. and Ślósarczyk, K., 2022. Isotopic signature of anthropogenic sources of groundwater contamination with sulfate and its application to groundwater in a heavily urbanized and industrialized area (Upper Silesia, Poland), *Journal of Hydrology*, *612*, 1-15.

Kassambara A. and Mundt F., 2020. factoextra: Extract and Visualize the Results of Multivariate Data Analyses. R package version 1.0.7, <https://CRAN.R-project.org/package=factoextra>.

Kennedy, B.V. and Krouse, H.R., 1990. Isotope fractionation by plants and animals: implications for nutrition research, *Canadian Journal of Physiology and Pharmacology*, *68*(7), 960-972.

Kleynhans, C.J. and Louw, M.D., 2007. *Module A: EcoClassification and EcoStatus determination'. River EcoClassification: Manual for EcoStatus Determination (version 2)* Water Research Commission, Report No. TT 329/08, Pretoria.

Koptsik, G. and Alewell, C., 2007. Sulphur behaviour in forest soils near the largest SO2 emitter in northern Europe, *Applied Geochemistry*, *22*(6), 1095-1104.

Kossoff, D., Dubbin, W.E., Alfredsson, M., Edwards, S.J., Macklin, M.G. and Hudson-Edwards, K.A., 2014. Mine tailings dams: Characteristics, failure, environmental impacts, and remediation, *Applied Geochemistry*, *51*, 229-245.

Lê, S., Josse, J. and Husson, F. 2008. FactoMineR: An R Package for Multivariate Analysis. Journal of Statistical Software, 25(1), 1-18.

Leavitt, W.D., Cummins, R., Schmidt, M.L., Sim, M.S., Ono, S., Bradley, A.S. and Johnston, D.T., 2014. Multiple sulfur isotope signatures of sulfite and thiosulfate reduction by the model dissimilatory sulfate-reducer, Desulfovibrio alaskensis str. G20, *Frontiers in Microbiology*, *5*, 1-16.

Lee, K.Y., Graham, L., Spooner, D.E. and Xenopoulos, M.A., 2018. Tracing anthropogenic inputs in stream foods webs with stable carbon and nitrogen isotope systematics along an agricultural gradient, *PloS one*, *13*(7), 1-19.

Liu, J. and Han, G., 2021. Tracing riverine sulfate source in an agricultural watershed: Constraints from stable isotopes, *Environmental Pollution*, *288*, 1-10.

Lodhi, H.S., Khan, M.A., Verma, R.S. and Sharma, U.D., 2006. Acute toxicity of copper sulphate to fresh water prawns, *Journal of Environmental Biology*, *27*(3), 585-588.

Lowrance, R., Altier, L.S., Newbold, J.D., Schnabel, R.R., Groffman, P.M., Denver, J.M., Correll, D.L., Gilliam, J.W. and Robinson, J.L., 1997. Water quality functions of riparian forest buffers in Chesapeake Bay watersheds, *Environmental management*, 687-712.

Magalhães, N., Penniston-Dorland, S., Farquhar, J. and Mathez, E.A., 2018. Variable sulfur isotope composition of sulfides provide evidence for multiple sources of contamination in the Rustenburg Layered Suite, Bushveld Complex, *Earth and Planetary Science Letters*, *492*, 163-173.

Mayer, B., Fritz, P., Prietzel, J. and Krouse, H.R., 1995. The use of stable sulfur and oxygen isotope ratios for interpreting the mobility of sulfate in aerobic forest soils, *Applied geochemistry*, *10*(2), 161-173.

McGarigal, K., Cushman, S.A., Neel, M.C. and Ene, E., 2002. *FRAGSTATS: spatial pattern analysis program for categorical maps*, Computer software, University of Massachusetts, Amherst. Available from: www.umass. edu/landeco/research/fragstats/fragstats.

Meier, J., Babenzien, H.D. and Wendt-Potthoff, K., 2004. Microbial cycling of iron and sulfur in sediments of acidic and pH-neutral mining lakes in Lusatia (Brandenburg, Germany), *Biogeochemistry*, *67*, 135-156.

Merriam, E.R., Strager, M.P. and Petty, J.T., 2022. Source water vulnerability to elevated total dissolved solids within a mixed-use Appalachian River basin, *PLOS Water*, *1*(8), 1-17.

Mitchell, M.J. and Likens, G.E., 2011. Watershed sulfur biogeochemistry: shift from atmospheric deposition dominance to climatic regulation, *Environmental science & technology*, *45*(12), 5267-5271.

Mitchell, M.J., Krouse, H.R., Mayer, B., Stam, A.C. and Zhang, Y., 1998. 'Use of stable isotopes in evaluating sulfur biogeochemistry of forest ecosystems' In Kendall, C. and McDonnel J.J. (eds) *Isotope tracers in catchment hydrology,* pp. 489-518, Elsevier.

Morrissey, C.A., Boldt, A., Mapstone, A., Newton, J. and Ormerod, S.J., 2013. Stable isotopes as indicators of wastewater effects on the macroinvertebrates of urban rivers, *Hydrobiologia*, *700*, 231-244.

Nakai, N. and Jensen, M.L., 1967. Sources of atmospheric sulfur compounds, *Geochemical Journal*, *1*(4), 199-210.

Nielsen, D.L., Brock, M.A., Rees, G.N. and Baldwin, D.S., 2003. Effects of increasing salinity on freshwater ecosystems in Australia, *Australian Journal of Botany*, *51*(6), 655-665.

Nielsen, H., 1974. Isotopic composition of the major contributors to atmospheric sulfur, *Tellus*, *26*(1-2), 213-221.

Nordstrom, D.K. and Southam, G., 1997. 'Geomicrobiology of sulfide mineral oxidation', In Banfield, J.F. and Nealson, K.H. (eds.), *Geomicrobiology: Interactions between microbes and minerals*, pp. 361-390, Washington DC, USA.

Novák, M., Bottrell, S.H. and Přechová, E., 2001. Sulfur isotope inventories of atmospheric deposition, spruce forest floor and living Sphagnum along a NW–SE transect across Europe, *Biogeochemistry*, *53*, 23-50.

Novák, M., Vile, M.A., Bottrell, S.H., Štěpánová, M., Jačková, I., Buzek, F., Přechová, E. and Newton, R.J., 2005. Isotope systematics of sulfate-oxygen and sulfate-sulfur in six European peatlands, *Biogeochemistry*, *76*, 187-213.

Ochieng, G.M., Seanego, E.S. and Nkwonta, O.I., 2010. Impacts of mining on water resources in South Africa: A review, *Scientific Research and Essays*, *5*(22), 3351-3357.

Ofukany, A.F., Wassenaar, L.I., Bond, A.L. and Hobson, K.A., 2014. Defining fish community structure in Lake Winnipeg using stable isotopes (δ13C, δ15N, δ34S): Implications for monitoring ecological responses and trophodynamics of mercury & other trace elements, *Science of the Total Environment*, *497*, 239-249.

Otero, N. and Soler, A., 2002. Sulphur isotopes as tracers of the influence of potash mining in groundwater salinisation in the Llobregat Basin (NE Spain), *Water Research*, *36*, 3989-4000.

Otero, N., Canals, A. and Soler, A., 2007. Using dual-isotope data to trace the origin and processes of dissolved sulphate: a case study in Calders stream (Llobregat basin, Spain), *Aquatic Geochemistry*, *13*, 109-126.

Penniston-Dorland, S.C., Mathez, E.A., Wing, B.A., Farquhar, J. and Kinnaird, J.A., 2012. Multiple sulfur isotope evidence for surface-derived sulfur in the Bushveld Complex, *Earth and Planetary Science Letters*, *337*, 236-242.

Penniston-Dorland, S.C., Wing, B.A., Nex, P.A., Kinnaird, J.A., Farquhar, J., Brown, M. and Sharman, E.R., 2008. Multiple sulfur isotopes reveal a magmatic origin for the Platreef platinum group element deposit, Bushveld Complex, South Africa, *Geology*, *36*(12), 979-982.

Pool-Stanvliet, R.W.C.N.C.B., 2013. A history of the UNESCO Man and the Biosphere Programme in South Africa, *South African Journal of Science*, *109*(9), 1-6.

R Core Team. 2023. R: A Language and Environment for Statistical Computing. R Foundation for Statistical Computing, Vienna, Austria.

Rice, K.C., Scanlon, T.M., Lynch, J.A. and Cosby, B.J., 2014. Decreased atmospheric sulfur deposition across the southeastern US: When will watersheds release stored sulfate?, *Environmental science & technology*, *48*(17), 10071-10078.

Romahn, F., Pedergnana, M., Lotola, D., Aptiuley, A., Sneep, M. and Veefkind, J.P., 2023. 'Sentinel-5 precursor/TROPOMI Level 2 Product User Manual Sulphur Dioxide SO_2', Document No. S5p-L2-DLR-PUM-400E, German Aerospace Center.

Scheepers, A. 2017. *Proposed installation of Sulphur Dioxide (SO2) abatement equipment at Anglo American Platinum Limited: Polokwane Smelter – Environmental and Social Management Programme*, WSP Environmental (Pty) Ltd.

Schippers, A., 2004. Biogeochemistry of metal sulfide oxidation in mining environments, sediments, and soils, *Special Papers-Geological Society of America*, 49-62.

Sharpley, A., Richards, P., Herron, S. and Baker, D., 2012. Case study comparison between litigated and voluntary nutrient management strategies, *Journal of Soil and Water Conservation*, *67*(5), 442-450.

Shi, P., Zhang, Y., Li, Z., Li, P. and Xu, G., 2017. Influence of land use and land cover patterns on seasonal water quality at multi-spatial scales, *Catena*, *151*, 182-190.

Shikwambana, L., Mhangara, P. and Mbatha, N., 2020. Trend analysis and first time observations of sulphur dioxide and nitrogen dioxide in South Africa using TROPOMI/Sentinel-5 P data, *International Journal of Applied Earth Observation and Geoinformation*, *91*, 1-13.

Skinner, S.J.W., 2018. Platinum Tailings Review-A comparison of the water quality in the tailings dam to the surrounding groundwater, *IMWA*, 733-737.

Soucek, D.J. and Kennedy, A.J., 2005. Effects of hardness, chloride, and acclimation on the acute toxicity of sulfate to freshwater invertebrates, *Environmental Toxicology and Chemistry: An International Journal*, *24*(5), 1204-1210.

South African Government, 2005. *No 39 of 2004 National Environmental Management: Air Quality, Act 2004*, Government Gazette Vol. 476 No. 27318, Pretoria.

South African Weather Service (SAWS). Climate data 2007 to 2022 of A21K, from http://www.weathersa.co.za/climate.

Srayko, S.H., Jardine, T.D., Phillips, I.D., Morrissey, C.A. and Chivers, D.P., 2023. Sulfur stable isotopes as a tracer of insect migration and consumption by fish predators. *Freshwater Science*, *42*(3), 000-000.

Takahashi, H., Kopriva, S., Giordano, M., Saito, K. and Hell, R., 2011. Sulfur assimilation in photosynthetic organisms: molecular functions and regulations of transporters and assimilatory enzymes, *Annual review of plant biology*, *62*, 157-184.

Thormann, L., Buchspies, B., Mbohwa, C. and Kaltschmitt, M., 2017. PGE production in southern Africa, part I: production and market trends, *Minerals*, *7*(11), 1-22.

Trust, B.A. and Fry, B., 1992. Stable sulphur isotopes in plants: a review, *Plant, Cell & Environment*, *15*(9), 1105-1110.

Turchyn, A.V., Tipper, E.T., Galy, A., Lo, J.K. and Bickle, M.J., 2013. Isotope evidence for secondary sulfide precipitation along the Marsyandi River, Nepal, Himalayas, *Earth and Planetary Science Letters*, *374*, 36-46.

Wanderi, E.W., Gettel, G.M., Singer, G.A. and Masese, F.O., 2022. Drivers of water quality in Afromontane-savanna rivers, *Frontiers in Environmental Science*, *10*, 1-20.

Wang, H. and Zhang, Q., 2019. Research advances in identifying sulfate contamination sources of water environment by using stable isotopes, *International journal of Environmental Research and Public Health*, *16*(11), 1-13.

Wayland, M. and Hobson, K.A., 2001. Stable carbon, nitrogen, and sulfur isotope ratios in riparian food webs on rivers receiving sewage and pulp-mill effluents, *Canadian Journal of Zoology*, *79*(1), 5-15.

Woodborne, S., Huchzermeyer, K.D.A., Govender, D., Pienaar, D.J., Hall, G., Myburgh, J.G., Deacon, A.R., Venter, J. and Lübcker, N., 2012. Ecosystem change and the Olifants River crocodile mass mortality events, *Ecosphere*, *3*(10), 1-17.

Wu, S., Jeschke, C., Dong, R., Paschke, H., Kuschk, P. and Knöller, K., 2011. Sulfur transformations in pilot-scale constructed wetland treating high sulfate-containing contaminated groundwater: a stable isotope assessment, *Water research*, *45*(20), 6688-6698.

Yucel, D.S., Balci, N. and Baba, A., 2016. Generation of acid mine lakes associated with abandoned coal mines in Northwest Turkey, *Archives of Environmental Contamination and Toxicology*, *70*(4), 757-782.

Zak, D., Hupfer, M., Cabezas, A., Jurasinski, G., Audet, J., Kleeberg, A., McInnes, R., Kristiansen, S.M., Petersen, R.J., Liu, H. and Goldhammer, T., 2021. Sulphate in freshwater ecosystems: A review of sources, biogeochemical cycles, ecotoxicological effects and bioremediation, *Earth-Science Reviews*, *212*, 1-23.

Zhang, H. B., Hu, A. Q., Lu, C. Z. and Zhang, G.X., 2002. Sulfur isotopic composition of acid deposition in South China Regions and its environmental significance, *China Environ. Sci.*, 22(2), 165-169.

Zhang, Q., Wang, H. and Lu, C., 2020. Tracing sulfate origin and transformation in an area with multiple sources of pollution in northern China by using environmental isotopes and Bayesian isotope mixing model, *Environmental Pollution*, *265*, 1-11.

Zunckel, M., 1999. Dry deposition of sulphur over eastern South Africa, *Atmospheric Environment*, *33*(21), 3515-3529.

Zunckel, M., Robertson, L., Tyson, P.D. and Rodhe, H., 2000. Modelled transport and deposition of sulphur over Southern Africa, *Atmospheric Environment*, *34*(17), 2797-2808.

Zuur, A.F., Ieno, E.N., Walker, N.J., Saveliev, A.A. and Smith, G.M., 2009. Mixed effects models and extensions in ecology with R, Springer, New York.

4.6.3. Supplementary material

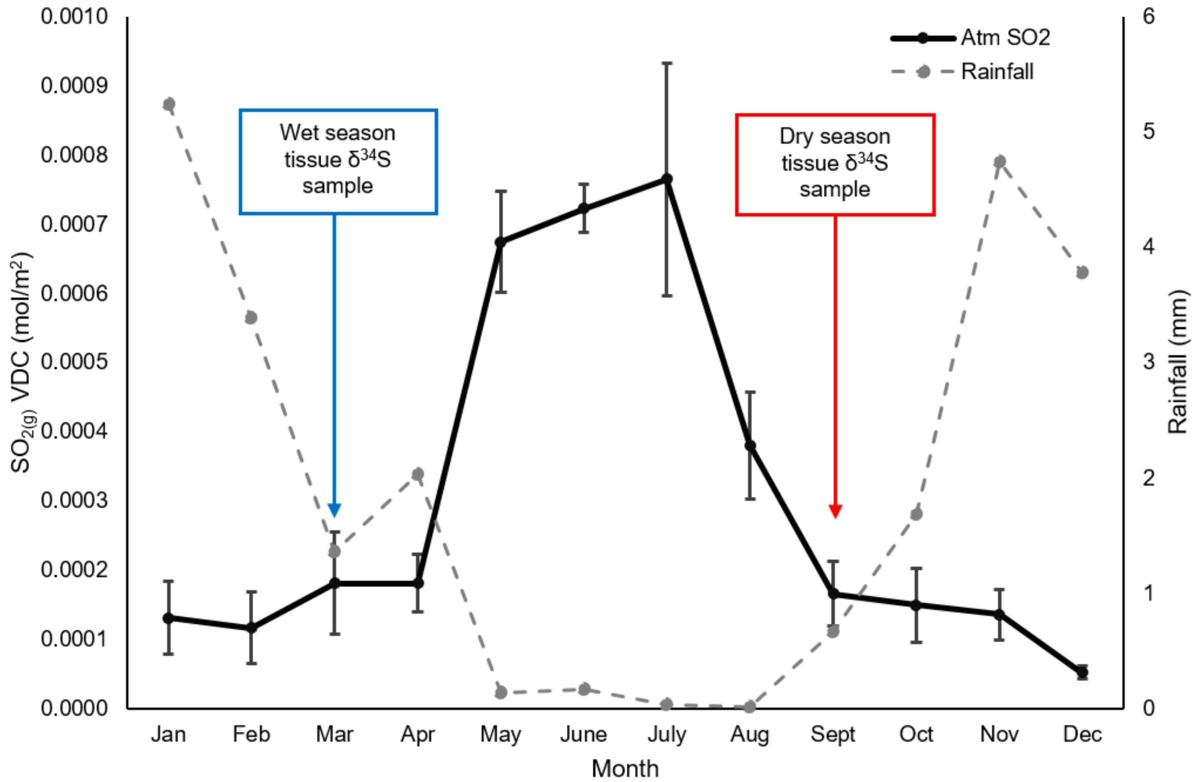

Figure S4-1: Seasonal (temporal) trend of the Sentinel-5P Copernicus TROPOMI sensor sulfur dioxide (SO_2) vertical column density (VCD) in units of mol/m^2 (black solid line) averaged over the study area for the years 2019-2021. The seasonal standard deviation for each yearly time series is represented as error bars. The mean rainfall data (grey-broken line) is collected from Climate Hazards Group InfraRed Precipitation with Station data (CHIRPS) dataset for the same time-period as the atmospheric $SO_{2(g)}$ (Funk et al., 2015). There is a significant negative correlation (r = -0.84, p < 0.01) between averaged atmospheric $SO_{(g)}$ and rainfall. The blue and red arrows denote the month in 2021 where the collection of fish tissue samples began for the wet and dry seasons respectively.

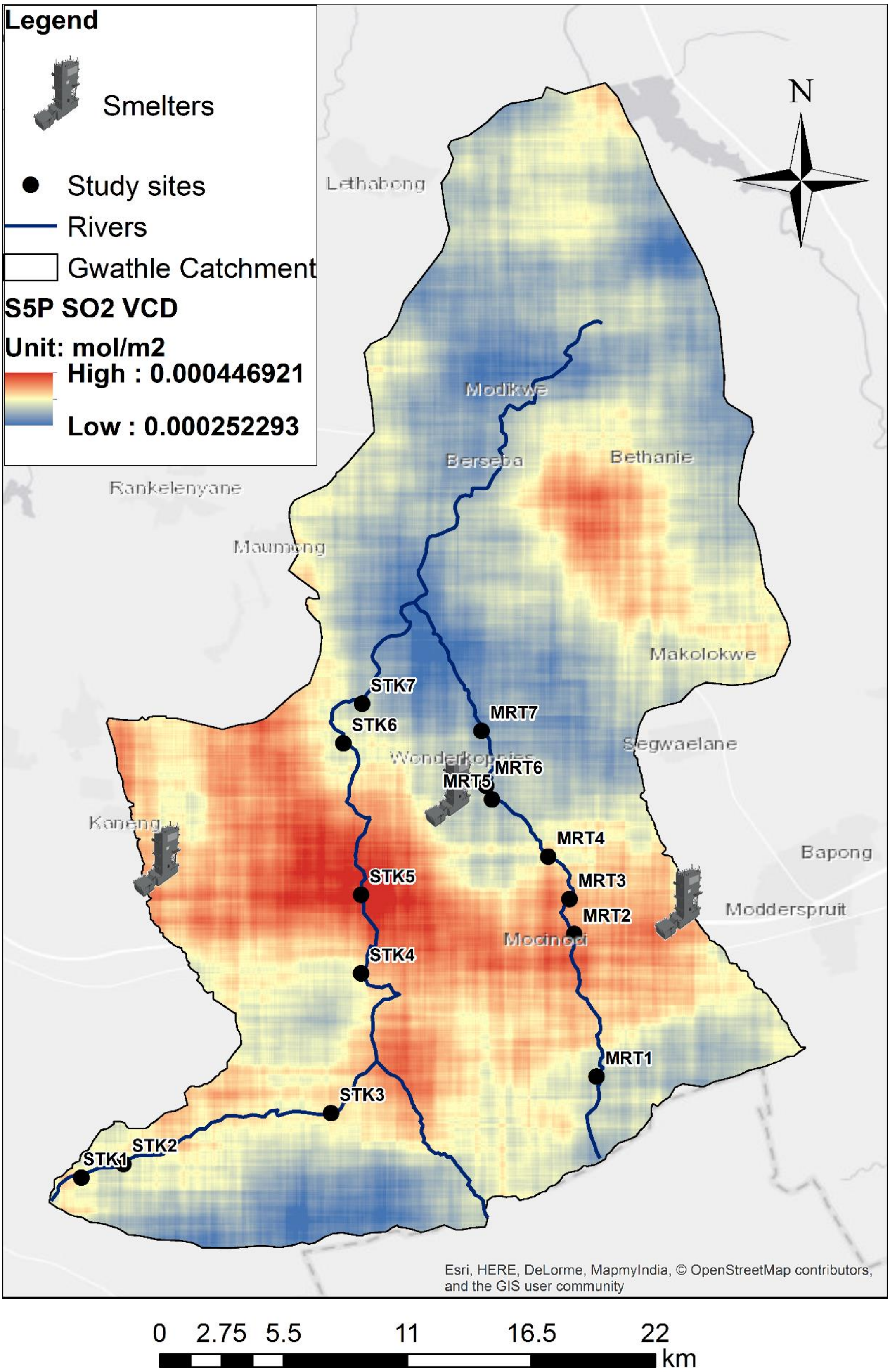

Figure S4-2: The average spatial sulfur dioxide (SO_2^-) vertical column density (VCD) distribution in units of mol/m^2 over the Gwathle Catchment (A21K) with data collected between January 2019 and December 2021 to determine long-term $SO_{2(g)}$ variability and potential key atmospheric-aquatic ecosystem exposure driving fish tissue δ^{34}S variability.

Table S4-1: The variable loadings associated with the Principal Components Analysis (PCA) as performed and labelled **Figure 4-3** in determining the catchments key water quality variables in relation to the fish tissue $\delta^{34}S$ mean (pristine corrected) data (bolded black). The red highlighted variables denote the water quality parameters with the highest loading in each principal component.

Principal Component (PC)	Variable	Loadings	p value
PC 1 (accounting for 34.54% of the datasets variation)	**TDS**	**0.95**	**0.00**
	Sulfate	0.94	0.00
	Mg	0.92	0.00
	Zn	0.92	0.00
	Cr	0.91	0.00
	Cu	0.67	0.00
	pH	0.64	0.00
	Nitrate	0.63	0.00
	River MRT	0.59	0.00
	Temp	0.52	0.00
	Fe	0.39	0.04
	$\delta^{34}S$ mean	**-0.46**	**0.01**
	River STK	-0.59	0.00
PC 2 (accounting for 12.25% of the datasets variation)	**Ortho-phosphate**	**0.78**	**0.00**
	Turbidity	0.70	0.00
	Ammonium	0.64	0.00
	DO	-0.37	0.05
PC 3 (accounting for 10.56% of the datasets variation)	River STK	0.62	0.00
	Ammonium	**0.59**	**0.00**
	River MRT	-0.60	0.00

Table S4-2: The tissue derived $\delta^{34}S$ values averaged and standard derivation (SD) over the two seasons together with the sites total dissolved solids and spatial-scale specific SO^2 as vertical column density measured in mol/m^2 calculated for the respective season between Jan 2019 – Dec 2021

Site and Season	$\delta^{34}S$ (‰) mean	$\delta^{34}S$ (‰) SD	$\delta^{34}S$ (‰) mean (corrected)	$\delta^{34}S$ (‰) SD (corrected)	TDS (g/L)	Sub-basin atm. SO_2 VCD (mean)	Sub-basin atm. SO_2 VCD (SD)	Cumulative-basin atm. SO_2 VCD (mean)	Cumulative-basin atm. SO_2 VCD (SD)
STK1W	-0.3	0.2	-0.3	0.2	0.01	0.000135	0.000089	0.000135	0.000089
STK2W	-0.6	1	0	1	0.01	0.000127	0.000073	0.000128	0.000075
STK3W	3	0.4	3.6	0.4	0.04	0.000126	0.000044	0.000126	0.000044
STK4W	1.9	0.4	3	0.6	0.29	0.000140	0.000057	0.000132	0.000043
STK5W	-1.4	3.7	-0.8	3.7	0.32	0.000129	0.000073	0.000131	0.000043
STK6W	2.5	0.8	2.1	0.3	0.03	0.000157	0.000067	0.000132	0.000042
STK7W	2.4	0.6	3	0.6	0.27	0.000146	0.000055	0.000136	0.000044
MRT1W	2.6	0.4	0	0.4	0.01	0.000132	0.000105	0.000132	0.000105
MRT2W	4.9	0.5	2.3	0.5	0.13	0.000157	0.000065	0.000150	0.000070
MRT3W	4	1.9	1.4	1.9	0.14	0.000154	0.000084	0.000150	0.000071
MRT4W	-1.4	2.4	1.4	1.9	0.41	0.000139	0.000072	0.000145	0.000060
MRT5W	-1.3	1.5	-3.9	1.5	0.37	0.000135	0.000062	0.000141	0.000053
MRT7W	-1	1.3	-3.5	1.3	0.78	0.000144	0.000068	0.000141	0.000051
STK1D	0.9	0.8	0.6	0.7	0.02	0.000556	0.000084	0.000556	0.000084
STK2D	-0.1	0.6	0	0.6	0.02	0.000538	0.000089	0.000540	0.000088
STK3D	3.5	0.3	3.6	0.3	0.11	0.000503	0.000069	0.000507	0.000064
STK4D	2	0	2.1	0	0.18	0.000516	0.000072	0.000511	0.000054
STK5D	2.3	1.1	2.4	1.1	1.18	0.000567	0.000103	0.000517	0.000053
STK6D	4.2	1	4.3	1	0.03	0.000617	0.000141	0.000525	0.000055
STK7D	2.5	0.8	2.7	0.8	0.28	0.000588	0.000084	0.000550	0.000060
MRT1D	3.1	0.5	0	0.5	0.02	0.000518	0.000080	0.000518	0.000080
MRT2D	5.1	0.8	2	0.8	0.13	0.000536	0.000096	0.000532	0.000089
MRT3D	5.1	0.6	2	0.5	0.19	0.000576	0.000108	0.000539	0.000089
MRT4D	-0.9	0.9	-3.9	0.9	0.35	0.000578	0.000116	0.000557	0.000091
MRT5D	-2.9	1.1	-5.9	1.1	0.67	0.000566	0.000091	0.000561	0.000085
MRT6D	1.6	1.1	-1.5	1.1	1.91	0.000597	0.000059	0.000565	0.000088
MRT7D	1.4	0.6	-1.7	0.6	2.87	0.000501	0.000147	0.000553	0.000095

Table S4-3: The five FRAGSTATS derived class-level variables (four stressors) at each of the study sites recorded within their respective assessed hydrological spatial scales, quantified as using the Percentage of Landscape (PLAND) metric.

Site and Season	SB Agri PLAND	SB Urban PLAND	SB Fallow PLAND	SB Mining PLAND	SB Natural PLAND	CB Agri PLAND	CB Urban PLAND	CB Fallow PLAND	CB Mining PLAND	CB natural PLAND
STK1	0.00	0.00	0.00	0.00	100.00	0.00	0.00	0.00	0.00	100.00
STK2	9.97	0.11	0.75	0.00	89.10	8.72	0.09	0.66	0.00	90.47
STK3	7.98	1.20	7.90	0.00	82.90	8.04	1.09	7.13	0.00	83.71
STK4	6.50	1.28	1.54	0.06	88.33	7.39	1.17	4.69	0.05	85.70
STK5	12.67	3.81	13.05	8.48	61.93	7.99	1.48	5.65	1.05	82.92
STK6	10.02	31.05	21.23	5.59	31.90	8.15	3.59	6.80	1.37	79.25
STK7	15.67	1.97	23.95	16.30	42.05	11.17	2.94	13.69	7.38	64.28
MRT1	0.00	0.00	0.00	0.00	100.00	0.00	0.00	0.00	0.00	100.00
MRT2	18.72	2.68	2.24	0.00	76.34	14.80	2.15	1.79	0.00	81.25
MRT3	25.36	16.04	8.02	0.21	50.38	16.37	4.31	2.77	0.10	76.43
MRT4	26.07	2.26	12.20	5.67	53.75	20.98	3.40	7.24	2.70	65.64
MRT5	7.88	5.03	9.99	6.30	70.35	15.13	4.12	8.48	4.32	67.72
MRT6	15.86	1.90	12.39	31.78	38.05	15.18	3.86	8.94	7.28	64.53
MRT7	12.34	2.28	24.25	11.77	49.35	14.71	3.57	11.66	8.10	61.80

Chapter 5 – Synthesis and conclusion

This chapter presents a synthesis of the research findings from the empirical chapters **two** through **four**. These chapters explored contrasting tools and approaches for the potential development of a tailored environmental forensic toolbox, capable of improving South African catchment management. The rationale for this ecohydrological study is that the complex interaction of multiple catchment stressors over hydrological spatial scales poses major challenges for currently accepted aquatic ecosystem monitoring best practices, thereby hindering effective management interventions to alleviate pressure on river health. There is a critical need in the current Resource Directed Measures (RDM) and Source Directed Control (SDC) mechanisms for a supplemental environmental forensic toolbox, that combines spatially explicit pollutant fingerprinting methods, capable of attributing observed abiotic and biotic responses (i.e. ecosystem condition) to specific catchment stressors (source of impact). Disentangling the relationship between catchment stressors is vital for developing targeted river health management strategies and strengthening environmental enforcement capabilities.

To fulfill the current water resource management gaps, my research was designed and conducted in the Gwathle River catchment experiencing extensive land intensification with three broad aims: (**Chapter two**) disentangling and identifying dominant stressors influencing specific water quality responses across a land-use intensification gradient using a multi-hydrological-scale approach, (**Chapter three**) to track the movement of in-stream metals across the catchment by conducting a comparative geospatial assessment of dissolved and sediment-bound metals using two media-linked analytical techniques, and (**Chapter four**) to disentangle the effects of key terrestrial aquatic stressors in the catchment, using fish tissue $\delta^{34}S$ across differing spatio-temporal scales. In this final synthesis chapter, I highlight the key findings of the research, the implications that can address versatile catchment management needs, with the potential to improve fine-scale to catchment management in South Africa, as well as scope for future research.

5.1. Spatial considerations for river water quality stressor identification

My study has advanced the understanding that a multi-spatial scale investigation of co-existing catchment stressors can best explain responses in river water quality and trace metal behaviour in two media (**Chapters two** and **three**), as well as fish tissue

$\delta^{34}S$ as an effective aquatic stress-tracer (**Chapter four**). Interactions between different stressors are often considered complicated and spatially variable, making it difficult to pinpoint the leading cause of a negative effect on a river system (Sabater et al., 2021; Xu et al., 2020). In different spatially aligned studies investigating stressor-aquatic constituent relationships, class-level metrics (derived from the computer software FRAGSTATS), are often considered to explore the spatial patterns and characteristics of specific stressors (McGarigal et al., 2002; Ding et al., 2016). These may include the 1) percentage cover of each land cover class (PLAND) metric as well as the 2) physical connectedness of each land cover class (COHESION) metric for each stressor (class) (Allan, 2004; Ding et al., 2016). In such cases, there is generally high redundancy among such metrics for particular catchments (**Chapter one**) (Uuemma et al., 2006), this led to the selection of one overarching metric, PLAND, for stressor investigative purposes in the remaining chapters (**Chapter two** and **three**).

I explored how class-level composition (PLAND) and connectedness (COHESION) of land use stressors, as well as different topographic features (slope and elevation), at four hydrological spatial scales (sub-basin scale, cumulative basin scale, and the 100 m riparian buffers at each of the latter two scales) drive characteristic catchment water quality responses (**Chapter two**). While past spatial studies have sought the optimal spatial scale to link characteristic river water quality responses to stressors (Zhang et al., 2020), I demonstrated the importance of a multi-spatial scale assessment in identifying the specific scale-dependent sources of such in a multi-user catchment. Of the four different hydrological spatial scales I assessed in **Chapter two**, three were effective in linking key water quality responses to stressors. This is owing to ecohydrological processes and land-uses interacting at different scales, modifying mobile constituents in particular ways, showing the “one-scale fits all” approach to be inadequate (in agreement with; Wang et al., 2023). In addition, no other spatially aligned study to date has explored how common catchment stressors (urbanisation and agriculture) interact with extensive mining activities to drive changes in river water quality.

5.2. Aquatic stress-tracing using dissolved and sediment metals

Although four spatial scales were assessed in **Chapter two**, the sub-basin scale together with its nested derivative (i.e. cumulative scale) were used in further investigations (**Chapters three** and **four**); as they accounted for most of the river water quality variation. In **Chapter three**, I assessed at which of the latter two spatial scales trace metals, specifically conservative Cr and reactive Zn, were best predicted by catchment stressors as represented by the class-level PLAND metric. This was determined by analysing each metal in the two in-stream media using distinct techniques: water samples were measured by inductively coupled plasma mass spectrometry (ICP-MS), while sediment samples were evaluated using energy dispersive X-ray fluorescence (EDXRF). A novel addition in **Chapter three** was assessing whether each individual trace metal from dissolved and sediment-bound media at two hydrological spatial scales, provide complimentary or divergent information for use in disentangling catchment stressors. This was a pertinent question as currently only dissolved metals, which are sensitive to short-term fluctuations, are widely used in South African (national) river health assessments (Beck et al., 1991, DWAF, 2004).

In the statistical analysis, I accounted for the PGE-rich lithological context of the catchment. This is due to natural weathering processes facilitating metal mobilization (Almécija et al., 2017), and to isolate the potential metal source (stressor) it was important to account for catchment lithology as a confounding factor. Having collected dissolved and sediment samples during wet and dry seasons dissolved and sediment-bound Cr (conservative metal) demonstrated substantial stress-tracking capacity (agreement) at the cumulative basin scale. This indicated that Cr from both media effectively tracked changes in nested stressor patterns along river continua, where its variability in both media was primarily driven by mining stress. This finding provided fresh evidence supporting the ability of conservative sediment-bound metals to be used to trace legacy pollution activities in a multi-user catchment as opposed to only relying on dissolved, transient samples (Förstner and Müller, 1981). Sediment-Cr also demonstrated effectiveness in capturing nested mining pollution significantly above background levels, with enrichment factors exceeding 1.5 (Garcia-Ordiales et al., 2014).

Unlike dissolved Cr, dissolved zinc (reactive metal) was best predicted for at the sub-basin scale by geological factors, supporting its local scale attenuation as observed by Gozzard et al. (2011), while sediment-bound Zn at the cumulative basin scale (c.f. Jin et al., 2019) with its cumulative variability driven as much by urban stress as the lithology. The reactive Zn demonstrated behavioural differences in both media (c.f. Gozzard et al., 2011; Jin et al., 2019), leading to no stress-tracking agreement between the two. In addition, I demonstrated that sediment-derived Zn enrichment factors did not exceed 1.5 (i.e., no more than 0.2 EF) and were not significantly different from background levels (Garcia-Ordiales et al., 2014). While these low EFs could indicate a limited ability to detect prominent stressor effects, they may also reflect the absence of substantial Zn pollution sources within the studied catchment. Further investigation of potential Zn contamination sources and their influence on sediment enrichment is needed to fully assess Zn's performance as a pollution indicator in this system.

The multi-scale (model) findings of the two Zn media, do suggest that reactive metals, such as Zn, may be subject to more scale-dependent processes, leading to divergent results between water and sediment media that do not provide complementary information about stressor effects along a land-use intensification gradient. As a result, water and sediment media may not be effectively paired for identifying pollution sources when considering reactive metals like Zn. In contrast, behaviourally conservative Cr demonstrated consistent spatial detection patterns which tracked stressor Cr input effects downstream in both water and sediment samples. This thereby signifying the feasibility of coupling these media for identifying sources of aquatic Cr metal pollution in this study catchment and beyond. This comparative analysis highlights the efficacy and value of rapid sediment screening using the cost-effective EDXRF method to identify persistent trace metal accumulation, particularly from mining activities and to complement routine water quality monitoring. Notably, this approach proves valuable even for complex contaminants that may undergo phase transformations between dissolved and particulate forms.

5.3. Fish tissue-derived $\delta^{34}S$ as ecotoxicological aquatic stress tracer

Aquatic tissue derived stable isotopes, particularly $\delta^{15}N$, have been used globally (Lee et al., 2018) and in South Africa (Motitsoe et al., 2022) to identify key stressor sources of aquatic N-loading. Although attempts have been made internationally to use fish-tissue $\delta^{34}S$ to trace a few catchment sources of aquatic S-loading, such as industry and urban wastewater (Wayland and Hobson, 2001), no aquatic ecosystem study in South Africa nor abroad has applied it in a multi-user catchment with interactive mining effects. I used fish tissue $\delta^{34}S$ as a novel key ecotoxicological tracer of multi-user catchment stress (including agriculture, urbanisation and mining), at the two hydrological spatial scales used in **Chapter three**. Just as the sediment-bound Cr in **Chapter three** provided a time integrated signal of metal contamination, $\delta^{34}S$ in fish tissue assessed in **Chapter four**, also provides a time-integrated signal of catchment stress on river systems (Hesslein et al., 1991), however, the $\delta^{34}S$ was effective in disentangling agricultural and mining stress as opposed to the metals, which in **Chapter three** only identified mining as an overwhelming (key) driver of metals. This result demonstrated $\delta^{34}S$ to be a key indicator of chronic and acute pollution episodes from multiple stressors other than those that contribute to metal pollution.

An important additional novel consideration in the identification of terrestrial stressors on river ecosystems using fish tissue $\delta^{34}S$ in **Chapter four**, was accounting for atmospheric $SO_{2(g)}$ deposition influencing spatio-temporal tissue $\delta^{34}S$ variability (between scales and over seasons). This was because the catchment is likely subjected to $SO_{2(g)}$ concentrations above those of an equally sized unindustrialized catchment, particularly one without extensive open-cast mining and sulfide ore smelting (ore-roasting) activities (Nielsen, 1973; Koptsik and Alewell, 2007; Shikwambana et al., 2020). Like catchment lithology was accounted for in **Chapter three** as a confounding factor, so too was the spatio-temporal atmospheric $SO_{2(g)}$ (average and heterogeneity). I obtained spatially and temporally comparable $SO_{2(g)}$ vertical column density (mol/m^2) data for each of the two hydrological spatial scales across each season (wet and dry) to account for its spatio-temporal influence in the statistical models.

Through **Chapter four**, I demonstrated that by pairing spot sampled (instantaneous) total dissolved solids (a broadly applicable pollution indicator) with the simultaneously collected tissue-assimilated $\delta^{34}S$ (from each site) on biplots, water resource managers can rapidly visualise stressor groupings without extensive statistical knowhow. However, through more advanced geospatial statistical approaches, I demonstrated that agricultural stress at the sub-basin scale was the significant driver of enriched tissue-assimilated $\delta^{34}S$ relative to pristine conditions among the catchment stressors. While at the cumulative-basin (nested) scale, I determined mining to be the significant driver of relatively depleted tissue $\delta^{34}S$ values within the catchment. The assessment of terrestrial mining stress on river catchments using fish tissue $\delta^{34}S$ is novel, as previous studies investigating mining stress have largely used dissolved $\delta^{34}S_{SO4}$ rather than time-integrated tissue-based $\delta^{34}S$ values (Otero and Soler, 2002; Yucel et al., 2007).

Furthermore, in this **Chapter four**, I highlighted that terrestrial agricultural and mining stressors in the Gwathle Catchment were shown to have an overwhelming effect on tissue-based $\delta^{34}S$ variation when compared to the effects of atmospheric $SO_{2(g)}$ across scales and seasons. This is due to both atmospheric $SO_{2(g)}$ metrics (seasonal average and heterogeneity - SD) presenting as non-significant drivers of fish tissue $\delta^{34}S$ following statistical modelling. As with **Chapters two** and **three**, this **Chapter four** demonstrated effective stressor tracing abilities at hydrological spatial scales that are immediately relevant to local water resource management decision making. These findings demonstrate that spatially-assessed tissue-based $\delta^{34}S$ is a well-suited tracer tool for disentangling complex catchment intensification effects, to identifying the key source(s) of local aquatic ecosystem impact(s) to advise adaptive catchment management.

5.4. Management Implications

The results from my research have shown that when attempting to disentangle complex relationships between catchment stressors and associated aquatic ecosystem effects, (1) seasonally collected water quality can be driven by multiple stressors, each operating at different hydrological spatial scales (relevant to local catchment management), due to differing ecohydrological processes, (2) there is complementarity between conservative dissolved Cr (ICP-MS analysed) and legacy sediment-derived Cr (EDXRF analysed) trace metals in tracking mining stressor inputs at the hydrological cumulative basin scale, (3) that fish tissue $\delta^{34}S$ (as an ecotoxicological tracer) is effective at identifying terrestrial catchment stressors, where such stressors overwhelmed any significant seasonal atmospheric $SO_{2(g)}$ effects on the fish $\delta^{34}S$ variation, having accounted for spatio-temporal atmospheric $SO_{2(g)}$ concentrations.

In **Chapter two,** my findings suggest that using a multi-scale approach to modelling water quality responses to stressors can provide important insight and an improved understanding of distinct ecohydrological processes, interacting with different land-use stressors and water quality constituents. In-stream ammonium, copper, and turbidity concentrations were significantly driven by localized impervious urban runoff, mining effluent from direct discharge and decant waters, and agricultural soil erosion respectively, at the sub-basin scale. In contrast, pH shifted with cumulative basin scale changes in catchment slope variation, likely reflecting nested geological transitions and their influence on alkalinity. At the riparian interface, sulfate concentrations were closely tied to mineralized discharge and leaching from mine waste within the cumulative 100 m stream buffer. Analysing water quality change at multiple complementary spatial scales can assist water resource managers in better understanding and identifying scale and stressor-specific processes acting on mobile constituents influencing aquatic ecosystem health.

South Africa's national river water quality monitoring protocols currently do not consider hydrological spatial scales in the collection nor analysis of the data (DWAF, 2004; Kleynhans and Louw, 2008). There are however, freshwater resource strategies, including the National Freshwater Ecosystem Priority Areas (NFEPA) project, that do make provision for aspects of place-based monitoring to uphold a particular resource's RQOs. Each FEPA is tied to a particular "status" guiding localized management objectives (Driver et al., 2011). The NFEPA delineates spatial priorities for the country's waterways into FEPAs to support sustainable resource use, via sub-quaternary spatial catchments, analogous to the sub-basins in **Chapters two** through **four**. In addition, it allows for monitoring nodes (sites) to be positioned downstream of individual FEPAs, to maintain and/or improve the localized management objectives of each FEPA. While NFEPA links monitoring sites to FEPAs, it does not provide guidance on how the collective FEPA units can be used in identifying sources of catchment stress that drive river water quality responses.

Based on the findings of **Chapter two**, a supplementary protocols document outlining a forensic geo-spatial abiotic modelling approach could be integrated into the NFEPAs Project. By spatially analysing stressors and modelling their metrics (i.e. PLAND and COHESION) against river water quality responses, **Chapter two** demonstrated the forensic utility of this approach for effectively attributing sources of catchment water quality responses. Such an approach can be developed into a protocol document (as a forensic SDC tool) that could leverage the current monitoring nodes located downstream of each FEPA, to effectively link FEPA-aligned abiotic water quality responses with the source of impact, and from that, apply suitable remediation action, thereby better supporting individual NFEPAs objectives and thus catchment RDMs (see Kleynhans and Louw, 2008, pp. A2-7). In addition, such a developed protocol would provide the CMAs with the necessary stressor-response evidence allowing precisely targeted key maintenance and/or remedial actions geared towards overall improving catchment conditions.

The findings from **Chapter three**, which revealed the complementary ability of dissolved and sediment-bound (time-integrated) Cr to track metal contamination and its geo-spatial forensic capability, strongly suggest that trace metal monitoring in sediment should be incorporated into South Africa's national water resource management strategy. A portion of this research, without the forensic capabilities, but still using the rapid metal-sediment assessment (using EDXRF), can be refined into a national protocols document. Such a document can be facilitated and executed under the ‘monitored system drivers’ to rapidly assess ‘sediment contamination’ within the River Eco-status Monitoring Programme (REMP) and act as a supplementary addition to the dissolved analysis (DWAF, 2004; Kleynhans and Louw, 2008, pp. A2-4; Mogakabe and van Ginkel, 2008; Thirion and Jafta, 2019).

Currently, the national Water Resource Quality Monitoring sampling protocol only provides for the procedural collection of dissolved metals (DWAF, 2004). In addition, the forensic geo-spatial sediment-derived metal monitoring approach, as presented in **Chapter three**, can be further developed into a national stress-tracing protocol (using EDXRF). This protocol, with the aim of pinpointing key source(s) of active and legacy aquatic metal pollution, can be facilitated under the SDCs framework, and integrated as a forensic tool to assess compliance within the ‘Pollution Prevention and Minimization of Impacts’ guideline for the protection of water resources in the South African mining sector (DWAF, 2008).

Adopting such a sediment-metal (legacy capable) tracking approach, using the cost-effective EDXRF (**Chapter three**), may reduce the national budgetary and logistical requirements for dissolved metal sampling. The current inorganic sampling protocol by DWAF (2004) suggests that the optimal sampling frequency of dissolved monitoring should be at the discretion of the Resource Quality Services at national government level (DWAF, 2004). However, in the event of irregular/missed dissolved sampling, sporadic pollution events may go uncaptured in later spot analysed, dissolved samples. Sediment-derived trace metal monitoring via the cost-effective EDXRF can fill such a shortfall in dissolved sampling by providing a time-integrated metal signal, capable of capturing such sporadic pollution, negating the potential need for as frequent dissolved metal monitoring.

Moreover, dissolved inorganic sampling is rendered unsuitable when monitored river reaches become stagnant (DWAF, 2004), which may occur during periods of drought. In South Africa, many rivers and streams experience periods of low or no flow during the dry season, which can lead to some developing stagnant reaches while others may dry up completely (Day et al., 2019). These are non-perennial rivers and the interruptions in flow can last for weeks to months. Rainfall patterns are expected to become more variable in southern Africa in the coming decades, including an increasing likelihood of severe droughts (Jackson et al., 2020). With these projected hydrological shifts, coupled with the anticipated higher surface water demand, it can thus be argued that an increasing number of South Africa's rivers and streams will experience stagnant reaches for extended time periods (Day et al., 2019; du Plessis, 2023), thereby further disrupting dissolved inorganic water quality monitoring schedules.

To overcome the shortfall imposed by low flow conditions on dissolved monitoring (DWAF, 2004), sediment-derived samples can be collected and analysed using the rapid EDXRF method. This additional monitoring tool would provide water resource managers with suitable short-term and/or legacy metal pollution signatures (depending on sample depth), that would have otherwise not have been collected pending the return of suitable flow regimes to resume dissolved monitoring. In this context, sediment sampling offers a valuable complementary approach to assess metal contamination during low flow river conditions, providing insights into both recent and historical pollution that would otherwise be missed by relying solely on dissolved sampling.

The key implication of **Chapter four** is with regards to the use of seasonally collected fish tissue $\delta^{34}S$ to disentangle aquatic S-linked agricultural and mining spatial-stressor effects on river systems, while accounting for confounding atmospheric $SO_{2(g)}$ deposition in a multi-user catchment. As a geo-spatially integrated tool, it demonstrated forensic versatility in tracing and pinpointing pollution sources that likely do not follow sustainable land-management practices, that would otherwise be aimed at limiting pollution. Such practices may include the excessive application of agricultural fertilizers, as well as improper waste disposal and ineffective storage in the mining sector (Navarro et al., 2008; Xu et al., 2022). Fish tissue $\delta^{34}S$ can therefore offer a powerful time-integrated forensic tool for South African freshwater resource management. It can also complement the shortfalls of abiotic monitoring, which are limited by fluctuating transient effects (Beck et al., 1991), as well as biotic monitoring tools that are subject to hydrodynamic influences e.g. responding to flood pulses rather than water quality (Foord and Fouché, 2015).

Although fish tissue $\delta^{34}S$ for this research was analysed by an international laboratory, recent investment by the International Atomic Energy Agency (IAEA) in South Africa (Project: RAF 7021) will enhance local stable isotope analysis capabilities and thus the capacity to allow on-demand analysis of aquatic tissue $\delta^{34}S$. With such analysis being locally accessible, this would permit regular use of such a geo-spatially linked stable isotope forensic tool in aquatic ecosystem management and enforcement. This could also allow for the development of a novel and national, spatially-related aquatic forensic tool to identify aquatic pollution at the source, thereby forming part of the national SDCs framework, which is separate from the REMP 'Biological Response' tools e.g. SASS5, that carry a PES and do not have the forensic abilities to identify the sources of aquatic ecosystem stress (Kleynhans and Louw, 2008; DWS, 2023). Such a tool would offer complimentary forensic capabilities, whereby linking the REMP biological response results with specific source(s) of stress; which is critically lacking in the current REMP and thus bolstering the local freshwater resource management toolbox.

If integrated to support the current biotic REMP components, expert-derived, stressor-specific $\delta^{34}S$ response patterns could be established, from which ecosystem assessors can validate their linkages between ecosystem impacts and the contributing stressors. Realising the full potential of $\delta^{34}S$ as an ecotoxicological forensic tracer requires countrywide field research to develop distinct stressor-specific (source) $\delta^{34}S$ response signatures. Additionally, a standardized protocol is needed for consistent statewide sample collection, laboratory analysis, geospatial analysis and data interpretation. This would align with and strengthen South Africa's freshwater conservation goals and evidence-based enforcement capabilities. Overall, locally-enabled tissue $\delta^{34}S$ analysis, paired with current abiotic and biotic monitoring, offers a major advancement for identifying watershed activities that require regulation thereby improving local sub-basin scale and catchment wide management.

5.5. Knowledge gaps identified and research limitations

This doctoral thesis explores self-contained forensic tools and approaches as part of a proposed environmental forensic toolbox to bolster local freshwater resource management capabilities, by disentangling complex aquatic ecosystem stressors in a multi-user catchment. There is still, however, much work that is required to validate the effectiveness and responses of each tool within this proposed toolbox when applied in different river catchments, experiencing additional stressors of varying magnitudes.

Although this assessment considered no more than two FRAGSTAT-derived class-level metrics, accounting for land use composition (PLAND) and spatial configuration (COHESION), it is suggested that future follow up water quality response modelling assessments include additional metrics to enhance the representation of catchment land use patterns. This is because other metrics that account for the diversity (e.g. Shannon's diversity index) as well as shape (e.g. landscape shape index) have been demonstrated to be strongly correlated with such responses (Sun et al., 2014; Xu et al., 2020). In addition, the geo-spatial assessment throughout **Chapters two** through **four** could be expanded to include additional hydrological spatial scales, to potentially produce more informative parsimonious models. Some studies have for instance assessed water quality responses to stressors using multiple riparian buffer scales, ranging from 100 m to 1000 m (Xu et al., 2020), which may capture additional ecohydrological processes and interactions (Ledesma et al., 2016).

Chapter four explored fish tissue $\delta^{34}S$ as an ecotoxicological tracer, effectively disentangling catchment mining and agricultural and stressor effects. Previous research has linked fish tissue $\delta^{34}S$ with industrial stressor effects (pulp-mill effluents) on aquatic ecosystems (see Wayland and Hobson, 2001), while others have attempted to identify urban wastewater inputs using macroinvertebrate tissue $\delta^{34}S$ (e.g. Morrissey et al., 2013; Corson, 2017). To date, however, no published research has integrated both fish and macroinvertebrate trophic levels in a joint aquatic stressor assessment. Furthermore, no research has jointly investigated source derived $\delta^{34}S_{SO4}$ (e.g. Cravotta, 1997; Jakóbczyk-Karpierz and Ślósarczyk, 2022) and the consequential stepwise change in aquatic tissue $\delta^{34}S$ as a result of its input into the ecosystem from the source. Integrating fish and macroinvertebrate trophic levels in a joint aquatic stressor assessment using tissue $\delta^{34}S$, while simultaneously investigating the cascading effects of source-derived dissolved $\delta^{34}S_{SO4}$ on aquatic tissue $\delta^{34}S$, can enhance our insight into the fundamental biogeochemical cycling of sulfur and the ecological impacts of S-pollutants across aquatic food webs.

Although independently assessed in peer-reviewed literature, no multi-isotopic research has explored how aquatic food web integrity metrics respond to shifts in aquatic consumer $\delta^{34}S$ values when used as an ecotoxicological tracer of catchment stress (i.e. linking functional responses to abiotic drivers). Food web integrity metrics assess aquatic ecosystem food web structure and function and are computed using $\delta^{13}C$ and $\delta^{15}N$ (see Hill et al. 2015 and Jackson et al. 2011). Such metrics can be used to assess the trophic redundancy, niche space and evenness among others (Jackson et al., 2011; Brind'Amour and Dubois, 2013). Providing a seamless, full ecosystem integrity-to-stressor response multi-isotopic toolbox that links ecological condition (i.e. integrity) to pollution, would have significant implications in supporting the national resource sustainability mandate of the National Water Resource Strategy 3 that aims to uphold the integrity of aquatic ecosystems (DWS, 2023).

During the initial thesis conceptualisation and proceeding into aquatic tissue data collection, I intended to pair (link) aquatic tissue $\delta^{34}S$, as a quantifiably determined ecotoxicological tracer of catchment stress, with aquatic ecosystem integrity responses. This, however, was not conducted due to half the collected and packaged in-stream aquatic food web samples intended for $\delta^{13}C$ and $\delta^{15}N$ analysis remaining unanalysed by the contracted stable isotope laboratory at the time of thesis submission. This delay was caused by laboratory renovation, equipment repair, maintenance, and analysis backlogs on the locally sourced stable isotope ratio mass spectrometer.

Currently, there is no estimated time of completion for the analysis of the outstanding samples. An imbalanced seasonal analysis between fish tissue $\delta^{34}S$ and the $\delta^{13}C$ and $\delta^{15}N$ data would have prevented conclusive seasonal food web responses from being drawn in response to catchment stressors experiencing, often seasonally driven ecohydrological processes. Once the outstanding $\delta^{13}C$ and $\delta^{15}N$ data do become available, I anticipate conducting a quantitative food web ecological integrity – stressor response assessment using the $\delta^{34}S$ ecotoxicological tool in **Chapter four**. In addition, when made available, the data will also expand upon the descriptive presentation of only half of available $\delta^{13}C$ and $\delta^{15}N$ data in my previous research, Levin et al. (2023).

In addition, there are further outstanding $\delta^{34}S$ macroinvertebrate data for both the wet and dry sample seasons. This outstanding data was intended to be included in the **Chapter fours** analysis of the aquatic tissue $\delta^{34}S$ ecotoxicological tracer of catchment stressors. The outstanding processed and delivered samples are awaiting analysis following sample backlogs at an international laboratory that was commercially contracted. Upon receiving the outstanding samples (date still to be confirmed), I anticipate producing a $\delta^{34}S$ ecotoxicological tracer paper, investigating the responses of both secondary (currently unavailable) and tertiary consumers. This would aim to validate and expand upon the current findings, while considering further trophic level linked details, such as the potential $\delta^{34}S$ fractionation between trophic levels.

5.6. Conclusion

This research has been submitted at a pertinent time in the history of South Africa's water quality woes and remediation attempts. South Africa's essential, socio-economic supporting river systems are in a dire state, with many drinking water sources, including the Vaal system, being compromised by pollution from various sources (Bega, 2024; du Plessis, 2024; Nyathi, 2024). National government departments including the Department of Water and Sanitation as well as the Department of Forestry, Fisheries and Environment have together with appointed committees to urgently assess potential integrated solutions to river systems that are of national concern (Le Roux, 2024). These solutions include identifying sources of stress for targeted management action, as well as suitable remediation measures to improve aquatic ecosystem conditions. This research offers a multi-tooled approach towards the development of a tailored environmental forensic toolbox, aimed at enhancing water resource management in South Africa.

In it, I have demonstrated that a multi-spatial scale, as opposed to a single-scale approach, is essential in identifying the leading drivers (stressors) of key water quality responses. In doing so, we refine our understanding of the complex interactions between ecohydrological processes and catchment stressors. Although not yet integrated nationally, the rapid and cost-effective sediment-derived trace metal analysis (via EDXRF) can be paired/supplemented with traditionally used dissolved inorganic analysis (via ICP-MS), particularly that of conservative trace metals (e.g. Cr). This overcomes the limitations of infrequent and unsuitable dissolved sampling conditions to identify the source of and assess legacy stress on aquatic ecosystems. This research has uniquely advanced the understanding of how aquatic tissue-derived $\delta^{34}S$ responds to multiple-interacting catchment stressors, particularly agricultural and mining activities. This supports its use as a forensic tool in disentangling sources of aquatic ecosystem stress.

Collectively, this environmental forensic toolkit offers complementary and novel power to equip water resource managers. It enables identifying sources of stress and applying relevant local and transboundary integrated catchment management actions. Overall, this multi-faceted approach meaningfully advances our understanding of ecohydrological aspects and water resource analysis in South Africa. By elucidating key stressors and their complex interactions, it equips water resource managers with critical new evidentiary tools to aid enforcement and ensure the improvement and protection of aquatic ecosystems.

5.7. References

Allan, J.D., 2004. Landscapes and riverscapes: the influence of land use on stream ecosystems. *Annual Review of Ecology, Evolution, and Systematics*, *35*, 257-284.

Beck, M.B., Adeloye, A.J., Finney, B.A. and Lessard, P., 1991. Operational water quality management: transient events and seasonal variability, *Water Science and Technology*, *24*(6), 257-265.

Bega, S., 2024. *Vaal River residents say water lettuce is 'national crisis'*, viewed 20 February 2024, from: https://mg.co.za/the-green-guardian/2024-02-14-vaal-river-residents-say-water-lettuce-is-national-crisis/.

Brind'Amour, A. and Dubois, S.F., 2013. Isotopic diversity indices: how sensitive to food web structure?, *PloS one*, *8*(12),1-9.

Cravotta, C.A., 2002. *Use of stable isotopes of carbon, nitrogen, and sulfur to identify sources of nitrogen in surface waters in the Lower Susquehanna River Basin, Pennsylvania*, U.S. Geological Survey Water-supply paper No. 2497, Pennsylvania Department of Environmental Protection, US Government Printing Office.

Day, J.A., Malan, H.L., Malijani, E. and Abegunde, A.P., 2019. Water quality in non-perennial rivers. *Water SA*, *45*(3), 487-500.

Ding, J., Jiang, Y., Liu, Q., Hou, Z., Liao, J., Fu, L. and Peng, Q., 2016. Influences of the land use pattern on water quality in low-order streams of the Dongjiang River basin, China: A multi-scale analysis, *Science of the total environment*, *551*, 205-216.

Driver, A., Nel, J.L., Snaddon, K., Murry, K., Roux, D.J, Hill, L., Swartz, E.R., Manuel, J. and Funke, N. 2011. Implementation Manual for the Freshwater Ecosystem Priority Areas, Water Research Commission, Report No. 1807/1/11, Pretoria.

Du Plessis, A., 2023. *South Africa's Water Predicament: Freshwater's Unceasing Decline* (Vol. 101), Springer Nature, Switzerland.

du Plessis, A., 2024. *Another victim of inaction, reactive management and questionable decisions*, viewed 6 March 2024, from: https://www.iol.co.za/pretoria-news/opinion/another-victim-of-inaction-reactive-management-and-questionable-decisions-3bfacdf6-380b-4dc6-9810-e1d9d44c2896.

DWAF, 2004. *Water Resource Quality Monitoring Volume 1 – sampling protocol for Inorganic chemical analysis*, Resource Quality Services Department of Water Affairs, Pretoria, South Africa.

DWAF, 2004. *Water Resource Quality Monitoring Volume 1 – sampling protocol for Inorganic chemical analysis*, Resource Quality Services Department of Water Affairs, Pretoria, South Africa.

DWAF, 2008. Series 2A Guidelines for Water Management for Mine Residue Deposits, Best practice guidelines for water resource protection in the South African Mining Industry, Directorate: Resource Protection and Waste, Pretoria.

DWS, 2023. *The National Water Resources Strategy Third Edition (NWRS-3) March 2023*, Department of Water and Sanitation, Pretoria, South Africa.

Foord, S.H. and Fouché, P.S.O., 2016. Response of instream animal communities to a short-term extreme event and to longer-term cumulative impacts in a strategic water resource area, South Africa, *African Journal of Aquatic Science*, *4*, 29-40.

Förstner, U. and Müller, G., 1981. Concentrations of heavy metals and polycyclic aromatic hydrocarbons in river sediments: geochemical background, man's influence and environmental impact, *GeoJournal*, *5*, 417-432.

Garcia-Ordiales, E., Loredo, J., Esbrí, J.M., Lominchar, M.A., Millan, R. and Higueras, P., 2014. Stream bottom sediments as a means to assess metal contamination in the historic mining district of Almadén (Spain), *International Journal of Mining, Reclamation and Environment*, *28*(6), 357-376.

Gozzard, E., Mayes, W.M., Potter, H.A.B. and Jarvis, A.P., 2011. Seasonal and spatial variation of diffuse (non-point) source zinc pollution in a historically metal mined river catchment, UK, *Environmental Pollution*, *159*(10), 3113-3122.

Hesslein, R.H., Capel, M.J., Fox, D.E. and Hallard, K.A., 1991. Stable isotopes of sulfur, carbon, and nitrogen as indicators of trophic level and fish migration in the lower Mackenzie River basin, Canada, *Canadian Journal of Fisheries and Aquatic Sciences*, *48*(11), 2258-2265.

Hill, J.M, Kaehler, S., Hill, M.P. and Coetzee, J., 2011. *A stable isotope approach for the early detection and identification of N loading in aquatic ecosystems*, Water Research Commission, Report No. KV 280/11, Pretoria.

Jackson, A.L., Inger, R., Parnell, A.C. and Bearhop, S., 2011. Comparing isotopic niche widths among and within communities: SIBER–Stable Isotope Bayesian Ellipses in R, *Journal of Animal Ecology*, *80*(3), 595-602.

Jackson, M.C., Fourie, H.E., Dalu, T., Woodford, D.J., Wasserman, R.J., Zengeya, T.A., Ellender, B.R., Kimberg, P.K., Jordaan, M.S., Chimimba, C.T. and Weyl, O.L., 2020. Food web properties vary with climate and land use in South African streams, *Functional Ecology*, *34*(8), 1653-1665.

Jakóbczyk-Karpierz, S. and Ślósarczyk, K., 2022. Isotopic signature of anthropogenic sources of groundwater contamination with sulfate and its application to groundwater in a heavily urbanized and industrialized area (Upper Silesia, Poland), *Journal of Hydrology*, *612*, 1-15.

Jin, Z., Ding, S., Sun, Q., Gao, S., Fu, Z., Gong, M., Lin, J., Wang, D. and Wang, Y., 2019. High resolution spatiotemporal sampling as a tool for comprehensive assessment of zinc mobility and pollution in sediments of a eutrophic lake, *Journal of hazardous materials*, *364*, 182-191.

Kleynhans, C.J. and Louw, M.D., 2008. *Module A: EcoClassification and EcoStatus determination'. River EcoClassification: Manual for EcoStatus Determination (version 2)* Water Research Commission, Report No. TT 329/08, Pretoria.

Koptsik, G. and Alewell, C., 2007. Sulphur behaviour in forest soils near the largest SO2 emitter in northern Europe, *Applied Geochemistry*, *22*(6), 1095-1104.

Le Roux, C., 2024. *What next!? Task team to tackle 'sewage-loving' water lettuce crisis in Vaal River*, viewed 6 March 2024, from: https://www.citizen.co.za/news/vaal-river-rand-water-lettuce-sewage-pollution-dws-task-team-latest-5-march-2024/.

McGarigal, K., Cushman, S.A., Neel, M.C. and Ene, E., 2002. *FRAGSTATS: spatial pattern analysis program for categorical maps*, Computer software, University of Massachusetts, Amherst. Available from: www.umass. edu/landeco/research/fragstats/fragstats.

Mogakabe, D.E., and van Ginkel, C.E., 2008. *The water quality of Bospoort Dam*, Department of Water Affairs and Forestry, National Eutrophication Monitoring Programme, Report number: N/000/00/DEQ/0108, Pretoria.

Morrissey, C.A., Boldt, A., Mapstone, A., Newton, J. and Ormerod, S.J., 2013. Stable isotopes as indicators of wastewater effects on the macroinvertebrates of urban rivers, *Hydrobiologia*, *700*, 231-244.

Motitsoe, S.N., Hill, J.M., Coetzee, J.A. and Hill, M.P., 2022. Invasive alien aquatic plant species management drives aquatic ecosystem community recovery: An exploration using stable isotope analysis, *Biological Control*, *173*, 1-12.

Navarro, M.C., Pérez-Sirvent, C., Martínez-Sánchez, M.J., Vidal, J., Tovar, P.J. and Bech, J., 2008. Abandoned mine sites as a source of contamination by heavy metals: a case study in a semi-arid zone, *Journal of Geochemical exploration*, *96*(2-3), 183-193.

Nielsen, H., 1974. Isotopic composition of the major contributors to atmospheric sulfur, *Tellus*, *26*(1-2), 213-221.

Nyathi, M., 2024. *Sewage crisis means Vaal water lettuce is here to stay*, viewed 01 March 2024, from: https://mg.co.za/the-green-guardian/2024-02-06-sewage-crisis-means-vaal-water-lettuce-is-here-to-stay/.

Otero, N. and Soler, A., 2002. Sulphur isotopes as tracers of the influence of potash mining in groundwater salinisation in the Llobregat Basin (NE Spain), *Water Research*, *36*, 3989-4000.

Sabater, S., Elosegi, A. and Ludwig, R., 2021. Framing biophysical and societal implications of multiple stressor effects on river networks, *Science of the Total Environment*, *753*, 1-9.

Shikwambana, L., Mhangara, P. and Mbatha, N., 2020. Trend analysis and first time observations of sulphur dioxide and nitrogen dioxide in South Africa using TROPOMI/Sentinel-5 P data, *International Journal of Applied Earth Observation and Geoinformation*, *91*, 1-13.

Sun, Y., Guo, Q., Liu, J. and Wang, R., 2014. Scale effects on spatially varying relationships between urban landscape patterns and water quality, *Environmental Management*, *54*, 272-287.

Thirion, C. and Jafta, N., 2019. *River Ecostatus Monitoring Programme State of Rivers Report 2017-2018*, Department of Water and Sanitation, Report Number: N/000/00REMP/2019, Pretoria.

Uuemaa, E., Roosaare, J. and Mander, Ü., 2007. Landscape metrics as indicators of river water quality at catchment scale, *Hydrology Research*, *38*(2), 125-138.

Wang, Y., Song, Z., Bai, H., Tong, H., Chen, Y., Wei, Y., Wang, X. and Yang, S., 2023. Scale effects of land use on river water quality: a case study of the Tuojiang River Basin, China, *Environmental Science and Pollution Research*, 30(16), 48002-48020.

Wayland, M. and Hobson, K.A., 2001. Stable carbon, nitrogen, and sulfur isotope ratios in riparian food webs on rivers receiving sewage and pulp-mill effluents, *Canadian journal of zoology*, *79*, 5-15.

Wayland, M. and Hobson, K.A., 2001. Stable carbon, nitrogen, and sulfur isotope ratios in riparian food webs on rivers receiving sewage and pulp-mill effluents, *Canadian Journal of Zoology*, *79*(1), 5-15.

Xu, H., Tan, X., Liang, J., Cui, Y. and Gao, Q., 2022. Impact of agricultural non-point source pollution on river water quality: evidence from China, *Frontiers in Ecology and Evolution*, *10*, 1-11.

Xu, S., Li, S.L., Zhong, J. and Li, C., 2020. Spatial scale effects of the variable relationships between landscape pattern and water quality: Example from an agricultural karst river basin, Southwestern China. Agriculture, Ecosystems & Environment, 300, 1-13.

Yucel, D.S., Balci, N. and Baba, A., 2016. Generation of acid mine lakes associated with abandoned coal mines in Northwest Turkey, *Archives of Environmental Contamination and Toxicology*, *70*(4), 757-782.

Zhang, J., Li, S. and Jiang, C., 2020. Effects of land use on water quality in a River Basin (Daning) of the Three Gorges Reservoir Area, China: Watershed versus riparian zone, *Ecological Indicators*, *113*, 1-11.